

Visual constraints upon avian behaviour

Alexandra Louise Pollard

September 2009

**Thesis submitted for the degree of Doctor of
Philosophy, Cardiff School of Biosciences, Cardiff
University**

UMI Number: U585391

All rights reserved

INFORMATION TO ALL USERS

The quality of this reproduction is dependent upon the quality of the copy submitted.

In the unlikely event that the author did not send a complete manuscript and there are missing pages, these will be noted. Also, if material had to be removed, a note will indicate the deletion.



UMI U585391

Published by ProQuest LLC 2013. Copyright in the Dissertation held by the Author.
Microform Edition © ProQuest LLC.

All rights reserved. This work is protected against
unauthorized copying under Title 17, United States Code.

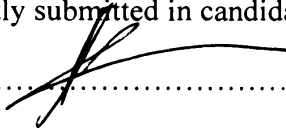


ProQuest LLC
789 East Eisenhower Parkway
P.O. Box 1346
Ann Arbor, MI 48106-1346

Declarations


DECLARATION

This work has not previously been accepted in substance for any degree and is not concurrently submitted in candidature for any degree.

Signed  (candidate) Date ...30/9/09.....

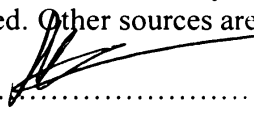
STATEMENT 1

This thesis is being submitted in partial fulfillment of the requirements for the degree of PhD.

Signed  (candidate) Date30/9/09.....

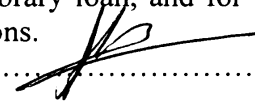
STATEMENT 2

This thesis is the result of my own independent work/investigation, except where otherwise stated. Other sources are acknowledged by explicit references.

Signed  (candidate) Date30/9/09.....

STATEMENT 3

I hereby give consent for my thesis, if accepted, to be available for photocopying and for inter-library loan, and for the title and summary to be made available to outside organisations.

Signed  (candidate) Date30/9/09.....

Acknowledgements

Throughout the course of my PhD studies I have received support and advice from many people, to whom I am indebted. Firstly I would like to thank my supervisors Rob Thomas, Peter Ferns and Kate Buchanan for their advice and guidance on the project and thesis.

I am grateful to my advisor Jon Erichsen for his contributions to the project and the use of his microscope. I would like to thank Dave Kelly and Nicola Marples for their valuable insights and ideas on my project.

I would not have been able to complete my studies without the fieldwork assistance and help with observations by Katherine Booth Jones, Heather Coats, James Chen, Peter Jenkins, Soski Nagano, Matt Postles, Lucy Rowse and Frances Thistlethwaite.

I would also like to thank the following: The Tamplin family, Forestry Commission, Tower of London, EMRIC, Natural History Museum (London and Tring), Turbary Owl Sanctuary (Whitestake), Naturalis (Leiden), A Rocha Portugal, Ed Drewitt, Peter Howlett, Nicola Goodship, Claire Bale, James Orpwood, Wendy Fernandes, Gabi Juma, Renata Medeiros, Viola Ross-Smith and Loys Richards-Hobbs, and the rest of the office past and present for providing friendship and tea.

These acknowledgments would not be complete without expressing my gratitude to my mum and dad, and Chris who provided support, love and motivation. I am especially grateful to Emily for providing perspective.

Summary

The aim of my PhD research was to investigate how avian behaviours may be constrained by eye design and visual capabilities. As great diversity exists across bird species in the design of the visual system, I utilised this variation to examine and explain the links between vision and behaviour. Several methods were employed in order to gain ocular information from species: including measuring eye size, retinal image brightness and retinal topographic analysis. I applied and developed these methods in studies ranging from a microscopic scale analysis of retinal structure, to studies comparing whole eye size and morphology, to gain an insight into how the timing of different behaviours may be constrained by visual capability, and how artificially modified visual constraints can lead to behavioural plasticity. Specifically, I compared the visual ability of extant diurnally and nocturnally active avian species with that of *Archaeopteryx*, finding that this early bird was likely to have been diurnal in the timing of its activity. Following on from this, I found that eye size, controlling for body mass, is an important predictor in the timing of onset of dawn song for species around the world. This relationship is stronger in circumstances when twilight length is longer. This study also revealed how species richness may affect the timing of behaviours, suggesting that tropical birds are able to partition their dawn choruses to reduce masking of acoustic signals. When the presence of artificial lighting modifies the visual constraints at twilight and night, I found that European robins *Erithacus rubecula* correspondingly modified their singing, foraging and mass regulation behaviour. Overall, my research highlights the great diversity of avian visual adaptations, and emphasises that understanding the differences between them is intrinsic to appreciating the way in which behaviour is constrained by visual ability.

Table of contents

Title page	i
Declaration	ii
Acknowledgments	iii
Summary	iv
Table of contents	v

Chapter 1 An introduction to avian vision and sensory ecology

Introduction	1
Evolution of the eye	2
Eye size and function	6
The refractive eye	12
Supporting and protecting the eye	24
Processing light information – the retina and neural centres	31
Optical specialisations for underwater vision in diving birds	53
Avian vision in context: Sensory Hierarchies	56
Conclusion	61

Chapter 2 Methods of assessing avian eye design

Abstract	62
Introduction	63
Measuring eye size and eye morphology	64
Measurements using ultrasound	68
Measurements using magnetic resonance imaging	72
Estimating maximum retinal image brightness	75
Case study – Was Archaeopteryx diurnal or nocturnal?	80



Refinement of the calculation of retinal image brightness	82
Constituent eye structures: Measuring retinal design	91
Testing the methodology – a case study: Do nocturnal species have higher retinal image brightness estimates than diurnal species and can any inference be made on the activity patterns of <i>Archaeopteryx lithographica</i> ?	93
Introduction	93
Methods	95
Results	96
Discussion	99

Chapter 3 How does a night-migrating bird differ in its visual ability when compared to a diurnally active species?

Abstract	102
Introduction	103
Hypotheses	112
Methods	113
Results	119
Discussion	123

Chapter 4 Visual constraints on the timing of onset of dawn song around the world

Abstract	126
Introduction	127

Methods	137
Results	
A: Testing for Phylogenetic Autocorrelation	149
B: The relationship between visual ability and the onset of dawn song	152
C: Variation with distance from the equator in the slope of the relationship between eye size and the onset of dawn song	167
D: Variation with twilight length in the slope of the relationship between eye size and the onset of dawn song	172
E: Variation in the onset of dawn song start time	176
F: Are estimates of retinal image brightness better than eye size measures in predicting the timing of the onset of dawn song?	180
Discussion	
The relationship between visual ability and the onset of dawn song	191
Variation in the slope of the eye vs. song relationship with distance from the equator and with twilight length	194
Comparing eye size and maximum retinal image brightness as predictors of the timing of the onset of dawn song	197

Chapter 5 Effects of artificial lighting on the behaviour of European robins

Abstract	201
Introduction	202
Methods	
A. Study of free-living robins	206

B: Study of aviary-held birds	210
Results	
A. Study of free-living robins	217
B: Study of aviary-held birds	226
Discussion	235
Chapter 6 Conclusions	242
References	249
Appendices	306

Chapter 1 An introduction to avian vision and sensory ecology

The purpose of my study is to examine variation in eye design among birds, and determine how this variation is related to variation in behaviour and ecology. Birds have remarkably large eyes for animals of their body mass, reflecting the central role of vision in guiding their behaviour (Tansley and Erichsen, 1985). Bennett and They (2007) describe birds as “visually guided creatures with extraordinary eyes; indeed, they have perhaps the most richly endowed visual system of any vertebrate.” Birds have extremely varied eye designs, which have been studied in detail for a considerable time (see for example Ramon y Cajal’s 1889 study on avian retinal morphology). The wealth of available literature addresses many aspects of avian eye design. In this first chapter, I introduce key areas of animal spatial vision in general, and avian vision in particular, that are relevant to understanding the links between visual adaptations and the behaviour and ecology of birds. I discuss the evolution, structure and function of the avian eye, and give examples of visual constraints on bird behaviour in different circumstances. Following on from this first chapter, the thesis progresses with increasing ocular magnitude, beginning at methodologies employed in my studies (Chapter 2), with a case study using extant birds’ eye designs to predict the timing of Archaeopteryx behaviours and food type. I then provide details of a study comparing retinal design in the European storm petrel and the European starling (Chapter 3). I then examine the complex relationships between overall eye size and the timing of onset of dawn song in species from around the world in Chapter 4, and then investigate whole-organism level behaviours (how artificial light affects the singing, foraging and mass regulation behaviours of the

European robin) mediated by visual cues (Chapter 5). The final chapter (Chapter 6) summarises and discusses my findings.

The Evolution of the Eye

Prior to the evolution of optically sophisticated eyes, many organisms could perceive light using non-directional light-sensitive cells to allow simple phototaxis, moving towards or away from ambient light. With the advent of more complex photoreceptor arrays allowing formation of a visual image (spatial vision; Land and Nilsson, 2002), more effective visually-guided behaviour could occur. Visual systems capable of spatial vision first appeared in the fossil record over 500 million years ago during the Cambrian explosion (Lamb, Collin and Pugh, 2007).

It is very likely that the evolution of the eye as an organ began in an aquatic environment, because most (if not all) multicellular organisms lived in water at this time (Land and Nilsson, 2002; Parker, 2003). It is therefore also likely that only a relatively narrow wavelength range was perceived at this time, due to the wavelength-dependent attenuation of light transmitted through water (Fernald, 2004; Warrant and Locket 2004). The acquisition of spatial vision (as distinct from simple light sensitivity) is likely to have provided an important selective advantage: for example, by enabling visual predators to find and catch blind prey easily. As a result, evolutionary “arms races” between predators and prey may have favoured the evolution of more elaborate and sensitive eyes. Indeed, selection pressure from newly evolved visually-guided predators may have driven the rapid diversification of multicellular animal taxa during the Cambrian explosion (Parker, 2003).

Today, approximately one third of extant metazoan phyla have no ocular specialisation, whilst two thirds have a light sensitive organ allowing some degree of

spatial vision, or a specialised image-forming eye. Indeed, those species that have image-forming eyes constitute 96% of the known species alive today (Fernald, 2004), reflecting the importance of vision in guiding behaviour among extant animal taxa.

Hypothetically, natural selection could cause a patch of light sensitive cells to evolve into a complex lens eye in as little as 1,830 sequential 1% incremental changes, in approximately 365000 generations (Nilsson and Pelger, 1994). There has therefore, assuming a generation time of 1 year, been sufficient time in the 500 million years since the Cambrian period for complex eyes to have evolved more than 1500 times. However, a complex eye is not useful without sufficiently evolved processing power in the brain, and the mechanical means by which to act upon visual information (Nilsson and Pelger, 1994). More realistic estimates therefore place the number of times the eye has independently evolved at between one (Gehring, 2005) and 40-65 (Land and Fernald, 1992).

The presence of the gene families *Pax6*, *otx* and *six* (which all are important in development and differentiation of retinal cells and eye structure) in a wide diversity of invertebrates and vertebrates (Bandah *et al.*, 2007) may indicate a monophyletic origin of the eye (i.e. all modern eye types arising from a single common ancestor) (Arendt, 2003). Similarly, all extant visual systems utilise the membrane protein opsin, connected to a light-reactive component retinal, to form the photoreceptive pigment rhodopsin (Land and Nilsson, 2002). While there is some evidence that the organism possessing the ancestral opsin was not photosensitive, there are similarities between regions within this molecule and other chemoreceptive molecules, indicating that chemoreception may have been a precursor to photoreception (Fernald, 2004; Tessmar-Raible *et al.*, 2005).

Furthermore, while opsin is the key light detecting molecule common to all animal taxa, the two major opsin classes differ between vertebrates and invertebrates, perhaps indicating independent evolutionary origins of these opsin classes (Fernald, 2006). Further evidence for multiple evolutionary origins includes the different origins of the eyes in embryological development of different taxa, e.g. cephalopod eyes arise from the epidermis, while vertebrate eyes arise from the neural plate, which in turn induces the epidermis to form the lens (Fernald, 2004).

The Urbilatarian ancestor (the last common ancestor of vertebrates and invertebrates), which had both rhabdomeric and ciliary receptor types (in addition to a third, non-opsin based visual system, cytochrome) gave rise to groups containing all three systems, in varying degrees (Nilsson, 2005). Rhabdomeric receptors have photosensitive pigment located within microvilli. These differ from ciliary receptors which have photosensitive pigment within cilia (Land, 2005), not only by their structure, but by their differing phototransduction cascades (i.e. processes by which light causes a biochemical reaction within the photoreceptor). Whilst both employ G-protein-coupled signalling cascades (i.e. allowing a reaction cascade to occur across a membrane), rhabdomeric receptors depolarize in response to light and ciliary receptors hyperpolarize in response to light (Lamb, Collin and Pugh, 2007). Both types of receptor have been found in the marine ragworm which has ciliary photoreceptors in its brain (active in photoperiodism and maintaining circadian rhythms) and rhabdomeric receptors in its eyes as visual photoreceptors (Arendt *et al.*, 2004). This provides a possible pathway and an explanation for the evolution of the wide range of photoreceptor types in modern eyes. It is hypothesised that vertebrates either lost the rhabdomeric receptor cells or that these cells evolved into the unpigmented retinal ganglion cells (Fernald, 2006).

Both rhabdomeric and ciliary receptors have different opsin (pigment) types. Arendt (2003) suggested that this is because the last common ancestor (Urbilaterian) had the genetic capacity for both receptor types, as it carried two *opsin* genes (*c-opsin* and *r-opsin*) each responsible for ciliary and rhabdomeric receptors, respectively. The rhabdomeric cell type associated with pigment cells to form simple eyes, while the ciliary type formed a photosensitive part of the brain with a role in photoperiodism. In vertebrates both cell types may have been incorporated into the retina.

There are several different eye types present in modern organisms (Land and Nilsson, 2002): pit eyes (e.g. planarians), basic compound eyes (e.g. ark clams), apposition compound eyes e.g. diurnal insects, refracting superposition compound eyes (e.g. moths), single chamber eyes (e.g. the scallop *Pecten*) and reflecting superposition eyes (e.g. lobsters), aquatic lens eyes (e.g. fish), and corneal lens eyes (e.g. humans). The physical properties of light constrain the number of possible eye types available, and help to explain the convergence in eye designs observed among widely divergent taxa, such as the remarkably convergent lens eyes of vertebrates and cephalopod molluscs (Sivak, 2004). Birds, in common with other terrestrial vertebrates, have corneal lens eyes. Within the class aves, there are a wide diversity of variations on the theme of the basic corneal lens eye design, including examples of extreme adaptations for solving particular visual tasks such as high resolution, extreme sensitivity and the ability to resolve images in both air and water. Birds, therefore provide an ideal taxon to examine in detail the adaptive relationships between aspects of eye design and aspects of behaviour and ecology.

Eye size and function

The largest vertebrate eyes belong to birds and primates, with birds having the largest eyes for their body size in the animal kingdom (Brooke, Hanley and Laughlin, 1999; Kiltie, 2000): they are up to 36% larger than other vertebrate eyes (Howland, Merola and Basarab, 2004). In chapter 2, I outline some of the methods utilised to measure eye size in both skeletal and live specimens, and in Chapter 4, I compare the time of onset of dawn song, as a measure of the timing of onset of daily activity, from birds around the world, with reference to eye size. Eye size has important implications for two key aspects of visual capability, namely resolution and sensitivity.

Visual resolution

Resolution (or resolving power) is the “precision with which an eye splits up light according to its direction of origin” (Land and Nilsson, 2002), i.e. eyes with higher levels of resolution are able to see finer details of their environment. Large eyes have large axial lengths i.e. the distance from the front of the eye to the retina, and therefore are more likely to have longer focal lengths enabling projection of a larger image upon the retina than species with smaller eyes. They thus have a higher resolving power because the larger image allows greater spatial discrimination by the photoreceptors of the retina (Walls, 1967).

In addition to the size of the eye, resolution is also affected by the diameter and density of photoreceptors in the retina, photoreceptor “wiring” within and beyond the retina, and pupil aperture. The greater the photoreceptor density, the greater the resolution, as the image formed upon the retina is sampled by a larger number of photoreceptors. The narrower the individual photoreceptors are, the higher the resolution because each photoreceptor is able to provide image information over a

smaller area than would a larger one. Nevertheless, photoreceptors are only efficient at capturing light if their diameter is greater than approximately 1000 nm (near the red end of the visual spectrum, 800 nm), otherwise total internal refraction cannot occur within the cell, and light “leaks” out of the photoreceptor without being captured. The two types of photoreceptor associated with spatial vision (rods and cones) are “wired” differently and therefore are each associated with either high sensitivity or high acuity, respectively. If each photoreceptor is individually “wired” (as in the case of cone photoreceptors), then the resolution will be high due to the lack of spatial summation or pooling (which refers to the process by which the information from several photoreceptors is amalgamated at the level of the retinal ganglion cell).

The blurring effect of diffraction can also be diminished by having wide pupil apertures, also increasing resolution. Diffraction occurs when the central part of the light wavefront passing through the lens slows down more than its edges, curving the wavefront. When it meets the point of focus, it then interacts with itself causing blurring. A large pupil aperture allows the wavefront to curve less, therefore causing less blurring at the focal point. (However a large pupil is associated with other aberrations, see below).

An example of a high acuity eye is that of the wedge-tailed eagle *Aquila audax*, which has a foveal cone cell density that approaches the theoretical limit according to wave theory, allowing the eye (at high light intensities) to resolve at up to 143 cycles per degree (the angular resolution) (Reymond, 1985). While this specialisation allows the eagle to see high levels of detail, for example when it is locating prey at a height, it is not able to resolve as well in dimmer light, for example at dawn or dusk, and this is reflected in the lack behavioural observations of raptors foraging at these times (Martin, 1986b). Another species, the American kestrel *Falco*

sparverius was found to have even higher resolving power at up to 160 cycles per degree (Fox, Lehmkuhle and Westendorf, 1976), however these results were based on behavioural studies and no measurements of the eye itself were undertaken.

Visual sensitivity

Sensitivity is an eye's ability to capture and process light, to obtain visual information. Maximising the light available for capture and processing, maximises sensitivity. This can occur by several methods: having a large eye, spatial or temporal summation, the presence of a tapetum (see below), high rod densities (or a high rod: cone ratio), increasing the angle over which photoreceptors accept light and increasing photoreceptor length (Warrant and Nilsson, 1998; Land and Nilsson, 2002).

A large eye generally has a large pupil aperture which allows more light into the eye than a smaller aperture would, and so large eyes tend to be more sensitive than smaller eyes. Most visually guided nocturnal species have large eyes (Hall and Ross, 2007). This finding forms the basis for my hypotheses (in Chapters 2, 4 and 5) testing the relationship between eye size and the timing of behaviour. Additionally, increasing the angle through which a photoreceptor can accept light i.e. increasing the photoreceptor diameter, allows a large proportion of light to enter a single cell, however, this reduces the resolution of the eye. Therefore it is not a particularly advantageous method of increasing sensitivity in organisms (such as birds) where the ecological light levels are highly variable. Instead, increasing the size of the receptor pool over which summation occurs (i.e. spatial summation) or increasing the duration of retinal sampling (i.e. temporal summation) allows light to be gathered over a

greater amount of space or time (or both). This is similar, but more flexible than would be achieved by increasing photoreceptor width.

A rod-rich retina is characteristic of highly sensitive eyes, due to spatial summation occurring only for this type of photoreceptor. Summation occurs at the expense of resolution due to the reduction in detail that can be sampled from an image at the retina when multiple adjacent rod cells all contribute to a single output. Therefore there is a trade-off between resolution and sensitivity, although a large eye benefits both. In species where vision is important, such as most birds, large eyes are therefore prevalent. Among birds, species requiring higher levels of resolution (e.g. for detecting prey at long distance, fast flight, etc.) or high sensitivity (e.g. for nocturnal activity) have particularly large eyes (Brooke, Hanley and Laughlin, 1999).

Some nocturnal organisms have evolved a mirror-like structure between the retina (behind the photoreceptor layer) and retinal pigment epithelium called the tapetum or *tapetum lucida*, which causes a characteristic eye-shine when viewed under direct artificial light at night (e.g. cats eyes). This structure allows any light that has not been absorbed by the photoreceptors to be reflected back into the eye, for a second opportunity of photoreceptor stimulation (Ollivier *et al.*, 2004). Of all the nocturnal birds so far studied, only the nighthawk *Chordeiles minor*, common poor-will *Phalaenoptilus nuttallii*, common pauraque *Nyctidromus albicollis* and chuck-will's-widow *Caprimulgus carolinensis* (all Caprimulgiformes) have been shown to have a tapetum (Nicol and Arnott, 1974), suggestive of their highly sensitive eyes. The presence of a tapetum reduces the resolution of the eye as the light is likely to be more scattered after reflection. This, in addition with evidence that the retina of such birds is extremely sensitive (due to the densely packed photoreceptors), suggests that Caprimulgiformes use vision to orient generally in dim light, and are able to forage

upon silhouetted prey (e.g. looking up from below at a flying moth, against the night sky), but are not able to resolve small prey items against dark backgrounds (Martin 1990; Martin *et al.*, 2004).

An example of an extremely sensitive eye is that of the oilbird *Steatornis caripensis* which has the highest rod density documented for any vertebrate, with approximately 1,000,000 rods mm⁻². This value exceeds the theoretical limit of photoreceptor packing density; however the rods are arranged in a banked structure, overcoming this limit by allowing more rods per unit area than could be packed into a flat surface (Martin *et al.*, 2004). However, no tapetum was found in this species, highlighting that there are several ways in which a species can maximise sensitivity and highlighting the variation seen within the avian eye.

A further example of a diurnal species with relatively high sensitivity is the European robin *Erithacus rubecula*. This species is one of the first to begin song at dawn and often is heard singing under artificial lighting, however little is known regarding the consequences on energetics or the timing of onset of foraging. The effects of artificial manipulation of light levels on the behaviour of this species is investigated in Chapter 5.

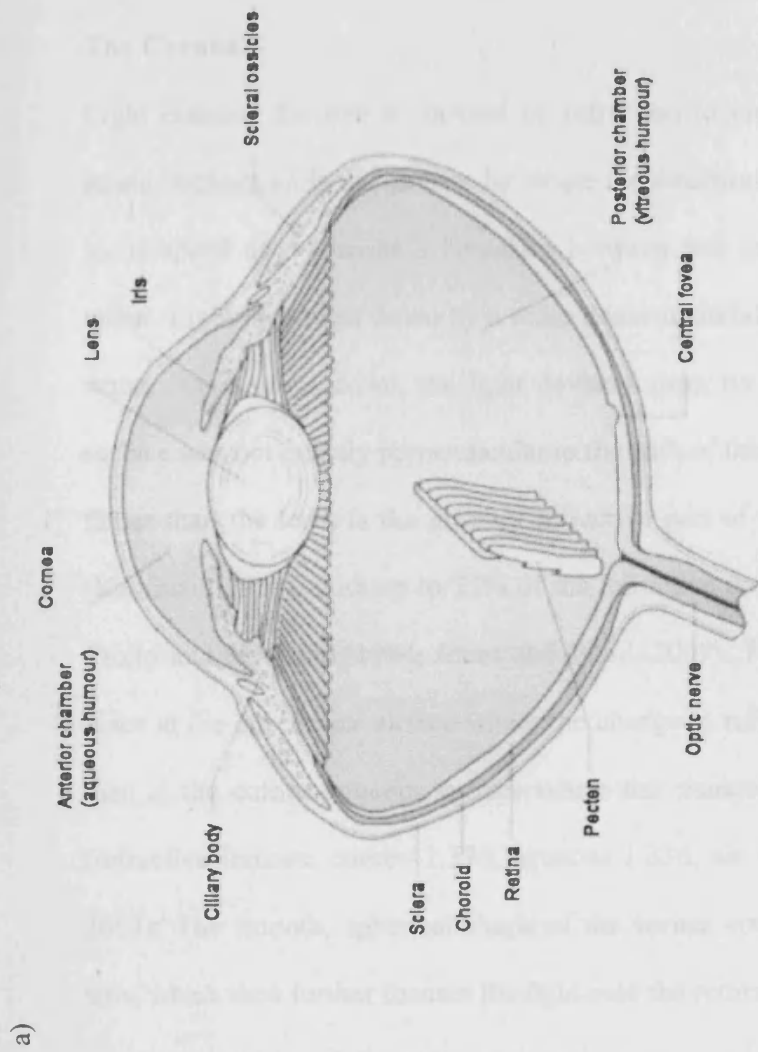


Figure 1.1. The basic structure of the avian eye in horizontal section: a) Schematic representation of the avian eye (from Colville and Bassett, 2002); b) Vertical section of a flattened type eye (barn swallow *Hirundo rustica*), where sco = scleral ossicles, bc = ciliary body, no = optic nerve, p = pecten; c) Horizontal section of a tubular type eye (tawny owl eye *Strix aluco*), where c = cornea, ch = choroid, cr = lens, cs = canal of Schlemm (aqueous-blood transport), lp = pectinate ligament (lenticular support), no = optic nerve, p = pecten, pc = ciliary process, r = retina, sco = scleral ossicles, z = zonule (connects lens and ciliary body). Photographic sections from Rochon-Duvigneaud, 1943.

Structure and function

The avian eye, while conforming to a fairly uniform basic design, is remarkable in the specialised adaptations exhibited by individual taxa. The general anatomy of a typical avian eye structure is shown in Figure 1.1. In the subsequent section, I will outline the constituent parts of the eye, giving examples of variations on the basic design, with reference to visually mediated behaviours.

The Refractive Eye – Cornea, Lens and Accommodation

The Cornea

Light entering the eye is focused by refraction to create an inverted image on the retina. Refraction is the process by which the direction of light is altered by a change in its speed as it crosses a boundary between two materials differing in refractive index. Light is slowed down by a more dense material e.g. when moving from air to water. As it slows down, the light deviates from its original path, if the boundary surface was not exactly perpendicular to the path of the light. The cornea (Figure 1.1), rather than the lens, is the primary refractive part of the terrestrial corneal-lens eye (Kaufman, 1988), with up to 75% of the refractive power of the whole eye (Glasser, Troilo and Howland, 1994; Jones and Ward, 2007). The majority of refraction takes place at the air-cornea surface where the change in refractive index is greatest, rather than at the cornea-aqueous surface where the change in refractive index is smaller (refractive indices: cornea 1.376; aqueous 1.336; air 1.00029, Katzir and Howland, 2003). The smooth, spherical shape of the cornea converges the light rays into the lens, which then further focuses the light onto the retina.

The cornea is also very important in accommodation (i.e. focusing); the process where the eye is able to adjust the degree of refraction of light, in order to maintain sharply focused images on the retina when viewing distant objects at optical infinity, or when viewing objects much closer to the eye (Glasser and Howland, 1996). The more curved the cornea is made, the greater the refraction and therefore the greater the accommodation (see below for the additional accommodation performed by the lens). Accommodation is measured in diopters (D) and is calculated by taking into consideration the corneal radius of curvature and corneal refractive index (Murphy and Howland, 1983). There is a large amount of variation across avian eyes as to the degree of corneal accommodation possible, which influences upon the behaviour and ecology of each species. For example, the eagle owl *Bubo bubo* is a nocturnal predator of large prey items, and which locates prey at a distance of several metres. It has a relatively low accommodative range (0.7 D), and cannot focus on objects less than approximately 1 m from its eyes (Murphy and Howland, 1983). The screech owl *Megascops asio*, has a larger accommodative range (up to 6 D) and is able to focus on objects as close as 0.26 m from its eyes. This owl, whilst also nocturnal, forages on smaller prey, is able to catch prey items whilst in flight and often forages at ground level (Gelbach, 1995). The amount of accommodation possible therefore relates well to the behaviour and ecology of the eagle and screech owls.

The cornea is avascular, refractive and transparent, and, at least in primates, is typically comprised of six layers (Figure 1.2; Thomas, 1955; Donaldson, 1971). These are (1) the corneal epithelium, which is a continually replaced (Woods, 2005) moisture-trapping layer of five or six cells thick; (2) the epithelium basement membrane, which is important in maintaining the order of the stratifications and

injury healing (Nishida, 2005); (3) Bowman's membrane which provides support to the cornea (Margaritis *et al.*, 1976); (4) the stroma (or *substantia propria*) which is the largest part of the cornea (90%) and is made of striated collagen bundles (Linsenmayer *et al.*, 1986); (5) Descemet's membrane which separates the endothelium from the stroma and is impervious to blood vessels and cell invasion; and (6) the endothelium which continually regulates fluid absorption from the aqueous humour by the stroma, preventing the diameter and spacing of the collagen fibrils changing, thus maintaining the cornea's transparency (Verkman, 2003).



Figure 1.2. Histological section through the vertebrate cornea (human). 1 = epithelium, 2 = epithelium basement membrane, 3 = Bowman's layer, 4 = stroma, 5 = Descemet's membrane and 6 = endothelium. From Nishida (2005).

The corneal stroma is formed from stress-bearing collagen fibrils arranged into two distinct regions: a central area of orthogonally arranged fibrils with increased strength, and an outer region of locally reinforced tangentially arranged fibrils (Boote *et al.*, 2008). The perpendicular arrangement of each region of collagen fibrils is extremely important in maintaining transparency (Trelstad and Kang, 1974) as an absence (Clark, 2004) or disorganisation of collagen fibrils results in opacity, (Connon *et al.*, 2004) as does damage or swelling caused by injury (Cox *et al.*, 1970). The lamellae, consisting of collagen fibrils of approximately 25 nm in diameter (Lisenmayer *et al.* 1986), are between 0.25-1.5 μm thick. It has been suggested that the lamellae could function as diffraction elements, producing optical effects that stimulate the photoreceptors (Bruns, Press and Gross, 1987). However, there seems to be more evidence that the arrangement of collagen is structural (Boote *et al.* 2008). The structure of the avian cornea is extremely stable and the collagen arrangement in the stroma continues as a band uninterrupted into scleral collagen, which then inserts into the scleral ossicles.

The avian ciliary body (Figure 1.1) contains musculature responsible for both lenticular (i.e. lens-based) and corneal accommodation, although the action is primarily upon the cornea (Pardue and Sivak, 1997). Unlike mammalian ciliary muscle (see Stafford, 2001), the avian ciliary body is comprised of striated muscles acting directly upon the lens and cornea (Sivak, 2004). The ciliary muscle can be divided into three fibre groups: anterior (Crampton's), internal (Müller's) and posterior (Brücke's) fibres (Pardue and Sivak, 1997). Anterior fibres are responsible for reducing corneal curvature on contraction; posterior fibres are responsible for lenticular accommodation; and internal fibres play a role in both lenticular and

corneal accommodation. Species that have a greater proportion of anterior fibres than internal or posterior, principally use corneal accommodation. Examples of these are American kestrels, domestic chickens *Gallus gallus domesticus* and domestic pigeons *Columba livia* (Pardue and Sivak, 1997). Diving birds, such as hooded mergansers *Lophodytes cucullatus*, however, have more posterior and internal fibres, suggesting that their accommodation is mostly lenticular (Pardue and Sivak, 1997; Sivak 2004), as discussed below.

The Lens

The lens (Figure 1.1 and Figure 1.3) is a crystalline structure derived embryologically from ectodermal epithelial cells. Like the cornea, it is transparent, and its main function is to refract light. The lens fibres are mostly comprised of high levels of crystallin (structural) proteins (Ihanamaki *et al.*, 2004). There are three major classes of crystallin generally found within the vertebrate lens: α -crystallin, β -crystallin and γ -crystallin. Within the avian lens, however, no γ -crystallin is present (Wistow and Piatigorsky, 1988) and the major class is the δ -crystallin (Sampaleanu *et al.*, 1999). The γ -crystallin seems to carry a selective disadvantage in bright light, in that it is susceptible to cataract formation. The absence of γ -crystallin is therefore evidence that the avian common ancestor was diurnal. Other minor classes of crystallins found within the bird lens are τ - and ϵ -crystallins (Wistow and Piatigorsky, 1988). Avian crystallins are often enzyme-derived, unlike mammalian crystallins, and act as molecular chaperones, preventing thermal and UV-induced aggregation. There is little or no cell turnover in the lens and so to maintain transparency, the crystallins display a high degree of structural integrity (Rao *et al.*, 1994).

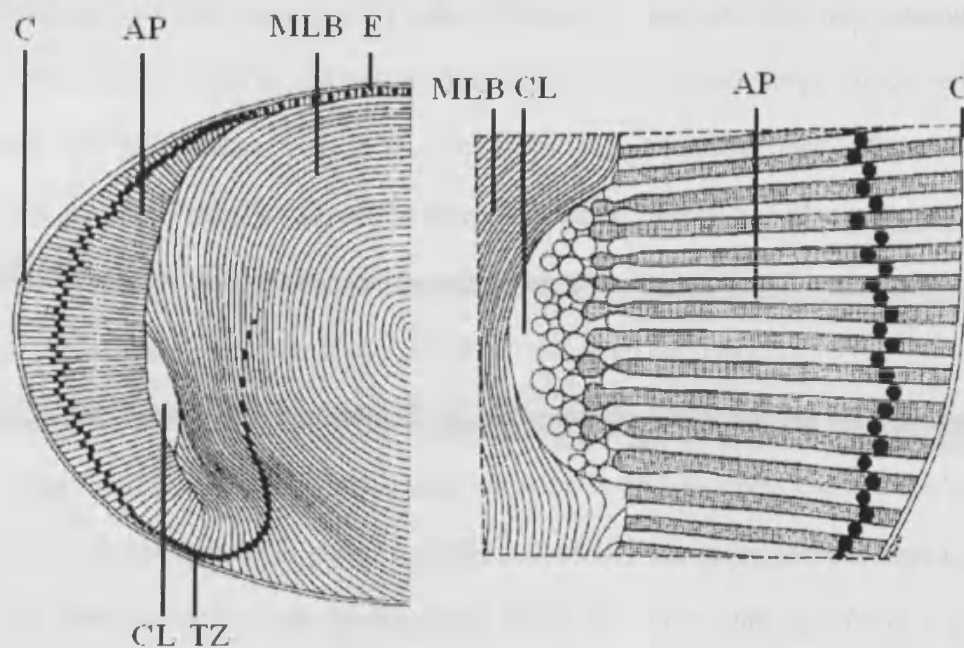


Figure 1.3. Diagram of the anatomy of the avian lens, from Willekens and Vrenson (1985). The left hand illustration shows a half section of the lens and the right hand illustration a magnified view of the junctions within the *cavum lenticuli*. C = capsule, AP = annular pad, MLB = main lens body, E = epithelium, CL = *cavum lenticuli*, TZ = transitional zone. The black dots represent the position of the cell nuclei.

The avian lens comprises two regions, the annular pad and the main lens body, separated by a *cavum lenticuli*. (Figure 1.3) This structure lends itself to the malleability required for the bulging of the lens involved in accommodation (Willekens and Vrenson, 1985). The avian annular pad generally consists of hexagonal smooth fibres. The main lens body also has hexagonal smooth fibres, studded with ball and socket junctions, enabling structural stability during accommodative deformation: as the fibres move they can lock into their new position rather than slipping back to the original position (Lo and Reese, 1993). The study by Willekens and Vrenson (1985) also revealed that while the domestic chicken, kestrel

Falco tinnunculus and song thrush *Turdus philomelos* share a similar lens structure, the canary *Serinus canaria* lens has an annular pad with twisted fibres studded with ball and socket junctions. This is in contrast to the mammalian lens, where such junctions are constrained to the cortex layer. The *cavum lenticuli* is also a feature of the avian eye, as it facilitates accommodation, by allowing gliding movement of the annular pad over the main lens body (Willekens and Vrenson, 1985).

Avian lenses are considered to be optically superior to non-primate mammalian lenses, due to their lack of lens sutures (where lens fibres end at the edges of the lens in lines, instead of points as in the avian lens). However, there is increased structural disorganisation and decreased lens focussing power with age (Banh *et al.*, 2006), therefore, lens degradation may therefore limit visual capability in long-lived individuals.

Optical Aberrations

Aberrations are imperfections in image formation; their presence reduces image quality. Aberrations may be monochromatic (caused by the shape of optical structures) or chromatic (caused by light dispersion properties of the ocular media). The most important aberration to consider in the avian eye is that of chromatic aberration (Lind, Kelber and Kröger, 2008). The refractive state of the ocular media is wavelength dependent, with shorter wavelengths (at the blue end of the visual spectrum) being dispersed further than longer wavelengths (at the red end of the spectrum). This means that when light crosses a refractive surface (e.g. the lens), short wavelengths are strongly refracted, therefore falling short of the retina (myopic), while long wavelengths are weakly refracted, falling behind the retina (hyperopic) (Sivak and Mandelman, 1982). This blurring of colour information is termed

longitudinal chromatic aberration. Transverse chromatic aberrations occur when the incident light is off the optical axis, causing differences in the angular displacement of the retinal image at different wavelengths (Marcos *et al.*, 1999). An animal that uses colour vision is susceptible to such aberrations, especially in bright light. Most birds are diurnal, and many operate under intensely bright light conditions, such as on the open ocean surface under direct sunlight. Chromatic aberration is therefore a potential constraint on visual capability in such circumstances, and birds with larger eyes generally use the violet sensitive visual pigments as opposed to ultraviolet sensitive visual pigments in order to improve image quality as ultraviolet light is scattered by the ocular media due to chromatic aberration, more than violet light. Similarly birds which view objects at a distance (e.g. common buzzard, *Buteo buteo*) employ the same strategy to minimise blurring prospectively caused by the scattering of ultraviolet light by the atmosphere (Hart and Hunt, 2007).

Many vertebrates compensate for longitudinal chromatic aberration and spherical aberrations by having multifocal ocular systems or Matthiessen lenses (Land and Nilsson, 2002; Lind, Kelber and Kröger 2008). These generally involve a concentric zonation of a refractive index gradient within the refractive media e.g. the lens. Most birds have multifocal eye systems (Lind, Kelber and Kröger, 2008), which may be related to the UV sensitivity of many birds. UV light is very strongly refracted and so would fall well in front of the retina if focused by a unifocal lens. Therefore, having a multifocal lens allows UV light to be focused onto the retina (Lind, Kelber and Kröger, 2008). Although these multifocal visual systems do reduce the amount of aberration, there is still some aberration remaining due to some light falling upon non-optimum zones, and there is also some loss of spatial resolution due to the zonation of the lens.

Another important aberration effect to consider is defocus. Eyes with a small f -number (shorter focal length relative to aperture size) have more image blurring caused by defocus aberration, than do eyes with larger f -numbers, due to the circles of blur scaling with size (Land and Nilsson, 2002). Nocturnal, crepuscular and aquatic animals generally have eyes with a small f -number, and so are more likely to have blurred images (Malmström and Kröger, 2006). Owl eyes have a very small f -number, providing a relatively bright retinal image, and so image blurring is a potential constraint on resolution in owls. However, barn owls *Tyto alba* were found to have very low amounts of high order aberrations (including spherical aberration, see below), and while some astigmatism and defocus effects were found, these did not impact upon the retinal image quality, implying that the barn owl eye is adequately able to respond to nocturnal conditions (Harmening *et al.*, 2007).

The following aberrations, termed high order aberrations (HOA), are not well studied in birds, with only sparse references to avian examples (e.g. Harmening *et al.*, 2007). Their definitions are included here for completeness sake. Spherical aberrations occur when more curved edges of ocular media (e.g. the edge of the lens) focus light more strongly than flatter areas (e.g. the centre of the lens), so species with more spherical lenses or corneas are likely to have more aberration if no corrective mechanism is in place (Land and Nilsson, 2002). Astigmatism aberrations occur when two perpendicular planes of light from a single object each have a separate point of focus. Comatic aberrations are those which occur for objects that are located off the optical axis: light rays from these objects do not converge symmetrically and the image produced has a bright centre and a dimmer offset region (similar to a comet and its tail). Tilt aberrations are also from objects located off the optical axis, but are rotated and result in similarly blurred retinal images (Bores, 2001).

The Pupil

The avian pupil is simply a hole surrounded by both striated and smooth muscle to reduce or increase its diameter. The cornea refracts light through the pupil and into the lens, which is located directly behind the pupil. Due to excessive light being damaging to the eye, its entry must be controlled by the constriction of the pupil to minimise scattering, photoreceptor bleaching and free radical damage. On the other hand, in dim conditions the pupil is able to dilate to allow more light to enter the eye, in order to increase visual sensitivity. Pupil aperture may also be influenced by autonomic stimulation. Light-independent pupil response has been explained by emotive display shown via the pupils in response to stimuli such as food, prospective mate presence and aggression in chickens, cephalopods and humans (Douglas *et al.*, 2005; Tombs and Silverman, 2004).

The speed of pupil constriction in bright light also varies across species, with cuttlefish and birds having the quickest responses (Douglas *et al.*, 2005). The great horned owl *Bubo virginianus* has a remarkable speed of constriction (176 ms) which is consistent with the high speed of contraction of striated muscle (found concentrically through the avian iris). The speed of pupil dilation, in contrast, is much slower and is attributed to the slower contraction of smooth muscle fibres (found radially through the iris). The speed of both contraction and dilation does however vary between avian species and may result from species differences in musculature (Oliphant *et al.*, 1983).

Pupil shape

Across all lens-eyed organisms, there is considerable variation in pupil shape. The shape is important in optimising the quality of the image under a range of light conditions. In a multifocal-lens eye, a circular pupil when constricted would prevent some wavelengths from being focused onto the retina (due to the pupil blocking the light path), while a slit pupil allows light to reach each lens zone, and therefore is able to be focused correctly onto the retina. Indeed, most multifocal-lens eyes (except those of birds) have slit pupils (Malmström and Kröger, 2006). Crescent shaped pupils are known to increase the field of view, reduce spherical aberration, enhance contrast at high spatial frequencies, and maintain a small depth of field (Murphy and Howland, 1991). Multiple pupils as seen during occasions of high light intensity in species of geckos which are both diurnally and nocturnally active (e.g. helmet gecko *Tarentola chazaliae*) allow the multifocal lens to be sampled similarly to the slit type pupil, in addition to perhaps being used in daytime distance estimation; the four apertures allow a single focus point on the retina only when properly focussed, otherwise there are four images produced (Roth *et al.*, 2009).

Birds (most of which so far examined have multifocal lenses) generally have circular pupils, with only four species documented to have alternative shaped apertures: The black skimmer *Rhynchops niger* pupil under constriction, forms a slit (Zusi and Bridge, 1981). This species is a tactile forager, with a diet comprising mainly of fish (Mariano-Jelicich, Favaro and Silva, 2003; Martin, McNeil and Rojas, 2007) and is active both at night and during the day. The slit pupil may therefore be of importance when foraging during the day, for reasons similar to the helmet gecko described above.

Other pupils documented to form non-circular shapes when constricted belong to the emperor penguin *Aptenodytes forsteri*, king penguin *A. patagonicus* and some homing pigeons *C. livia*, which form diamond, square and oval shapes, respectively. The emperor penguin does not have a multifocal lens and its pupil shape may be a result of the mechanics involved in having an extremely large range of pupil apertures, required for combining deep-sea foraging with activity in sun-lit snowfields (Lind, Kelber and Kröger, 2008). Similarly, the closely related king penguin may also have a pupil shape dictated by musculature rather than for optical properties. Not all domestic pigeons exhibit oval shaped pupils (pers. obs; Lind, Kelber and Kröger, 2008), but the oval pupils observed in some individuals may be an unintended result of artificial selection (similarly, different pigeon breeds show marked differences in estimates of their retinal image brightness; Pollard AL, unpublished studies).

Lind, Kelber and Kröger (2008) explain the presence of circular pupils in a multifocal lens system by proposing that birds are able to utilise a high gain mechanism i.e. they dilate or constrict only in response to a narrow range of light intensities. For example, many species that they examined maintained a wide pupil aperture even at relatively high light intensities (though this was not apparent in diving species or owls). Maximising pupil aperture allows more of the lens to be available for focusing varying wavelengths of light when a circular pupil is present, over a wide range of light intensities, and minimises aberrations caused by pupil constriction. In particular, ural owls *Strix uralensis* seem to avoid constricting their pupils under bright light conditions. Of course, nocturnal owls are not normally active under bright light conditions, and so the lack of pupillary response may simply be due to adaptation to nocturnality and these birds may lack appropriate musculature for major pupil constriction. In contrast, the snowy owl *Bubo scandiacus* constricts its

pupil further than *S. uralensis*, corresponding to the snowy owl's activity during the day, in bright reflected light conditions in snowy environments (Blix, 2005).

Supporting and Protecting the Eye

The eye needs protection and both mechanical and nutritional support to remain operational on a daily basis. Most of the structures discussed below provide one or both of these roles.

The Sclera

The avian sclera's role is to provide mechanical support and protection. It contains connective tissue and a layer of hyaline cartilage. It also contains the scleral ossicles (or sclerotic rings, Figure 1.1), which are small, overlapping and/or adjacent bones ("plates") surrounding the cornea of the avian eye. These plates form a "truncated cone" structure at the front of the eye. There is considerable variation across species as to the depth of this cone, the overall size of the ring, and the shapes and the number of plates present (Curtis and Miller, 1938). The number of plates (from 11 to 20) does not scale with size of the ring; for example, both the relatively small Aegithalidae and relatively large Corvidae have 14 plates. It is suggested that birds faced with elevated pressure such as that experienced underwater or when flying at high speeds require more anterior eye support, provided by the sclerotic ring. Indeed, diving birds such as *Uria*, Gaviiformes and *Fratercula* have very steep-sided and heavily boned sclerotic rings. Similarly, fast flying taxa such as Apodidae have very steep-sided but light-weight sclerotic rings; here the steep-sidedness may allow the overall weight of the rings to be reduced in order to minimise flight costs (Curtis and Miller, 1938).

The Choroid

The choroid (Figure 1.1) lies between the retinal pigment epithelium (RPE) and the sclera, and is comprised of highly vascularised and innervated cartilaginous tissue (Schroedl *et al.*, 2004). The choroid fulfils many roles in the avian eye: maintaining intraocular pressure; maintaining a constant retinal temperature; meeting the nutritional and oxidative demands of the avascular retina; and altering the axial length of the eye as part of the process of visual accommodation.

The avian choroid differs from the mammalian choroid in that in addition to blood vessels, this tissue also contains a lymphatic system and smooth muscle cells. These components are together involved in the regulation of intraocular pressure (IOP). The muscle cells surrounding the capillaries are able to constrict and dilate, allowing IOP to increase or decrease (DeStefano and Mugnaini, 1997a); while drainage and regulation of ocular fluid by the lymphatic system allows further control of IOP (DeStefano and Mugnaini, 1997b).

Maintaining a constant retinal temperature is important to ensure that it functions properly. As the avian retina is avascular, it cannot reduce its temperature by regulating blood flow centrally. The choroid fulfils this role and allows changes in ambient temperature to have little effect on retinal temperature (Geiser *et al.*, 2003).

The high level of vascularisation of the choroid lends itself to a transport and exchange system, maintaining (with the pecten, see below) the nutritional needs of the avascular retina (Bito, DiBenedetto and Stetz, 1982). Damage to the choroid or interruption of its blood flow causes retinal degradation, and visual impairment (Kimble, Fitzgerald and Reiner, 2006).

The choroid may be responsible for an accommodation mechanism additional to those provided by the cornea and lens. A study by Wallman *et al.*, (1995)

demonstrated that domestic chicks *G. gallus* that were experimentally made either myopic or hyperopic, controlled their choroid thickness to diminish the defocusing effect of the experimental procedure. However, this effect was not seen in dim light. It therefore may be an adaptation to providing additional focusing power in bright light conditions, as light intensity influences choroidal blood flow (Kimble, Fitzgerald and Reiner, 2006). A comparative study (Schroedl *et al.*, 2004) found that varying densities of intrinsic choroidal neurons (i.e. a type of neuron that innervates the choroid) were associated with retinal regions of high visual acuity, and were involved in the adjustment of choroidal thickness to allow these retinal regions to be brought precisely onto the image plane. Longer light wavelengths seem to stimulate more response in choroid thickness, suggesting that the choroid is not only important in reducing the effects of monochromatic aberrations (defocus) but also longitudinal chromatic aberrations (Rucker and Wallman, 2008).

In birds which face extreme variations in external pressure, for example diving birds and raptors, a structure within the choroid complex, the membrane fusca, stops the choroid detaching from the sclera. It provides cushioning support to the choroid by being highly elastic and compact (DeStefano and Mugnaini, 1997a).

The Pecten

A uniquely avian structure, the pecten (or pecten oculi) is extremely vascularised and protrudes from the retina into the vitreous humour, over the optic disc (Figure 1.1). Adjacent to the numerous capillaries running throughout this structure are pigmented cells (melanocytes) which may provide a supportive role in maintaining the erectile quality of the pecten, or to protect the blood vessels from UV light (Kiama *et al.*, 1994). Many suggestions have been given as to the pecten's function, including as a

pressure moderator, a temperature sensor, a heating filament, a cooling device at high altitude, providing shading of the retina from strong light, an absorber of scattered light, an image clarifier, a contrast softener when bright images are viewed against the sky, an aid to navigation and an aid to viewing moving or flickering objects (Brach, 1977; Kiama *et al.*, 2001; Pettigrew, Wallman and Wildsoet, 1990). However, the most widely accepted theory on the function of the pecten is that it is a transport organ, in association with the choroid (Schroedl *et al.*, 2004; Bito, DiBenedetto and Stetz, 1982). It distributes nutrients to the vitreous humour, oxygen to the retina, and may be especially active during saccadic eye movements (Gunturkun, 2000; Smith *et al.*, 1996). It allows nutrient and oxygen flow to and from the avascular regions of the eye, especially the retina, removing products of photooxidative stress, maintaining interocular stability and preventing light scattering which would otherwise be detrimental to visual ability.

The size and structure of the pecten varies from species to species and this variation can be associated with differences in behaviour and ecology. There are three morphological variants of pecten: conical (e.g. in the brown kiwi, *Apteryx australis*), vaned (e.g. in the ostrich *Struthio camelus*) and pleated (e.g. in the great horned owl), of which the pleated is the most studied (Kiama *et al.*, 2006). The number of folds in the pleated pecten depends upon the species, for example the emu *Dromaius novaehollandiae* has three or four thick folds (100-120 μm) (Braekevelt, 1998), the galah *Eolophus roseicapilla* has 20-25 folds (Braekevelt and Richardson, 1996) and the American crow *Corvus brachyrhynchos*, has 22-25 folds (Braekevelt, 1994). Smith *et al.*, (1996) state that the more visually oriented a species is, the larger its pecten will be and the more folded, to provide their more metabolically active retinas with a nutritive transport route. For example kiwis (Apterygidae family) have very

small pecten which may be a reflection on these species being reliant on smell and tactile cues, and not vision for their survival (Yu, Schwab and Dubielzig, 2009). Other nocturnal species such as the great horned owl, the barred owl *Strix avaria* and the spotted eagle owl *Bubo bubo africanus* have reduced microfolds within the pecten structure (Kiama *et al.*, 2006) suggesting that these species rely on hearing, or that higher demands are placed upon the pecten during diurnal vision, for example, in removal of photooxidative products. The red-tailed hawk *Buteo jamaicensis* conversely has a large pecten consisting of 17–18 folds which is typical of a highly visually active diurnal raptor (Braekevelt, 1993).

Not only does the size of the pecten differ in different species, but also the degree of vascularisation. The pecten of the diurnally active black kite *Milvus migrans* has a larger number of pleats, a larger pecten surface area, higher capillary luminal surface area and higher pecten blood volume than the nocturnally active spotted eagle owl and the diurnally active domestic chicken, even though the owl eye volume was highest (Kiama *et al.*, 2001). In addition, Kiama *et al.*, (2006) reported that endothelial specialisations within the pecten for increasing the surface area for nutrient flow, are diminished or absent in some species, and this could be explained by a reduction in reliance on vision. However, several owl species (great horned, spotted eagle and barred owls) are noted to have reduced endothelial specialisations, and are otherwise renowned for their high visual acuity (Martin and Gordon, 1974). Overall then, the current evidence suggests that the species that require high oxygen and nutrient delivery from a large and specialised pecten seem to be those reliant on good visual acuity alone for survival.

The Vitreous and Aqueous Humours

The aqueous and vitreous humours (see Figure 1.1) fill the anterior and posterior internal cavities of the eye respectively, providing physical and metabolic support to the eye's avascular structures. The humors are permeable to oxygen and nutrients, and transparent to reduce visual aberrations and light scattering (Balazs *et al.*, 1965).

The aqueous humour (henceforth "aqueous") is a liquid (as its name suggests) filling the anterior chamber of the eye. It has a high rate of turnover, being constantly produced by the ciliary body in response to variation in intra-ocular pressure, while being simultaneously drained by the aqueous sinus (Nakabayashi, 1999). The aqueous is a biochemically complex solution, providing the lens and cornea with nutrients and removing waste products.

For birds whose visual sensitivity extends into the ultraviolet, some ultraviolet radiation must obviously be allowed to reach the retina. However, protection of the eye from oxidative stress that would be caused by too much UV radiation entering the eye is important in species exposed to high intensity light. For example, in some water birds (e.g. mallard *Anas platyrhynchos*) and savannah species (e.g. ostrich), a currently unknown compound causes a red-shifted UV absorbance spectrum which could result in protecting the eye from UV damage (Ringvold *et al.*, 2003). The aqueous provides an alternative UV oxidation protective mechanism via the presence of the free radical scavengers urate (a primary UV screen) and ascorbate (Ringvold, Anderssen and Kjønnsen, 2000).

Unlike the relatively homogenous liquid aqueous, the vitreous humour (henceforth "vitreous") has both gel-like and liquid constituents, and fills the posterior chamber of the eye. It is principally made from hyaluronic acid and hydroxyproline (collagen) and where the two are combined, the gel forms (Kinnear and Lauber,

1978). In the chicken, the vitreous composition changes as the bird matures following hatching; after the first two weeks during which the vitreous is predominantly gel, the liquid component increases. This composition then remains the same throughout the bird's life. A difference between mammalian and avian vitreous composition is that the adult avian vitreous is comprised primarily of liquid vitreous, while mammalian vitreous is mainly gel (Balazs *et al.*, 1965). The gel vitreous is associated with the lens, with the liquid vitreous filling the remaining space in the posterior chamber. From personal observation, the gel vitreous is also associated with the pecten in domestic pigeons and common pheasants *Phasianus colchicus*. Vitreous is produced mainly by the retina during eye development and also by hyalocytes (vitreous-producing cells) within the vitreous body itself (Newsome, Lisenmayer and Trelstad, 1976). Over-production of the liquid vitreous results in glaucoma in birds reared in constant light, characterised by increased intraocular pressure, decreased corneal curvature and impaired drainage of vitreous or aqueous out of the eye (Kinnear and Lauber, 1978). This may be caused by light damaging the hyalocytes which are embedded in the cortical layers of vitreous gel (Seaman and Storm, 1965). The vitreous provides a means of metabolite transport from the pecten to the retina, which is highlighted by the production of vitreous at the vitreoretinal and vitreopectinal junction areas (Balazs *et al.*, 1965).

Sunshades, Nictating Membranes and Eyelids

Some species, for example, southern ground hornbills *Bucorvus leadbeateri* and southern yellow-billed hornbills *Tockus leucomelas*, have widely spaced eyelash-like feathers which operate as sunshades, casting shadows upon the cornea in bright light (Martin and Katzir, 2000). The positioning of these shadows can be manipulated by

postural changes in the angle of the head relative to the sun (Martin and Coetzee, 2004).

The nictitating membrane and its musculature (the quadratus and pyramidalis muscles) enable the cornea to be kept moist by wiping a screen of moisture across the surface, replenishing the tear film (Curio, 2001). Many species make use of a UV-filtering but otherwise transparent nictitating membrane to protect the eye from UV damage, especially during flight (Ringvold *et al.*, 2003). In addition, the nictitating membrane and eyelids protect the eye from mechanical damage, and also act as “wipers” removing debris and exogenous material, as seen in the American dipper *Cinclus mexicanus*, which removes mist and water splashes from the eye surface in this way (Cordier, 1927). Curio (2001) found that birds use their eyelids in taxon specific ways, mainly to protect the eye from mechanical impacts: Negros bleeding heart pigeon *Gallicolumba keayi* close their upper lid when feeding on dragonflies but keep the lids open when feeding on non-mobile items such as berries; and scops owl *Otus scops* close both lids unilaterally (i.e. the nearest eye to the direction of prospective damage) when grooming a mate or feeding on potentially damaging prey.

Processing light information – the retina and neural centres

The avian retina (Figure 1.1) is avascular and is stratified with nine layers (from back of the retina to the front): retinal pigment epithelium, photoreceptor inner and outer segments, outer nuclear, outer plexiform, inner nuclear, inner plexiform, retinal ganglion cell, nerve fibre layers and an inner limiting membrane (see Figure 3.1, Chapter 3). There are three types of pigmented photoreceptor cells (Figure 1.4) found within the outer nuclear layer: rods associated with scotopic (monochromatic) vision, single cones associated with photopic (chromatic) vision and double cones

associated with movement detection, texture discrimination and photopic vision (Jones and Osorio, 2004; Hart, 2001).

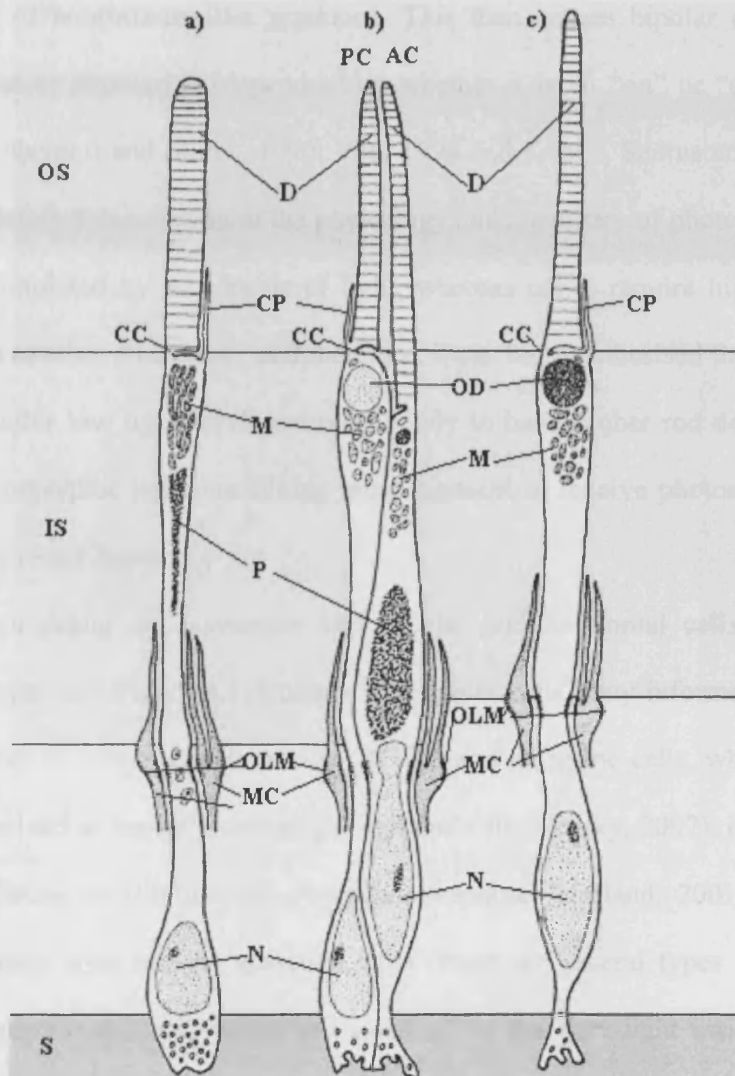


Figure 1.4. Avian photoreceptors. a) Rod; b) double cone; c) single cone. OS = outer segment region, IS = inner segment region, D = discs, S = synaptic region, CC = ciliary connection, CP = calycal process, M = mitochondria, P = paraboloid, OLM = outer limiting membrane, MC = Müller cell, N = nucleus, OD = oil droplet, PC = principle cone, AC = accessory cone. Adapted from Morris and Shorey (1967).

These photoreceptor cells are stimulated when light photons fall upon the rhodopsin molecules, located within the discs contained within the cells (see Figure 1.4). This triggers an internal cascade reaction resulting in hyperpolarisation and a reduction in the amount of neurotransmitter produced. This then causes bipolar cells to either hyperpolarize or depolarize (dependent on whether it is an “on” or “off” type cell) (see Rayer, Naynert and Stieve, 1990; Yau, 1994 and Kohen, Santus and Hirschberg, 1995 for a detailed description of the physiology and chemistry of phototransduction). Rods are stimulated by low levels of light, whereas cones require higher levels of illumination to elicit a response, and therefore, it can be hypothesised that species that are active under low light levels are more likely to have higher rod densities, and a thicker photoreceptor layer containing more pigment to receive photons, for a more sensitive eye (see Chapter 3).

Photoreceptor cells synapse with bipolar and horizontal cells at the outer plexiform layer (see Figure 3.1, Chapter 3). Bipolar cells relay information from the photoreceptors to retinal ganglion cells (RGCs) and amacrine cells, while horizontal cells are involved in lateral processing (Field and Chichilnisky, 2007), image contrast and in mediating an illumination dependent response (Hasland, 2001). Within the inner plexiform layer are the amacrine cells (there are several types dependent on different neurotransmitters) which are involved in the dark-light switch, which is important in signalling day-night transitions (Morgan and Boelen, 1996) and may have an output role in the avian centrifugal visual system (see below for further description) (Uchiyama and Stell, 2005) i.e. in focal attention (Ohno *et al.*, 2004). RGCs gather information from the photoreceptors indirectly, and their efferents form the optic nerve (see Figure 3.1, Chapter 3), taking information towards the optic tectum of the brain for further processing (Figure 1.5).

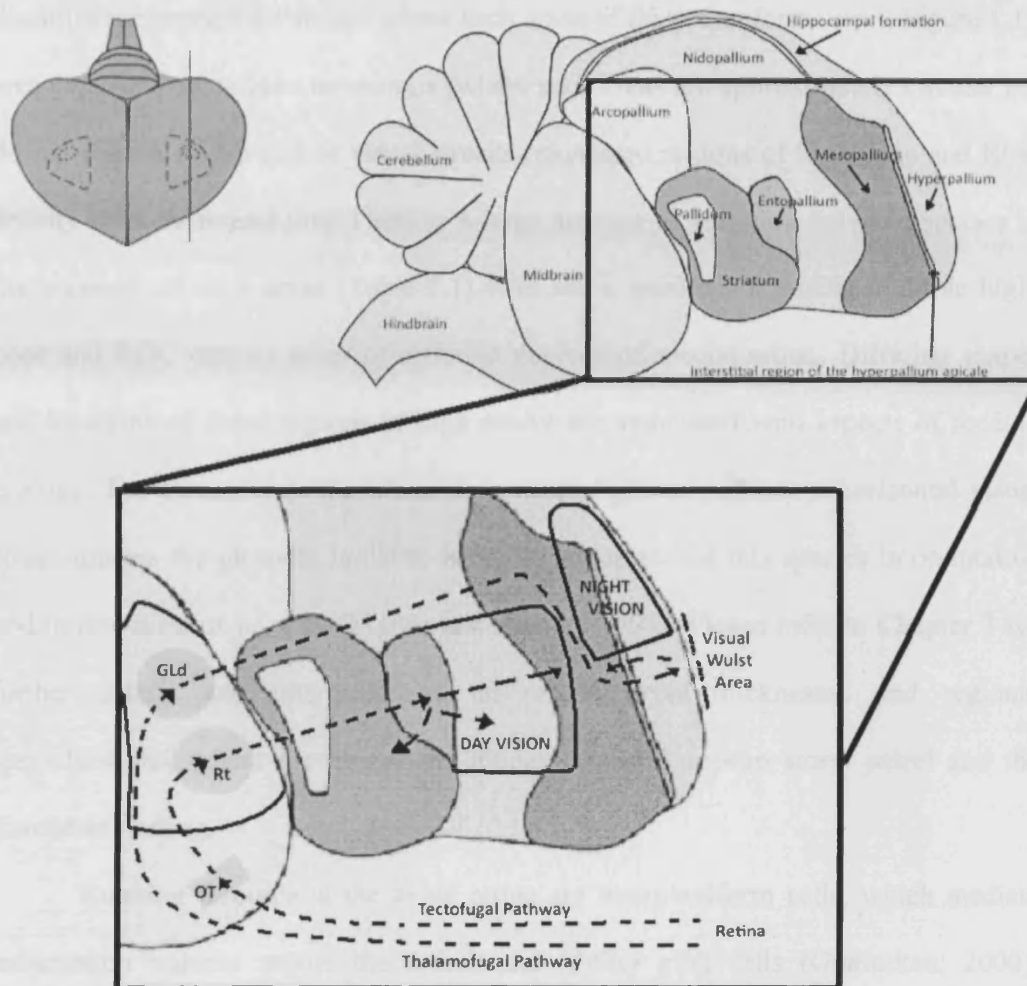


Figure 1.5. (a) Dorsal view of avian brain in top left shows the orientation of the night vision area, and the location of the section drawn. (b) Schematic illustration of the avian brain. (c) Enlargement of schematic drawing of (b) showing the relative locations of the day- and night-vision (otherwise known as Cluster N) activated brain regions in a night-migrant songbird, along with the thalamofugal and tectofugal visual pathways, in coronal section. GLd, lateral geniculate nucleus, dorsal part; Rt, nucleus rotundus; OT, optic tectum; From Mouritsen *et al.*, (2005).

Areas within the retina containing high cone cell and retinal ganglion cell densities are termed the fovea (where such areas of the retina forms a pit, Figure 1.1), area centralis, dorsalis or temporalis (where such areas are approximately circular but do not form a foveal pit) or visual streaks (elongated regions of high cone and RGC density with no retinal pit). There is a large amount of variation between species in the presence of such areas (Table 1.1) with some species possessing multiple high-cone and RGC density areas of different degrees of specialisation. Differing shapes and locations of these regions of high acuity are associated with aspects of feeding ecology. For example, in the Manx shearwater *Puffinus puffinus* a horizontal visual streak images the physical horizon, which is important for this species in orientation and in detection of its prey (Martin and Brooke, 1991). Please refer to Chapter 3 for further details and interpretations on retinal layer thicknesses and regional specialisations, where I compare the retinas of the European storm petrel and the European starling.

Running throughout the avian retina are interplexiform cells, which mediate information transfer across the retina, and Müller glial cells (Gunturken, 2000). Müller glial cells are very important in that they are able to differentiate into other retinal cell types after significant damage to the retina, i.e. acting as retinal stem cells. This cell behaviour has not been shown in mammalian retina, and while cells are present in avian eyes that are potentially capable of neurogenesis, any regeneration is not as complete as that seen in cold-blooded vertebrates (Fischer, 2005).

The outer segments of the photoreceptors are embedded in the retinal pigment epithelium (RPE). The RPE is characterised by the presence of melanin and its various functions include helping to maintain the blood-retinal barrier, maintaining retinal adhesion and thus shape, aiding water and ion flow between the retina and the

choroid, absorbing scattered light which would otherwise degrade the visual image, protecting against free radicals, controlling retinoid metabolism and carrying out

Table 1.1. Different avian species with different areas retinal specialisation. These retinal specialisations confer high acuity and comprise of high densities of retinal ganglion and cone cells. Please see the text for the definitions of the specialisations.

Continued overleaf.

Common Name	Species	Retinal Specialisation	Reference
Barn owl	<i>Tyto alba</i>	Area Centralis and Horizontal Streak	Bravo and Pettigrew, 1981
Black vulture	<i>Coragyps atratus</i>	Fovea and Area Centralis	Inzunza <i>et al.</i> , 1991
Burrowing owl	<i>Speotyto cunicularia</i>	Area Centralis	Bravo and Pettigrew, 1981
Chilean blue eagle	<i>Buteo fuscens</i> <i>australis</i>	Fovea x2	Inzunza <i>et al.</i> , 1991
Chimango caracara	<i>Milvago chimango</i>	Fovea and Area Centralis	Inzunza <i>et al.</i> , 1991
Condor	<i>Vultur gryphus</i>	Fovea and Area Centralis	Inzunza <i>et al.</i> , 1991
Domestic chicken	<i>Gallus domesticus</i>	Area Centralis	Straznicky and Chehade, 1987
Great kiskadee	<i>Pitangus sulphuratus</i>	Fovea and Horizontal Streak	Coimbra <i>et al.</i> , 2006
Indian blue-shouldered peafowl	<i>Pavo cristatus</i>	Area Centralis	Hart, 2002

Common Name	Species	Retinal Specialisation	Reference
Japanese quail	<i>Coturnix coturnix japonica</i>	Fovea and Area Centralis	Budnik <i>et al.</i> , 1984
Jungle crow	<i>Corvus macrorhynchos</i>	Area Centralis	Rahman <i>et al.</i> , 2007
Laughing kookaburra	<i>Dacelo gigas</i>	Fovea x2	Moroney and Pettigrew, 1987
Magellanic penguin	<i>Spheniscus magellanicus</i>	Area Centralis	Suburo, Herrero And Scolaro, 1991
Mallard	<i>Anas platyrhynchos</i>	Area centralis	Rahman, Aoyama and Sugita, 2007
Manx shearwater	<i>Puffinus puffinus</i>	Horizontal Streak	Hayes, Martin and Brooke, 1991
Ostrich	<i>Struthio camelus</i>	Horizontal Streak	Boire <i>et al.</i> , 2001
Rock pigeon	<i>Columba livia</i>	Area Centralis	Binggeli and Pauli, 1969
Rusty marginated flycatcher	<i>Myiozetetes cayanensis</i>	Fovea and Horizontal Streak	Coimbra <i>et al.</i> , 2006
Sacred kingfisher	<i>Halcyon sancta</i>	Fovea x2	Moroney and Pettigrew, 1987
Sparrow hawk	<i>Falco sparverius</i>	Fovea x2	Inzunza <i>et al.</i> , 1991
Mouse-colored tyrannulet	<i>Phaeomyias murina</i>	Fovea, area temporalis and weak horizontal streak	Coimbra <i>et al.</i> , 2009
Yellow-bellied elaenia	<i>Elaenia flavogaster</i>	Fovea, area temporalis and weak horizontal streak	Coimbra <i>et al.</i> , 2009

phagocytosis of the outer segment of the photoreceptors, ensuring their renewal (Schraermeyer and Heimann, 1999).

Not only is the retina important in the perception of static images, but also in motion perception. All birds require a level of motion perception for survival. Detection of motion occurs only if an object moves across the visual field within a defined speed range. If an object is moving too fast, it will not register a response, and if it is too slow, it will not be perceived as moving (Ali and Klyne, 1985). Lettvin *et al.*, (1968) suggested that the mechanism for motion perception at the retina involved the detection of temporal and spatial variation of local light intensity. More specifically, Luksch, Khanababaie and Wessel, (2004) found that avian wide-field tectal neurons (situated in the optic tectum) that are sensitive to moving stimuli alone, form direct synaptic contact with retinal ganglion cell axons, inferring a direct relationship between the retina and motion detection.

Whilst the avian retina is considered a relatively good processor of information (compared to the mammalian retina) due to the complexity of its interconnecting neurons, further higher level processing is required to combine all the ocular information. Neural pathways project from the retina to the brain via the optic nerves (Figure 1.1), which cross at the optic chiasma, so that the left hemisphere processes retinal information from the right eye, and vice-versa. However, some ipsilateral projections have been demonstrated in the chick and quail (Weidner *et al.*, 1985; Jeffery, 2001).

The two major visual pathways elucidated for birds are the tectofugal and thalamofugal pathways (Figure 1.5). The tectofugal pathway projects retinal information to the optic tectum, then to the nucleus rotundus and then to the visual Wulst (a brain area where the visual pathways reach the telencephalon). This pathway is associated with diurnal vision, binocular vision, colour vision, motion detection and pattern discrimination (Rogers, 1996; Mouritsen *et al.*, 2005). The thalamofugal

pathway projects from the retina to the dorsal lateral geniculate nucleus then to the visual Wulst, and is associated with both diurnal and nocturnal vision, lateral stimulus detection and spatial discrimination (Rogers, 1996; Mouritsen *et al.*, 2005; Heyers *et al.*, 2007). Also present is a retinal-brain feedback system termed the centrifugal visual pathway, which may have various roles including gaze stabilisation, selective visual attention and coordination of pecking behaviour, though these functions are still to be clarified (Repérant *et al.*, 2007). There are species differences in this centrifugal visual pathway, with Columbiformes, Galliformes and Passeriformes having a higher level of complexity than Anseriformes, raptors and insectivorous birds that feed on the wing (Repérant *et al.*, 2006). These taxonomic differences show that there is some evolutionary plasticity in the avian brain, accommodating adaptations to differing environmental circumstances and behaviours.

Eye size and neural processing

Larger eyes have space for greater numbers of photoreceptor cells, and may therefore be expected to require a greater neural processing capacity in the brain. The relationship between body mass and eye size has been described by several studies, with eye size scaling allometrically with body mass (Chapter 4; Howland *et al.*, 2004; Brooke, Hanley and Laughlin, 1999): axial length (mm) = 14.91 * mass (kg)^{0.19}. Garamszegi *et al.* (2002) found that even after taking into account the scaling of eye size with body mass, and phylogeny, eye mass and brain mass are also positively correlated, supporting the hypothesis that larger eyed species require larger brain areas to process the visual information than do smaller eyed species. Garamszegi *et al.* (2002) also suggest that eye size and brain size coevolved in response to nocturnality and perhaps capture of mobile prey items. There do, however, seem to be

some differences in the scaling of brain size and eye size between passerines and non-passerines. Generally passerines range from 4.6 g (short-tailed pygmy-tyrant *Myiornis ecaudatus*) to 1 kg (raven *Corvus corone*), while non-passerines range from 2.2 g (bee hummingbird *Mellisaga helenae*) to 110 kg (ostrich *Struthio camelus*), which is a size range over 100 times larger (Schmidt-Nielsen, 1984; Dunning, 2008). Burton (2008) found that non-passerine eye size correlates more strongly with brain size than body size whereas among passerines, eye size correlates more strongly with body size. This difference in relationship is attributed to the higher amounts of variation in body morphology among the non-passerines, with larger members of this group having larger bodies in proportion to their heads. For hypotheses concerning the timing of onset of behaviours (as in Chapters 4 and 5), it is imperative that body mass effects are considered, not only due to the mass of the eyes being comprised within overall body mass, but also due to the energetic constraints imposed with having smaller or larger body masses. For example, Thomas et al., (2002) found that small birds began to sing earlier than larger birds, with the explanation being attributed to the need for smaller birds to begin their day earlier to recoup their overnight energetic losses. In Chapter 4, the effect of body mass on the onset of dawn song is considered in addition to eye size (as a measure of visual sensitivity).

In addition to overall eye size scaling with brain size, Iwaniuk *et al.* (2008) presented evidence that birds with more frontally placed eyes and broader binocular fields have larger Wulst volumes. The Wulst (dorsal hyperstriatum) is part of the telencephalon or forebrain which is the recipient area of the thalamofugal pathway (Figure 1.3), and is particularly well developed in owls, which have highly converged visual fields (Iwaniuk and Wylie, 2006). *In vivo* neuronal studies (Baron *et al.*, 2007) and behavioural studies (McFadden and Wild, 1986) show that binocular integration

and disparity detection, and selection of orientation and motion detection occurs to a high degree within this specialised brain region. However this study did not find any correlation between eye size and either Wulst volume or optic tectum volume, suggesting that the evidence of eye size scaling with overall brain size described by Garamszegi *et al.* (2002) is due to space limitations constrained by head size rather than processing power (Burton, 2008). Furthermore, as overall eye size is not the only measure of visual ability; neural processing areas may be more inclined to scale with photoreceptor or RGC densities (Iwaniuk *et al.*, 2008).

Colour Vision

The avian eye is in general capable of perceiving a wide range of colour information. It is well established that most birds have tetrachromatic vision, with at least four cone types present in the retina (Herrera *et al.* 2008), and are able to see into the UV range (Wilkie *et al.*, 1998). Birds have one class of rod photoreceptor, four classes of single cones, and one class of double cone. Cone cells may also contain coloured oil droplets, which primarily modify the cone cell's absorbance spectrum by acting as wavelength-dependent filters.

Cone photoreceptors are often described according to their wavelength sensitivity: ultra-violet (UVS), short-wavelength (SWS), medium-wavelength (MWS) and long-wavelength (LWS) sensitive, in addition to the double cone (DC). The DC can be subdivided into its principal and accessory members, each of which may contain pigments sensitive to different wavelengths. The accessory member of a double cone does not usually contain an oil droplet, but instead contains a carotenoid (A-type) within the distal region of the inner segment, and which displays a characteristic triple peaked absorbance spectrum (Bowmaker *et al.* 1997).

The oil droplets are named according to their colour (i.e. their colour as perceived by human observers using histological techniques), with transparent (T), colourless/pale green (C), golden yellow (Y), red (R) and pale (P). These oil droplet colours are almost always associated with particular cone types as follows: UVS+T, SWS+C, MWS+Y, LWS+R, DC+P (Hart *et al.*, 2000c). The oil droplets are functionally diverse in that they may act as long-pass cut-off filters by narrowing the wavelengths to which the cone is sensitive, protecting the cone outer segments from short wavelength oxidative damage, providing relief from chromatic aberration and concentrating light upon the outer segment of the cone (Varela *et al.*, 1993; Martin and Muntz, 1978). Some species of bird have particular types of oil droplet concentrated in particular regions of the retina. For example, the pigeon ventral retina has Y- type oil droplets with a mean $\lambda_{\text{cut-off}}$ at 513nm, whereas the dorsal retina has Y-type oil droplets with a mean $\lambda_{\text{cut-off}}$ at 539 nm (Bowmaker *et al.*, 1997).

Due to the variation in the wavelength sensitivity of the UVS cone type, some birds have a relatively low λ -max sensitivity at, e.g. 355 nm (Peking robin *Leiothrix lutea*), whereas others have a relatively high λ -max sensitivity e.g. 424 nm (common peafowl *Pavo cristatus*) (Maier and Bowmaker, 1993; Hart, 2002). This implies that while some similarities exist, there is considerable variation in different species' UV sensitivities, with some only sensitive to near-UV wavelengths and others not sensitive to wavelengths beyond the human visual spectrum. This species variation in the λ -max sensitivity peak of the chromatic ocular disposition (i.e. the total ability of the species to perceive colour through cone frequency, oil droplet and ocular filters such as cornea and lens) has proved to be important in reconstructing the evolutionary history of colour vision in birds. It seems that the ancestral state of short wavelength

sensitivity is towards the violet part of the spectrum, with UV sensitivity evolving independently within some taxonomic groups later on (Ödeen and Håstad, 2003).

Table 1.2 illustrates some of the variation found in avian λ -max sensitivities, from published data. Note that the overlap seen with the P type oil droplet and C and Y oil droplets can be explained by some of the values for the P oil droplet being a mean of two wavelengths i.e. the oil droplets from the principle member and the accessory member of the double cone, and therefore can cover a wide range of wavelengths. Indeed, it has been proposed that the double cone is primarily utilised in movement sensitivity rather than colour vision, and that the oil droplet is does not act as a cut-off filter as it does not cause a shift in the peak sensitivity of either the principle or accessory member of the cone (Hart, 2001). Not all studies included in Table 1.2 include data for all types of cone or oil droplet, as some were carried out before modern techniques had been devised to elucidate accurate measurements of wavelength sensitivity. It is also important to note that the T type oil droplet $\lambda_{\text{cut-off}}$ of mean absorbance spectrum value is a maximum figure, in that many studies do not find a peak absorbance at the given value, and presume that the maximum is below the currently available threshold for obtaining data (i.e. the equipment is not able to read values lower than this figure). Therefore the mean $\lambda_{\text{cut-off}}$ for T type oil droplets is likely to be far lower than represented in Table 1.2.

It is essential to note that birds' combined ocular media (i.e. the cornea, aqueous humour, lens and vitreous humour) also act as a light filters for very short wavelengths of light. No light is transmitted to the retina below 300 nm in plum-headed finches *Neochmia modesta*, white-headed munia *Lonchura maja* or gouldian finches *Erythrura gouldiae*, with 50% transmittance occurring at 316 nm, 318 nm and 317 nm, respectively (Hart *et al.*, 2000b). Similarly, the wavelength of half

transmission is 317 nm in the blue tit *Cyanistes caeruleus* and 343 nm in the blackbird *Turdus merula* (Hart *et al.*, 2000a), and no transmittance occurs at 300 nm and 312 nm respectively. Das *et al.*, (1999) found that canary *Serinus canaria* lens absorbs an increasing proportion of incident light, the lower the wavelength becomes (for wavelengths below 380 nm). The observed species differences in absorbance of short wavelengths may indicate that birds which live in habitats where there are increased possibilities of UV damage occurring to the eye minimise the risk by having more absorbent ocular media at low wavelengths (Das *et al.*, 1999).

Many birds have differing proportions of the different types of cones, in different sections of the retina, and in each eye. Hart (2001) found that the pied cormorant *Phalacrocorax varius* has a larger proportion of double cones (associated with movement, as described above) within the ventral retina. This reflects the pied cormorant's predatory behaviour, in that it is able to swim below prey items, remain countershaded and therefore camouflaged, and see the prey item silhouetted against the surface of the water. Some birds have differing proportions of photoreceptor type in each eye. For example, the European starling *Sturnus vulgaris* has more single cones in the left retina, and more double cones in the right retina (Hart *et al.*, 2000a). This infers that birds utilise their eyes for different roles – for instance one eye for primarily colour vision and one eye primarily for movement detection.

Table 1.2. Cone pigment and oil droplet maximum sensitivity wavelengths (nm). Where Sens. λ -max = Maximum wavelength sensitivity, UVS = ultra-violet wavelength sensitive cone pigment, SWS = short wavelength sensitive cone pigment, MWS = medium wavelength sensitive cone pigment, LWS = long wavelength sensitive cone pigment, T = transparent oil droplet, C = colourless/pale green oil droplet, Y = golden yellow oil droplet, R = red oil droplet and P = pale oil droplet. All values are in nm. Filled cells indicate no data available, while an asterisk indicates that a cone type is present but no sensitivity data could be obtained.

Common Name	Latin Name	VS/UVS		SWS		MWS		LWS		Double Cone		Reference
		Sens. λ -max	T	Sens. λ -max	C	Sens. λ -max	Y	Sens. λ -max	R	Sens. λ -max	P	
Blackbird	<i>Turdus merula</i>	373	<330	454	414	504	514	557	570	557-556	415-472	Hart <i>et al.</i> , 2000b
Blue tit	<i>Cyanistes caeruleus</i>	371	<330	448	414	503	508	563	573	565-563	417	Hart <i>et al.</i> , 2000b
Bobolink	<i>Dolichonyx oryzivorus</i>	373	<350			505	412	56	503	566/403	535/561	Beason and Loew, 2008
Bobwhite quail	<i>Colinus virginianus</i>					500						Sillman, 1969
Brown towhee	<i>Pipilo fuscus</i>					500						Sillman, 1969
Burrowing owl	<i>Athene cucularia</i>					503						Sillman, 1969
California quail	<i>Callipepla californica</i>					500						Sillman, 1969
Canary	<i>Serinus canaria</i>	369	<370	444	412	500	504	571	578	571	413	Das <i>et al.</i> , 1999
Cowbird	<i>Molothrus</i> sp					501						Sillman, 1969
Cut-throat finch	<i>Amadina fasciata</i>	370	<330	447	423	500	516	563	574	564-564	420-425	Hart <i>et al.</i> , 2000a

Domestic chicken	<i>Gallus gallus domesticus</i>	418	<370	455	~43 0	507	~49 0	569	~54 8	565- 570	430- 480	Bowmaker <i>et al.</i> , 1997
Domestic pigeon	<i>Columba livia</i>	409	<370	453	~44 0	507	513- 539	567	~56 0	565- 570	440- 480	Bowmaker <i>et al.</i> , 1997
Domestic turkey	<i>Meleagris gallopavo</i>	420	330	460	437	505	490	564	514	564	436	Hart <i>et al.</i> , 1999
Gouldian finch	<i>Erythrura gouldiae</i>	370	<330	440	422	500	513	562	572	565	419- 422	Hart <i>et al.</i> , 2000a
Green-backed firecrown hummingbird	<i>Sephanoides sephanioides</i>	371		444		508		560		560		Herrera <i>et al.</i> , 2008
House finch	<i>Carpodacus mexicanus</i>					502						Sillman, 1969
Humboldt penguin	<i>Spheniscus humboldti</i>	403	<400	450	475	543	525					Bowmaker and Martin, 1985
Japanese quail	<i>Coturnix japonica</i>	420	<370	458	434	505	516	567	580	567	430- 440	Bowmaker <i>et al.</i> , 1993
Mallard	<i>Anas platyrhynchos</i>	420	<370	452	450	502	515	570	580	570	475- 500	Jane and Bowmaker, 1988
Manx shearwater	<i>Puffinus puffinus</i>	402		452		*		*				Bowmaker <i>et al.</i> , 1997
Mourning dove	<i>Zenaida macroura</i>					502						Sillman, 1963
Ostrich	<i>Struthio camelus</i>	405		445	417	506	507	570	555	570	498	Wright and Bowmaker, 2001
Peafowl	<i>Pavo cristatus</i>	424	<330	458	449	505	511	567	569	566	479- 500	Hart, 2002
Pekin robin	<i>Leiothrix lutea</i>	355	<370	453	400	501	506	567	568	568	405	Maier and Bowmaker, 1993
Plum-headed finch	<i>Neochmia modesta</i>	373	<330	442	415	500	514	565	568	562- 564	414- 421	Hart <i>et al.</i> , 2000a

Poor-will	<i>Phalaenoptilus nuttallii</i>									506								506							Sillman, 1969
Rhea	<i>Rhea americana</i>						447	417	506	504	571	555	571	496				506							Sillman, 1969
Ringneck dove	<i>SStreptopelia risoria</i>								502									502							Sillman, 1969
Roadside hawk	<i>Buteo magnirostris</i>								500									500							Sillman, 1969
Shell parakeet	<i>Melopsittacus undulatus</i>	371	<370			444	~40	508	0	~48	564	~55	565-	415-			508	570	480						Bowmaker <i>et al.</i> , 1997
Starling	<i>Sturnus vulgaris</i>	361	<350			449	399	504	514	565	572	563-	407-	478			504	563-	559						Hart <i>et al.</i> , 1998
Tawny owl	<i>Strix aluco</i>	463				503		555									555								Bowmaker and Martin, 1978
Wedge-tailed shearwater	<i>Puffinus pacificus</i>	406	<370			450	445	503	506	566	562	566	413				503	566	562						Hart, 2004
White-crowned sparrow	<i>Zonotrichia leucophrys</i>							502									502								Sillman, 1969
White-headed munia	<i>Lonchura maja</i>	373	<330			446	422	500	510	562	567	563-	419-				500	564	489						Hart <i>et al.</i> , 2000a
Zebra finch	<i>Taeniopygia guttata</i>	360-380	<370			430	~40	506	9	568	~56	565-	425-	480			506	570	480						Bowmaker <i>et al.</i> , 1997

Cones have low absolute sensitivity compared to rods (Kohen, Santus and Hirschberg, 1995). Nocturnal birds therefore have relatively few cones, and these have spectrally distinct oil droplets which lack the dense pigmentation found in the cone oil droplets of diurnal birds. Among owls (Strigidae), only approximately 10% of cones contain orange/ yellow oil droplets, with the remaining 90% containing colourless oil droplets. This is likely to be an adaptation to increase the sensitivity of the few cones present under the low illumination levels at dawn and dusk (Hart, 2001). Aerial insectivores are similar to nocturnal species in that they have fewer red and yellow oil droplets than other diurnal birds. However, their retinas are double-cone dominant, emphasising the reliance on motion detection that such aerial foragers as the barn swallow *Hirundo rustica* require in high speed aerial pursuit of prey (Hart, 2001; Goldsmith, Collins and Licht, 1984).

While some marine species (e.g. northern gannet *Morus bassanus*) which look through the air-water interface at their prey may have more long wavelength sensitive (i.e. red) cones and more red and orange oil droplets than terrestrial species (Partridge, 1989), others (e.g. noddy tern *Anous minutus*) have more short wavelength sensitive cones. Hart (2001) suggests that having longer wavelength sensitive cones in species that look through the air/ water interface is maladaptive in that the optimum wavelengths for seeing through this interface are between 425 nm and 500 nm. However, all of the species examined so far do have some sensitivity in this range, and so the long wavelength sensitivity may arise as a result of another evolutionary pressure, e.g. to avoid glare. Lythgoe (1984) states that for fish at least, coastal waters would require visual pigments to be maximally sensitive in the range 530 nm to 560 nm for optimal vision. Freshwater red-eared slider turtles *Trachemys scripta elegans* have red and yellow oil

droplets but ocean living green turtles *Chelonia mydas* do not, and at certain times of day, red light is more reflected than blue light. This suggests that the colour of the water (i.e. dependent on the turbidity and substrate), and timing of day are important factors in selection for spectral sensitivity (Dvorak and Granda, 1990).

Visual fields

The visual field is the total area around the animal from which visual information can be obtained (Fernández-Juricic, Erichsen and Kacelnik, 2004). The placement and mobility of the eyes mean that different species have very different fields of view. Visual fields in birds can be classified by foraging behaviour into three main types: (1) visual guidance in foraging using the bill, such as in European Starling; (2) non-visual guidance when taking food with the bill, such as in Eurasian woodcock *Scolopax rusticola*; (3) non-visual guidance when taking food with the feet such as in tawny owl *Strix aluco*. Some overlap between these types is seen, for example where short-toed eagles *Circus gallicus* follow and take prey visually using their feet (i.e. a combination of types 1 and 3) (Fernández-Juricic, Erichsen and Kacelnik, 2004; Martin and Katzir, 1999). Generally, the bill does not protrude into the visual field, however, in starlings and hornbills (southern ground hornbills and southern yellow-billed hornbills) the bill tip is seen within the frontal visual field, allowing the bird to see what is contained between the mandibles during foraging. This is seen as an adaptation allowing high levels of precise manipulation of food items within the bill (Martin and Coetzee, 2004).

Binocularity

Binocular vision occurs if the visual fields of the two eyes overlap. Birds and mammals exhibit a large amount of interspecific variation in the placement of the eyes, and hence the degree of binocularity (Heesy, 2004). Humans are able to see the world with a mostly binocular view (a 140° binocular field). Similarly, most diurnal birds of prey and owls also have forward-facing eyes with a large binocular field, albeit smaller than humans (e.g. barn owl binocular field width is 44°; Iwaniuk *et al.*, 2008). In contrast, most other birds have their eyes positioned laterally, with the degree of binocularity dependent on the amount that the eyes converge towards the front of the head (Cassin and Soloman, 1990), for example the cattle egret *Bubulcus ibis* has a binocular field of 22° (Iwaniuk *et al.*, 2008).

One function of binocularity is for distance perception through stereopsis (Iwaniuk and Wylie, 2006). This is the “perception of three-dimensional space achieved through binocular vision and the detection by neural processes of the disparity in the images of the two eyes” (Martin and Katzir, 1999). Another possible function of binocularity is movement perception through the removal of the ambiguity of signals from each individual eye, in rotational and directional motion. For example, if a bird is moving forwards, each eye will have the same neuronal responses for the direction, but if the bird is turning to the right, each eye will have opposite neuronal responses (Wylie and Frost, 1990). Pigeon, zebra finch *Taeniopygia guttata*, little owl *Athena noctua* and barn owl have all been shown to have convergent processing of monocular neurons in the visual Wulst (Pettigrew and Konishi, 1976; Casini *et al.*, 1992; Deng and Wang, 1993; Wylie and Frost, 1999; Schmidt and Bischof, 2001; Voss and Bischof, 2003).

Despite the apparent importance of stereopsis, studies on pigeons landing after flight has revealed that because distance perception by stereopsis is a relatively slow process, monocular cues of depth are more important when a bird is in imminent danger of collision (Martin and Katzir, 1999). In addition, some species of bird are able to move each eye independently, reducing or increasing binocularity, and so individual control over binocularity is possible (Martin and Katzir, 1994). There is an obvious trade off between the benefits of binocular vision and the ability to view large proportions of the animal's environment. The size of the blind area correlates with the size of the binocular field, with birds that have large binocular areas also having large blind areas. To compensate, birds with larger blind areas tend to spend more time being vigilant. For example, wigeon *Anas penelope* have a larger blind area than shoveler *A. clypeata*, and correspondingly spend more time undertaking vigilant behaviour i.e. in a head-up posture (Guillemain, Martin and Fritz, 2002). Fernández-Juricic *et al.*, (2008) found that the ground feeding house sparrows and house finches are capable of foraging and scanning for predators at the same time, but this level of vigilance may be used for motion detection and not for detailed inspections of predator approaches, which occur when the head is up.

Costs of Vision

All sensory perception involves some costs. Eyes are metabolically expensive because the retina has a high metabolic rate and in birds eyes, comprise a large percentage of the overall body mass, affecting overall metabolic rate (Brooke, Hanley and Laughlin, 1999). Carrying around relatively large fluid-filled “balls” requires more energy expenditure, particularly in flight, for individuals with larger and heavier eyes than those with smaller

and lighter eyes (Thomas, Kelly and Goodship, 2004). Visual specialisation also requires further neural processing to allow information gained from the specialisation to be beneficial (Iwaniuk, Clayton and Wylie, 2006). The cost here is primarily metabolic, with additional nutritional resources being used to process information. Larger eyes require larger brains for processing larger amounts of visual information, with the optic lobes scaling proportionally to retinal information (Brooke, Hanley and Laughlin, 1999; Garamszegi, Møller and Erritzøe, 2002). These larger brains required are heavier still, incurring additional flight costs. Birds with larger brains also have smaller pectoral muscles (Isler and van Schaik, 2006), reflecting the trade-off between locomotion and brain size.

Other costs of vision relate to foraging: birds that exhibit cranial kinesis during feeding (i.e. mobility of the upper beak relative to the brain case) and those with large eyes have skulls that are less stable than those with relatively smaller eyes. A more kinetic skull produces less of a bite force whilst feeding (Bout and Zweers, 2001), and it is suggested that this reduces foraging efficiency in larger-eyed birds.

Birds with a wide binocular field, and thus a correspondingly wide blind area, are liable to costs imposed by the need for increased vigilance during foraging, especially on prey items that are particularly difficult to obtain. Blue jays *Cyanocitta cristata* in a cryptic (i.e. difficult) food detection task required high levels of attention in the frontal field, and were not monitoring their lateral fields. To minimise the risk of predation, they would have to become more vigilant whilst foraging on cryptic prey (Fernández-Juricic, Erichsen and Kacelnik, 2004): reducing the time spent actually foraging.

A case study in visual ecology: Optical specialisations for underwater vision in diving birds

The air-cornea interface of an avian eye contributes much of the refractive power of the eye as a whole. However, the refractive index of the cornea is similar to water, and so when a terrestrial cornea is immersed in water it becomes unable to accurately focus light onto the lens and retina (i.e. the eye is no longer emmetropic with an image accurately focused on the retina, but becomes hyperopic or myopic). It was once suggested that the nictitating membrane was able to counteract the negation of corneal refractive power underwater in birds. However, Sivak, Bobier and Levy (1978) were able to show that the membrane does not have a refractive function, as its refractive index is similar to that of the cornea (1.37). The lens therefore becomes the major refractive medium underwater (Sivak, Hildbrand and Lebert, 1985), and so diving birds, which use vision underwater, require specialisations of the lens to achieve accommodation in both air and water.

Specialisation for underwater vision can include changing the shape of the lens. A more spherical lens allows light to be more strongly focussed upon the retina, and a graded refractive index within such a lens minimises spherical aberrations (see above). Indeed, wholly aquatic organisms such as teleost fish generally have graded spherical lenses (Sivak, 2004), as this is the only refractive element of the eye; the cornea having no refractive function in water. Among birds, penguins have been shown to have relatively spherical lenses in comparison to wholly terrestrial birds, reflecting their aquatic lifestyle (Suburo and Scolaro, 1990).

Several species of diving bird have been shown to employ lenticular accommodation to counteract the negating refractive effect of water upon the refractive properties of the cornea, with some demonstrating their ability to achieve an emmetropic

state (or close to this) underwater. Anseriforme species foraging underwater on active prey, such as the hooded merganser and goldeneye *Bucephala clangula*, are able to accommodate by 70 – 80 D underwater to project a fully focussed image onto the retina (Sivak, Hildbrand and Lebert, 1985). An example of a species which forages underwater upon molluscs, plants and occasionally small fish i.e. not always pursuing prey actively, is the redhead *Aythya americana*, which is able to accommodate underwater by only 16 D. This degree of accommodation represents an intermediate adaptation between terrestrial and amphibious accommodation (Sivak, Hildbrand and Lebert, 1985).

Another adaptation to loss of corneal refraction underwater is to have a relatively flat cornea. For example, the cornea of the humboldt penguin *Spheniscus humboldti* has a refractive power of 29 D (c.f. that of the European starling which has a refractive power of 124.6 D) (Martin and Young, 1984). King penguins, forage principally upon lantern fish Myctophidae (which have many photopores producing small points of light) during the both the night and day. They, like other penguins, have very flat corneas, which minimises the reduction in corneal refractive power (10.2 D) under water, and large eyes overall (large axial length), which allows the eye to be sensitive at low light levels i.e. the conditions under which foraging occurs. In addition to these adaptations, king penguins have an extremely small and square-shaped pinhole pupil when fully constricted (see section on pupil aperture above), which allows the retina to become pre-adapted to the dim conditions deep underwater before the penguin begins its dive (Martin, 1999). Several penguin species are known to reach an approximately emmetropic state below water: gentoo *Pygoscelis papua*, rockhopper *Eudyptes chrysocome*, Magellanic *S. magellanicus*, king, Humboldt, and Adelie *P. adeliae* (Sivak and Millodot, 1977; Howland and Sivak 1984; Sivak, Howland and McGill-Harelstad, 1987). Both grey-

headed and black-browed albatrosses (*Diomedea melanophris* and *D. chrysostoma*) also have corneas of relatively low refracting power (22.8 D and 23.3 D respectively), demonstrating their visual adaptation to an amphibious lifestyle, pursuing prey at and beneath the water surface (Martin, 1998).

The American dipper provides a further example of visual adaptation to an amphibious lifestyle. This species has larger iris (Figure 1.1) musculature than other closely related species (e.g. American robin *Turdus americanus*) and experimentally derived data, using nicotine to stimulate a response on excised eyes suggest that it may be able to accommodate up to 48 D underwater (Goodge, 1960). Larger iris musculature may be an adaptation to increasing the lenticular accommodative power. Contraction of the iris sphincter in combination with contraction of the ciliary muscle causes the lens to be pushed against the iris disc. The central lens then is able to bulge through the pupil (Levy and Sivak, 1980).

Whilst the penguins, albatrosses and shearwater mentioned above are quite closely related, and could conceivably have an amphibious common ancestor, the anseriforms and dipper (passerine) are not closely related (Hackett *et al.*, 2008), and the oldest known avian fossil (*Archaeopteryx lithographica*) is believed to have been non-aquatic (Burnham, 2007). Therefore, it is likely that the remarkably similar amphibious visual adaptations apparent in such a wide range of taxa, is a result of convergent evolution.

Avian vision in context: Sensory Hierarchies

Whilst vision is very important for the majority of bird species, the other senses are employed to different extents in different species and circumstances. When one sensory mechanism is not a viable option, another will be used; e.g. where visual information is inadequate, other senses such as olfaction and audition may be utilised. When a particular sense confers a selective advantage, the species often will have a corresponding anatomical or physiological specialisation, according to the “use it or lose it” theory (Liman, 2006). The senses of audition, echolocation, magnetoreception, olfaction and touch, alone or in combination with each other and with vision are exhibited in a variety of species, and are discussed briefly below.

Hearing

Some species of owl (e.g. barn owl, saw-whet owl *Aegolius acadicus*) can use sound alone to locate their often highly camouflaged or hidden prey (e.g. mice beneath grass tunnels), in circumstances where use of vision would not be possible (Knudsen, 1981). These nocturnal hunters have an enlarged area in the brain (avian auditory midbrain nucleus or “MLd”) which confirms that such species have placed greater emphasis on audition, when compared to other species without hypertrophied MLd. Some species that do not have an enlarged MLd nevertheless have other auditory specialisations, for example, the oilbird, which is able to navigate through caves using echolocation (Iwaniuk, Clayton and Wylie, 2006).

Echolocation

When vision is not possible, a sensory mechanism used by a few species is echolocation. Echolocation is a means of locating objects even in complete darkness, by emitting high amplitude pulsed sound, and orienting according to the reflected echoes (Suthers and Wallis, 1970). Avian echolocation has been described only in two groups; Oilbirds, and in the Collocalini (swiftlets) tribe of the Apodidae, both of which roost and nest deep within caves. However, unlike echolocating bats, birds emit relatively low frequency sounds (either clicks or pulse series) and so are only able to orientate using echolocation and cannot forage using echolocation alone, as the spatial resolution is too low (Konishi and Knudsen, 1979; Thomassen *et al.*, 2007). The nocturnal oilbirds are frugivorous and find fruit by sight and smell (Martin *et al.*, 2004). Diurnal swiftlets also do not forage using echolocation, but use vision to find their insect prey (Price, Johnson and Clayton, 2004). Echolocation in birds therefore is an adaptation to orientating in complete darkness, rather than for foraging purposes.

Magnetoreception

Avian magnetoreception is a bird's ability to sense the earth's magnetic field of approximately 50 μT (Rodgers and Hore, 2009), and use it for orientation and navigation. Birds are able to use a combination of magnetite particles in the beak and light-dependent radical-pair processes (likely to involve cytochromes) in the retina (Mouritsen and Ritz, 2005), implying that vision is still important at least in part for this sensory adaptation. European robins *Erithacus rubecula* are able to orient in a fixed-direction in complete darkness (therefore using the magnetite system alone as a compass). The magnetite system also allows birds to gauge the magnitude of the magnetic field they are passing

through (Stapput *et al.*, 2008). Possible mechanisms for the light-dependent radical-pair system are outlined extensively in Rodgers and Hore (2009). Mouritsen *et al.*, (2005) found that night-migrating songbirds have an area within the brain (termed Cluster N) that is active only during night vision (see figure 1.4) and may be involved in integration of magnetosensory and visual cues in migratory navigation. Other visual orientation mechanisms which may work in combination with each other and with magnetoreception, include the star-compass (e.g. in indigo bunting *Passerina cyanea*: Emlen, 1967), the sun-compass (e.g. in American golden plover *Pluvialis dominica*: Alerstam *et al.*, 2001) and orientation using visual landmarks (e.g. in domestic pigeon: Biro *et al.*, 2007).

Olfaction

Olfaction is used for several behaviours: detecting predators, intraspecific communication, navigation and foraging. Olfactory acuity relates to the number of functional olfactory receptor (OR) genes, with nocturnal species such as the brown kiwi and the kakapo *Strigops habroptilus* generally possessing a relatively large number of these genes, when compared to diurnal species (Steiger *et al.*, 2009). Species with high olfactory acuity generally have a highly developed olfactory bulb in the brain (Ioalé and Papi, 1989) One exception to this pattern is the snow petrel *Pagodroma nivea*, which was found to have small amounts of OR genes yet a relatively large olfactory bulb. This result was explained by the snow petrel having a high sensitivity to a small range of odours (Steiger *et al.*, 2008). The timing of daily activity is correlated with the size of the olfactory bulb: Nocturnal species are more likely to have larger olfactory bulbs than their diurnal counterparts (Healy and Guilford, 1990), reflecting the increased role of olfaction in circumstances where vision is impaired by low light levels.

Olfaction has recently been found to play a role in predator avoidance in passerine species that are generally considered to be visually-guided. For example, when exposed to mammalian predator faeces (cat), house finches *Carpodacus mexicanus* responded as though they were in danger, minimising the overall time spent at a feeder and the feeding bout length (Roth, Cox and Lima, 2008). Blue tits also demonstrated anti-predator responses when exposed to the scent of a predator within their nest boxes, delaying entry and minimising the time spent provisioning their chicks (Amo *et al.*, 2008).

Other studies have shown that birds are able to recognise conspecifics (i.e. mates and other individuals) using body odour, and their nests. For example, European storm petrel *Hydrobates pelagicus* chicks are able to find their own nest burrows using scent (Mínguez, 1997); and Antarctic prions *Pachyptila desolata* can differentiate between their own scent, an unknown conspecific's, and a mate's, and actively avoid their own scent (Bonadonna, Hesters, and Jouventin, 2003; see Hagelin and Jones, 2007, for a review on odour as a means of intraspecific communication). Wallraff (2004) provides a comprehensive review of the evidence surrounding avian olfactory navigation, where birds are able to assimilate odour cues to navigate. For example, domestic pigeons are able to deduce positioning information and navigate to their "home" loft using atmospheric trace gases (Bingman and Benvenuti, 1996).

The use of olfaction to find prey items has been documented in many procellariiform species. Wandering albatrosses *Diomedea exulans* detect almost half their prey (45.5%) using olfaction (Nevitt, Losekoot and Weimerskirch, 2008). Black-footed albatrosses *Diomedea nigripes*, sooty shearwaters *Puffinus griseus*, pink-footed shearwaters *Puffinus creatopus*, Manx shearwaters, Buller's shearwaters *Puffinus bulleri*, short-tailed shearwaters *Puffinus tenuirostris*, blue petrels *Halobaena caerulea*, white-

chinned petrels *Procellaria aequinoctialis*, black-bellied storm-petrels *Fregetta tropica*, Wilson's storm-petrel *Oceanites oceanicus* and northern fulmars *Fulmarus glacialis* are all highly attracted to dimethyl sulfide and/or food-related odours (Hutchison and Wenzel, 1980; Nevitt and Bonadonna, 2005a; 2005b). These species utilize olfaction to find patchy foraging resources in the open ocean, particularly in adverse weather conditions preventing perception of visual cues (Nevitt, 2008).

Touch

Some species are able to perceive and utilise tactile cues from their environment. As previously mentioned, black skimmers are tactile foragers, and they employ a feeding strategy combining tactile and visual cues. They gather prospective prey items within their bill by skimming across the water surface, detecting prey by touch, and then visually assess the prey caught for suitability while it is held in the bill-tip (Martin, McNeil and Rojas, 2007). Kiwis have specialised bill tips, packed with sensory pits, within which lie mechanoreceptors which project to extremely large neural processing areas. Martin *et al.*, (2007) show that two kiwi species (brown kiwi *Apteryx mantelli* and spotted kiwi *A. haastii*) use a combination of tactile and olfactory cues, rather than vision, to forage at night. Indeed these birds have very small optic nerve diameters and their optic tectum and Wulst are small in comparison with other avian species.

Conclusion

As the above examples show, comparisons of different species' visual capabilities often allow a more complete understanding of bird behaviour. In Chapter 2, I aim to provide a comprehensive overview of techniques and methods that are widely used and which I have used in my studies. Within this chapter, I also outline a brief case study employing these methods, using the relationship between retinal image brightness and the timing of activity and food type, to predict aspects of Archaeopteryx's lifestyle. In Chapter 3 I then go on to compare the retinal structure and morphology of the European storm petrel *Hydrobates pelagicus* and common starling *Sturnus vulgaris*, aiming to distinguish nocturnal retinal specialisations in the European storm petrel and relating my findings to their behaviour. In Chapter 4, I compare the differences in eye size and the time of onset of dawn song for many species around the world both with species level and comparative analyses. In this chapter I aim to untangle the complex relationships that exists between visual ability, body mass, the timing of onset of dawn song and the latitude. In Chapter 5 I investigate how artificial lighting causes behavioural differences in the European robin *Erithacus rubecula*, using studies of captive and wild birds. Here I aim to provide evidence on the consequences of artificial illumination on birds, and recommendations for mediation. Chapter 6 concludes this thesis with a general discussion, providing areas for future study and expansion, and the implications of my studies.

Chapter 2: Methods of assessing avian eye design

Abstract

In this chapter I discuss in detail several different methods for measuring avian eye design, that I have utilised in my studies to assess avian visual ability. There are often several techniques available to gain the same information. For example, ultrasound, magnetic resonance imaging (MRI), simple measurements of excised eyes and measurements of skeletal eye sockets can all be used to obtain information on overall eye size; however, there are costs and benefits of each method. I used an ultrasound technique to obtain information on eye size of the domestic pigeon *Columba livia*, comparing my findings with published literature. I used a photographic method to obtain retinal image brightness estimates for a range of non-passerine and passerine species of known activity timing, which I then compared to *Archaeopteryx lithographica*. This analysis reveals that the “first bird” was likely to be diurnal in its activity. I provide details of refinements to the calculation of retinal image brightness estimates, using both MRI scans of “intact” dead specimens and measurements from skulls. I describe the techniques employed to obtain data on retinal morphology and topography, which I apply in Chapter 3 to compare the retinas of two species with contrasting lifestyles. I also give details of methods for directly measuring exposed corneal diameter, and for estimating this measurement from measurements of orbital diameter made from skulls. These methods are applied in Chapter 4, to explain the timing of the onset of dawn song in bird communities around the world.

Introduction

Most birds are visually guided animals and so knowledge of their visual adaptations is vital to fully understand their behaviour. This chapter describes in detail the methods that I have adopted and developed for my own studies of avian visual ecology that I describe in the subsequent chapters. There are many methods available that can be used to measure aspects of visual capacity in birds, and here I concentrate on measuring three key aspects of eye design: (i) overall eye size, (ii) estimates of retinal image brightness and (iii) retinal structure. These three measures are important for understanding the links between visual constraints and behaviour because they relate directly to (i) overall investment in vision, (ii) the brightness of the image available for detection by the retina, and (iii) the ability of the retina to detect and process that image.

When assessing avian visual adaptations, the techniques involved depend heavily on the type of specimen available for study. For example, different measurements can be obtained from live birds than can be obtained from skins or skulls, but the use of live birds may involve ethical issues. Also, several methods are logistically impossible in some situations, for example the use of large specialised equipment, such as MRI scanners, in remote field locations. Therefore utilising technologically simpler methods to obtain the same or similar data may be favoured in the field. It is also important to validate the methods used, to allow comparisons to be made between data obtained with the different methods.

Measuring eye size and eye morphology

a) Measurements from excised eyes

Many methods have been used in the literature to assess eye size. Historically, enucleated eyes were used for eye size measurements, with the animal being euthanized and the eyes immediately removed (Slonaker, 1918; Rochon-Duvigneaud, 1943). Once the eye is removed, the axial length (i.e. the length of the eye from the front of the cornea to the back of the eye) can be directly measured. The eye can be dissected for further measurement of the internal structures, for example the lens, pecten and retina.

Decomposition of ocular tissue occurs fairly rapidly post mortem, leading to leakage of the vitreous and aqueous humour (Bito and Salvador, 1970). As a result, the shape of the eye can change post-mortem, rendering any measurements inaccurate unless the eye is properly “fixed” (i.e. decomposition halted) soon after death. Fresh eyes that are measured or “fixed” up to 30 minutes after death are considered useable for detailed microscopic work as the level of decomposition is low within this time period. Although no studies have yet demonstrated the decay rate and suitability of using eyes after different periods of time post mortem for avian species, chick *Gallus gallus domesticus* eyes were found to be able to fully recover from ischemia (lack of blood supply) 30 minutes after the blood supply was cut off but not after 40 minutes (Nakazaki, Nao-I and Sawada, 1998). This implies that fixation at up to 30 minutes post mortem would yield more useful results than from an eye obtained after this time. Some studies (see Hall, 2008) use fixed eyes in studies of eye morphology and size, and try to overcome the problems associated with using dead tissue by inflating the eye to a maximum level by injecting liquid into it before measurements are taken. However, fixatives generally cause

shrinkage within tissues, with different fixatives causing different levels of shrinkage within different tissues and cells (Latendresse *et al.*, 2002). Therefore, such measurements are not readily comparable to measurements from living specimens.

b) Measurements of exposed corneal surface

A bird's pupil aperture cannot usefully be wider than the transparent area of the exposed corneal surface. Maximum pupil aperture can therefore be estimated by measuring the maximum diameter of the exposed corneal surface, between the eyelids and mucous membrane surrounding the eye (Figure 2.1). This measurement is easily obtained from live birds, and does not assume sphericity of the eye. Corneal diameter can be measured directly using callipers or by scaled digital photography (Figure 2.1). To measure the scaled digital photographs taken throughout my studies I used ImageJ software (Abramoff, Magelhaes and Ram, 2004). Corneal diameter is highly correlated with orbital diameter, controlled for body mass (adjusted $R^2 = 0.870$, $F_{2, 40} = 141.8$, $P < 0.0001$) and both are highly repeatable measures (Thomas *et al.*, 2002; Methods, Chapter 4, adjusted $R^2 = 0.991$, $F_{13, 36} = 364.7$, $P < 0.001$). Thus, measurements of orbital diameter from museum skull specimens (see below, Figure 2.2) can be used to estimate corneal diameters for species for which live birds are unavailable (see Chapter 4).

c) Measurements from skulls

Measuring skulls is a valuable way in which to obtain data on visual capability. It is a particularly useful way to obtain information from species that are not easily accessible or are only present within the fossil record (see below for *Archaeopteryx lithographica*). For example, the skull of a kakapo *Strigops habroptila* (a nocturnally active species of

parrot) would be more easily measured than would a live wild adult, due to it being highly elusive and critically endangered (BirdLife International, 2009). It is also a cost effective and efficient method, as many species from around the world are often housed in a single collection at one location, allowing photographs and measurements to be taken from a large number of specimens in a short time.

The overall morphology and size of the eye socket can be measured easily either directly, (i) using Plasticine®, metal or plastic spheres, or (ii) by using digital photography.

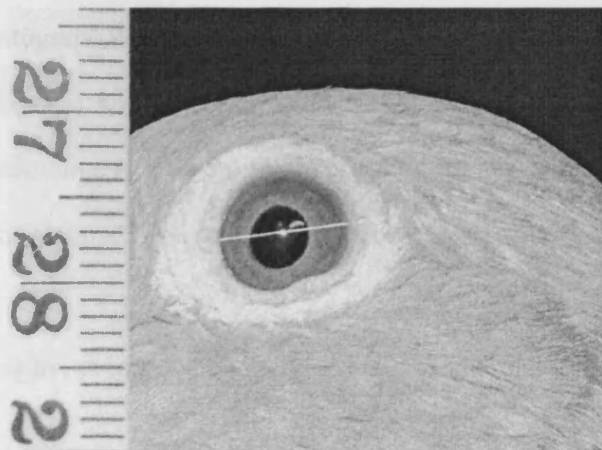


Figure 2.1. Corneal diameter (or “eye surface diameter”) on a pigeon *C. livia* is represented by the white line. Note the ruler held adjacent to the eye for scaling purposes.

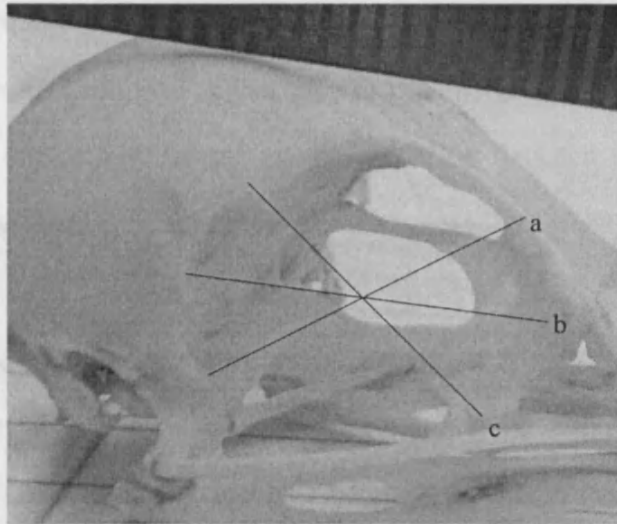


Figure 2.2. An average of distances a, b and c are measured to provide orbit diameter measurements (photograph of an arrow-marked babbler *Turdoides jardineii* skull). Note ruler at top of photograph, adjacent to the skull.

In my studies, measurements were taken from scaled photographs of skulls held at the National Museum of Natural History, Tring, UK and at Naturalis, Leiden, Netherlands.

(i) Fitting spheres into eye sockets

A method employed in several recent studies is to measure the diameter of “best-fitting” steel ball bearings (Thomas *et al.*, 2006) and Plasticine balls (Brooke, Hanley and Laughlin, 1999) placed within the eye socket. The benefit of using ball bearings over Plasticine is that they remain consistently spherical, whereas Plasticine easily becomes deformed, though both Brooke, Hanley and Laughlin’s (1999) measurements using Plasticine and Thomas *et al.*’s (2006) measurements using ball-bearings were found to be highly repeatable. Steel ball bearings can be heavy relative to a small and potentially fragile skull; therefore, hollow plastic alternatives may be

used instead (Pollard A. L., Goodship, N. M. and Thomas R. J., unpublished studies). However, these methods assume that the eye is spherical and axial length estimates may therefore differ from actual measurements of flattened eyes (e.g. domestic pigeon *Columba livia*) or tubular eyes (e.g. tawny owl *Strix aluco*).

(ii) Scaled digital photography

To obtain estimates of orbit diameter, scaled digital photographs of skulls are taken with the skulls aligned so that the orbit aperture is parallel to the camera lens, and in the same plane as a ruler (to provide the scale). Modelling clay can be used to stabilise the skull and ruler in a fixed position. I used this method for as many of my study species as were available in museum collections, with 1 to 6 individuals being photographed per species. The aperture of the eye socket was then measured directly from the digital photographs, in three orientations, using Image J software (Figure 2.2). The three measurements were then averaged to provide a mean eye socket aperture. Measurements of eye sockets obtained by this method are highly repeatable within species: A repeatability analysis (following Harper, 1994) using measurements of orbit diameter for 14 species ranging from approximately 9 g to 900 g, with 2 – 4 (average $N = 3.477$) replicates for each species, revealed such orbit measurements to be very highly repeatable within species (adjusted $R^2 = 0.991$, $F_{13, 36} = 364.7$, $P < 0.001$).

Measurements using ultrasound

A more technologically advanced technique for measuring eye size and morphology is ultrasound. Ultrasound is used very successfully in medicine and veterinary science to

image humans and other animals internally, without the need for invasive surgery. This technique can be applied to imaging the internal structure of the eyes of living animals, using an ultrasound scanner positioned over the corneal surface. A stationary pose is required, and so mild anaesthesia or sedation is used to restrain the animal during the procedure. In addition, application of water-based sonographic gel is required to minimise discomfort and aid transduction of the sound waves across the corneal surface (Schmid, 2006). As contact between the scanner head and the gel-covered corneal surface is required, the technique cannot be termed non-invasive.

Ultrasound imaging is a technique that is most useful in live or very freshly dead specimens in order to measure the distances between ocular structures and hence their physical relationships. Sound waves pass through the eye and are reflected off the internal structures. Two types of scan can be implemented: A-scans which image tissue along a single axis sound beam, or B-scans which emit a broader beam of sound to image a wider section of tissues. In the present study, A-scans were used as the measurements of interest lie along a single axis, i.e. the axial length of the eye. The time lag between the production of the signal and the reception of the resulting echoes can then be used in locating the position of structures including the corneal surface, the iris, the faces of the lens, and the retina. I describe and present below the results of a pilot study on the use of ultrasound in obtaining information on eye size and design, and examining how the eye dimensions may change following death.

Ultrasound imaging of the eye was completed for two domestic pigeons *Columba livia* during euthanasia. These birds were euthanized under a UK Home Office licence as part of research on neural homing mechanisms, and the ultrasound scan was administered as part of a preliminary study on ocular ultrasound procedures in small birds (J.

Guggenheim and J. Erichsen, personal communication). Each bird was administered an intra-peritoneal injection of sodium pentobarbital at 100-150 mg/kg and held in a cage until the anaesthetic had taken effect. Once the bird was adequately sedated, sonographic gel was placed upon the corneal surface, and the ultrasound transducer applied (see Cottrill and McBrien, 1996).

Table 2.1. *Post mortem* changes of the pigeon eye (n = 2).

Pigeon ID	<i>Pre/post mortem</i>	Eye	Anterior chamber depth (mm)	Lens thickness (mm)	Vitreous chamber depth (mm)	Axial length (mm)
1	Pre	Right eye	1.898	2.893	6.793	11.583
		SEM	0.01	0.019	0.005	0.007
1	Post	Left eye	1.918	2.905	6.78	11.603
		SEM	0.008	0.009	0.01	0.002
2	Post	Right eye	1.98	2.698	6.748	11.425
		SEM	0.009	0.007	0.009	0.01
2	Pre	Left eye	1.933	2.65	6.748	11.33
		SEM	0.008	0.038	0.036	0.004
	Pre	Combined	1.916	2.772	6.7705	11.457
		SEM	0.0175	0.1215	0.0225	0.1265
	Post	Combined	1.949	2.802	6.764	11.514
		SEM	0.031	0.1035	0.016	0.089

Measurements of axial length, anterior chamber depth, vitreous chamber depth and lens thickness were obtained for each bird, before and less than 5 minutes after death (right eye prior to death, then left eye after death in one pigeon, and *vice versa* for the second bird).

The measurements derived using ultrasound (axial length = 11.49 mm) were similar to the measurements found when examining dissected eyes to form a schematic eye model (axial length = 11.46 mm, Marshall, Mellerio and Palmer, 1973; 11.62 mm, Martin and Brooke, 1991) and from hemisected eyes (axial length = 11.13 mm, Rochon Duvigneaud, 1943), verifying that the ultrasound measurements were accurate and reliable.

One post-mortem change observed in the pigeon eye was that it marginally elongated after death (Table 2.1), with the overall axial length and the anterior chamber depth increasing by approximately 1% of the *ante mortem* distance. Whilst this effect may simply be due to measurement error (the average magnitude of the increase is only 0.058 mm), the increase may be also due to the muscles surrounding the eye and the ciliary muscle controlling the cornea (and lens) relaxing immediately following death, allowing the cornea to become more convex. The overall axial length became larger by the same extent as the change in anterior chamber depth, suggesting that only the musculature affecting the cornea (i.e. the anterior and internal ciliary fibres) causes the change in eye length at death.

Whilst this pilot study does not provide any conclusive evidence of intraocular changes at death in the pigeon, it does allow a demonstration of a valuable technique in ocular measurements that can validate the measurements obtained from dead specimens. Both the previously published schematic eye and dissected eye measurements for *C. livia*

are reliant on information from dead specimens and obtaining similar accurate measurements would be very difficult in a live specimen without the use of this ultrasound technique. However, consideration of the stress of handling and anaesthesia is imperative prior to use of ultrasound imaging techniques. Although the birds in this study were euthanized, in other applications, recovery and release is possible, as demonstrated by its use in veterinary practice (Gumpenberger and Kolm, 2006).

Measurements using magnetic resonance imaging

Magnetic resonance imaging (or MRI) is a relatively new technique, at least within the field of visual ecology (Jeppard and Clare, 2001), and can be used for a variety of purposes. The physics behind the scanning technology is based on the miniature magnetic fields created by the spin of positively charged nuclei of atoms with an odd number of protons, neutrons or protons and neutrons (i.e. those with nuclear spin, e.g. ^1H). Information is obtained by inducing electromagnetic signals from these miniature magnetic fields: A radio frequency pulse of energy is transmitted via an electromagnetic coil surrounding the specimen, which causes the ^1H protons to spin in a particular direction and at a particular frequency (Wirtschafter *et al.*, 1992). Once the radio frequency pulse is switched off, the protons return to their natural state and release the energy from the pulse, which is detected by a receiver antenna. This information is processed by computer software (via a Fourier transform), along with information from the gradient coils which produce the electromagnetic signals, to determine the location of the protons' energy signal, and so to produce the images (Millar, 1995). The resulting images are visual sections or slices through the specimen, similar to those produced

histologically, but obtained without the need for dissection. Imaging software can provide a range of 2D and 3D models of the scanned anatomy and it is possible to recreate different viewing orientations post-scan. Although primarily used for human clinical studies and diagnosis, MRI is increasingly being used as a powerful imaging tool in a range of non-clinical fields. For example, a MR spectroscopy scan of a region of tissue can reveal its chemical composition, and a functional MRI scan can show internal changes over time in response to a stimulus in brain tissue.

In my study, I have applied the emerging technology of MRI to obtain detailed morphometric data on avian eye design from intact heads of freshly dead and chemically “fixed” birds (see Chapter 3, Figure 3.2). Advantages of MRI for such measures are (i) the high contrast between tissue types that is revealed by MRI (due to the different elemental composition of different tissues) and (ii) the clear photograph-like images that result from a successful scan, allowing the measurement of internal biometrics that are unavailable by any other technique. Furthermore, MRI scans allow internal structures to be observed and measured without the need for dissection, allowing the specimen to be utilised again and removing the possibility of dissection-related damage.

Using MRI on live birds is certainly possible as demonstrated by the wealth of literature available (starlings *Sturnus vulgaris*, Van Meir *et al.*, 2006; zebra finches *Taeniopygia guttata*, Boumans *et al.*, 2007; bald eagles *Haliaeetus leucocephalus*, Stauber *et al.*, 2007; chickens *Gallus gallus*, Li *et al.*, 2003; African grey parrot *Psittacus erithacus*, Fleming *et al.*, 2003; domestic pigeon *Columba livia*, Romagnano *et al.*, 1996). However, often these birds are laboratory animals and/or are euthanized after the experimental procedure, or they are veterinary patients undergoing diagnostic tests. Live animals must be restrained under anaesthesia whilst being scanned, to prevent movement

and therefore inaccuracies in the images produced. For example, head movement will cause the position of the eyes to change in each “section” making comparisons and measurements difficult. When MRI is used in the course of veterinary and licensed experimental procedures, anaesthesia is often already in use, whereas using anaesthesia solely for the purposes of gaining anatomical images may not be seen as ethically justified. In addition wild-caught birds would have to be transported to the scanner, anaesthetised and monitored during the scan and then returned to catch sites for release. Therefore MRI would not always be logistically possible for use with birds caught in remote field locations. MRI is also an expensive technique and may be prohibitively costly in some studies.

Using dead birds removes many of the issues and difficulties of studying live birds (housing, anaesthesia, recovery, release / euthanasia). Many of the bird specimens used in my study are borrowed from museum collections of frozen corpses (e.g. Manx shearwaters *Puffinus puffinus* killed in storms were obtained from National Museum of Wales), donated by members of Cardiff University’s Biodiversity and Ecological Processes research group (e.g. common kingfisher *Alcedo atthis*) or obtained as by-products of other studies (e.g. storm-killed Leach’s storm petrel *Oceanodroma leucorhoa*). This approach follows the ethical principles of the “3 Rs” (i.e. Reduction, Refinement & Replacement of animals in research) in that it reduces the numbers of live animals used because fewer individuals need to be killed for the purposes of the study, and researchers are sharing the specimen for its constituent parts, for use in more than one study. All birds examined throughout the study were obtained within the letter and spirit of the Wildlife and Countryside Act 1981, as well as the ASAB guidelines for use of animals in behavioural research and teaching (ASAB, 2006).

It is preferable to carry out MRI scanning of a bird as soon after death as possible, to gain the most accurate representation of its ocular anatomy before post-mortem changes occur (see above). However, this is not always possible and within this study frozen birds and those fixed in formaldehyde have been used. Some of the samples scanned showed considerable decay and so were not used in further analyses, and most specimens had sunken eyes as a result of post mortem dehydration. No measurements were taken incorporating structures deformed or displaced due to these effects, so that they do not contribute to any measurement error.

The MRI scanner used in this study was a 9.4 Tesla (400MHz) MRI scanner (Bruker BioSpin MRI GmbH, Ettlingen, Germany) at the Experimental MRI Centre (EMRIC) at Cardiff University. Short scans (~15 minutes) were performed in all cases, except for 16 hour and 25 hour scans for Leach's petrel and European storm petrel. Shorter scans were used to maximise the number of species scanned within the allocated scan time whilst still maintaining adequate resolution (slice thickness = 0.5-1.0mm) for gross internal anatomy to be measured. Longer scans increase the resolution (slice thickness = 0.1mm) and allows detailed 3D models of the head to be developed. After scanning, the appropriate images were selected using ParaVision 4.0 (Bruker Biospin 2006) and measured using Image J (Abramoff, Magelhaes and Ram, 2004).

Estimating maximum retinal image brightness

The maximum retinal image brightness (RIB_{max}) is defined as the maximum brightness of an image falling on the bird's retina, relative to that of other eye designs at an equivalent light intensity. RIB is inversely proportional to square of the minimum F-number of the

eye, where the F-number is the focal length of the eye (f) divided by the diameter of the entrance pupil (d). The calculation of RIB_{\max} is shown by Equation 2.1. (Martin and Young, 1984; Martin, 1990).

Equation 2.1. Measurements are in mm.

$$\text{Relative maximum image brightness (RIB}_{\max}) = 1 / F_{\min}^2$$

where $F_{\min} = \text{Focal length (f) / Maximum pupil aperture (D)}$

$$\text{Axial length} = (\text{Cornea to cornea distance} - 1) / 2$$

$$\text{Focal length (f)} = 0.63 \times \text{Axial length}$$

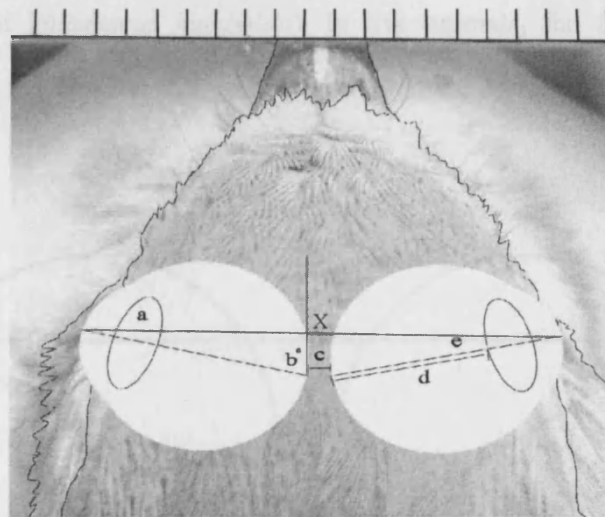


Figure 2.3. Dorsal view of the positioning of the eyes within a bird's head; a = lens, b° = angle of convergence, c = septum between the eyes, mm, d = focal length, mm, e = axial length, mm, X = cornea to cornea distance, mm. Note ruler at top of photograph (sketch overlay of European robin *Erithacus rubecula*).

While overall eye size takes into consideration both the resolution and sensitivity of the eye (generally larger eyes have increased sensitivities and resolution), maximum retinal image brightness (RIB_{max}) is a useful measure of how much light actually is available to be perceived by the retina, and therefore is expected to be important in considering the animal's behaviour, especially with reference to activity patterns.

Calculating retinal image brightness requires measurements of (i) the eye's focal length and (ii) maximum pupil aperture. In previous studies, these measurements have been obtained from excised and dissected specimens of dark adapted eyes (e.g. see Martin and Young, 1984, for details of methodology used in their study on the eye of the Humboldt penguin *Spheniscus humboldti*). In live animals, the focal length can be calculated through the use of scaled photographs (Figure 2.3), by MRI, or by ultrasound.

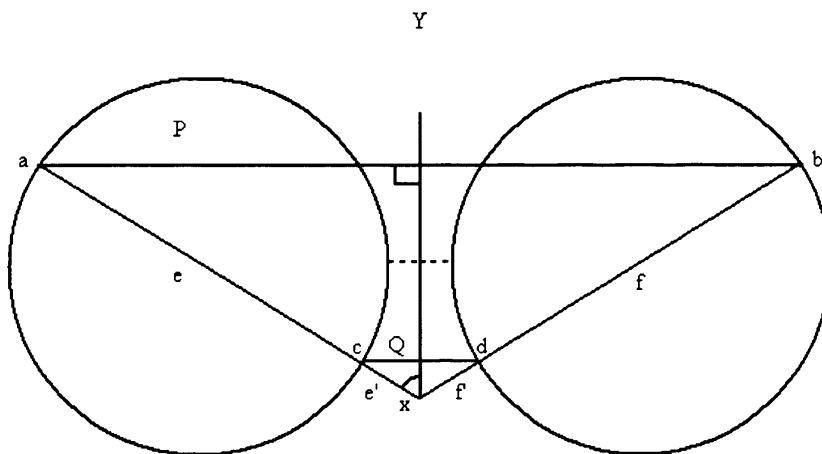


Figure 2.4. A dorsal representation diagram of the orientation of the eyes, where distance ab = cornea to cornea measurement, cd = assumed septum width, ac ($e - e'$) = bd ($f - f'$) = axial length of eye. Direction of the beak is at Y. The dotted line represents the minimum septum distance measured. Angle of convergence is denoted by x . P and Q represent half distances of the cornea to cornea distance and septum width respectively.

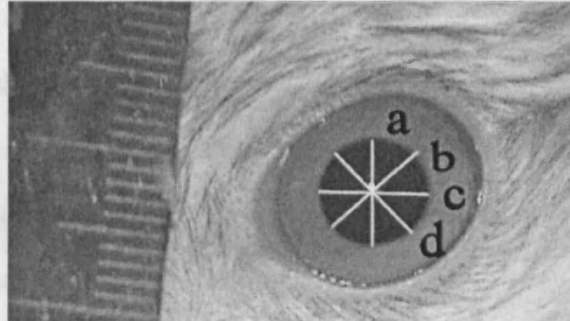


Figure 2.5. Infra-red still shot taken from film of a red kite eye. The bird was held in darkness for 5 minutes prior to filming commenced. Four pupil aperture measurements were taken at a, b, c and d using ImageJ software. Note the ruler is held adjacent to the eye.

(i) Measuring/estimating focal length

The focal length is the distance from the posterior nodal point of the optical system (the point in a schematic eye model where the angle of light exiting this system is the same as the angle of light entering it) to the retina (Hall and Ross, 2007). The focal length can be estimated from scaled photographs of live birds, showing a view of both corneal surfaces as shown in Figure 2.3 and 2.4. Because the eyes of most birds are so large, the eyes almost touch in the centre of the skull, separated by only a small septum of connective tissue (pers. obs.). The cornea-to-cornea distance can be accurately measured from a scaled photograph (dorsal view), and assuming that the eyes are exactly laterally oriented and assuming a septum width of 1 mm (Thomas, Kelly and Goodship, 2004), the axis length of a single eye can be calculated. Estimation of the focal length then involves

multiplying the axis length by 0.63 (the ratio of axial length to focal length that is broadly consistent across avian taxa; Murphy and Howland, 1987; Martin, 1993).

(ii) Measuring maximum pupil diameter

Measuring pupil diameter in vivo allows a real-life quantification of the amount of light that is able to reach the retina. Post-mortem changes in the ciliary muscles controlling the pupil aperture can cause the aperture to initially dilate and then constrict during and after rigor mortis (Prasad, 2003), and so live measurements provide a far more accurate representation of pupil aperture in a living bird. Pupil aperture measures taken after death may not be wholly representative of the accurate range of the pupil i.e. post-mortem dilation above the live range may give a large aperture result, but it is not realistic of the conditions normally faced by the bird. Post-mortem pupil aperture measurements from skins and approximations from MRI, skulls and dissection are still valuable as the measurement is a representative of the species, as long it is clear that the measurements are derived after death and are not directly comparable with measurements from live specimens.

As calculations of RIB assess the maximum light gathering potential of the eye, the maximum pupil aperture measurement is required. Therefore, a maximally dilated pupil is photographed: The bird is held in a dark room or specially constructed dark box for a short period (approximately 5 minutes) to allow the pupil aperture to equilibrate at its effective maximum, and then the eye is filmed with an infra-red camera (Sony Handicam ® range). A ruler is held next to the eye to allow scaled measurements to be taken digitally using ImageJ software (Figure 2.5). Care must be taken when choosing the still image to take measurements from as pupil aperture can vary in size around a baseline

level after reaching dark adaptation. For example in the domestic chicken *Gallus gallus domesticus*, the pupil dilates to an effective maximum after being held in the dark for several minutes, but the pupil does not remain stable at the same dilation. It dilates and constricts around a baseline dilation level consistent with the pupil aperture after acclimatising to the dark conditions (Figure 2.6). Therefore the footage of the eye must be viewed for a period of time to allow the viewer to assess the mean pupil aperture. This “pupil noise” has been described in humans (see Stark, Campbell and Atwood, 1958) and may be correlated to blood pressure, heat stress and respiratory fluctuations (Calcagnini *et al.*, 2000; Borgdorff, 1975). Therefore it may be more pronounced at times of stress (Cabanac and Guillemette, 2001). To minimise stress effects, the bird is restrained throughout the photography session using standard holding positions and is released promptly after all photography is completed, within timescales recommended in UK bird ringing protocols (Redfern and Clark, 2001).

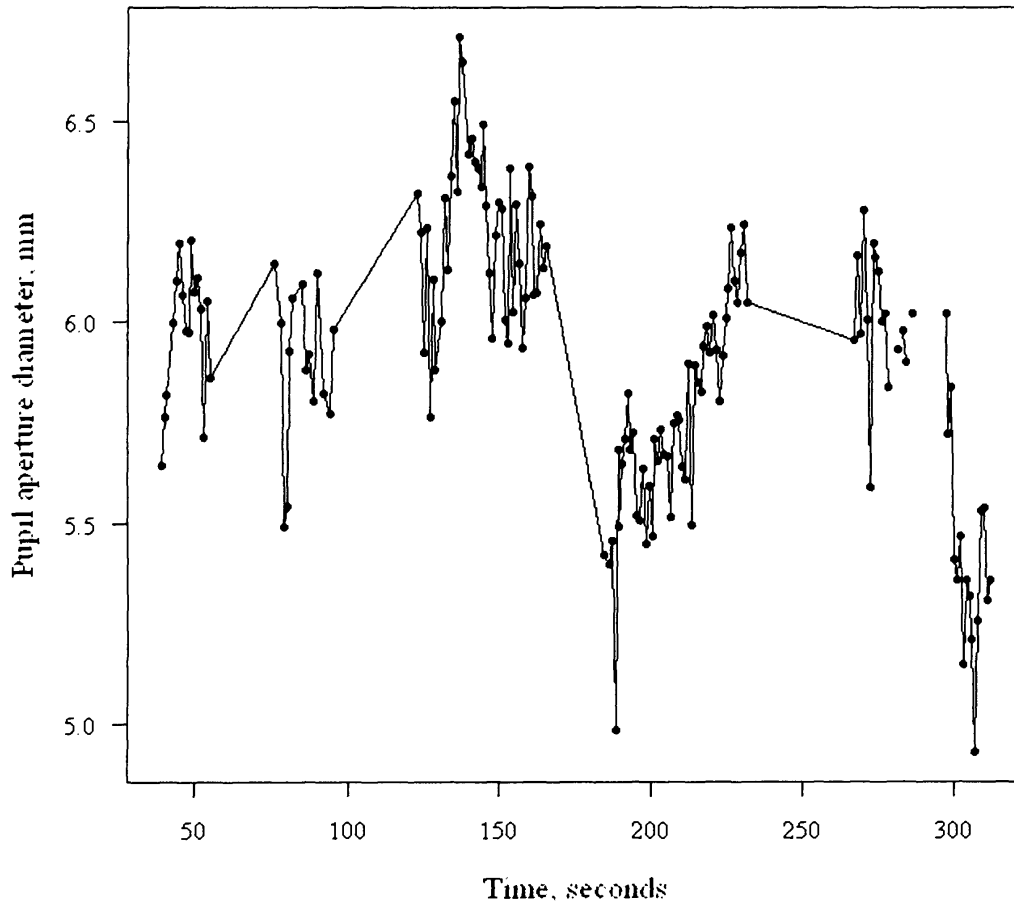


Figure 2.6. Pupil aperture diameter fluctuates over time. Data from domestic chicken held in a dark room ($N = 1$, mean diameter = 5.91 mm, range = 4.93 – 6.71 mm).

Equation 2.1 combines the measures of maximum pupil aperture and focal length, to calculate the estimate of maximum retinal image brightness. A great number of species can be assessed for a measure of their retinal image brightness using this technique as it is non-invasive and quick (see Appendix A.1.1 for list of species assessed). Many of the birds photographed were caught in the course of routine BTO bird-ringing, minimising the need for trapping birds specifically to measure their eyes, and thus minimising the

impacts of stress caused by capture (see Lynn and Porter, 2008, for a study on the impacts of trapping on the stress response of house sparrows *Passer domesticus*).

This simple photography-based method for estimating RIB is valuable as it is non-invasive, is easily used in the field and has now successfully been used on a wide variety of species. Some caution is needed, however, in the use and interpretation of such data. Scaled photos allow only an approximation of focal length to be measured as the angle of the convergence of the eyes and the width of the septum between the eyes cannot be accurately assessed. However, measurements from MRI scans can be used to check the assumptions outlined above, and to validate the method in general (see below for adjusted calculations).

Refinement of the calculation of retinal image brightness

As described above, Equation 2.1 is useful in providing estimates of retinal image brightness in non-laboratory conditions and in live birds. However, this equation makes two key assumptions; (i) that the septum between the eyes is uniform between species (at 1 mm), and (ii) that the eyes are oriented at 90 degrees to the anterior-posterior axis of the head. In this section, I use measurements from MRI scans of bird heads, to assess the validity of these assumptions.

(i) Measuring the width of the septum between the two eyes

The assumption made in Equation 2.1, that the septum (i.e. the gap between the retinas of the two eyes) is 1 mm, seems unlikely to be valid across all species as overall body size varies by several orders of magnitude between avian taxa. The septum is comprised of

bone and/or connective tissue, and initial dissections indicated that the dimensions of these appeared to vary between different species (personal observations).

Morphological measurements from MRI scans

a) Width of the septum separating the two eyes

The minimal distance between the choroid of each eye was measured from MRI scans (transverse orientation) and linear models were used to assess the relationship between the septum width and body mass (Dunning, 2008), as it was noted in handling the skulls that smaller birds often had thinner (or no) bony septum than larger birds. Septum width was found to be variable between species in this sample ($n = 19$ species, $SD = 1.503$, minimum: Willow warbler *Phylloscopus trochilus* 0.759 mm; maximum: leach's petrel *Oceanodroma leucorhoa* 5.603 mm). A tawny owl *S. aluco* was excluded from this analysis, due to the tubular shape and forward-facing orientation of the eyes of owls. Therefore, the septum width in owls cannot be estimated in the same way as it can be for birds with the more usual eye shape (spherical-flattened) and orientation (lateral).

The median septum width across all species measured was 2.000 mm. However, septum width was significantly and positively associated with overall body mass ($N = 19$ species, adjusted $R^2 = 0.515$, $F_{1,17} = 20.11$, $P < 0.001$). Equation 2.2 and Figure 2.9 show the relationship between septum width and body mass.

$$y = (0.399 x) - 0.707 \quad \text{Equation 2.2}$$

where y = natural log transformed septum width (mm)

x = natural log transformed body mass, g.

Wilcoxon signed rank tests revealed that the septum widths calculated by Equation 2.2 (median: 1.613) were not significantly different from the actual septum widths measured from MRI scans (median: 2.000), but were highly significantly different from a standard value of 1 mm as used in the original calculation (Equation 2.1) (real septum vs. calculated septum value: $V = 79$, $N_1 = N_2 = 19$, $P = 0.541$; real septum vs. calculation using a standard 1 mm septum: $V = 184$, $N_1 = N_2 = 19$, $P < 0.001$). The minimum septum distance is related to the assumed septum width as in Figure 2.10 and Equation 2.3. The refined calculation for estimating retinal image brightness can now be expressed as in Equation 2.4.

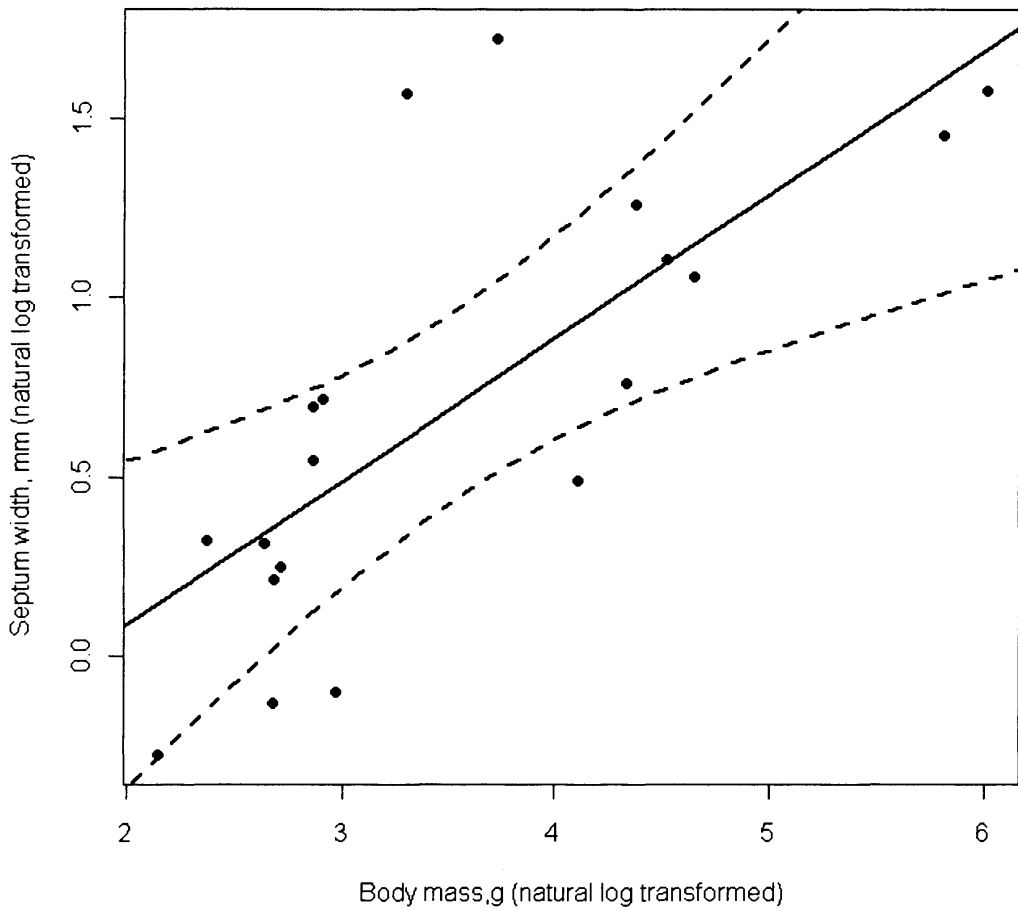


Figure 2.9. The relationship between avian body mass and width of the septum separating the orbits. Dashed lines represent 95% confidence limits (based on R package “car: Companion to Applied Regression” by Fox, 2009).

$$bx = (ab/2)/\sin x = f + f'$$

$$f' = \text{Exp} (0.399 \ln (\text{body mass}) - 0.707) / 2 / \sin x$$

$$B = f' (\sin x)$$

$$C = (bx - f') / 2$$

$$A = (C + f') (\sin x)$$

$$S = A - C$$

Equation 2.3

where the letters correspond to those in Figure 2.10.

$$\text{Focal length (mm)} = 0.63 ((\text{cornea to cornea distance} - (\text{Exp} (0.399 * \ln (\text{body mass}) - 0.707))) / 2)$$

$$\text{RIB} = 1 / (\text{Focal length} / \text{pupil diameter})^2$$

Equation 2.4

(ii) Measuring the orientation of the eyes in the head

Another possible refinement to Equation 2.1 would be to include information on the orientation of the eyes. Equation 2.1 assumes that the eyes are aligned exactly laterally, so that the axes of both eyes run along the same straight axis perpendicular to the axis of the head. However, it is well understood that the degree of ocular convergence (i.e. the degree to which the optic axes deviate from parallel) varies between species. For example, the domestic pigeon *C. livia* has a relatively large binocular field (22° wide) when compared with other species, for example the Manx shearwater *P. puffinus* (11° wide) (Martin and Brooke, 1991). Martin and Katzir (1999) suggest that such differences are associated with foraging method, so that species requiring visual inspection of food

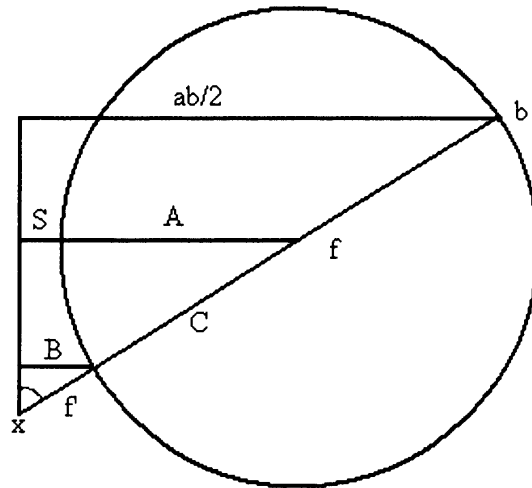


Figure 2.10. The relationship between the assumed septum width ($2B$) and the minimum septum width ($2S$) is found, assuming at least the posterior half of the eye is spherical, by Equation 2.4. Angle x = angle of convergence, $ab/2$ = cornea to cornea distance/ 2, B = assumed septum width/ 2, C = radius, f = axial length, S = minimum septum width/ 2. Other letters indicate terms used within Equation 2.3.

items and those that use precision foraging techniques (i.e. pecking) have larger binocular fields (thus more frontally facing eyes) than those that employ tactile or chemical foraging methods, or those that do not provision their chicks (Martin, 2007). Owls generally have very wide binocular fields: for example, Tawny owls have a binocular field of approximately 50° (Martin, 1984). This may not be primarily due to nocturnality alone, as two other night-active species; oilbirds *Steatornis caripensis* and pauraques *Nyctidromus albicollis*, have binocular fields of 38° and 25° respectively (Martin *et al.*, 2004). While owls may use their feet to grab mobile prey, bringing their feet into their binocular field prior to capture (implying a precision based visual foraging method),

these factors alone do not explain the large binocular fields present in owls. Owls generally have a highly developed auditory capacity, often locating prey items using hearing alone (Knudsen, 1981). The area of highest auditory accuracy is known to be within the binocular field and so owls may require such a wide binocular area in order to ensure that binaural and binocular cues can be fully overlapped (Martin and Katzir, 1999). Skull size may also constrain ocular orientation, so that the large auditory brain areas of owls may force the eyes into a more frontal position (Martin, 2007).

Measuring the angle of the orientation of the eyes (see Figure 2.11) is relatively simple using the images produced from MRI scans and from dorsal views of skulls. When the angle of convergence is known (for those used in this study, see Appendix A .1.2), the focal length can then be calculated as in Equation 2.5. Utilising this refined calculation to estimate retinal image brightness allows both the width of the septum and the angle of convergence to be incorporated into the estimate of RIB_{max} .

Figure 2.12 was constructed by applying Equation 2.5, using hypothetical angles of convergence of 45° , 60° and 90° (i.e. the angle assumed for the basic RIB calculation in Equation 2.1), to illustrate how the angle of convergence affects the retinal image brightness estimate, if the angle of convergence actually differs from the assumption of 90 degrees. Figure 2.12 shows that assuming an angle of convergence of 90° inflates the estimate of the true retinal image brightness of eyes converging at 45 degrees by over 200 % (using mean values).

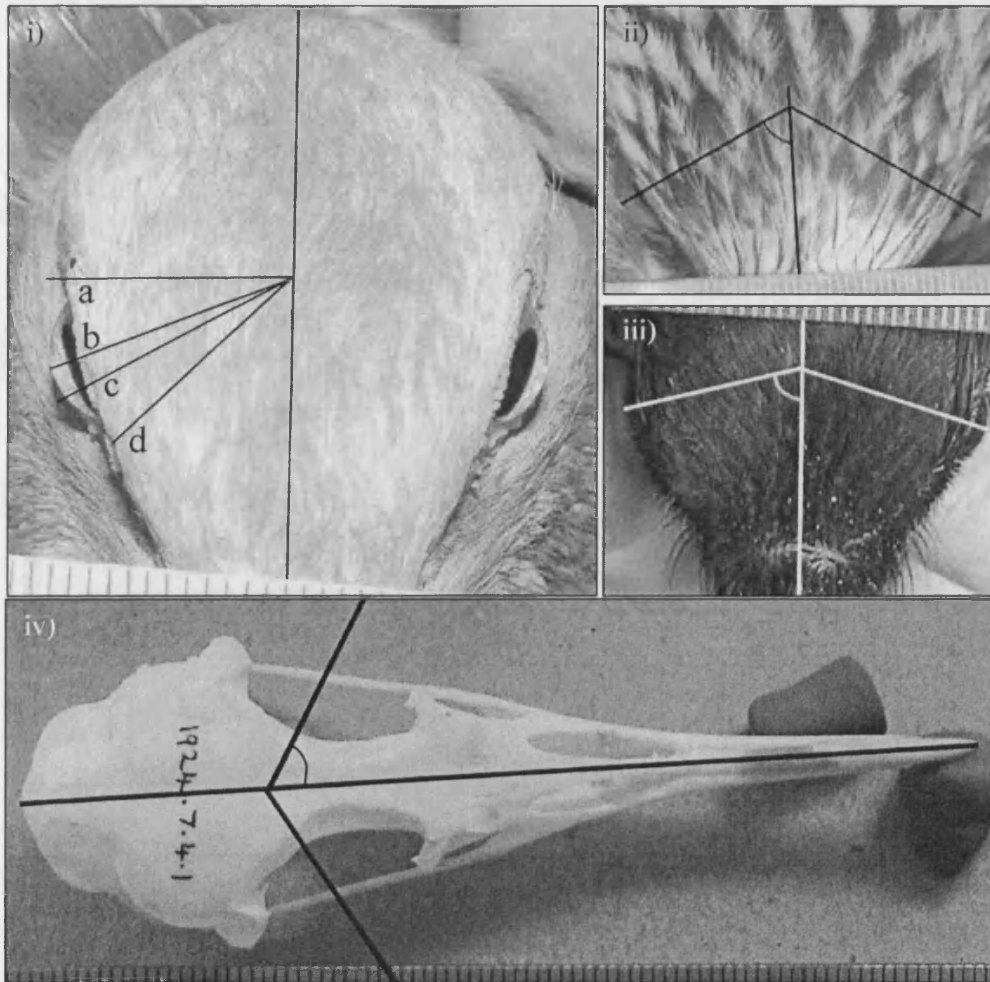


Figure 2.11. Measuring convergent angles: i) domestic pigeon *Columba livia* (angle a = 90° , b (actual measurement) = 68.02° , c = 60° and d = 45°); ii) red kite *Milvus milvus* (59.29°), iii) magpie *Pica pica* (73.53°) and iv) Manx shearwater *Puffinus puffinus* (57.68°). The angle from a skull is measured by drawing the midline and taking the angle from the position of the back of the eye socket at the deepest point on the midline to the estimated optic axis line. The angle derived here is similar to that found in Martin and Brooke's (1991) study on the visual fields and optical structure of the Manx shearwater (59.5°).

$$\text{Focal length (mm)} = 0.63 \left(\frac{ab}{2} / \sin x \right) - \left(\frac{\left(\exp(0.399 \ln(\text{body mass}) - 0.707) \right) / 2}{\sin x} \right)$$

$$\text{RIB} = 1 / \left(\frac{\text{Focal length}}{\text{pupil diameter}} \right)^2 \quad \text{Equation 2.5}$$

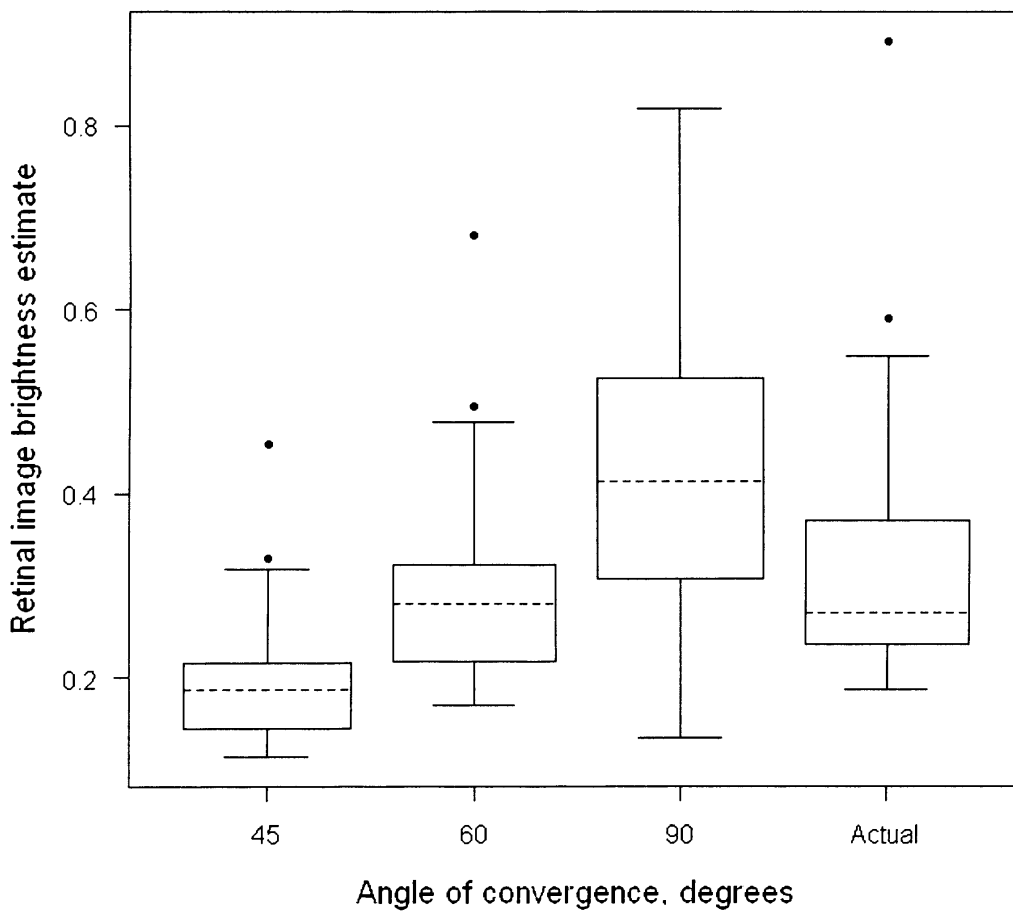


Figure 2.12. Constructing estimates of retinal image brightness using Equation 2.5, with hypothetical angles of convergence (45°, 60°, 90°) and actual angles of convergence measured from MR images and skulls (see text for details).

As birds vary considerably in their ocular convergent angle, assuming a 90 degree angle of convergence may therefore lead to misleading estimates of RIB for many taxa. However, by utilising previously published angles of convergence for different species, by measuring eye orientation in skulls or by estimating the angle from photographs (Figure 2.11), the estimate of retinal image brightness can be refined further.

Constituent eye structures: Measuring retinal design

Estimating the brightness of the image falling on the retina, as described above, does not provide a complete description of the eye's visual capabilities, since visual sensitivity and resolution (as well as other capabilities such as colour perception and motion detection), depend critically on how the retinal image is captured and processed. Studies of the retina's structure and function are therefore important in understanding visual capabilities and constraints. Using a comparative approach to measuring retinal structure also allows interspecific differences in retinal composition to be related to behavioural parameters, such as the timing of activity.

Several approaches have been used to investigate retinal structure and function.

- (i) Whole-mounted retinas are useful for examination of the entire retina. Stone, (1981) gives detailed methodology for the preparation and analysis of retinal whole-mounts. Such whole-mounts have been used, for example, to compare retinal ganglion cell densities in different regions of the retina of the common quail *Coturnix coturnix japonica* (Budnik *et al.*, 1984), or to investigate the

distribution of efferent neural fibres in the domestic chicken retina (Lindstrom *et al.*, 2009).

- (ii) Thin (10 – 100 nm) or semithin (0.25 – 0.5 μm) retinal sections are used in neural connectivity studies (Cohen-Cory and Lom, 2004), and in pathological studies. For example, Zeiss and Dubielzig (2006) used such preparations to observe that lentoids (lens-like crystalline structures) form in the retina of several different avian species, arising from Müller glial cells following retinal lesion.
- (iii) Homogenized retinas are used to investigate the chemical composition of cell contents, for example, in the study of the retinoid cycle (Muniz *et al.*, 2009).

Two recent studies have related retinal structure to the timing of behaviours such as singing and foraging: McNeil, McSween and Lachapelle's (2005) study found that all retinal layers examined, except the outer plexiform layer, were found to vary in thickness in different locations within the same retina and also between the species studied. Specifically, American robin *Turdus migratorius* and hermit thrush *Catharus guttatus*, which start to sing very early at dawn, have thicker inner nuclear and inner plexiform layers than common grackle *Quiscalus quiscula* or mourning dove *Zenaida macroura*, which start to sing later. The outer nuclear layer is thickest in the hermit thrush *C. guttatus*. Rojas *et al.*, (1999) studied the retinas of six wading bird species differing in their activity patterns (yellow-crowned night heron *Nycticorax violaceus*; great blue heron *Ardea Herodias*; roseate spoonbill *Ajaia ajajal*; cattle egret *Bubulcus ibis*; tricolored egret *Egretta tricolour*; and American White Ibis *Eudocimus ruber*). They

found that the species adopting active pursuit mechanisms of obtaining their prey (cattle egret *B. ibis* and tricolored egret *E. tricolour*) had thickened areas of outer nuclear, inner nuclear and inner plexiform layers. The thickening of these layers may be explained by the requirement for movement detection and contrast perception in the foraging techniques of these species.

Following these recent studies on retinal structure and the timing of behaviour, I similarly used transverse semi-thin sections to examine the differences in retinal layer morphology in two species (European starling *S. vulgaris* and European storm petrel *Hydrobates pelagicus*) with reference to behaviour (see Chapter 3).

Testing the methodology – a case study

Do nocturnal species have higher retinal image brightness estimates than diurnal species and can any inference be made on the activity patterns of *Archaeopteryx lithographica*?

Introduction

In order to see under low light levels, for example by star or moonlight, the eye must be sensitive enough to gather the available light to form an image. Therefore, birds that are active under low illuminations are likely to have more sensitive eyes than their diurnal counterparts. As explained above, estimations of RIB allow a measure of such sensitivity. However, many nocturnal species have poor vision and have alternative specialised sensory capabilities. For example, the brown kiwi *Apteryx australis* has relatively poor vision but utilises its keen sense of smell (Martin *et al.*, 2007). Species that need to

discriminate detail in their food items under low light, for example in distinguishing cryptic prey, may require more sensitive vision than would species that forage upon static and invariable food items (Rojas *et al.*, 1999). In this brief study I examine how RIB estimates vary with activity pattern and diet and I relate these findings with the possible behaviour of the extinct *A. lithographica*.

A. lithographica, while unlikely to be a direct ancestor of modern birds, is considered to be the first avian in the fossil record, showing several avian characteristics such as feathers (Feduccia and Tordoff, 1979), pronounced optic lobes of the brain (Alonso *et al.*, 2004) and flight capabilities (Norberg, 1985). It is therefore of considerable interest in terms of eye design, as it can potentially provide insights into the visual capabilities, and hence the behaviour, of birds early in their evolutionary history.

Only ten *A. lithographica* specimens have been found so far, and each fossil is different in size and is incomplete in some way. Very little can be noted about the behaviour of this species due to its fossil nature, however the limb structure and braincase suggests it was, both neurally (Alonso *et al.*, 2004) and anatomically (Norberg, 1985), capable of flapping flight. Due to its claw structure and lack of a reversed toe (therefore unable to perch very well), it was likely to take prey from the ground or by climbing tree trunks (Glen and Bennett, 2007; Mayr *et al.*, 2007) and it has teeth that are capable of slicing larger prey items (i.e. prey that cannot be swallowed whole), and which are similar to marine predators, suggesting that it was capable of catching relatively large invertebrate or vertebrate prey (Paul, 2002). Here I test the hypothesis that *A. lithographica* was a diurnal species, following related studies by Schmitz *et al.* (2007) and Hall (2008).

Methods

Similarly to Hall (2008), I used the Berlin specimen (plaster cast, photographed with permission from the British Museum of Natural History, London), which has a clearly visible, right side sclerotic ring present. I took calliper measurements of the inner sclerotic ring to obtain the maximum possible diameter of the pupil aperture. Hall observed that the sclerotic ring inner diameter can be used as an approximation of the corneal diameter with these variables being highly correlated ($r^2 = 0.936$). As the axial length of the eye cannot be estimated through the fossil plaster cast due to the way in which the specimen is lying, I used a scale diagram of the skull (Figure 2, in Houck *et al.*, 1990), where the skull had been reconstructed using all available specimens. This reconstruction was to examine the size differences present in the specimens and so this was considered in my calculations: Orbit depth was found to increase with ontogeny by a factor of 1.63, with younger individuals having shallower orbits than older individuals. Houck *et al.*'s Figure 2 corresponds with a larger individual (London or Solnhofen specimens) and so measurements derived from this reconstruction must therefore be scaled down to the proportions of the Berlin specimen by a factor of 0.8, as the Berlin specimen is thought to be a juvenile.

I compared the results from the *A. lithographica* specimen with a dataset of extant species retinal image brightness estimates, measured using the photographic method described above. Between 1 and 9 individuals were measured for each species (mean = 1.74 individuals). Retinal image brightness is a highly and significantly repeatable measure within each species (repeatability analysis using 32 different passerine and non-passerine species estimates of retinal image brightness: $r = 0.741$, $F_{31,52} = 8.49$, $P <$



0.001), and so using single specimens as representative of a species is not detrimental to the analyses.

Extant species were split into either nocturnal or diurnal groupings, or a category which includes species that are active both at night and during the day. These categories were determined by the literature (del Hoyo *et al.*, 1992 - 2008; BWPi, 2007) or through eye witness accounts (E. O'Brien, Dublin Zoo). The nocturnal category also included nocturnal-crepuscular species (two caprimulgid species). Similarly, the species were assigned a diet category according to their food type, based on the same literature sources. Where species are known to consume several food types, the principal type is used in these analyses. Analyses were completed using Kruskal-Wallis tests and Nemenyi-Damico-Wolfe-Dunn test for multiple comparisons (Hollander and Wolfe, 1999) within significant results, using R (R Core Development Team, 2005; packages: coin, Hothorn *et al.*, 2009; multcomp, Hothorn, Bretz and Westfall, 2008).

Results

A. lithographica had an approximate maximum retinal image brightness of 0.422, with an estimated corneal diameter of 6.823 mm. I found that nocturnal species had significantly larger RIB_{max} estimates than either diurnal species or those that are active both at night and during the day (Figure 2.7; nocturnal+diurnal, N = 4: median = 0.281, maximum = 0.522, minimum = 0.126; nocturnal, N = 6: median = 0.782, maximum = 1.160, minimum = 0.597; diurnal, N = 58: median = 0.406, maximum = 0.797, minimum = 0.126. Kruskal-Wallis test: $\chi^2 = 16.006$, $df = 2$, $P < 0.001$, Nemenyi-Damico-Wolfe-Dunn test for multiple comparisons: p-value Nocturnal+diurnal vs. Nocturnal < 0.001 , $P_{Diurnal vs. Nocturnal} = 0.004$).

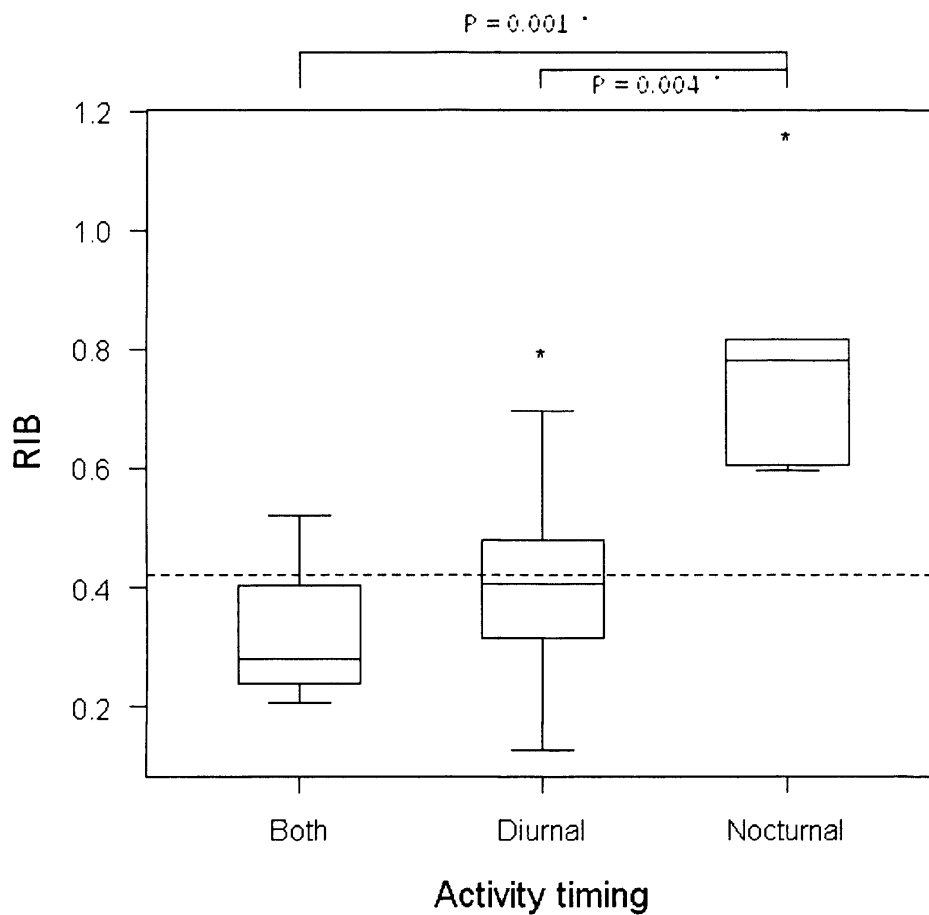


Figure 2.7. Retinal image brightness estimates for a range of avian species with different activity timings. Nocturnally active birds have significantly larger RIB estimates than either diurnally active or those species which are active both at night and during the day. The dashed line represents where *A. lithographica* would be placed. Significant relationships are marked above the boxplot.

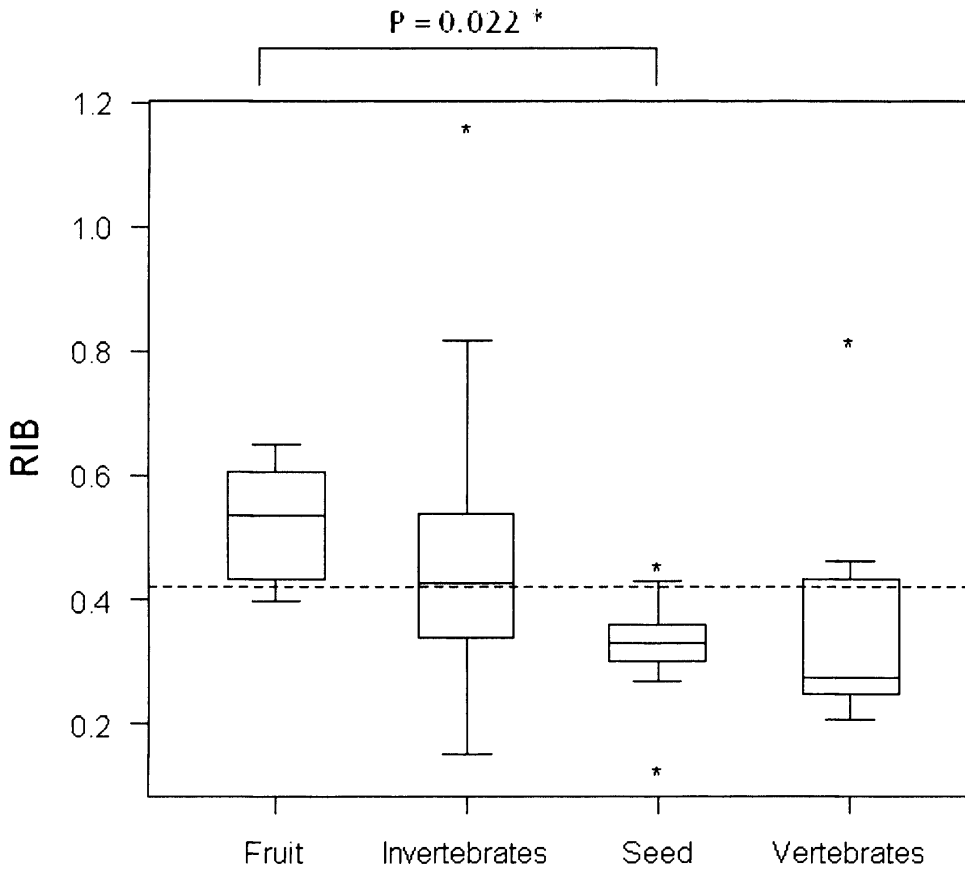


Figure 2.8. Retinal image brightness estimates for a range of avian species with different diets. “Fruit” includes nectar, and “Seed” includes nuts and grain ($N_{\text{Invertebrate}} = 46$, $N_{\text{Seed}} = 9$, $N_{\text{Vertebrate}} = 7$, $N_{\text{Fruit}} = 6$). The dashed line represents where *Archaeopteryx lithographica* would be placed. The significant relationship is marked above the boxplot.

Also, birds which forage upon fruit have significantly larger RIB estimates than do those that forage upon seed (Figure 2.8., Kruskal-Wallis test: $\chi^2 = 10.2071$, $df = 3$, $P = 0.017$, Nemenyi- Damico-Wolfe-Dunn test for multiple comparisons: $P_{\text{Seed vs. Fruit}} = 0.022$). No other dietary categories were significantly different from each other. Note that

these comparisons treat values for different species as statistically independent data points, but RIB_{max} , the timing of activity and diet may each be phylogenetically constrained (Harvey & Pagel, 1991). The sample sizes for RIB_{max} for non-diurnal species obtained in this study were too small for phylogenetically corrected analyses to be conducted, but a full phylogenetic comparative analysis of eye design in relation to the timing of activity is presented in Chapter 4.

Discussion

The RIB estimate obtained for *A. lithographica* placed this species close to the median of the diurnal species category, and outside the range of the nocturnal category (although it does fall within the interquartile range of the nocturnal+diurnal category). However, no conclusions can be drawn regarding dietary habits due to the RIB estimate ambiguously falling within the range for all four food types.

While not surprising that nocturnally and crepuscularly active species have higher RIB estimates than diurnal species, it is interesting that birds that are active both at night and during the day do not have intermediate RIB estimates. Within this category are four species (European storm petrel *Hydrobates pelagicus* $RIB_{max} = 0.26$, Manx shearwater *Puffinus puffinus* $RIB_{max} = 0.26$, herring gull *Larus argentatus* $RIB_{max} = 0.21$, common nightingale *Luscinia megarhynchos* $RIB_{max} = 0.45$) which are perhaps “special cases,” requiring an individual explanation of their activity timings. Both the European storm petrel (see Chapter 3) and the Manx shearwater are predated upon by gulls and due to the risk of attack when coming ashore to their breeding colonies, are nocturnal during this stage of their live history (Brooke and Cox, 2004). However, both are also active by day, spending this time foraging out at sea (Martin and Brooke, 1991; Thomas, Medeiros and

Pollard, 2006). A relatively low RIB estimate for both of these species may be due to them having olfactory specialisations (Bonadonna and Francesco, 2009) and therefore they may not be reliant on vision alone for survival.

Many *Larus* sp are noted to forage both by night and day and herring gulls have been noted scavenging from fishing boats nocturnally and diurnally (Garthe and Huppopp, 1996). Emond *et al.*, (2006) found that in *Larus delawarensis* and *Larus modestus*, while their retinas were cone rich (cone: rod = 3:1 in central retina, 2:1 elsewhere), unlike strictly diurnal species, they have a uniform distribution of rods throughout the retina. This adaptation is likely to allow a good level of resolution and sensitivity throughout the visual field. This may also be the case for the closely related herring gull.

Common nightingales are active both night and day: Male nightingales sing nocturnally to attract a mate, diurnally to defend their territories, while females visit prospective mates nocturnally and both forage during the day (Amrhein, Korner and Naguib, 2002; Roth *et al.*, 2009). Their RIB estimate of 0.522 is the highest in this category and, as it is above the median value for diurnal species, is intermediate between nocturnal and diurnal RIB estimates.

The main difference between species that consume fruit and those that consume seed perhaps lies in the habitat in which they live. The frugivorous species included in these analyses were typically tropical species, living in forest habitats. It is known that some birds are able to choose fruit based on its colour, recognising the antioxidant levels within it (Schaefer, McGraw and Catoni, 2008), and as colour perception is a visual task, the visual ability of frugivorous species may be greater than species that do not need to take visual cues from their food items. As RIB is a measure of sensitivity whereas colour perception is usually associated with cones (and therefore acuity), this explanation may

seem counter-intuitive. However, discriminating ripe (usually darkly coloured) fruit from a dark background, under the forest canopy may require high levels of sensitivity.

In a comparison with the overall eye sizes of other non-passerine species, Hall found *A. lithographica* to have an activity pattern intermediate between nocturnal and diurnal (tending towards diurnal), and did not draw any firm conclusions due to the error in measurement and low sample size of available fossil specimens. Schmitz *et al.* (2007) presented research on the London specimen, scaling the measurements taken down to the proportions of the Berlin and Eichstatt specimens. However, they also did not find any conclusive evidence of activity pattern due to the errors involved in the calculations. Also, there is no clear indication whether the birds that Schmitz and colleagues compared *A. lithographica* with were passerines, non-passerines or a combination of the two. While I have not used independent contrast analysis in this section, I have used it in Chapter 4, in the analysis of eye size and retinal image brightness estimates in relation to the timing of dawn song, where I found that species level analyses were similar to phylogenetically independent contrasts. Therefore the use of species level analysis here seems justified.

Similarly to Hall (2008) and Schmitz *et al.*, (2007), the error in the calculation must be considered, due to the fossil nature of the specimen, however all three studies so far completed suggest that *A. lithographica* is likely to be diurnal.

Chapter 3 How does a night-migrating bird differ in its visual ability when compared to a diurnally active species?

Abstract

In this chapter, I compare the visual capabilities of two species of bird: the European storm petrel *Hydrobates pelagicus* and the European starling *Sturnus vulgaris*, by studying their gross eye morphology and their retinal design. These two species were chosen for comparison due to their overall similarity in body size, eye size and gross eye design, but the striking difference in the timing of their foraging and breeding activity, which suggests that they are faced with activity under very different visual constraints. Both species are, however, capable of nocturnal as well as diurnal migration and so have to navigate under similar visual constraints at this stage of their annual cycles. The association between these similarities and differences in ecology, and the design of the eyes of the two species, is the focus of this chapter. I found that the storm petrel retina is better adapted to vision under low-light level than the starling retina, due to its longer photoreceptor outer segments and thicker outer plexiform layer, compared to the starling, which had thicker inner and outer nuclear, and inner plexiform layers, consistent with adaptations to a more diurnal way of life. The retinas of both species showed topographic variation in the thickening of retinal layers, implying there are areas of specialisation within each retina.

Introduction

Behaviour & Ecology

European storm petrels (henceforth “storm petrels”) are members of the avian order Procellariiformes and are the smallest of the Atlantic seabirds (18.4 – 31.0 g), as well as being among the smallest of the Procellariiformes (at the other extreme within the order is the wandering albatross *Diomedea exulans* at 6000 – 11000 g). Storm petrels spend much of their time feeding at sea on small fish, zooplankton, oily/fatty material (floating on the water surface), crustaceans and ships’ garbage. They forage by both day and night and studies have shown that the proventriculus contents often contain nocturnally active intertidal and pelagic crustacean species. These include prey species which are nocturnal vertical migrants to the sea surface, providing strong evidence of regular nocturnal foraging by storm petrels (D’Elbée and Hémery, 1997, Thomas, Mediros & Pollard, 2006). Storm petrels also migrate both nocturnally and diurnally, flying long distances from wintering grounds off southern Africa to breed in the Northern hemisphere (centred on the British Isles, Faroes and Iceland), covering 1-200 km per day. Storm petrels breed and nest on land in previously occupied burrows and rock crevices, in unsheltered and undisturbed areas, coming ashore nocturnally to prospect for nest sites, or to attend their nests, eggs and chicks (Cramp, 1977; Cramp, Perrins and Brooks 1994; Fowler, 2002).

European starlings (henceforth “starlings”) are members of the order Passeriformes, and though at 78g are heavier than storm petrels, they have comparable wing lengths (storm petrel: 360 – 390 mm; starling: 370 – 420 mm). While storm petrels are sexually monomorphic (Medeiros R., pers. com.), female starlings are smaller than males (body mass_{male} ~ 87g, body mass_{female} ~ 82.5g).

Starlings are opportunistic in their foraging habits taking invertebrates, fruits and seeds from a range of habitats including intertidal zones, low density forest, sewage treatment sites and urban areas. Urban areas generally support a resident population of starlings, but starling populations in the northern and eastern parts of their Eurasian breeding range migrate (both nocturnally and diurnally) to wintering grounds in western or southern Europe, northern Africa (north of Sahara), the middle east, and to the northern plains of India (Cramp. 1977, Cramp, Perrins and Brooks 1994). Like most passerine birds, starlings are diurnal foragers, and there are no records in the literature of starlings foraging during the middle part of the night.

Nocturnal migration

Both storm petrels and starlings are capable of both diurnal and nocturnal migration (Gwinner, 1975; Martin, 1986a; BWPi, 2007). Most otherwise diurnal birds that carry out long distance migrations do so at night (at least in Europe) and this strategy offers several advantages over daytime migration:

- 1) Nocturnal migration allows birds to keep restoring energy supplies at times where foraging is profitable and efficient (i.e. during the day) whilst travelling sufficient distances to reach their destination quickly and economically (Schmaljohann *et al.*, 2008).
- 2) As water is a limited resource for many migrants, minimisation of water loss is vitally important. Therefore, flying at night in cool air allows a reduction in loss of water by evaporation (Schmaljohann *et al.*, 2007).

- 3) The costs associated with the powering of flight by flapping flight are lower at night due to the diel fluctuations in air temperature and density. At night, birds (particularly heavy or large birds) are able to benefit from the cool dense air, and reduce their energetic costs of turning muscle action into forward momentum (Kerlinger and Moore, 1989)
- 4) Wind at night is more laminar than during the daytime, with peaks in daytime turbulence occurring especially at times of spring and autumn migration. By flying at night, costs associated with maintaining the correct flight path in variable wind conditions can be minimised (Kerlinger and Moore, 1989).
- 5) Predation risk is thought to be lower at night (Mukhin *et al.*, 2009; c.f. Kerlinger and Moore, 1989), with only one nocturnal predator documented as specialising on nocturnal migrants: Analysis of greater noctule bat *Nyctalus lasiopterus* fecal pellets revealed that this species preys upon migrating passerines during the peak migration periods and insects for the rest of the year (Ibáñez *et al.*, 2001).

Several ideas have been put forward to explain how birds manage to successfully utilise their senses in order to orientate and navigate nocturnally. Olfaction seems especially important for the Procellariiformes, perhaps allowing them to follow defined regions of scent for example an ocean ridge, where productivity is high resulting in odour plumes (Nevitt, 2008). Use of star and geomagnetic compasses requires a degree of visual sensitivity in order to operate successfully. Migratory songbirds have been found to have a specialised brain region active only at night in processing visual information (Mouritsen *et al.*, 2005; Solov'yov and Greiner, 2009). Neural integration of olfaction and visual information, coupled with a longitudinal navigation system (Chernetsov,

Kishkinev and Mouritsen, 2008) may occur to provide a more complete representation of the environment by night. Neither starlings nor storm petrels have been studied specifically as yet with reference to their method of nocturnal navigation, although it is known that starlings are unlikely to use polarised light in day time migratory movements (Greenwood *et al.*, 2003) but may use olfaction for longer journeys (Wallraff *et al.*, 1995).

Timing of activities

Whilst both species can migrate by night, the timing of their behaviour for the rest of the year is strongly contrasting. Storm petrels remain active at night at the breeding colony, only coming ashore to their nest burrows or sites after dark, with non-breeding birds remaining exposed in order to find a mate or breeding site. Whilst this is perhaps a strategy to minimise predation risk (Oro *et al.*, 2005), it can be exploited by great skuas *Stercorarius skua* which actively hunt storm petrels nocturnally at the petrels attend their breeding colonies on St Kilda, UK, (but this foraging behaviour is not documented at Icelandic sites), taking both European storm petrels and Leach's storm petrels *Oceanodroma leucorhoa* which make up to 40% of great skua diet (analysis of regurgitated pellets by Votier *et al.*, 2006). Gulls also predate upon storm petrels at breeding colonies, with individual gulls' predation rate positively correlated with local storm petrel nocturnal activity (e.g. specialist yellow-legged gulls *Larus michahellis*, Oro *et al.*, 2005). However, risky nocturnal activity, such as coming ashore to nest burrows, no doubt provides some protection from predation (Watanuki, 1986).

By day, storm petrels forage out at sea, often in highly productive regions where there are high concentrations of prey items, and more than likely utilising a combination

of visual cues and olfaction to locate and obtain prey. Procellariiformes are noted as having among the largest olfactory bulbs of all birds, with the Northern fulmar *Fulmarus glacialis* having twice as many mitral cells (these are cells that are involved in processing odour information and enhancing odour contrast information) than rats (Nevitt, 2008). Several studies have demonstrated that petrel species are attracted to and utilise odourous signals in their foraging strategies (Nevitt, Reid and Trathan, 2004; Bonadonna *et al.*, 2006; Nevitt, 2008). Whilst on migration, during the day, rafts of storm petrels may be seen resting and feeding offshore and dietary evidence suggests that by night they also forage upon small *Eurydice* species of isopod, both pelagically and along beaches (Medeiros, Thomas and Pollard, 2006). Martin and Price (2001) suggest that, although olfaction is important in this species in guiding Procellariiformes to an area of high prey density, vision is likely to play an important role in procurement of individual prey items (excepting perhaps the filter feeding prion species).

When starlings are not on long distance migrations, they follow a typical diurnal passerine routine, waking before sunrise, typically participating in a dawn chorus, foraging throughout the daylight hours and then roosting after a brief dusk chorus (Tinbergen, 1980). Starlings are visual foragers, utilising a specialised technique termed “prying” or “open-bill probing” to obtain their prey items from the top soil. Starlings are capable of relatively large eye movements in comparison with other similar sized birds, and are able to obtain binocular fields only 5° less than the tawny owl *Strix aluco*. This arrangement also affords starlings with an ability to remain vigilant whilst foraging, as their eye movements enable them to have a large visual field above the head (Martin, 1986a).

Current knowledge of visual capabilities

While very little is known regarding the visual abilities of the storm petrel, several studies have been completed on the starling. For example, Hart *et al.* (2000a) found that starlings have asymmetrical retinas (i.e. differences in retinal composition between the left and right eyes), implying that enhanced colour discriminations are possible by the left eye (due to increased numbers of single cones), and better movement detection abilities by the right eye (due to increased numbers of double cones).

Both the starling and the storm petrel eye seem to have similar light gathering capabilities. Martin (1986) states that the starling eye has a maximum retinal image brightness of approximately 0.28, which is similar to the pigeon and man (0.26 and 0.22 respectively). My own studies reveal that the storm petrel has very similar retinal image brightness (mean = 0.29, range 0.290 – 0.285, n = 2 individuals) to the starling. The schematic eye for the starling has been drawn (figure 4 with tables 1 and 2; Martin, 1986a), which is typical of a passerine eye shape (i.e. not globose or tubular). The eye is relatively mobile within its socket, enabling the starling's field of view to be manipulated, reducing the binocular field from 36° to 6° when oriented temporally (Martin, 1986a).

Although the storm petrel eye has not been extensively studied (c.f. Rochon-Duvigneaud, 1943), studies of other Procellariiform eyes have been published, from which information about the likely visual abilities of storm petrels can be inferred. Manx shearwater *Puffinus puffinus* eyes have a distinct visual streak containing high densities of small retinal ganglion cells, and like several other species (Kerguelen petrel *Lugensa brevirostris*, great shearwater *Puffinus gravis*, broad-billed prion *Pachyptila vittata*,

common diving petrel *Pelecanoides urinatrix*), have an area situated in the dorso-temporal area of the retina containing large sized retinal ganglion cells. The visual streak is positioned so that it is horizontally oriented (i.e. aligned with the horizon) when the bill is pointing downwards at an angle of 20° (i.e. the normal position of the head during level flight/ rest), and the peripheral area of large ganglion cells is within the binocular field region. This area may be associated with motion detection and its position within the binocular field perhaps allows quick response to catch prey or to navigate the changing water surface topography (Hayes, Martin and Brooke, 1991).

Differences between species in foraging strategy are often associated with measurable interspecific differences within the retina: white-chinned petrels *Procellaria aequinoctialis* and Antarctic prions *Pachyptila desolata* both have similar shaped binocular fields, however the positioning of the bill and the size of the field differs. The white-chinned petrel is a visually guided forager and has a relatively wide binocular field (49°) with its bill positioned near to the centre of this field. The Antarctic prion predominantly filter-feeds and has a narrower binocular field (14°) with the bill positioned towards the ventral edge of this field. These findings typify the different foraging methods employed by these species (Martin and Prince, 2001).

The retina of the wedge-tailed shearwater *Puffinus pacificus* suggests that this species is capable of colour vision, with four single cones, one double cone and one rod type photoreceptor present (Hart, 2004). This species also has a prominent horizontal visual streak similar to the Manx shearwater, and which contains highly dense cones with pale coloured oil droplets, compared with the more brightly coloured oil droplets from elsewhere on the retina. At the visual streak, spatial acuity is high and the dense arrangement and narrowed structure of the cones reduces the amount of light available

for capture by each cone. Thus having oil droplets present in the visual streak may seem counterintuitive as they would further reduce the amount of light entering the receptor (Hart, 2004).

There are many studies on the retinas of a small number of species (e.g. the domestic pigeon), but there is a deficit in the current literature relating to rarer or less easily obtainable species, such as the storm petrel. Whilst not classified as a IUCN Red List species (it is listed as Least Concern) (BirdLife International, 2009), the storm petrel is of UK amber conservation status, and there is evidence of population declines, especially as a response to rat invasion at breeding colonies (BirdLife International, 2009; de León *et al.*, 2006). Studies have also shown that artificial light causes mortalities in storm petrels, perhaps after disorientation and then exhaustion, when attracted towards a light source (although exactly why birds are attracted towards light sources remains unknown). Rodríguez and Rodríguez (2009) highlight that there is an urgent need for research in order to form mitigation measures to reduce the impacts of artificial lighting on Procellariiforms (including storm petrels). Through studying the retina of the storm petrel, an understanding of how this species uses its vision may provide some guidance for minimising the effects of nocturnal light pollution on this species.

Martin (1986) completed an extensive study on the eye of the starling, revealing valuable information on visual fields and schematic optics, and several studies have shown that retinal (and neural) lateralisation exists with behavioural implications (Hart *et al.*, 2000a; Templeton and Gonzalez, 2004; Templeton and Christensen-Dykema, 2008). However, little is known regarding the nocturnal visual ability of this normally diurnal species. In addition to its intrinsic value, potentially yielding information on how otherwise diurnally active but night migrating birds are able to navigate when on

nocturnal migration, the comparison between the storm petrel and starling retinas enables me to test the hypotheses listed below, relating interspecific differences in eye morphology and retinal design to corresponding differences in the timing of behaviour.

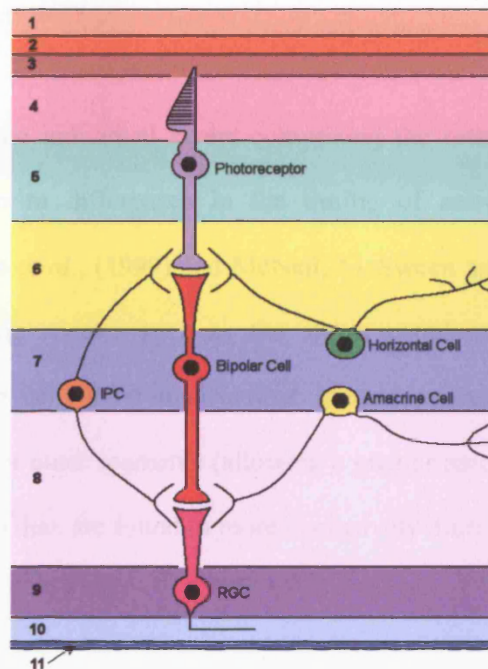


Figure 3.1. Representation of a section of vertebrate retina, showing the different layers and typical neurone locations. 1 = Sclera, 2 = Choroid, 3 = Retinal pigment epithelium, 4 = Photoreceptor outer and inner segments, 5 = Outer nuclear layer, 6 = Outer plexiform layer, 7 = Inner nuclear layer, 8 = Inner plexiform layer, 9 = Retinal ganglion cell layer, 10 = Neural fibre layer, 11 = Inner limiting membrane.

Specifically, the retinal layers of different species (Figure 3.1) may vary in thickness due to a combination of spatial constraints (i.e. large cells spread out and the layer becomes thinner overall) or increases in cells associated with neural processing. Therefore,

conclusions can be drawn regarding aspects of the species ecology and behaviour, where differences occur either between species or retinal areas.

Hypotheses

1. The thickness of the individual layers comprising the retina will vary between species in relation to differences in the timing of activity. Specifically, as suggested by Rojas *et al.*, (1999) and McNeil, McSween and Lachapelle (2005), nocturnally foraging species such as the storm petrel are predicted to have thickened ganglion cell, inner nuclear and inner plexiform layers, as well as longer photoreceptor outer segments (allowing a greater amount of photosensitive rhodopsin pigment) than are found in more exclusively diurnal species such as the starling.
2. There are specialised regions associated with high spatial resolution, in the retinas of both species, indicated by the thickening of the retinal ganglion cell layer. These are the foveas or visual streaks as documented in other studies (Martin 1986; Martin and Brooke 1990; Hayes, Martin and Brooke 1991). As the storm petrel is similar in its behaviour to the Manx shearwater, a prominent horizontal visual streak similar in to that found in Manx shearwaters is predicted to be present in storm petrels, whereas the starling retina is predicted to have a more circular area(s) of specialisation, similar to other diurnal songbirds.

Methods

Two techniques are used in this study to elucidate the visual abilities of the storm petrel and the starling. Firstly, thin sections of the eye enable microscopic analysis of retinal morphology, and secondly, magnetic resonance imaging (MRI) allows measurement of the overall morphology and orientation of the eyes within the head.

Histology

Fresh eyes were obtained from one European storm petrel (a bird-ringing casualty) and one Eurasian starling (a bird from an unmanipulated control group, euthanized as part of a study on chemical pollution; procedures completed under UK Home Office license PPL 30/2043, see Markman *et al.*, 2008 for study details). This follows the reduction principal of the “3R’s” ethical considerations, in that the starling used was also used for other studies.

The skin and feathers surrounding each eye were removed and a small temporal incision was made using a scalpel blade behind the cornea. A needle was inserted into the posterior chamber at the nasal corneal-scleral junction and the eye was gently flushed using formaldehyde solution 10% v/v in 0.9% NaCl solution (Fisher Scientific, UK). The whole head was then submerged in a container of 10% formalin saline for at least one month, until the eyes could be histologically processed. The eyes were then excised and standard dehydration and wax embedding protocols were followed (Table 3.1; carried out by Heather Phillips, Histologist, Cardiff School of Psychology).

Table 3.1. Schedule for dehydrating and embedding tissue in preparation for mounting on slides and staining. Steps 1-12 = dehydration and 13-18 = wax embedding procedures.

Step	Dehydration process/ embedding procedure	Time for each step
1	50% alcohol	30 minutes
2	70% alcohol	30 minutes
3	70% alcohol	1 hour
4	90% alcohol	2 hours
5	90% alcohol	overnight
6	90% alcohol	1 hour
7	100% alcohol	overnight
8	100% alcohol	1 hour
9	50/50 volume/volume mixture alcohol/xylene	15 minutes
10	50/50 alcohol/xylene	Overnight in fridge
11	100% xylene	1 hour
12	100% xylene	1 hour
13	Pour off most of xylene and warm by placing pot (lidded) into wax oven for 10 minutes	
14	Blot tissue on filter paper and place in wax in clean pot in wax oven	30 minutes
15	Transfer tissue to clean wax pot and leave to ensure wax has penetrated tissue	overnight in wax oven
16	Embed tissue in wax using a suitable sized mould on a refrigerated base	
17	Leave to harden and refrigerate	overnight

The eyes were sectioned sagittally (starling) and transversely (storm petrel), at 10 μm thickness. Sections were mounted on glass slides (3 sections per slide) and the sections on 1 in every 8 slides were stained with haematoxylin and eosin (the rest remained unstained and were stored). Only the left eyes were photographed and

measured. Realignment for comparison between the two retinas was done post-processing using the pecten and optic nerve as landmarks, in addition to the MRI scans (Figure 3.2).

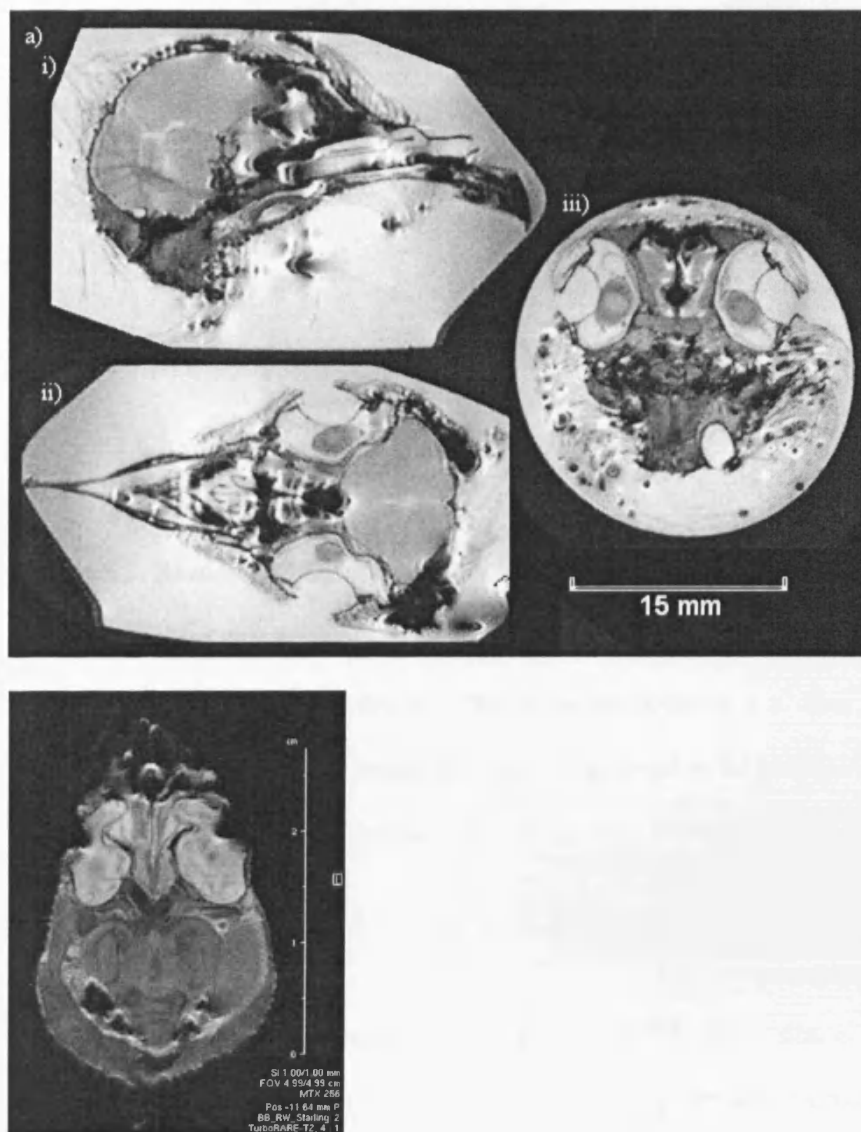


Figure 3.2. a) Storm petrel MRI scan in i) sagittal, ii) axial and iii) coronal planes of orientation and b) starling MRI scan image in axial orientation.

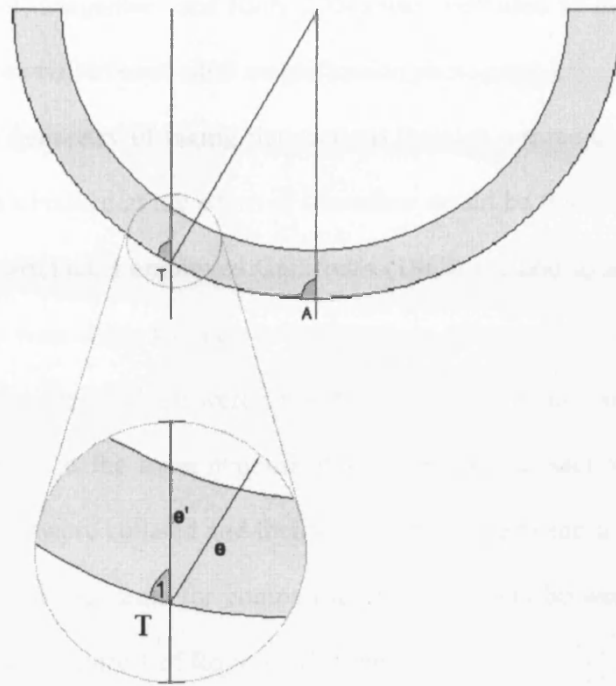


Figure 3.3. Reconstruction of the retina from off-meridian sections: The sections are cut at planes aligned perpendicular to A and T. The further from A, the thicker the sections will be due to the angle of the cut. The actual thickness $e = e' \sin T_1$. Therefore all measurements taken at planes other than the centre need to be transformed. Angle T_1 can be estimated from the total number of sections taken divided by 180° . From Gallifret, 1968.

A microscope (Axioskop, Carl Zeiss GmbH) with digital camera (Canon Powershot G6) attached was used to view and photograph approximately every fourth slide (equivalent to one section every 0.96 mm across the whole eye). A slide overview (at x 25 or x 50) magnification was photographed to provide the length of the whole retina in that section, and then each section was photographed at a higher (x400)

magnification, every 10° (Chapter 2, Figure 2.11) around the length of the retina. ImageJ software (Abramoff, Magelhaes and Ram, 2004) was then used to measure each retinal layer, in three places within each x400 magnification photograph).

Due to the geometry of taking flat sections through a three-dimensional concave retina, the sections obtained at the edges of the retina would be thicker than at the centre. To overcome this artefact, I employed Gallifret's (1968) method to adjust the thickness measurements that were made from the retinal sections (Figure 3.3). Measurements were initially recorded in pixels which were then transformed to a standard distance using a slide graticule viewed at the same magnification as the retinal sections were measured. These measurements were collated and their positions mapped onto a 2-dimensional grid that I divided into 36 segments for comparing measurements between the two species (Figure 3.4; following Figure 1 of Rojas *et al.*, 1999).

Comparisons of the two species' retinal layer thicknesses (outer segments, inner segments, outer nuclear, outer plexiform, inner nuclear, inner plexiform and retinal ganglion cell layers) were made using Wilcoxon signed rank tests or paired t-tests, where appropriate in R (R Foundation for Statistical Computing, 2008). These comparisons were made using one thickness measurement for each segment of the 2-dimensional grid described above. Thickness measurements for the two species were matched by location on this grid. Retinal topographies were computed using the complete grid-mapped dataset (i.e. not using subsamples based on segments) using the "lattice" package in R (Sarkar, 2008).

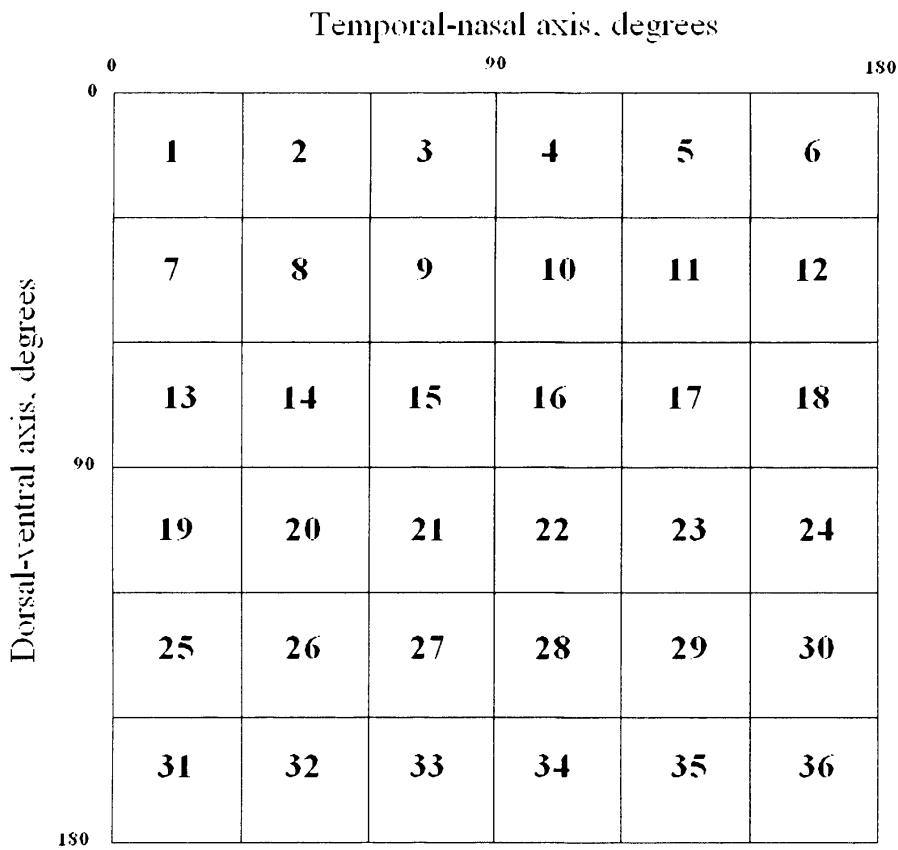


Figure 3.4. The concave retina was mapped onto a 2-dimensional grid, divided into 36 segments, to enable mapping of the thickness of the different retinal layers and comparisons of layer thicknesses between species (see text for details). The optic nerve and pecten attachment was located in segments 27 and 28 for both storm petrel and starling retinas. Dorsal is at the top and nasal is at the right hand side.

Magnetic Resonance Imaging

The starling specimen was obtained from a collection of frozen museum specimens (National Museum of Wales, Cardiff, UK). The storm petrel specimen was obtained in a similarly frozen state (Ed Drewitt, Bristol City Museum, Bristol, UK) and was

decapitated prior to scanning. Each bird's head was removed and placed in a sample tube, and then scanned.

The starling was scanned using a Turbo-Rare-T2 weighted protocol, making 50 scanned "slices" of 1mm thick, over a period of approximately 5 minutes. The storm petrel was scanned using a Turbo-Rare-3D EMRIC Scout protocol over 25 hours. There was much higher resolution derived from the longer scan and it was used to build a 3D view of the head and brain. The shorter scan was undertaken to measure basic ocular features and to locate the orientation of the eyes. ParaVision (Bruker Biospin), ImageJ (Abramoff, Magelhaes, and Ram, 2004) and Analyze (Mayo Biomedical Imaging Resource) software were used to process and measure the MRI scan data.

Results

Histology

I found several differences between the storm petrel and the starling retinas (Figure 3.5 and 3.6): The outer photoreceptor segment layer was significantly thicker in the storm petrel than in the starling (median \pm IQR_{starling} = $1.99 \text{ E}^{-4} \pm 1.48\text{E}^{-4}$ mm, median \pm IQR_{storm petrel} = $4.32\text{E}^{-4} \pm 2.46 \text{ E}^{-4}$ mm, pairwise Wilcoxon test: N = 30 matched pairs, $V = 30$, $P < 0.0001$). The inner segment (median \pm IQR_{starling} = $1.29 \text{ E}^{-4} \pm 1.03\text{E}^{-4}$ mm, median \pm IQR_{storm petrel} = $2.18\text{E}^{-4} \pm 1.96 \text{ E}^{-4}$ mm, pairwise Wilcoxon test: N = 33 matched pairs, $V = 83$, $P = 0.0004$) and the outer plexiform layer (median \pm IQR_{starling} = $1.17 \text{ E}^{-4} \pm 8.29\text{E}^{-5}$ mm, median \pm IQR_{storm petrel} = $2.72\text{E}^{-4} \pm 1.95 \text{ E}^{-4}$ mm, pairwise Wilcoxon test: N = 34 matched pairs, $V = 29$, $P < 0.0001$) was also significantly thicker in the storm petrel.

Conversely, the outer nuclear layer (mean \pm StDev_{starling} = $1.81 \text{ E}^{-4} \pm 1.01\text{E}^{-4}$ mm, mean \pm StDev_{storm petrel} = $1.13\text{E}^{-4} \pm 5.39 \text{ E}^{-5}$ mm, paired t-test: N = 34 matched pairs, df = 32, $T = 4.134$, $P = 0.0002$), the inner nuclear layer (median \pm IQR_{starling} = $4.73 \text{ E}^{-4} \pm 5.33\text{E}^{-4}$ mm, median \pm IQR_{storm petrel} = $1.60\text{E}^{-4} \pm 1.16 \text{ E}^{-4}$ mm, pairwise Wilcoxon test: N = 34 matched pairs, $V = 566$, $P < 0.0001$) and the inner plexiform layer (median \pm IQR_{starling} = $6.96 \text{ E}^{-4} \pm 5.2\text{E}^{-4}$ mm, median \pm IQR_{storm petrel} = $3.54\text{E}^{-4} \pm 3.32 \text{ E}^{-4}$ mm, pairwise Wilcoxon test: N = 35 matched pairs, $V = 507$, $P = 0.0002$) was thicker in the starling. The retinal ganglion cell layer was of similar thickness in both species (median \pm IQR_{starling} = $3.93\text{E}^{-4} \pm 4.73\text{E}^{-4}$ mm, median \pm IQR_{storm petrel} = $5.00\text{E}^{-4} \pm 4.44\text{E}^{-4}$ mm, pairwise Wilcoxon test: N = 35 matched pairs, $V = 249$, $P = 0.417$). Power analysis suggests that the non-significant result is not simply due to the sample size; a sample of 216 extra retinal sampling pairs would be needed to give a significant result at $P < 0.05$, given the observed effect size and data distributions.

Retinal layer topographies of the retinal ganglion cell and nerve fibre layer (Figure 3.7) reveal that, as expected, there is thickening towards the centre and optic nerve areas of both species' retinas. There is tentative evidence for an area of specialisation in the storm petrel retina with thickened retinal areas in the centre of the retina (see topographic maps, Appendix A 2.1 – A 2.6). Similarly thickened regions in the starling retina correspond to specialisations in the central retina (outer nuclear and inner segments) and central-nasal area (inner nuclear and inner plexiform).

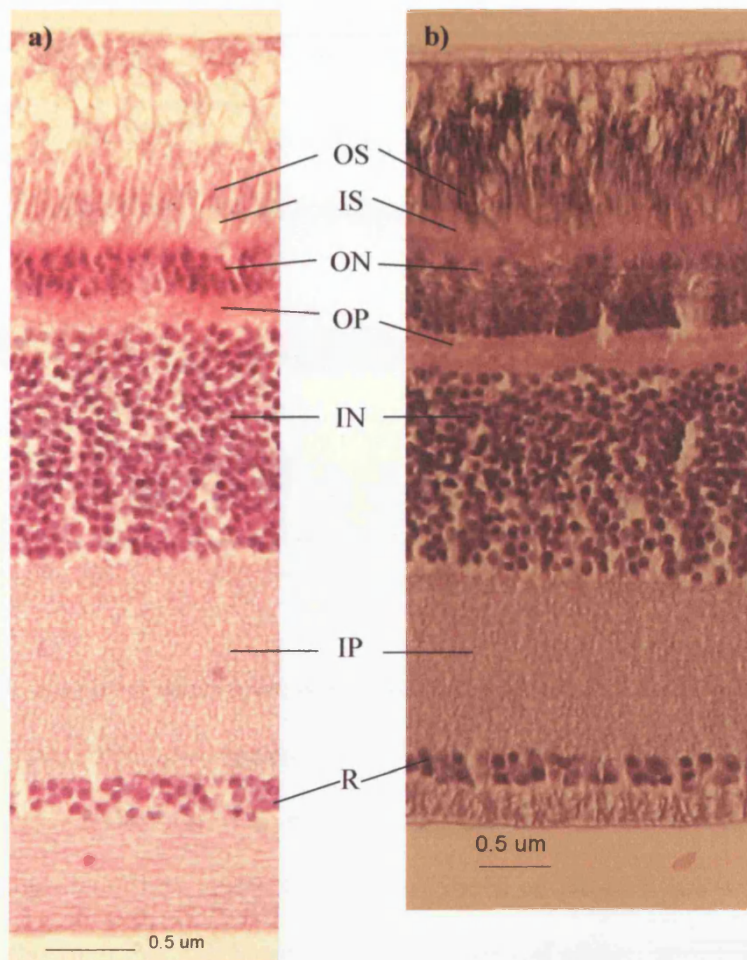


Figure 3.5. Retinal sections from the centre of the retina (i.e. at 90° on the dorsal-ventral axis and 90° on the temporal-nasal axis, top right corner of segment 21), for a) starling and b) storm petrel. OS = outer segments, IS = inner segments, ON = outer nuclear layer, OP = outer plexiform, IN = inner nuclear, IP = inner plexiform and R = retinal ganglion cell layer.

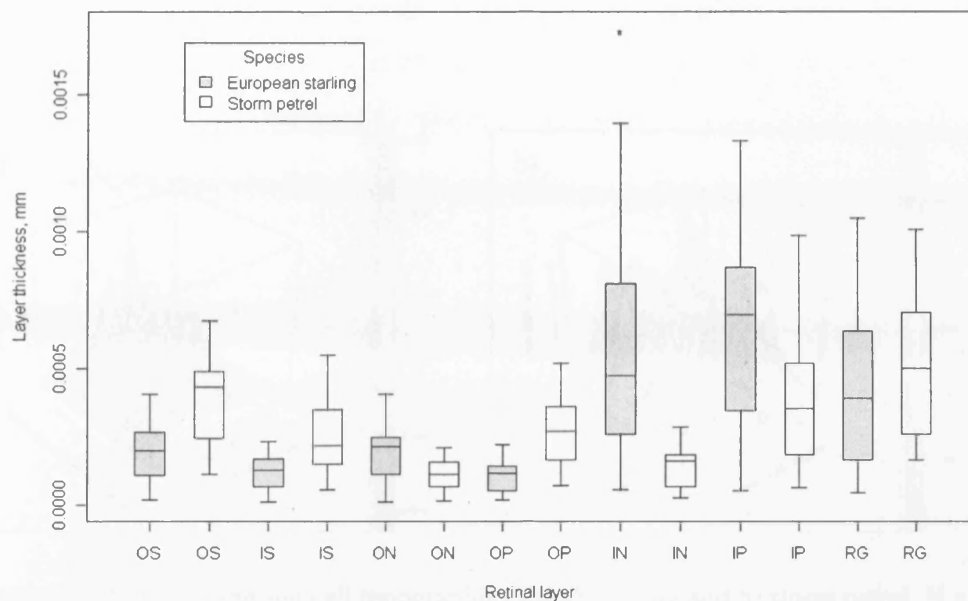


Figure 3.6. Retinal layer thicknesses of the European starling and storm petrel, where OS = outer segments, IS = inner segments, ON = outer nuclear layer, OP = outer plexiform layer, IN = inner nuclear layer, IP = inner plexiform layer, RG = retinal ganglion cell layer (including nerve fibre layer). Boxplots are based on 36 locations at the centres of the 2-D grid shown in Fig. 3.3. See main text for statistical comparisons between the two species.

Magnetic Resonance Imaging

The MRI scans images are shown in Figure 3.2. The information produced is mainly illustrative due to the low resolution of the scan that was obtained from the starling specimen. However, these scans were used to produce data for the refinement of the retinal image brightness calculations described in Chapter 2.

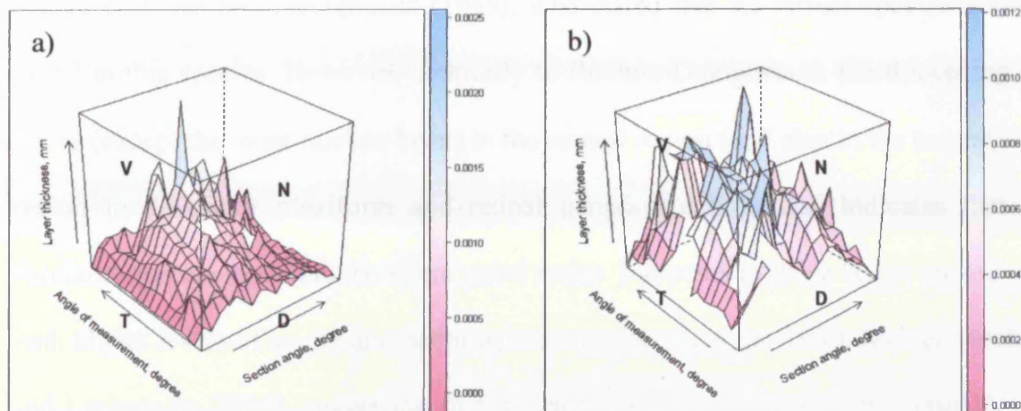


Figure 3.7. Retinal ganglion cell topographies for a) starling and b) storm petrel. N = nasal, V = ventral, D = dorsal, T = temporal (Axes: Y- Layer thickness (mm); X – Angle of measurement (degree); Z – Section angle (degree)). For other layers see Appendix A 2.1 – A 2.6.

Discussion

In hypothesis one, I suggested that marked differences in retinal layer thickness would be found between each species. Indeed, I found several major differences between the retinas of the storm petrel and the starling, namely that the outer segments, inner segments and outer plexiform layers are thicker in the storm petrel than the starling. The opposite is true for the outer nuclear, inner nuclear and inner plexiform layers, with these layers thicker in the starling. There are also major variations in layer thicknesses within each retina, indicating at least some degree of retinal specialisation. However, these findings are in contrast to Rojas *et al.* (1999).

Contrary to my second hypothesis that specialisations within the retina would exist, I did not find a prominent visual streak in the storm petrel. This concurs to some degree with Rochon-Duvigneaud (1943), who stated that no retinal specialisations are found in this species. However, contrarily to Rochon-Duvigneaud, the thickening of all layers (except the inner nuclear layer) in the central region (and also in the central-ventral region in the inner plexiform and retinal ganglion cell layers) indicates that some specialisation exists within the storm petrel retina. Increases in these layers are associated with higher levels of acuity and nocturnal activity (Rojas *et al.*, 1999; McNeil, McSween and Lachapelle, 2005), suggesting that the storm petrel is at least partly visually active under low illumination.

The starling was found to have regions of retinal thickening associated with areas shown by Hart *et al.* (1998) to be high acuity regions with high densities of cones. Therefore, the thicker areas may allow increased processing of the image information required for enhanced colour discrimination. It must be reiterated that only left eye retinas were examined in this study and this eye is associated with colour discrimination (at least in the starling: Hart *et al.*, 2000a). Therefore, future examination of the right retina would be advantageous for a full account and comparison of the visual abilities of each species.

The thicker retinal layers found within the storm petrel support the view that storm petrels have enhanced nocturnal vision compared to starlings. I found that the storm petrel retina had longer photoreceptor outer and inner segments than the starling retina. This reinforces the idea that storm petrels are visually active under low light levels, as the longer the outer segments are, the higher the capacity for arraying

photosensitive rhodopsin. Similar thickening of these layers was found in the nocturnally active great blue heron *Ardea herodias*, (Rojas *et al.*, 1999).

The thicker outer plexiform layer may be a result of the cell types contained within it. This layer is associated with horizontal cell placements (Figure 3.1). Tarrés, Baron and Gallego (1986) found that two owl species (little owl *Athene noctua* and barn owl *Tyto alba*) differed in their short-axon horizontal (H1) cell morphologies. The nocturnal barn owl had larger H1 cell bodies, axon lengths and dendritic trees (the spread-area of the dendrites) than the crepuscular little owl. These findings can be attributed to the increased requirement for more sensitive retinal circuitry, with the short-axon H1 cell involved in the perception of light intensity changes (Kolb *et al.*, 2001). They may also be due to the reduction in cone density in the barn owl, forcing H1 cells to become larger in order to make synapses to process and regulate information from well dispersed cone cells. However, future examination of the storm petrel rod and cone densities and distributions would be required for any definitive explanation to be made.

The starling has a thicker inner nuclear layer which may be a characteristic of birds requiring high acuity vision. Within the inner nuclear layer, bipolar cells are found, and high proportions (and presumably layer thickening) of certain types of these (i.e. midget bipolars) are associated with high acuity. This is because there is a 1:1:1 ratio between the cone, midget bipolar and the retinal ganglion cell (Quesada *et al.*, 1986; Kolb *et al.*, 2001). As the storm petrel does not have a similarly thick inner nuclear layer, it can be deduced that it has lower levels of acuity (lower cone density).

The thicker inner plexiform and nuclear layers found within the starling are characteristic of species that are active foragers, especially on the ground, with enhanced motion detection and directional selectivity occurring as a result of such a thickness

(Rojas *et al.*, 1999). These layers contribute to the ganglion cell layer, with correspondingly thicker layers usually seen in regions of high motion perception.

Along with the photoreceptors, retinal ganglion cells are probably the most studied cells of the avian retina, especially in comparative studies; however they are not as well understood as mammalian retinal ganglion cells (Rahman, Aoyama and Sugita, 2008). Areas of high densities of ganglion cells are associated with high acuity, for example in the *area centralis* and fovea (see Table 1.1, Chapter 1). The variation in ganglion cell densities seen in different species corresponds with their ecology and behaviour for example; diurnal birds have thicker ganglion cell layers than nocturnal species due to there being a higher proportion of cones and cones having a 1:1 relationship with ganglion cells. Similarly, the nerve fibre layer contains retinal ganglion cell efferents, and so where there are areas of high ganglion cell density, the nerve fibre layer must be proportionally thicker (Ali and Klyne, 1985).

However, in my study I did not find any difference in the thickness of the retinal ganglion cell layer (combined with the nerve fibre layer) between the two species. This may be due to the sampling method, taking into consideration both nerve fibres and ganglion cells. However, the equivalent thicknesses may be due to different, but equally neurally demanding, visual processes occurring in each species. Species active in visual foraging (such as the cattle egret *Bubulcus ibis*) have thicker retinal ganglion cell layers than non-visually active species (e.g. the Scarlet ibis *Eudocimus ruber ruber*) (Rojas *et al.*, 1999). As ganglion cells are associated with a greater capacity to discriminate detail, the evidence that the storm petrel does not have a thinner ganglion cell layer, suggests that it is able to discriminate similar detail to that of the starling. However, a lack of correspondingly thicker inner plexiform and nuclear layers suggests that there may be

other explanations. A wider inter-species comparison would therefore be beneficial in order to gain further insight into the level of detail that different ganglion cell layer thicknesses afford other species, with or without corresponding inner plexiform and nuclear layers.

To conclude, the storm petrel retina exhibits some characteristics of a retina suitable for sensitive vision under low-light levels, suggesting that this species is able to use visual cues at night. However, whether or not its visual capabilities extend to nocturnal detail discrimination that would be required for foraging at night remains to be seen. Future work including detailed photoreceptor and retinal ganglion cell counts would therefore be useful. My findings regarding the starling retina concur with other studies (Martin, 1986a; Hart *et al.*, 1998; 2000a) that the starling is capable of high acuity vision, and that it is not as well adapted for low light vision, as is the storm petrel.

Chapter 4 Visual constraints on the timing of onset of dawn song around the world

Abstract

Birds are highly vision-dependent organisms, so the timing of their behaviour is expected to be constrained by visual capability. I used eye size and retinal image brightness (RIB) as estimates of the ability of different avian taxa to see under low light conditions, to test hypotheses about how visual constraints may influence the time at which different species begin their dawn singing activity in different bird communities around the world. My first hypothesis is that as eye size becomes larger, time of onset of dawn song becomes earlier, and indeed at most locations studied, this negative relationship between eye size and time of dawn song onset was found. Eye size was generally a better predictor of the timing of dawn song, than was RIB or body mass. This relationship was apparent, both when considering species-level data, and when the data were corrected for phylogeny. I then compared the slope of the relationship between eye size and song onset, between bird communities at different locations, to explore the hypothesis that when twilight was protracted (e.g. at high latitudes in summer), the slope of the relationship would be shallower than when dawn breaks more rapidly. Contrary to this expectation, I did not find a decrease in the slope of the relationship with an increase in the duration of twilight. The results indicate that visual capabilities, and visual constraints imposed by low ambient light levels during dawn twilight, play an important role in defining interspecific differences in the timing of dawn song. However, when dawn breaks very rapidly, other factors such as the avoidance of acoustic

competition may force greater spacing in the timing of song than can be explained by the changes in ambient light intensity alone.

Introduction

The timing of the dawn chorus

The two main functions of bird song (in general) are: mate attraction and territory defence (Catchpole & Slater, 1995). It is well known that bird song output varies throughout the day, with increased song activity at the beginning of the day and a smaller peak in activity at the end of the day; these peaks in singing are known as the dawn and dusk choruses respectively (Staicer *et al.*, 1996). In this study, I test the hypothesis that interspecific differences in the timing of twilight song are due to differences in visual abilities and constraints on vision at low light intensities. I focus on the timing of the dawn chorus, since there are very few published comparative studies on the timing of the dusk chorus around the world.

Any explanation of the timing of the onset of dawn song needs to be made in the context of a functional explanation of the dawn chorus as a whole. Numerous non-mutually exclusive hypotheses for the function of the dawn chorus and why birds sing predominantly at dawn have been proposed (Table 4.1, reviewed in detail by Kacelnik & Krebs, 1982; Mace, 1987; Staicer *et al.*, 1996; Thomas, 1997).

However, some of these hypotheses accounting for the dawn chorus may be convincing for a few species or in specific circumstances, but not as a general explanation for the timing of the dawn chorus among birds in general, or around the

Table 4.1. The different hypotheses proposed for the existence of a peak in song output at dawn, i.e. the dawn chorus (based on Mace, 1984; Staicer *et al.*, 1996; Thomas, 1997; Gill *et al.*, 2002, and references therein).

Hypothesis name	Function type	Hypothesis
Circadian cycles	Intrinsic	Song is a non-functional consequence of elevated testosterone levels
Self-stimulation	Intrinsic	Singing itself changes hormone levels to prepare for social interactions
Mate attraction	Social	Song at dawn is the best time to attract receptive females
Mate stimulation	Social	Song at dawn is the best time to stimulate reproductive development of mate
Mate guarding/mate defence	Social	Song at dawn defends the pair-bond and repels prospecting males from extra-pair copulations, at a time when females are especially fertile
Territory defence	Social	Song advertises that the singer has survived overnight and holds the territory
Social dynamics	Social	Dawn song comprises inter-neighbour communication assessing any overnight change in dominance hierarchies and competitiveness
Handicap	Social	Singing is a signal of male quality if singing is more costly at dawn than at other times
Low predation	Environmental pressures	Dawn is a less costly time to sing because predation risk is low
Acoustic transmission	Environmental pressures	Song propagates further at dawn than in the middle of the day
Inefficient foraging	Environmental pressures	Low prey availability and/or inability to see prey items at dawn makes this the best time to sing
Unpredictable conditions	Environmental pressures	Excess energy resources are available for song after better than anticipated conditions overnight

world. For example, dawn song has been hypothesised to function as “acoustic mate-guarding” (Gill *et al.* 2005). Levin (1996b) presented evidence for acoustic mate-guarding (though not specifically as an explanation of the timing of the dawn chorus) in the bay wren *Thryothorus nigricapillus*, in which males may participate in duets with their female partners

to prevent them from attracting other males. However, not all species that participate in the dawn chorus sing duets, and many species sing when not mate-guarding. For example, in contrast to Levin's study on the bay wren, Gill *et al.* (2005) found that the mate guarding hypothesis did not explain the dawn song of the congeneric buff-breasted wren *Thryothorus leucostis*, whose song timing did not differ between different stages of the breeding cycle (i.e. pre-fertile or fertile periods), and had extremely low rates of extra-pair fertilisations. This implies that the buff-breasted wren either has (i) alternative strategies for guarding against extra-pair copulations, so that the dawn chorus is more likely to function in reproductive synchronisation and pair bonding (e.g. according to the mate stimulation, self-stimulation and mate defence hypotheses), or (ii) that there is limited benefit for male buff-breasted wrens to guard their mates, due to low genetic variation in the male population (Gill *et al.*, 2005).

Given that all functional hypotheses for the dawn chorus describe how the costs and benefits of singing (and alternative behaviours such as foraging) may vary over the diurnal cycle, there is no reason to suppose that there is just one true explanation for the dawn chorus. Rather, a varying combination of factors may favour dawn singing across a wide range of species, social circumstances, habitats and regions. For example, Dalziell and Cockburn's (2008) study on superb fairy-wrens *Malurus cyaneus* found that there are multiple explanations for the dawn chorus in this species: Territories of the superb fairy-wren are held by socially monogamous pairs along with up to four male helpers. The female initiates extra-pair copulations from outside the territory during the dawn chorus. Attractive male song was found to contain longer "trill" sections (supporting the mate attraction hypothesis) and dominant male song was found to contain more "chatter" sections (possible

for within-group social hierarchy maintenance). Thus, the dawn chorus functioned both to attract extra-pair females and to maintain a male hierarchy within the territory.

Despite the wide variety of hypotheses proposed to account for the dawn chorus, and the conflicting evidence from different field studies, most of these hypotheses do not offer any explicit explanation of interspecific differences in the timing of the onset of dawn song (rather than the peak of singing during the dawn chorus). One hypothesis which appears to provide a widely accepted explanation both for the peak of singing at dawn among a wide range of species, as well as interspecific differences in the onset of dawn song, is the inefficient foraging hypothesis, outlined below.

Visual capability and foraging efficiency

Kacelnik (1979) used data from his studies of great tits *Parus major* to argue that dawn may be an inefficient time for feeding and that this species therefore allocates its time to other activities such as singing instead, postponing feeding until later when light intensity has increased and foraging can become more successful. Staicer *et al.*, (1996) interpreted this to mean that prey items were unavailable at the time of the dawn chorus, and countered that many non-predatory species have dawn choruses. However, inefficient foraging may simply be due to not being able to see clearly enough to find sufficient food to make foraging worthwhile (Kacelnik, 1979; Kacelnik and Krebs, 1983; Thomas *et al.* 2002).

The inefficient foraging hypothesis therefore raises the suggestion that light intensity needs to be considered when trying to account for the timing of the dawn chorus, and the order in which birds join it. A species that has particularly good visual capabilities at low light intensities may be able to see well enough to forage earlier than species with poorer vision under these circumstances. Given that increasing eye size is associated with increasing

both visual sensitivity (ability to detect light of low intensity) and visual resolution (ability to resolve detail at a given light intensity) (Land & Nilsson, 2002); species that have larger eyes may be expected to begin to sing earlier at dawn than those with smaller eyes (Armstrong, 1963). Indeed, this has been found to be the case among passerine birds in Europe by Thomas *et al.*, (2002), who described an association between eye size and the onset of dawn song where larger eyes were associated with earlier singing. When controlling statistically for eye size, an association between body mass and the onset of dawn song was also detected where smaller body masses were associated with earlier singing). This association between body mass and timing of dawn song possibly arises because smaller birds lose a greater proportion of their energy reserves overnight, and therefore begin their daily activity earlier than larger birds, in order to recoup these reserves.

Subsequent studies have supported the hypothesis that the timing of dawn song is influenced by the birds' ability to see at low light intensities. Berg *et al.*, (2006) found that larger eye size was associated with earlier dawn song among both passerine and non-passerine species of a tropical forest bird community in Ecuador. Among passerines (but not among non-passerines) earlier dawn song was also associated with foraging higher in the forest canopy, where light intensities would generally be higher than on the forest floor.

Having larger eyes means that more light can reach the retina and allows a brighter image to be captured by the photoreceptors and processed by the neurons of the retina and visual centres of the brain. In addition to the effect of increasing eye size, ocular resolution can be increased by having increased numbers of retinal ganglion cells to process the signals from individual photoreceptors. These signals may be pooled at the level of the retinal ganglion cells (see Chapters 1 & 2), so a retina with greater number of retinal ganglion cells allows images to be processed with less pooling at low light levels than one with fewer cells

(potentially maximising visual resolution as well as sensitivity). McNeil *et al.*, (2005) found that the American robin *Turdus migratorius* and hermit thrush *Catharus guttatus* began their dawn song earlier and had more retinal ganglion cells than common grackle *Quiscalus quiscula* and the mourning dove *Zenaida macroura*, which start their dawn chorus later. Therefore, in general, having high visual sensitivity and resolution at low light intensities is associated with singing earlier at dawn. Taken together, these studies provide strong support for the idea that ambient light levels and the visual capability of different bird species influence the timing of dawn song.

The timing of the dawn chorus may therefore be explained by birds needing to sing at some point during the day to establish or preserve ownership of a territory, and while light levels remain below a threshold needed for efficient foraging at dawn, the benefits of foraging will remain low relative to the benefits of singing, and so birds use this time to sing. Only once light levels have increased further can it finally switch to foraging (Kacelnik, 1979). The threshold light intensity for foraging to be favoured over singing is likely to vary between species, depending on their visual capabilities at low light levels.

Other explanations for the dawn chorus need not be mutually exclusive with this inefficient foraging explanation: birds which have surplus energy reserves are likely to sing more at dawn as they are able to use these reserves to sing for longer rather than foraging (Thomas *et al.*, 2003). Indeed, as song is costly when compared to resting, birds which do not have surplus energy reserves or a highly variable food resource may not sing very much before they forage (McNamara *et al.*, 1987). It therefore follows that body reserves will also play a role in the onset of dawn song, with fatter birds singing more during the dawn chorus than leaner birds, as suggested by McNamara (1987) and confirmed empirically by Thomas & Cuthill (2002).

As the sun elevates towards sunrise, light intensity increases monotonically (Martin, 1990, Thomas *et al.*, 2002). However, the rate of change of light intensity and hence length of twilight (defined as the period from the onset of civil dawn twilight, to sunrise –see Table 4.2) can vary tremendously with latitude and the time of year. Figure 4.1 illustrates that at low latitudes, civil twilight length can be very short (e.g. approximately 20 minutes at the equator at the autumn and spring equinoxes) and at higher latitudes it can be very long (e.g. over 1 hour in Scotland, UK at the summer solstice). Whilst two studies mentioned above (Thomas *et al.*, 2002 and Berg *et al.*, 2006) investigate the relationship between eye size and the start time of the dawn chorus, there have to date been no studies comparing how the relationship between eye size and the start time of dawn song may vary between bird communities around the world, in response to these variations in twilight duration. Indeed, several studies have highlighted the need for research on the latitudinal differences in the timing of the dawn chorus, especially with reference to the tropics (Morton, 1996; Slater & Mann, 2004).

Table 4.2. Classification of twilight periods (Martin, 1990).

Twilight period	Range of degrees that the centre of the sun is below the horizon
Astronomical twilight	18 - 12°
Nautical twilight	12 - 6°
Civil twilight	6 - 0°

If the timing of dawn song is determined by visual constraints alone, then we would expect the duration of dawn twilight to influence the rate with which the different species join the dawn chorus. Specifically, when twilight is protracted the slope of the relationship is

expected to be shallower than when dawn breaks more rapidly. However, when twilight length is very short and where species richness is high, the timing of different species joining the dawn chorus may be influenced by acoustic competition between species, as well as by interspecific differences in visual constraints. For example, species may be forced to start singing earlier –or later- at dawn than might be predicted on the basis of their eye size alone, in order that their songs are not masked by overlapping with the songs of many other species that are all attempting to communicate effectively within the narrow time window of the tropical dawn twilight period. By spreading their song start times apart, birds may avoid competition for “acoustic space”, thereby transmitting their songs to potential mates or rivals without the songs being degraded by acoustic interference from the songs of other species.

Previous studies have found evidence of acoustic partitioning (i.e. limiting communication within discrete time blocks) between different songbird species, on a scale of seconds to minutes (Cody and Brown, 1969; Popp, Ficken and Reinhartz, 1985). Luther (2008) found evidence for acoustic partitioning within the dawn chorus for four tropical bird species (white-browed antbird *Myrmoborus leucophrys*, warbling antbird *Hypocnemis cantator*, chestnut-backed antshrike *Thamnophilus palliatus* and black-faced antthrush *Formicarius analis*), in a location where the twilight length was short and there was a highly diverse avian assemblage. Such an environment is therefore likely to cause a more protracted dawn chorus than might be predicted from visual capabilities alone, with the need for acoustic partitioning for effective communication driving the timing of each species’ vocalisations, rather than, or in addition to, light intensity and visual ability.

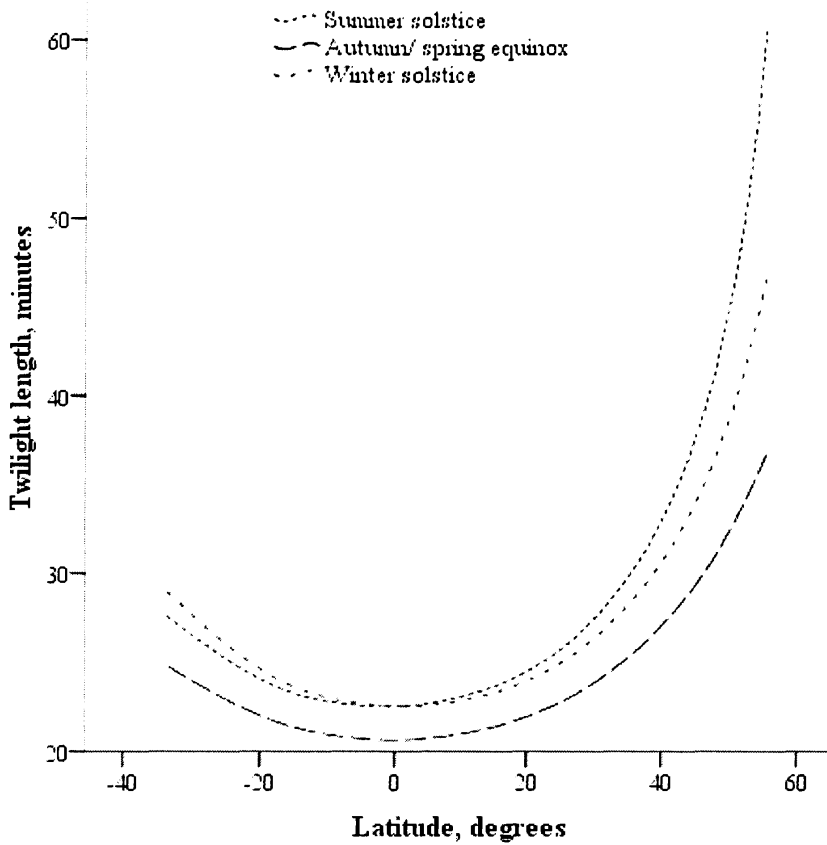


Figure 4.1. The length of civil twilight at the study sites, on the dates of the spring and autumn equinoxes, and the summer and winter solstices. The study sites were located between the latitudes of $-33^{\circ} 31' 29''$ and $55^{\circ} 25' 26''$. The length of twilight is measured from the start of civil twilight until sunrise. Note that the autumnal and spring equinox plots are identical.

My study combines information on visual ability and the timing of dawn song along with body mass and twilight length for species around the world, to test the following hypotheses:

1. Species differences in the timing of the onset of dawn song are associated with interspecific differences in visual sensitivity, at varying latitudes.
2. The duration of dawn twilight (determined by latitude and time of year) influences the rate at which different species join the dawn chorus.
3. Where twilight is very short, a greater temporal spacing is found between species than can be explained by light levels alone (i.e. the dawn chorus is more drawn out with each species having a adhering to a particular “song niche”).

In addition to my main analyses using overall eye size, maximum retinal image brightness estimates (RIB_{max}) was tested as an alternative measure of visual ability, in relation to the timing of dawn song. RIB_{max} is one measure of the sensitivity of the eye (based on the amount of light available to be detected by the retina –see Chapter 2) and so it was hypothesised that it is a better predictor of the time of first dawn song than overall eye size.

Methods

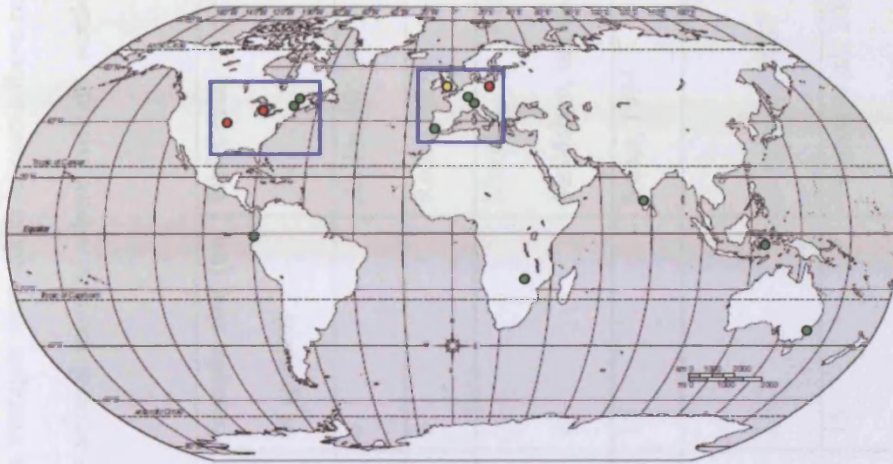
The timing of the onset of dawn song

The start times of dawn song of different species (i.e. the time at which each bird begins to sing each day) were collated from published studies, and from unpublished datasets from

twenty study sites located around the world (see table 4.3 and figure 4.1a & b). Published studies were selected if they included comparable data on the onset of the dawn chorus (henceforth referred to as “dawn song start time” or simply “start time”, as appropriate) for more than four species at a single location, and that the methods employed to collect the data were uniform. Studies were searched for using research databases such as ISI Web of Knowledge (Thomson Reuters) and were excluded if they did not give accurate locations of sampling or included data on too few species (similar selection methods to Söderström’s review of nest predation, 1999).

Data often comprised dawn song start times over a variable number of days. Where this was the case, a mean value for the start time of each species’ song was calculated, as well as the mean date of data collection. Generally the published studies gave the start time of song relative to sunrise or at a particular time at that location, for a range of species. To standardise the start time of song relative to sunrise, the US Naval Observatory sunrise calculator (<http://aa.usno.navy.mil/>) was used to calculate timings relative to sunrise at that location on the mean date for that dataset. This calculator takes into consideration latitude and longitude, date, time zone and the local daylight saving time status, to derive timings of twilight or sunrise. The timings of onset of dawn song could then be expressed as a standardised value in minutes relative to sunrise, allowing direct comparisons between locations to be made.

a)



b)



Figure 4.1a). Map of the world with locations of study sites (filled circles). All locations were included in the global analysis. Locations with red circles were excluded from the between-sites analysis relating to the duration of twilight, due to the data being collected over more than 1 month. The yellow circle represents multiple individual sites within the UK, see figure 1b. Sites within the blue rectangles were pooled for regional level analyses. b) Map of UK and Ireland with sites indicated by red or green filled circles, as in a). See table 4.1 for details of each location. Maps from Houghton Mifflin ©.

Table 4.3. Details of the observation sites with references. Shaded boxes indicate that averages were taken to assess these regional level locations. Sites with “NA” for twilight duration are those that occurred over several months, where twilight would vary considerably.

Site	Continent	Latitude	Longitude	Duration of twilight (minutes)	Sample size (no. of species)	Reference
Darwendale	Africa	-17° 41' 52"	30° 32' 36"	21:59	6	Rollin, 1953
Coonoor	Asia	11° 20' 56"	76° 47' 32"	22:56	6	Rollin, 1953
Wangi Wangi	Asia	-5° 18' 20"	123° 34' 52"	20:51	23	Marples, Kelly & McMahan, unpub. data
Ebenezer	Australia	-33° 31' 29"	150° 52' 52"	25:46	15	Keast, 1994
Manabi Province	South America	0° 39' 58"	-80° 4' 34"	21:27	21	Berg <i>et al.</i> , 2007
Cruzinha	Europe	37° 8' 11"	-8° 36' 52"	25:57	15	Thomas <i>et al.</i> , 2002
Guarda	Europe	46° 46' 30"	10° 9' 9"	39:06	10	Thomas <i>et al.</i> , 2002
Slupsk	Europe	54° 27' 50"	17° 1' 45"	NA	5	Gorska, 1991
Darmstadt	Europe	49° 52' 24"	8° 39' 20"	38:38	11	Scheer, 1950

Site	Continent	Latitude	Longitude	Duration of twilight (minutes)	Sample size (no. of species)	Reference
Glanton	Europe	55° 25' 26"	-1° 53' 22"	39:18	8	Rollin, 1953
Dublin	Europe	53° 20' 38"	-6° 16' 5"	39:10	14	Marples, Kelly & Dooley, unpub. data
Pwllgloyw	Europe	51° 59' 36"	-3° 24' 40"	48:54	12	Thomas <i>et al.</i> , 2002
Gwaelod-y-						
Garth	Europe	51° 32' 24"	-3° 16' 8"	47:52	18	Thomas <i>et al.</i> , 2002
Chew	Europe	51° 20' 47"	-2° 37' 20"	40:46	23	Thomas <i>et al.</i> , 2002
S Hampshire	Europe	50° 54' 31"	1° 11' 8"	NA	26	Marples, 1939
Henfield	Europe	50° 55' 57"	0° 16' 19"	38:39	11	Thomas <i>et al.</i> , 2002
Europe region	Europe			NA	51	
	North					
Mt Katahdin	America	45° 50' 56"	-68° 53' 55"	38:19	9	Allen, 1913
Jefferson	North					Wright, 1912;
Highlands	America	44° 22' 22"	-71° 26' 21"	36:44	53	Wright, 1913

Site	Continent	Latitude	Longitude	Duration of twilight (minutes)	Sample size (no. of species)	Reference
East Lansing	North America	42° 43' 50"	-84° 30' 4"	NA	9	Fisler, 1962
Ozark	North America	35° 39' 29"	-94° 4' 25"	NA	16	Zammuto & James, 1982
North America Region	North America			NA	63	

Pooling of information

Analyses were completed at the level of the individual study sites, but also at larger scale regional levels, pooling together data from multiple sites on the same continent i.e. North American and European sites, and at an overall global level by pooling data from all study sites. This allows an understanding to be gained of how variation in start times explained by the models computed at the site level compares with that explained by regional and global models.

Measuring visual ability

The methodology and justifications employed to assess eye size within this study are explained in detail in chapter 2, and are briefly summarised below.

Eye surface diameter

The diameter of the exposed corneal surface was measured from live birds in the hand. The eye was either measured directly using a calliper, or the eye was photographed adjacent to a ruler and measured post-hoc using Image J software. Such measurements are highly repeatable within species (Thomas *et al.*, 2002).

Measurements of eye size from skulls

Many of the species for which timing of song information was available in the literature, were not accessible to us for measuring eye surface diameter or estimation of retinal image brightness. For these species, the orbit diameters (from skulls) were measured instead, from scaled digital photographs of museum skulls, as described in chapter 2. For species where both eye surface diameter and orbit diameter were known (n=44 species),

regression analysis allowed prediction of eye surface diameter for species where only orbit diameter was known (results presented below). Note that some of the 44 species used for the regression analysis lacked song timing data, and were therefore excluded from the subsequent analyses of the timing of song.

Previous studies have shown that there are significant differences in the allometric relationships between eye size, body mass and brain mass, dependent on taxonomic grouping. For example, among passerine species, eye size is more highly correlated with brain mass than body mass, but psittacine eye size is more highly correlated with body mass than brain mass (Burton, 2008). Nevertheless, body mass is highly correlated with eye size for all avian taxa so far examined, scaling as $(\text{body mass})^k$, where k is 0.68 (Brooke *et al.*, 1999) or 0.67 (Kiltie, 2000). Therefore, to allow the model predicting eye surface diameter from orbit diameter to be as accurate as possible, body mass was included as a covariate. The body mass values used were obtained either from measurements of the live birds caught for eye measurements in the course of my study (where available), or from the body mass data collated by Dunning (2008).

Estimation of retinal image brightness

Retinal image brightness was estimated for as many species as became available through bird-ringing operations (see appendix A1.1; measurements made by myself, R. Thomas, D. Kelly & N. Marples). However, such data were mainly available for species found within Europe and Indonesia, due to the necessary experienced personnel and equipment present in these locations. Estimates of retinal image brightness for some species were obtained from individuals measured in zoos (e.g. the Blue-crowned motmot *Momotus momota* was photographed at Dublin Zoo). Only datasets that were of a large enough

sample size (i.e. Indonesia and Europe) were included in analysis of retinal image brightness data.

Explaining dawn song start times at each study site

General linear models were used to examine the effect of eye size (i.e. either actual eye surface diameter when available, or the eye surface diameter value predicted from orbit diameter) and/ or body mass, on the onset of dawn song.

Twilight length and latitudinal effects

Twilight length was calculated used in analysis, for those sites for which data collection dates were known and that were sampled over a relatively short period of time (less than 1 month). This approach avoided averaging song times over a large range of twilight durations for those studies which were carried out over a long period (e.g. the South Hampshire site was sampled over the course of an entire year, Marples 1939). Twilight length was calculated using a VBA Excel translation of the Sunrise/Sunset calculator by the National Oceanic and Atmospheric Administration (NOAA, United States Department of Commerce; <http://www.srrb.noaa.gov/highlights/sunrise/sunrise.html>).

Latitude (obtained from either the published studies or from maps) or twilight length were then included as the independent variable in weighted generalized additive models, with the dependent variable being the slope of association between dawn song start time and eye size (either eye size alone, controlling for body mass, or controlling for both body mass and the interaction between eye size and body mass). To take into account the level of confidence in these slope estimates, these models were weighted by $1/SE$ of the estimate of the slope of the relationship between eye size and start time at each study site.

Analysis of variability of dawn start times

An additional analysis was performed, to further examine the differences between study sites in the variation between species in the onset of dawn song. In this analysis, the dependent variable was the standard deviation of the onset times of dawn song, and the two independent variables used were (i) twilight duration and (ii) species richness. Species richness was included as an explanatory variable to account for possible effects of biodiversity and acoustic interference between sympatric species. This was done using published national avian species richness estimates from Ranjit Daniels *et al.*, (1992) for India, Myers *et al.*, (2000) for Indonesia and Hawkins *et al.*, (2003) for all other sites (Ireland was assumed to be similar to the UK estimates). Species richness in these studies were comparable and were determined by the number of mapped native, terrestrially feeding, breeding birds within a locality (Hawkins *et al.*, 2003) or by transect sampling (Ranjit Daniels *et al.*, 1992), or by compilation of field records and published literature (Myers *et al.*, 2000).

Statistical analyses

Analyses were completed within R (version 2.8.0). Packages used within R were: BDSA (Arnholt, 2008), gplots (Warnes *et al.*, 2009), MASS (Venables and Ripley, 2002) and mgcv (Wood, 2003 and Wood, 2006). Generalized linear models (Results sections B, C, D, E and F, below), generalized additive models (Results sections C and D) and linear models (Results sections B, C, D, E and F) were computed and assessed on both their significance values (i.e. parsimonious approach) and Akaike's Information Criterion (AIC) scores (see Posada & Buckley, 2004 for details of AIC calculation). The lower the AIC score obtained, the more adequately the model is able to explain the variance. In

section B, where no models were significant, AIC scores were used to select the simplest best model at each site. Where significant models were produced, simplification was completed using the P-values in a backwards stepwise procedure. In all simplification procedures, generalized likelihood tests (Wood, 2006) were used to test whether a significant amount of variation would be lost in removing a term from the model, and if so, the model was not simplified.

In section C, generalized additive models using thin plate regression splines (GAMs) were used to produce the best fitting model. As in Olivier and Wotherspoon (2005), the GAMs were used primarily as an exploratory tool and their graphical output provided insight into the correct transformation of the variables for subsequent GLM analysis (for simple and robust line equation derivation). Where a GAM was significantly more suitable than the most likely polynomial, the GAM results are presented. Finally, sign tests were employed to test the hypothesis that the slopes of association of eye size and the time of onset of dawn song differed significantly from zero.

Accounting for phylogeny

When comparing different species eye design, it is important to consider how likely that the differences and similarities are due to relatedness rather than a specific visual adaptation. Therefore to control for this relatedness (or phylogeny), independent evolutionary contrasts were calculated for all model variables (following Harvey & Pagel, 1991). An overall phylogeny was first constructed for all species for which song timing, body mass and eye size data were available (see appendix A.3.1). The phylogenetic tree was derived from published studies which vary in their methodology (primarily molecular studies), and from conventional zoological wisdom based on morphology and species distribution (Alström *et al.*, 2008; Arnaiz-Villena *et al.*, 2007; Chesser, 2004; Christidis,

1987; Cicero & Johnson, 2002; Clayton & Johnson, 2003; Crowe *et al.*, 2006; Driskell & Christidis, 2004; Ericson & Johansson, 2003; Groth, 1998; Hackett *et al.*, 2008; Haring *et al.*, 2007; Helbig & Seibold, 1999; Hughes, 1996; Irestedt *et al.*, 2004; Johansson *et al.*, 2002; Johnson *et al.*, 2001; Johnson *et al.*, 2002; Jonsson & Fjeldså, 2006; Klicka *et al.*, 2007; Klicka *et al.*, 2005; Lerner & Mindell, 2005; Moyle & Marks, 2006; Nguembock *et al.*, 2007; Rabosky & Lovette, 2008; Sato *et al.*, 2001; Sturmbauer *et al.*, 1998; Voelker & Spellman, 2004; Voelker *et al.*, 2007). Equivalent trees were also constructed for the region level and individual study site level analyses, using the global tree as the template.

Due to the assimilation of information from many phylogenies using different methods, no branch lengths were included in the global tree. Therefore, my analyses assume that branch lengths are equal (method described in Harvey & Pagel, 1991). No ancestral character states were known, and so a non-directional comparison analysis was used (Harvey & Purvis, 1991).

All nodes were labelled following Reeve & Abouheif (2003). Mean trait values were calculated for each node and contrasts were calculated by subtracting either node values or tip values. The software Phylogenetic Independence (PI) version 2.0 (Reeve & Abouheif, 2003) was used to check phylogenetic autocorrelation in the contrast data, over 1000 iterations. Where autocorrelation occurs it may be either negative or positive: negative autocorrelation implies that convergent evolution has caused non-random alternation of observations among sister taxa, whereas positive autocorrelation implies that similarity of adjacent observations is caused by shared evolutionary history (Abouheif, 1999).

Results

A: Testing for Phylogenetic Autocorrelation

Table 4A.1 shows the results of the test for serial independence (TFSI) analysis to assess the level of autocorrelation within the species-level and phylogenetic contrast datasets. The results show that the species level datasets are generally positively autocorrelated (38 out of 69 of the species-level trait analyses show significant positive autocorrelation), whereas the phylogenetically independent contrasts are generally not significantly autocorrelated (only 6 out of 69 contrasts trait analyses are significantly autocorrelated, including one significant negative autocorrelation). In all but one case, the positive autocorrelation in the contrasts datasets is weaker and less statistically significant than the autocorrelation the species level data.

Choosing between analysis of species level data or independent contrast data depends on whether or not there is a significant amount of autocorrelation within the dataset. These TFSI analyses indicate that overall, a phylogenetically based comparative method (PCM) is preferable over using species level data, because PCM controls statistically for similarities in trait values that can be attributed to shared phylogeny. The TFSI analysis reveals a few datasets in which the independent contrasts are themselves autocorrelated, suggesting a deviation from the assumed Brownian model of evolution (Blomberg *et al.* 2003). Abouheif (1999, figure 1) suggests that for such cases an alternate PCM taking into account branch lengths should be employed. However, the branch lengths in our phylogeny are largely unknown and the phylogeny used is considered appropriate for all of our datasets. Therefore, the same phylogenetic method based on an assumption of equal branch lengths appears to be the best available method for correcting for phylogeny across all of our datasets.

Table 4A.1 Analysis of randomized mean statistic values produced using PI software, to determine whether phylogenetic autocorrelation occurs within the dataset (Abouheif, 1999). The grey-shaded field indicates the single instance where the data are significantly negatively phylogenetically autocorrelated (see text for details). The p values indicate whether or not these relationships are significant, with significantly autocorrelated results underlined. Continued overleaf.

Site	Body Mass			Timing of dawn song			Eye size					
	Tip value	P value	Contrast P value	Tip value	P value	Contrast P value	Tip value	P value	Contrast P value			
Chew, UK	0.3527	<u>0.010</u>	-0.0095	0.495	0.2893	<u>0.044</u>	0.2793	<u>0.041</u>	0.5022	<u>0.003</u>	0.3033	<u>0.031</u>
Cruzinha, Portugal	0.4713	<u>0.008</u>	-0.1522	0.249	0.3033	0.089	0.1204	0.298	0.5231	<u>0.004</u>	-0.1382	0.219
Darmstadt, Germany	-0.0448	0.395	0.2170	0.205	0.5282	<u>0.010</u>	-0.2788	0.140	0.1246	0.246	0.2876	0.146
Dublin, Ireland	0.3643	<u>0.003</u>	0.3339	<u>0.033</u>	0.5296	<u>0.005</u>	0.0748	0.395	0.4333	<u>0.009</u>	0.4984	<u>0.030</u>
East Lansing, US	0.0919	0.370	-0.0731	0.383	-0.2351	0.132	0.1514	0.496	0.0532	0.476	-0.0199	0.504
Glanton, UK	0.3746	0.238	0.0820	0.463	0.4096	<u>0.027</u>	0.6089	0.181	0.3252	0.070	-0.2310	0.067
Guarda, Switzerland	-0.0387	0.523	0.1836	0.250	0.3118	0.059	-0.1180	0.358	0.1738	0.261	-0.0001	0.318
Gwaelod-y-Garth, UK	0.2680	0.069	0.0793	0.338	0.4271	<u>0.001</u>	0.0708	0.300	0.4487	<u>0.015</u>	0.0804	0.348
Henfield, UK	0.3902	<u>0.016</u>	0.1457	0.127	0.4489	<u>0.023</u>	0.0745	0.295	0.4640	<u>0.032</u>	-0.0024	0.496
Jefferson Highlands, US	0.2451	<u>0.015</u>	-0.0696	0.127	0.3546	<u>0.001</u>	-0.1310	0.125	0.4140	<u>0.001</u>	-0.0885	0.105
Mt Katahdin, US	0.4591	<u>0.005</u>	0.1021	0.510	0.1244	0.246	-0.2452	0.261	0.4571	<u>0.028</u>	0.1469	0.331
Ozark, US	0.1585	0.204	0.0504	0.390	0.0783	0.317	-0.0637	0.294	0.2002	0.058	-0.0349	0.420

Site	Body Mass			Timing of dawn song			Eye size		
	Tip value	P value	Contrast P value	Tip value	P value	Contrast P value	Tip value	P value	Contrast P value
Pwllgloyw, UK	0.3430	0.074	0.3284	0.6433	<u>0.010</u>	0.2205	0.4278	<u>0.027</u>	0.1691
South Hampshire, UK	0.7125	<u>0.001</u>	0.2938	0.2980	<u>0.018</u>	-0.0303	0.5659	<u>0.001</u>	0.0961
Slupsk, Poland	0.0345	0.396	0.0585	-0.2050	0.298	0.0342	-0.1240	0.517	0.0360
EU overall	0.6942	<u>0.001</u>	0.0276	0.3272	<u>0.001</u>	-0.0829	0.6317	<u>0.001</u>	0.0379
India	-0.0333	0.369	0.0213	0.2367	0.230	-0.4493	0.3921	0.069	-0.0626
Indonesia	0.3690	<u>0.010</u>	0.0945	-0.0709	0.345	0.0605	0.3344	<u>0.031</u>	0.2884
Australia	0.2293	0.058	0.1431	0.0184	0.443	0.1585	0.2093	0.089	-0.0159
Zimbabwe	0.2732	0.173	0.0176	0.2446	0.097	0.1313	-0.1397	0.394	-0.1244
Ecuador	0.2792	<u>0.039</u>	-0.0765	0.0757	0.280	-0.0395	0.3359	<u>0.013</u>	0.0453
US overall	0.3631	<u>0.001</u>	-0.0706	0.4126	<u>0.001</u>	-0.0173	0.4990	<u>0.001</u>	-0.1933
Global	0.6359	<u>0.001</u>	-0.0341	0.3159	<u>0.001</u>	0.0622	0.6301	<u>0.001</u>	-0.0099
			0.278	0.154		0.445			0.445

B: The relationship between visual ability and the onset of dawn song

The estimates of the overall relationship between eye size, body mass and the timing of onset of dawn song vary between the different study sites, and between the different techniques for model selection. However, across these datasets and methodologies, there was a consistent trend for eye size to be included as an independent variable in the best models explaining the timing of dawn song. Table 4B.1 shows the best models derived for each site, for the combined datasets US, EU and for the entire global dataset, using both species-level and phylogenetically independent contrast analyses. There is no single model structure that satisfactorily explains the interspecific variation in start times across all sites, but for the majority of sites, eye size is included in the best model -either alone, or with body mass, or with their interaction term. The results outlined in detail below are those for phylogenetically independent contrast analyses. The species level analyses are presented in Appendices A.3.3- A.3.11, and are qualitatively similar in outcome.

As expected, there was a strong and highly significant positive relationship between body mass and eye size (Figure 4B.1). To compare the scaling of eye size with body mass in my study with equivalent scaling factors reported in previous studies, I cubed the species level measures of eye size to obtain an estimate of volume, and then regressed this eye volume estimate with body mass (slope = 0.829 ± 0.026 ; adjusted $R^2 = 0.849$, $F_{1,178} = 1008$, $P < 0.001$).

This correlation between candidate variables for explaining the timing of dawn song can lead to different approaches to model refinement disagreeing about which combinations of independent variables comprise the “best” model. Where AIC scores and parsimonious methods of model refinement about the “best” model structure, in order to choose a best model, general likelihood ratio tests were employed (Wood, 2006). Within the phylogenetically independent contrasts analyses, this was necessary for only the Glanton, UK site. A simplification from the best model suggested by AIC score to the

simplest significant model did not significantly reduce the explanatory power of the model (generalized likelihood ratio test: contrast in time of dawn song ~ contrast in eye size x contrast in body mass, compared to contrast in time of dawn song ~ contrast in eye size + contrast in body mass: $F_{4,5} = 2.018$, $P = 0.228$), and so the simpler model was chosen.

Eye size (either as a main effect or as an interaction with body mass) was selected in the best model for explaining variance in the timing of dawn song, in 16 out of the 23 phylogenetically independent contrast datasets (i.e. individual sites, regions and the global dataset). Eye size was selected in the best model at 15 out of 20 individual study sites (the best models for the remaining five sites had body mass as the only independent variable). Eye size alone was favoured as a predictor for the time of onset of dawn song for 6 individual sites and 1 combined analysis (out of a total of 23 phylogenetically independent contrast analyses), using both parsimony and AIC methods of model selection.

There was a consistent trend for the slope of the relationship between eye size and onset of dawn song to be negative (i.e. species with larger eyes began to sing earlier at dawn). Tables 4B2-4 show the slopes of the relationships between eye size and dawn song onset, for phylogenetic independent contrast models containing only eye size (Table 4B2), eye size and body mass (Table 4B3), or eye size, body mass, and their interaction term (Table 4B3). Figures 4B.2 and 4B.3 illustrate this negative trend at the regional level (for the pooled European dataset) and for an individual site (Chew Valley Lake, UK). Signs tests upon the slopes of eye size vs. dawn song onset (either eye size alone, eye size controlled statistically for body mass, or eye size controlled statistically for body mass and their interaction) consistently showed that there were significantly more negative slopes than positive slopes, indicating that across our global sample of study sites, as eye size increases, the time of onset of dawn song becomes earlier (Table 4B.6). Equivalent

results for body mass (either as a main effect or as an interaction with eye size) are more variable than those for eye size, and are shown in Appendix A2.1 and A2.2.

Overall, these phylogenetically independent contrasts and the equivalent species-level analyses (see appendix) consistently support the view that while body mass can explain some of the interspecific variation in the timing of onset of dawn song at some locations; eye size is an important predictor of the onset of dawn song around the world, in that species with larger eyes begin their song earlier.

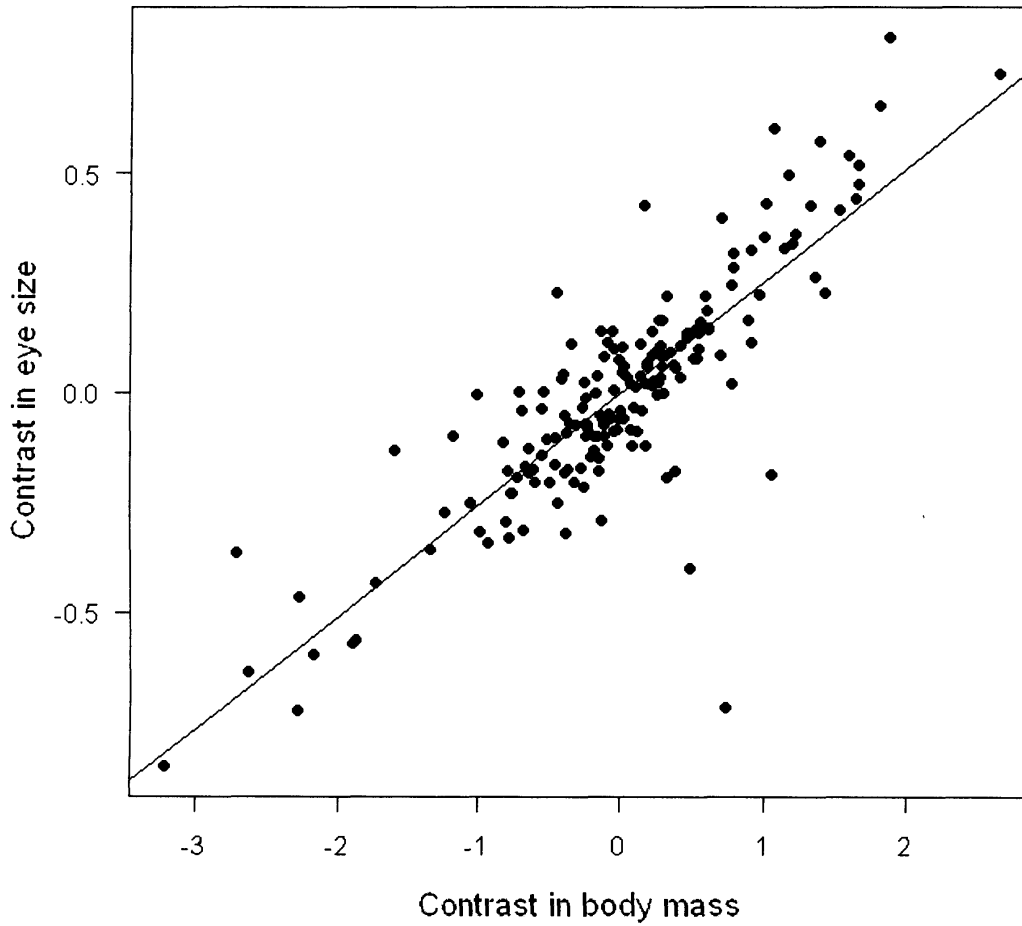


Figure 4B.1. The relationship between phylogenetically independent contrasts in body mass and eye size (adjusted $R^2 = 0.708$, $F_{1,178} = 434.8$, $P < 0.001$).

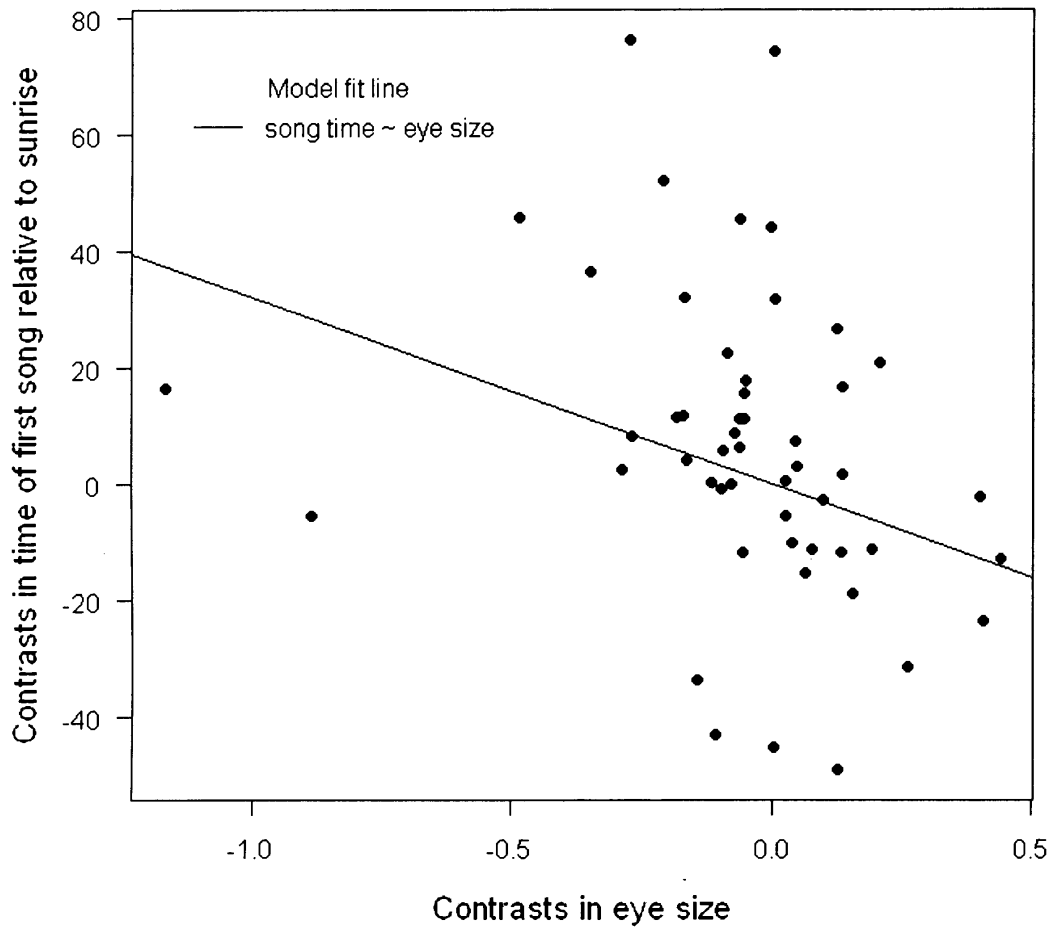


Figure 4B.2. The relationship between phylogenetically independent contrasts of the time at first song and eye size, for all European sites combined. The solid line represents the model including eye size alone (adjusted $R^2 = 0.086$, $F_{1,50} = 5.788$, $P = 0.020$, AIC = 479.924).

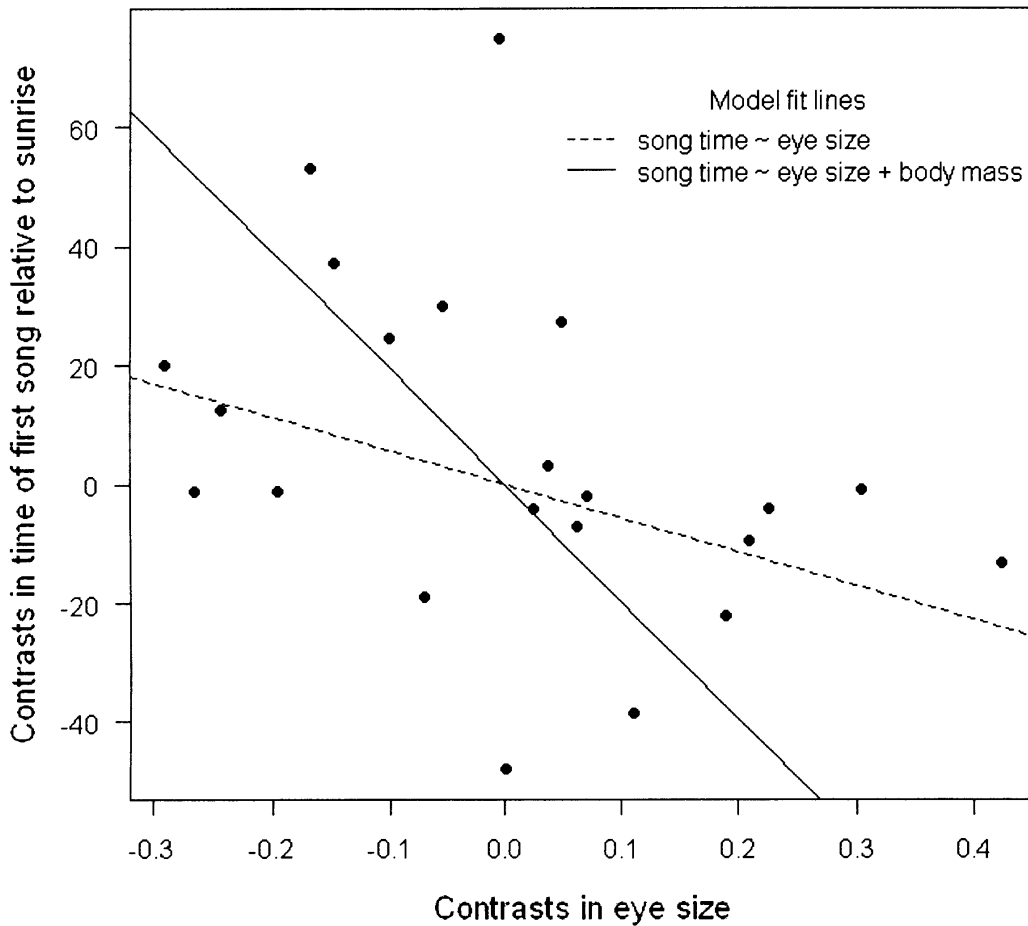


Figure 4B.3. The relationship between phylogenetically independent contrasts of the time at first song and eye size, at the Chew site. The dashed line represents the best fit of the model including eye size alone as a variable (adjusted $R^2 = 0.096$, $F_{1,21} = 3.325$, $P = 0.0825$, $AIC = 210.28$). The solid line represents the model including eye size statistically accounting for body mass (adjusted $R^2 = 0.335$, $F_{2,20} = 6.538$, $P = 0.006$, $AIC = 204.44$).

Table 4B.1. Best models for both species level and phylogenetically independent contrast analyses. Best models are represented by filled circles, selected by parsimony and/or AIC scores. Best models do not necessarily contain significant terms but may be derived on the basis of lowest AIC score. Grey fields reflect sites for which both species level and independent contrast analyses agree on the best model. A = AIC, P = parsimony, E = eye size alone, M = body mass alone, E + M = eye size and body mass, E x M = all terms including interaction between eye size and body mass. Continued overleaf.

		Species level analyses				Independent contrast analyses			
Site	Country	Method of model selection	Best model		Any other terms significant?	Method of model selection	Best model		Any other terms significant?
			E	M			E	M	
Coonoor	India	A	•			A	•		
Darwendale	Zimbabwe	A, P		•		A	•		
Wangi Wangi	Indonesia	A	•			A	•		
Ebenezer	Australia	A, P		•		A, P		•	
Manabi Province	Ecuador	A		•		A	•		
Cruzinha	Portugal	A, P	•			A	•		
Guarda	Switzerland	A, P	•			A	•		
Darmstadt	Germany	A		•		A		•	
Glanton	UK	A, P		•	Eye size	A, P		•	
Dublin	Ireland	A, P	•		Body mass	A, P	•		

		Species level analyses				Independent contrast analyses				
Site	Country	Method of model selection	Best model			Method of model selection	Best model			Any other terms significant?
			E	M	M + E		E	M	M + E	
Pwllgloyw	UK	A, P	•			A	•			
Gwaelod-y-Garth	UK	A, P	•			A	•			
Chew	UK	A, P	•			A, P	•			
Henfield	UK	A, P	•		Body mass	A		•		
Slupsk	Poland	A		•		A	•			
South Hampshire	UK	A, P	•		Eye size	A	•			
Average Europe	-	A, P	•		Body mass	A, P	•			Eye size
Mt Katahdin	USA	A		•		A		•		
Jefferson										
Highlands	USA	A, P		•		A		•		
East Lansing	USA	A, P		•		A, P		•		
Ozark	USA	A		•		A		•		
Average USA	-	A, P		•		A		•		
Average Global	-	A, P	•			A	•			
TOTAL			9	4	6	4	7	7	7	2

Table 4B.2. Results of General Linear Model analyses of the model: Contrasts of the time of onset of dawn song ~ contrasts of eye size + 0, for each site, for combined regional areas and overall. Hatched cells are used where no data is available due to averaging across sites or study took place over several months. Significance scoring: * $P < 0.05$, n = not significant. Continued overleaf.

Site	Latitude	Twilight length (minutes)	Slope of association of eye upon start time of dawn song	Eye significant?	SE	t value	p value	AIC
Coonoor, India	11.35	22:56	-5.398	n	71.489	-0.076	0.943	48.89
Darwendale, Zimbabwe	-17.70	21:59	-104.300	n	64.100	-1.627	0.179	46.17
Wangi Wangi, Indonesia	-5.31	20:51	20.050	n	16.530	1.213	0.239	222.14
Ebenezer, Australia	-33.52	25:46	-5.317	n	9.805	-0.542	0.597	118.97
Manabi Province, Ecuador	-0.69	21:27	-12.590	n	14.680	-0.858	0.402	185.62
Cruzinha, Portugal	37.14	25:57	-16.890	n	16.340	-1.034	0.32	115.13
Guarda, Switzerland	46.77	39:06	-40.380	n	24.400	-1.655	0.137	81.59
Darmstadt, Germany	49.87	38:38	-6.647	n	17.130	-0.388	0.707	86.16
Glanton, UK	55.42	39:18	4.829	n	8.759	0.551	0.601	72.31
Dublin, Ireland	53.36	39:10	-26.400	n	14.500	-1.821	0.094	111.83
Pwllgloyw, UK	51.99	48:54	-39.210	n	17.750	-2.209	0.052	90.39

Site	Latitude	Twilight length (minutes)	Slope of association of eye upon start time of dawn song	Eye significant?	SE	t value	P value	AIC
Gwaelod-y-Garth, UK	51.54	47:52	-48.670	n	24.870	-1.957	0.068	154.97
Chew, UK	51.35	40:46	-56.650	n	31.060	-1.824	0.083	210.28
Henfield, UK	50.93	38:39	-35.020	n	21.550	-1.625	0.139	85.82
Slupsk, Poland	54.46		-35.070	n	26.000	-1.349	0.270	36.08
South Hampshire, UK	50.91		-15.330	n	16.470	-0.931	0.361	240.76
Average Europe	49.82		-32.140	*	13.360	-2.406	0.020	479.92
Mt Katahdin, USA	45.85	38:19	-9.689	n	21.320	-0.454	0.663	74.87
Jefferson Highlands, USA	44.38	36:44	-3.963	n	13.800	-0.287	0.775	474.82
East Lansing, USA	42.74		-11.850	n	25.580	-0.463	0.660	69.84
Ozark, USA	35.66		-14.490	n	8.886	-1.631	0.125	118.96
Average USA	42.16		-1.649	n	12.203	-0.135	0.893	560.39
Average Global			-3.116	n	7.970	-0.391	0.696	1700.1

Table 4B.3. Results of General Linear Model analyses of the model: Contrasts of the time of onset of dawn song ~ contrasts of eye size + contrasts of body mass + 0, for each site, for combined regional areas and overall. Cells are hatched where no data is available due to averaging across sites or study took place over several months, cells are hatched. Significance scoring: * $p < 0.05$, ** $p < 0.01$. Continued overleaf.

Site	Latitude	Twilight length (minutes)	Slope of association of eye size upon start time of dawn song	Eye significant?	Mass significant?	SE	t value	p value	AIC
Coonoor, India	11.35	22:56	-7.366	n	n	78.080	-0.094	0.931	50.32
Darwendale, Zimbabwe	-17.70	21:59	-77.440	n	n	88.140	-0.879	0.444	47.75
Wangi Wangi, Indonesia	-5.31	20:51	30.112	n	n	34.706	0.868	0.396	224.02
Ebenezer, Australia	-33.52	25:46	-71.709	*	*	30.797	-2.328	0.038	116.06
Manabi Province, Ecuador	-0.69	21:27	31.330	n	n	36.890	0.849	0.407	185.84
Cruzinha, Portugal	37.14	25:57	-47.900	n	n	34.910	-1.372	0.195	116.00
Guarda, Switzerland	46.77	39:06	-61.744	n	n	79.405	-0.778	0.462	83.49
Darmstadt, Germany	49.87	38:38	-39.080	n	n	47.710	-0.819	0.437	87.51
Glanton, UK	55.42	39:18	29.411	**	**	7.062	4.165	0.009	63.20
Dublin, Ireland	53.36	39:10	37.550	n	n	43.790	0.858	0.409	111.30
Pwllgloyw, UK	51.99	48:54	-119.380	n	n	54.310	-2.198	0.056	89.79

Site	Latitude	Twilight length (minutes)	Slope of association of eye size upon start time of dawn song	Eye significant?	Mass significant?	SE	t value	p value	AIC
Gwaelod-y-Garth, UK	51.54	47:52	-116.640	n	n	72.910	-1.600	0.131	155.90
Chew, UK	51.35	40:46	-196.640	**	**	54.780	-3.590	0.002	204.44
Henfield, UK	50.93	38:39	-25.703	n	n	86.050	-0.299	0.773	87.81
Slupsk, Poland	54.46		-71.150	n	n	55.640	-1.279	0.329	37.08
South Hampshire, UK	50.91		4.360	n	n	22.320	0.195	0.847	241.03
Average Europe	49.82		-7.947	n	n	19.226	-0.413	0.681	478.93
Mt Katahdin, USA	45.85	38:19	-202.720	n	n	114.26	-1.774	0.126	73.69
Jefferson Highlands, USA	44.38	36:44	-54.569	n	n	36.125	-1.511	0.137	474.50
East Lansing, USA	42.74		-387.840	**	**	91.960	-4.217	0.008	61.44
Ozark, USA	35.66		36.470	n	n	48.810	0.747	0.468	119.71
Average USA	42.16		-40.715	n	n	30.631	-1.329	0.189	560.43
Average Global			-6.505	n	n	14.826	-0.439	0.661	1702.00

Table 4B.4. Results of General Linear Model analyses of the model: Contrasts of the time of onset of dawn song ~ contrasts of eye size * contrasts of body mass + 0, for each site, for combined regional areas and overall. Cells are hatched where no data is available due to averaging across sites or study took place over several months, cells are hatched. Significance scoring: * $P < 0.05$, ** $P < 0.01$. Continued overleaf.

Site	Latitude	Twilight length (minutes)	Slope of association of eye size upon start time of dawn song	Eye significant?	Mass significant?	Interaction term significant?	SE	t value	p value	AIC
Coonoor, India	11.35	22:56	-6.645	n	n	n	89.434	-0.074	0.948	51.65
Darwendale, Zimbabwe	-17.70	21:59	11.360	n	n	n	153.300	0.074	0.948	48.54
Wangi Wangi, Indonesia	-5.31	20:51	31.322	n	n	n	35.099	0.892	0.383	225.34
Ebenezer, Australia	-33.52	25:46	-75.595	*	n	n	33.905	-2.230	0.048	117.91
Manabi Province, Ecuador	-0.69	21:27	28.400	n	n	n	37.257	0.762	0.456	186.93

Site	Latitude	Twilight length (minutes)	Slope of association of eye size upon start time of dawn song	Eye significant?	Mass significant?	Interaction term significant?	SE	t value	p value	AIC
Cruzinha, Portugal	37.14	25:57	-18.028	n	n	n	44.344	-0.407	0.692	116.59
Guarda, Switzerland	46.77	39:06	-60.535	n	n	n	81.573	-0.742	0.486	84.58
Darmstadt, Germany	49.87	38:38	-87.030	n	n	n	51.620	-1.686	0.136	86.12
Glanton, UK	55.42	39:18	-27.761	n	n	n	40.754	-0.681	0.533	62.34
Dublin, Ireland	53.36	39:10	39.240	n	n	n	43.943	0.893	0.393	112.13
Pwllgloyw, UK	51.99	48:54	-122.615	n	n	n	57.698	-2.125	0.066	91.59
Gwaelod-y-Garth, UK	51.54	47:52	-105.520	n	n	n	74.230	-1.422	0.177	156.88
Chew, UK	51.35	40:46	-197.796	**	*	n	56.257	-3.516	0.002	206.36
Henfield, UK	50.93	38:39	-19.080	n	n	n	72.570	-0.263	0.800	85.04

Site	Latitude	Twilight length (minutes)	Slope of association of eye size upon start time of dawn song	Eye significant?	Mass significant?	Interaction term significant?	SE	t value	p value	AIC
Slupsk, Poland	54.46		-70.399	n	n	n	77.964	-0.903	0.532	38.99
South Hampshire, UK	50.91		3.691	n	n	n	22.901	0.161	0.873	242.94
Average Europe	49.82		-8.527	n	n	n	19.701	-0.433	0.667	480.90
Mt Katahdin, US	45.85	38:19	-218.446	n	n	n	127.451	-1.714	0.147	75.37
Jefferson Highlands, US	44.38	36:44	-54.411	n	n	n	37.998	-1.432	0.159	476.50
East Lansing, US	42.74		-422.838	*	*	n	107.334	-3.939	0.017	62.54
Ozark, US	35.66		38.115	n	n	n	51.593	0.739	0.474	121.67
Average USA	42.16		-42.073	n	n	n	31.954	-1.317	0.193	562.40
Average Global			-7.377	n	n	n	15.229	-0.484	0.629	1703.90

Table 4B.5. Sign tests of the slopes of associations of eye size with the onset of dawn song (either the direct association, or eye size controlled statistically for body mass, or eye size controlled statistically for body mass and their interaction), showing that there are significantly more negative slopes than positive ones.

Slope from model containing:	Category	N	Proportion	P value
Eye size	< 0	21	0.91	<0.001
	> 0	2	0.09	
Eye size + body mass	< 0	17	0.74	0.035
	> 0	6	0.26	
Eye size * body mass	< 0	17	0.74	0.035
	> 0	6	0.26	

C: Variation with distance from the equator in the slope of the relationship between eye size and the onset of dawn song

I examined whether the slope of the association between eye size and the onset of dawn song varied with distance from the equator, across the 22 study sites. To clarify the possible relationships: when the slope of the association is zero, there is no relationship between eye size and the time of onset of dawn song; when the slope is positive, as eye size increases, the time of onset of dawn song becomes later; and when the slope is negative, as eye size increases, the time of onset of dawn song becomes earlier.

Species level data

Figure 4C.1 shows how the slope of the species-level relationship between eye size and the onset of dawn song varies across study sites in relation to the distance of each site from the equator. All distances from the equator were made positive, i.e. southern hemisphere sites were plotted on the same scale as northern hemisphere sites.

The fitted line in Figure 4C.1 refers to a generalized additive model (GAM) analysis using the slope of association of eye size on the time of onset of dawn song, from models containing eye size alone; and equation 4C.1 describes the simplest significant relationship between these slopes and latitude.

$$y = (x^5 * -1.188E^{-07}) + 1.166 \quad \text{Equation 4C.1}$$

(where y is the slope of association of eye size upon the onset of dawn song, and x is the distance from the equator, in degrees).

This GAM analysis shows that the further from the equator the bird community is, the more negative the slope of the association between eye size and the onset of dawn song becomes. This implies that vision is more important in explaining the timing of onset of the dawn chorus at higher latitudes than at lower latitudes.

A similar but non-significant negative trend is identified by equivalent GAM analyses using slopes of association of eye size controlling for body mass on the onset of dawn song, and slopes of association of eye size, controlling for body mass and the eye*mass interaction term on the onset of dawn song.

Although these relationships between the slopes of association and latitude may not all be significant within GAM analyses, their intercepts are consistently significantly different from zero (except when using slopes derived from models incorporating eye size, body mass and their interaction term, see table 4C.1). All GAM intercepts are estimated to be negative, emphasizing that the overall relationship between eye size and the time of onset of dawn song is a negative one (i.e. as eye size increases, the time of first song becomes earlier).

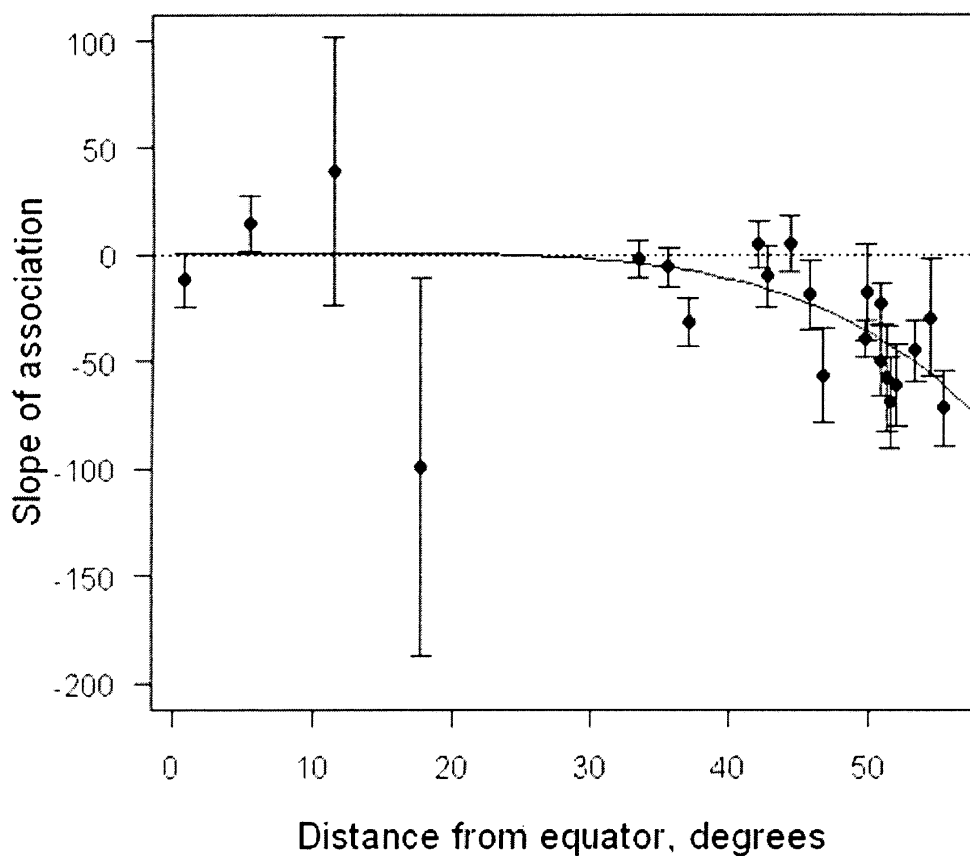


Figure 4C.1. Species-level analysis of the relationship between distance from the equator and the slope of association of eye size upon the time of onset of dawn song. Zero degrees represents the equator. (Adjusted $R^2 = 0.486$, $F_{1,20} = 20.85$, $P < 0.001$, $AIC = 199.07$). Error bars = SE.

Phylogenetically independent contrasts

GAM analyses of the phylogenetically independent contrasts identified similar non-significant negative trends to those found by analysis of the species level data. As with the species level GAM analyses, the intercepts of these GAM models were negative, and significantly so in all cases except when using slopes derived from models incorporating eye size and body mass, see table 4C.1.

Table 4C.1. Are the intercepts for the generalized additive models for both species level and phylogenetically independent contrasts analyses of slopes of association and distance from the equator, significantly different from zero? Model terms: eye size alone (E), body mass alone (B), eye size with body mass (E + B) or eye size, body mass and their interaction (E * B).

	Model terms	Intercept sig. different from zero?	t value	p value	Estimate	SE	Overall model significant?
Species level	E	***	-5.728	< 0.001	-24.86	4.34	**
	B	***	-5.883	< 0.001	-6.52	1.11	*
	E + B	***	-4.122	< 0.001	-59.92	14.54	Ns
	E * B	ns	-0.856	0.482	-41.80	48.81	Ns
Phylogenetically independent contrasts	E	**	-3.792	0.001	-16.09	4.24	Ns
	B	***	-3.931	< 0.001	-4.28	1.09	Ns
	E + B	ns	-1.975	0.063	-32.09	16.25	Ns
	E * B	*	-2.374	0.028	-40.82	17.20	Ns

D: Variation with twilight length in the slope of the relationship between eye size and the onset of dawn song

Relationships were examined between the slopes of association of eye size (or eye size and body mass, or eye size, body mass and their interaction term) and the length of twilight at each site for which comparable data were available (i.e. N = 16 sites at which song data were collected over a period of less than 1 month).

Species level data

As with the equivalent analyses in Section C above (which used distance from the equator as a predictor variable), GAM analyses identified negative associations between twilight length and the slopes of association between eye size and the onset of dawn song. Of these GAM analyses, significant negative associations between twilight duration and the slope of the association between eye size and the onset of dawn song, were found for the analyses using slopes from models containing eye size and body mass (figure 4D.1, equation 4D.1); and from models containing eye size alone (figure 4D.2, equation 4D.2)

$$y = (x * -4.638) + 80.355 \quad \text{(equation 4D.1)}$$

(where y is the slope of association of eye size and body mass upon the onset of dawn song, and x is twilight length, in minutes).

$$y = (x * -2.045) + 39.872 \quad \text{(equation 4D.2)}$$

(where y is the slope of association of eye size upon the onset of dawn song, and x is twilight length, in minutes).

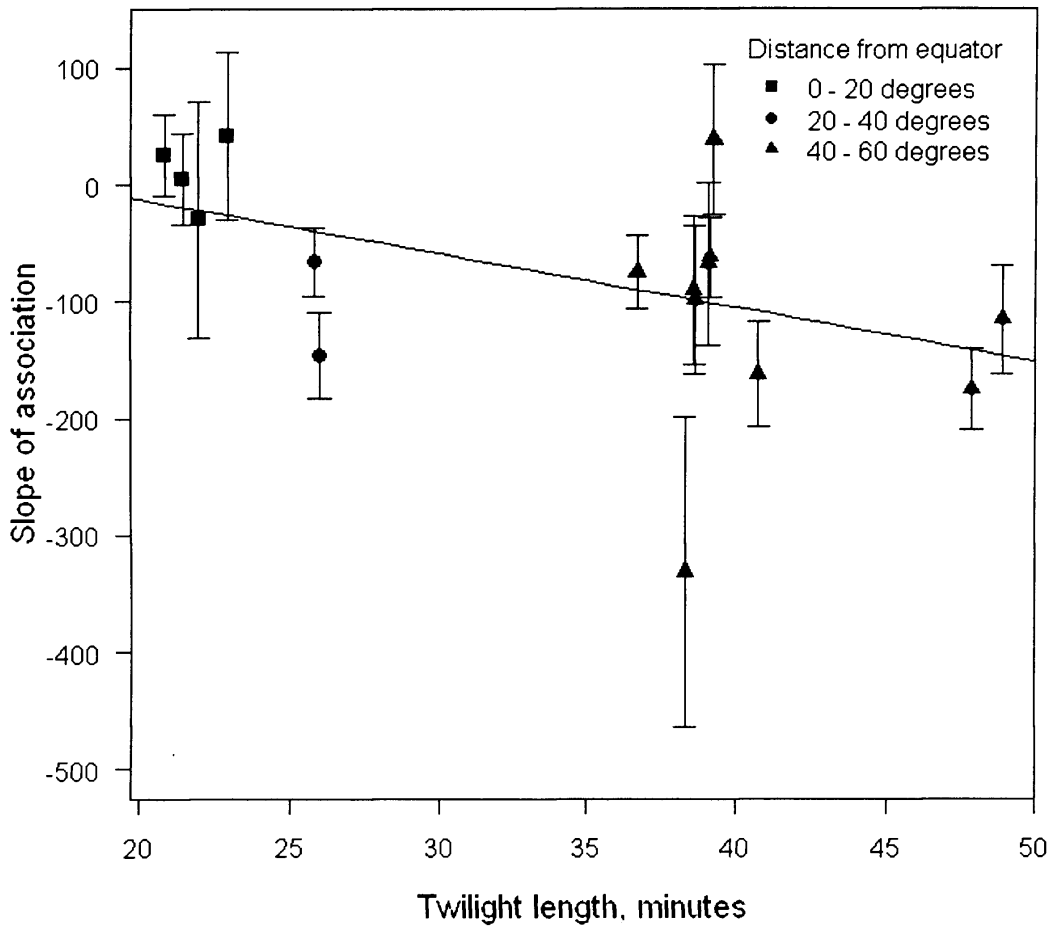


Figure 4D.1. A best fit straight line relationship exists within the species level data, between the slope of association of eye size on the time of onset of dawn song (controlling statistically for body mass), and twilight length (adjusted $R^2 = 0.273$, $F_{1,14} = 6.641$, $P = 0.022$). Error bars = SE. The latitudes of the bird communities sampled are indicated in the key.

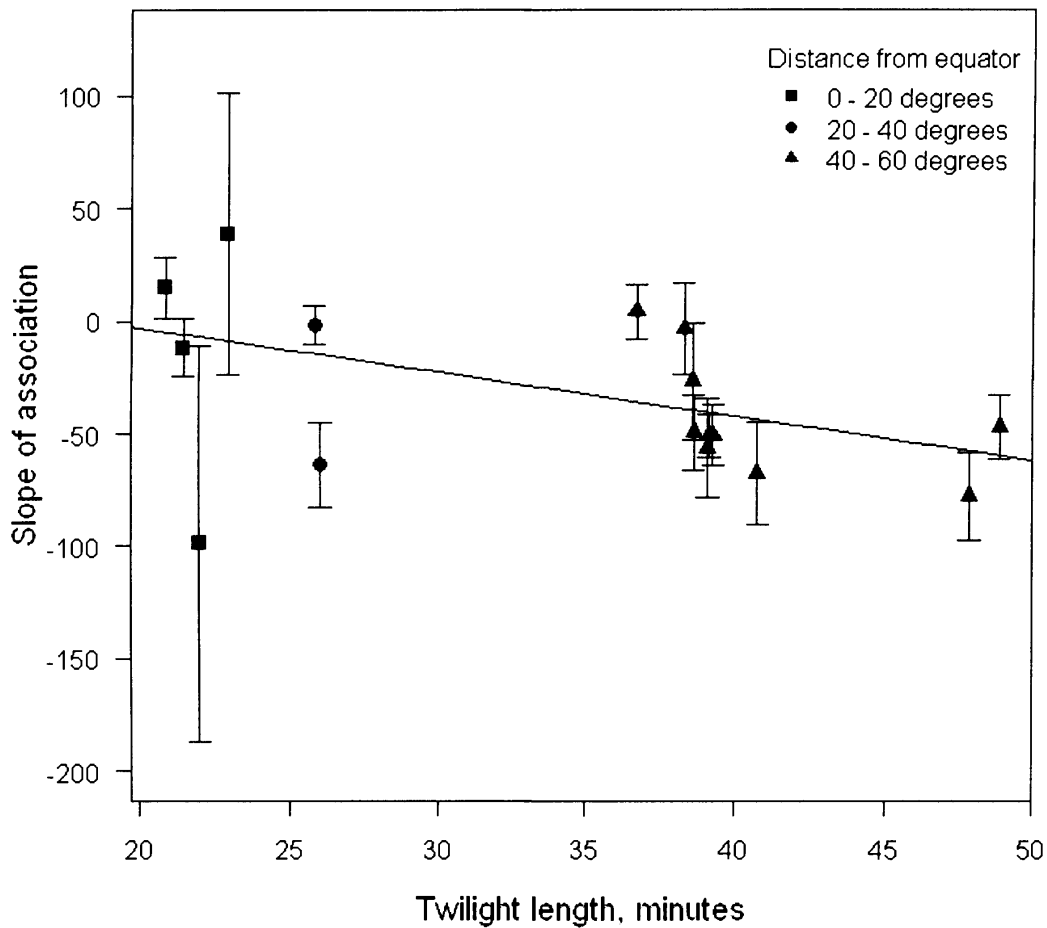


Figure 4D.2. A best fit straight line relationship exists within the species level data between the slope of association of eye size on the time of onset of dawn song, and twilight length (adjusted $R^2 = 0.303$, $F_{1,14} = 7.522$, $P = 0.016$). Error bars = SE. The latitudes of the bird communities sampled are indicated in the key.

Phylogenetically independent contrasts

As with the species-level analyses described above, the general overview of the analyses of the phylogenetically independent contrasts is that a negative trend exists for the relationship between slope of association and twilight length, for all GAM analyses (see tables 4B.2 – 4B.5). However, the only significant relationship is that between slope of association of eye size (controlling

statistically for body mass and their interaction term) on the time of onset of dawn song, and twilight length (figure 4D.3, equation 4D.3).

$$y = (x * -4.207) + 84.408 \quad \text{(Equation 4D.3)}$$

(where y is the slope of association of eye size and body mass upon the onset of dawn song, and x is twilight length).

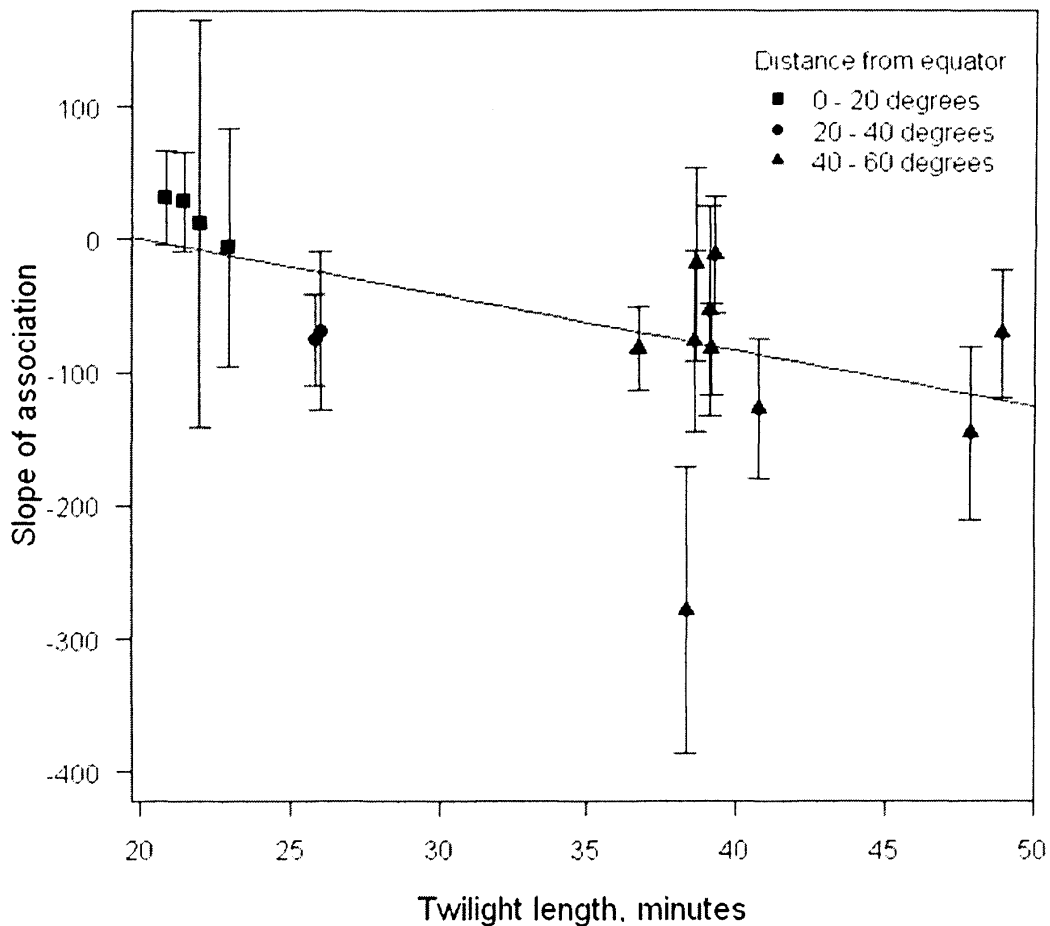


Figure 4D.3. A best fit straight line relationship exists within the phylogenetically independent contrasts between the slope of association of eye size (controlling for body mass and the eye*mass interaction term) on the time of onset of dawn song, and twilight length (adjusted $R^2 = 0.311$, $F_{1,14} = 7.754$, $P = 0.015$). Error bars = SE. The latitudes of the bird communities sampled are indicated in the key.

E: Variation in the onset of dawn song start time

Standard deviations of the dawn song onset times for the species in the bird communities present at each site were calculated. These were then included in a generalised linear model as the dependent variable, with twilight length and avian species richness (number of species in the local area, see methods) as independent

variables. Both independent variables explained a significant amount of variation (generalized linear model: adjusted $R^2 = 0.234$, $F_{2, 13} = 3.271$, $P = 0.071$, AIC = 100.28, $df = 13$, table 4E.1).

Table 4E.1. Influence of the variables twilight length and species richness on the standard deviations of the time of onset of dawn song at each site. The interaction term was not significant and so excluded from the final model. Asterisks imply degree of significance with a significant result ($* < 0.05$).

Explanatory variables	Regression coefficient	Standard Error	p-value
Intercept	2.446	7.398	0.746
Twilight length	0.440	0.180	0.030 *
Species richness	0.014	0.006	0.044 *

The positive regression coefficients in table 4E.1 indicate that as twilight length and species richness increase, the standard deviation in dawn song onset times increases also. This means that at sites which have longer twilights, the start time of dawn song is more variable than at sites with shorter twilights. At sites with high species richness, the onset of dawn song is also more variable. Figures 4E.1 and 4E.2 illustrate this relationship for each independent variable when controlling statistically for the other. Log transformed species richness was not used within the generalised linear model as the residuals were normally distributed when using the untransformed data. Species richness was only log transformed for the axis on figure 4E.2 and the accompanying regression for visualisation purposes.

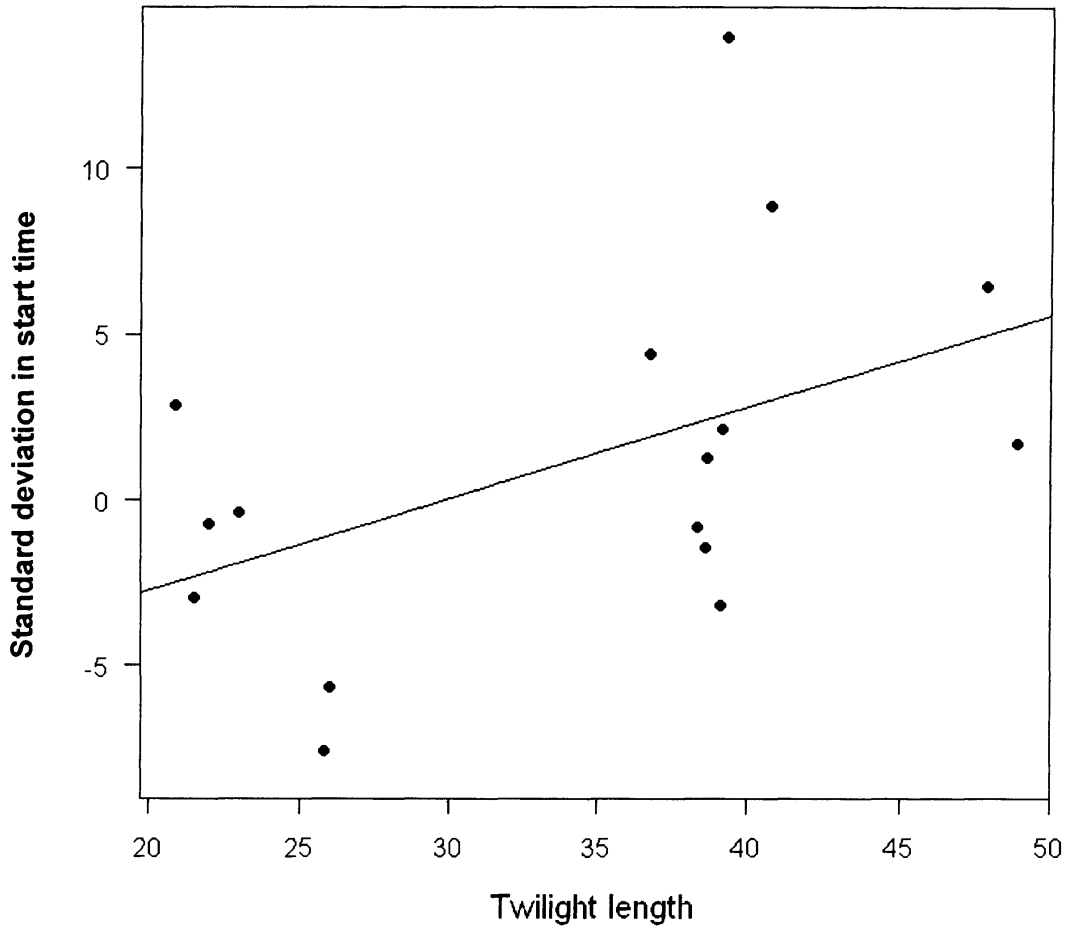


Figure 4E.1. The relationship between the standard deviation in the times of onset of dawn song, and twilight length, controlling statistically for species richness (adjusted $R^2 = 0.174$, $F_{1,14} = 4.165$, $P = 0.061$).

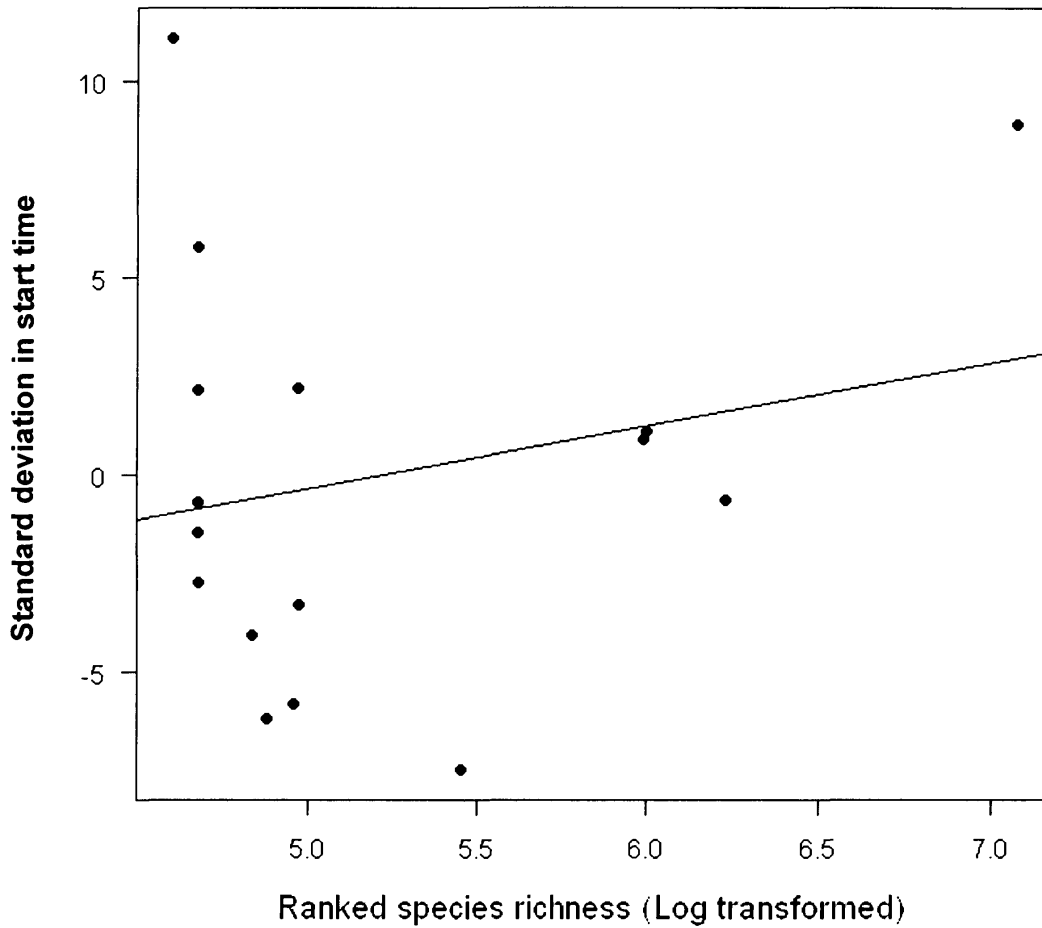


Figure 4E.2. The relationship between the standard deviation in the times of onset of dawn song, and species richness, controlling statistically for twilight length (adjusted $R^2 = -0.02$, $F_{1,14} = 0.706$, $P = 0.415$).

F: Are estimates of retinal image brightness better than eye size measures in predicting the timing of the onset of dawn song?

This set of analyses compared eye size and an estimate of maximum retinal image brightness (RIB_{max}), together with body mass, as candidate independent variables for explaining the timing of the onset of dawn song (the dependent variable). Following the phylogenetic autocorrelation analyses above (Results section A), analyses based on phylogenetically independent contrasts are presented below, though references to the equivalent species level analyses are made where appropriate. Further details of the species-level analyses can be found within the appendices (appendices A.3.4 – A.3.11). Data transformations were used as appropriate to normalize variables prior to calculation of phylogenetically independent contrasts.

Two sites were chosen (Gwaelod-y-garth and Chew, both UK), which were comparable with the findings of Thomas *et al.*, (2002), and for which estimates of retinal image brightness were available for many of the bird species present. However, as not all of the species within each dataset had estimates of retinal image brightness available, sample sizes for Chew were reduced to $N = 14$ (for species level analysis) and $N = 13$ (for phylogenetically independent contrasts). For Gwaelod-y-Garth, sample sizes were $N = 9$ (species level analysis) and $N = 8$ (phylogenetically independent contrasts).

Analysis of the pooled European dataset is also presented, to illustrate that trends that occur at the site level can disappear at a continent level, perhaps due to the averaging of song timing data across sites differing in twilight duration. The

analysis of the Indonesian dataset is provided to illustrate an interesting alternative trend to the European sites.

Chew, UK dataset

Analysis of the phylogenetically independent contrasts revealed that there is a significant negative relationship between eye size and the timing of onset of dawn song, when included in models 1 and 2 (table 4F.1) containing body mass and the interaction term as non-significant variables. This means that as eye size becomes larger (controlling for body mass), the time of onset of dawn song becomes earlier. The lowest AIC score belonged to the model containing eye size and body mass. The simplification from the model including the interaction term (also containing eye size as a significant term) to this model (i.e. model 1 to 2) does not significantly reduce the explanatory power of the model (generalized likelihood ratio test, table 4F.1: model 1 to model 2: $F_{10,11} = 0.117$, $P = 0.739$; Wood, 2006). Models containing RIB either alone or in combination with body mass, are not significant (models 5-7, table 4F.1) and have relatively high AIC scores, indicating that eye size is a better predictor of the timing of dawn song than is RIB_{max} . The species level analysis concurs with the phylogenetically independent contrast analysis (see Appendix A. 3.11).

Gwaelod-y-Garth, UK dataset

The phylogenetically independent contrast analysis of the Gwaelod-y-Garth dataset yielded similar results to the Chew dataset above. The model containing both eye size and body mass was significant in predicting the time of onset of dawn song, with both variables significant (figure 4F.2; model 2, table 4F.2). The

lowest AIC scoring model also included the interaction term. However, no significant loss of explanatory power occurs on simplification (generalized likelihood ratio test, table 4F.2: model 1 to model 2: $F_{5,6} = 4.366$, $P = 0.091$). RIB was not retained in any of the models, and models containing RIB had higher AIC scores than equivalent models containing eye size. The species level analysis concurs with these findings (see Appendix A.3.10).

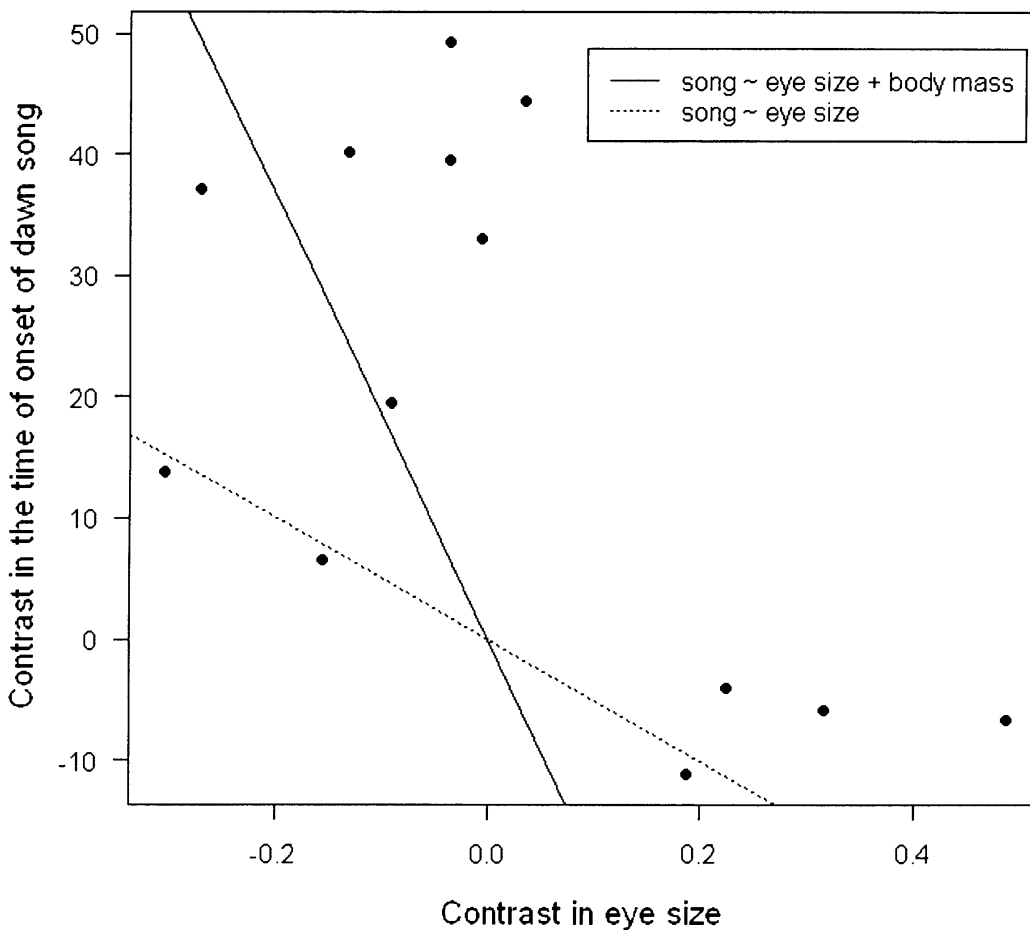


Figure 4F.1. Phylogenetically independent contrasts of the Chew dataset: continuous line -relationship of eye size (natural log transformed) and the onset of dawn song relative to sunrise; dotted line - relationship of eye size (natural log transformed) with body mass (natural log transformed), and the onset of dawn

song relative to sunrise, where zero is sunrise and earlier song production is negative. The regression is forced through the origin (see table 4F.1, models 2 and 3).

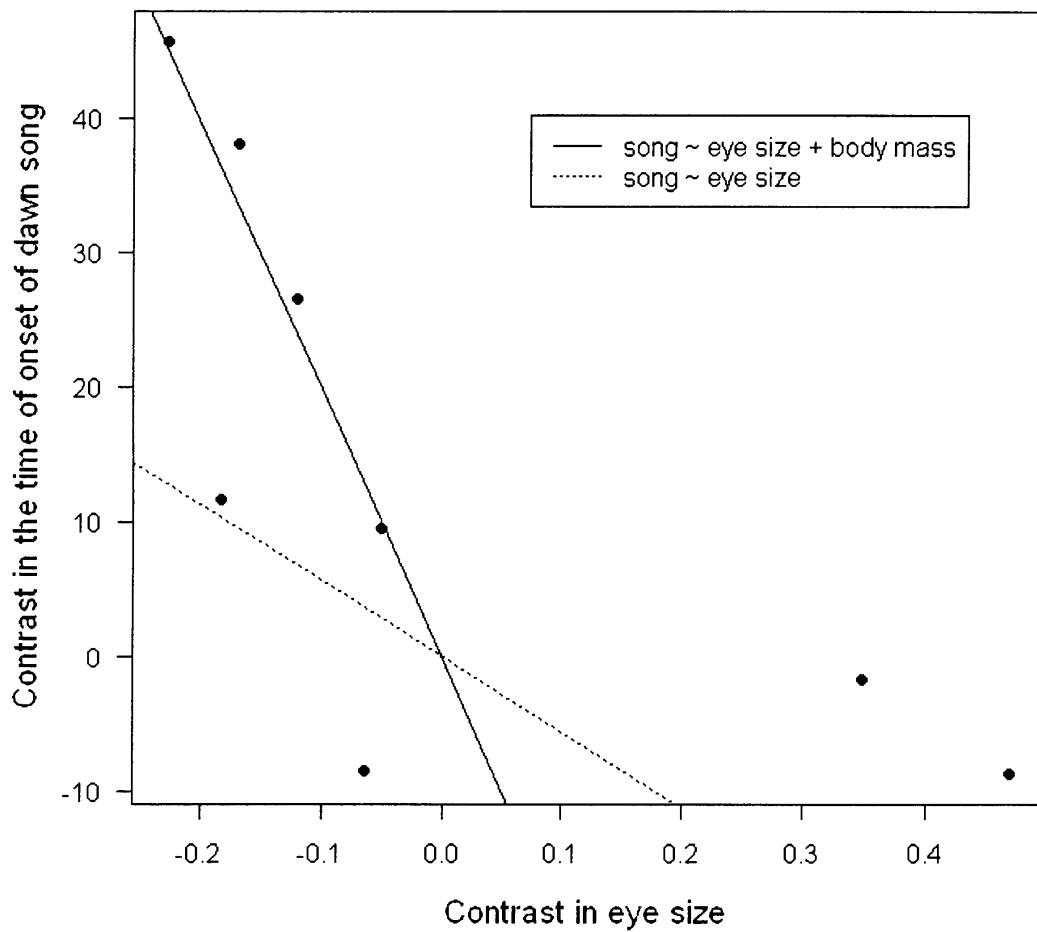


Figure 4F.2. Phylogenetically independent contrasts of the Gwaelod-y-Garth dataset: continuous line - relationship of eye size (natural log transformed) and the onset of dawn song relative to sunrise; dotted line - relationship of eye size (natural log transformed) with body mass (natural log transformed), and the onset

of dawn song relative to sunrise (where zero is sunrise and earlier song production is negative). The regression is forced through the origin (see table 4F.2, models 2 and 3).

Pooled European dataset

A European level phylogenetically independent contrast analysis was carried out, using song data averaged across European sites (N = 22 species; 21 independent contrasts). This analysis found no significant terms within starting models containing RIB or eye size along with body mass and the interaction term (RIB alone: adjusted $R^2 = -0.047$, $F_{1,20} = 0.060$, $P = 0.809$; eye size alone: adjusted $R^2 = 0.0092$, $F_{1,20} = 1.195$, $P = 0.287$; see table 4F.3 for results for other model structures). A species level analysis concurs with the finding that RIB_{max} is not a significant predictor of the time of onset of dawn song, but also identified a significant model containing eye size, body mass and their interaction term (Appendix A 3.9 model 1), with a negative slope for eye size, indicating that as eye size increases, the time of onset of dawn song becomes earlier.

Indonesian dataset

In contrast to all of the European analyses presented above, a phylogenetically independent contrast analysis of the Indonesian dataset (species level, N = 8; independent contrasts, N = 7) found that a model including RIB, body mass and their interaction term is significant (adjusted $R^2 = 0.768$, $F_{3,4} = 8.73$, $P = 0.031$),

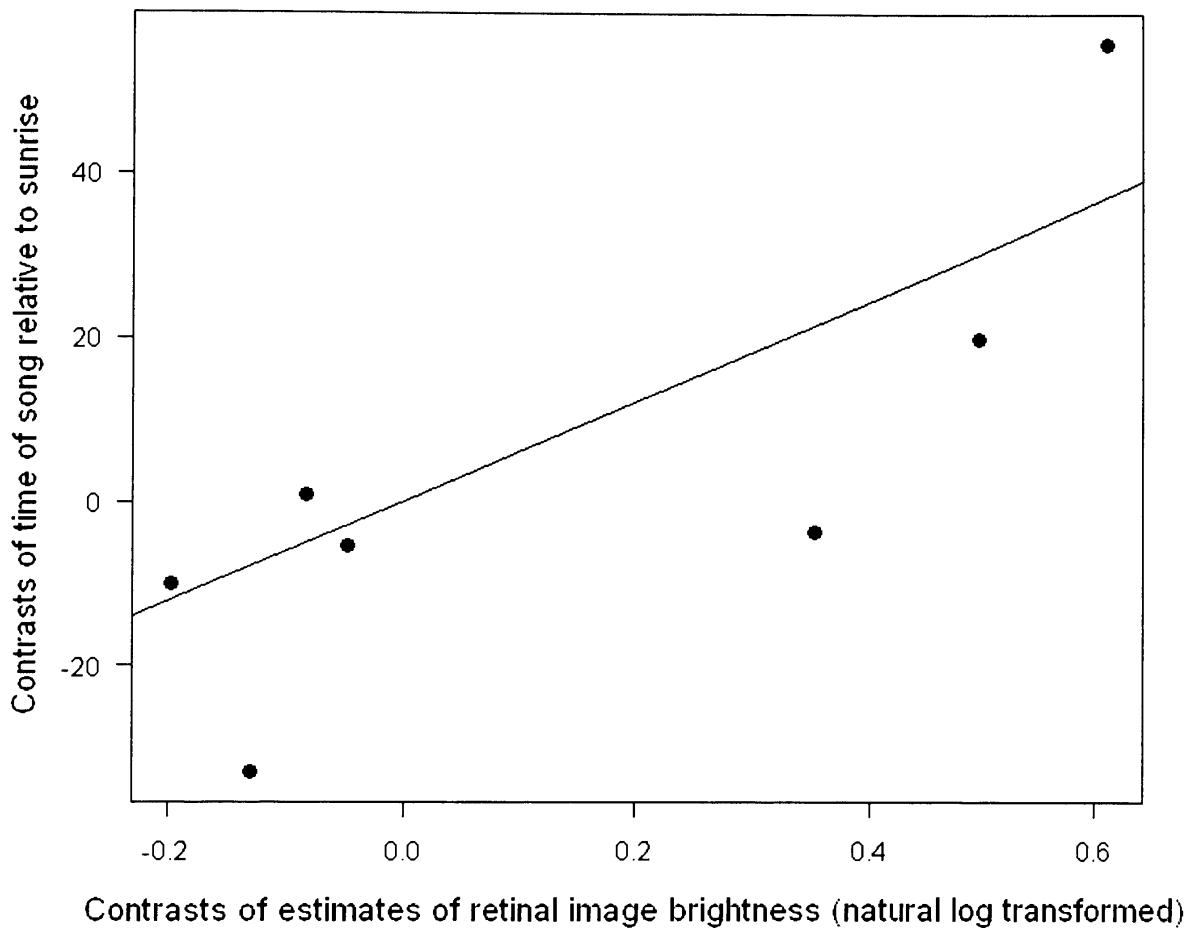


Figure 4F.3. Phylogenetically independent contrasts regression of Indonesian dataset estimates of retinal image brightness (natural log transformed) and the onset of dawn song relative to sunrise, where zero is sunrise and earlier song production is negative. The regression is forced through the origin (adjusted $R^2 = 0.570$, $F_{1,6} = 10.271$, $P = 0.019$).

with RIB as a significant term ($P = 0.012$). Simplification (on the basis of parsimony) to the simple model of RIB predicting the time of onset of dawn song alone does not significantly reduce the explanatory power of the model and so should be accepted as the best model, regardless of a higher AIC score being

derived for this simple model (generalized likelihood ratio test, table 4F.4: model 5 to model 6: $F_{4,5} = 1.643$, $P = 0.269$; model 5 to model 7: $F_{4,6} = 3.567$, $P = 0.129$). Within this dataset there is a surprising opposite trend to those found within the European sites datasets: a positive relationship exists between the onset of dawn song and measures of visual ability (figure 4F.3), indicating that as RIB increases, and therefore visual sensitivity, the start time of song becomes later. The species level analysis agrees with the phylogenetically independent contrast analysis (Appendix A.3.8).

Table 4F.1. Phylogenetically independent contrasts analyses for the Chew dataset. General linear models and regression analyses of eye size or RIB, body mass, and timing of dawn song in order of AIC score (lowest score indicating best model). Asterisks imply degree of significance with a significant result (***) < 0.0001, ** < 0.001, * < 0.05).

Model number	Explanatory variables	Adjusted R-squared	Regression coefficient	Standard Error	F (d.f.)	Within model p-value	Overall p-value	AIC
2	Eye size		-183.55	76.70		0.036 *		
	Body mass	0.244	45.18	23.74	3.097 (2, 11)	0.084	0.086	124.57
3	Eye size	0.079	-50.37	34.67	2.111 (1, 12)	0.172	0.172	126.27
1	Eye size		-180.91	80.34		0.048 *		
	Body mass		41.47	27.02		0.156		
	Eye size x body mass	0.178	12.83	37.48	1.938 (3, 10)	0.739	0.187	126.42
4	Body mass	-0.054	-6.65	11.48	0.335 (1, 12)	0.573	0.573	128.02
7	RIB	-0.082	5.39	38.40	0.020 (1, 12)	0.89	0.891	128.36
6	RIB		9.35	40.06		0.820		
	Body mass	-0.144	-7.12	12.13	0.182 (2, 11)	0.569	0.836	129.96
5	RIB		9.27	42.53		0.832		
	Body mass		-7.06	13.56		0.614		
	RIB x body mass	-0.258	-0.98	75.94	0.110 (3, 10)	0.990	0.952	131.96

Table 4F.2. Phylogenetically independent contrasts analyses for the Gwaelod-y-Garth dataset. General linear models and regression analyses of eye size or RIB, body mass, and timing of dawn song in order of AIC score (lowest score indicating best model). Asterisks imply degree of significance with a significant result (***) < 0.0001, ** < 0.001, * < 0.05).

Model number	Explanatory variables	Adjusted R-squared	Regression coefficient	Standard Error	F (d.f.)	Within model p-value	Overall p-value	AIC
1	Eye size		-195.30	48.91		0.010*		
	Body mass		28	16.2		0.144		
	Eye size x body mass	0.721	51.58	24.68	7.877 (3, 5)	0.091	0.024*	67.623
2	Eye size		-199.05	61.07		0.017*		
	Body mass	0.564	44.57	17.65	6.17 (2, 7)	0.045*	0.035*	70.644
3	Eye size	0.229	-56.17	30.59	3.37 (1, 7)	0.109	0.109	74.439
4	Body mass	-0.036	-8.77	10.25	0.723 (1, 7)	0.423	0.423	76.798
7	RIB	-0.076	-20.6	31.24	0.435 (1, 7)	0.531	0.531	77.101
6	RIB		-16.108	33.12		0.644		
	Body mass	-0.163	-7.653	11.07	0.440 (2, 6)	0.515	0.663	78.488
5	RIB		-6.73	41.43		0.877		
	Body mass		-16.4	23.08		0.509		
	RIB x body mass	-0.343	50.13	113.34	0.319 (3, 5)	0.677	0.812	80.181

Table 4F.3. Phylogenetically independent contrasts analyses for the European dataset. General linear models and regression analyses of eye size or RIB, body mass, and timing of dawn song in order of AIC score (lowest score indicating best model).

Model number	Explanatory variables	Adjusted					Overall p-value	AIC
		R-squared	Regression coefficient	Standard Error	F (d.f.)	Within model p-value		
4	Body mass	0.019	-7.64	6.45	1.40 (1, 20)	0.250	0.250	198.14
3	Eye size	0.009	-15.86	14.51	1.20 (1, 20)	0.287	0.287	198.35
7	RIB	-0.047	6.65	27.16	0.06 (1, 20)	0.809	0.809	199.5
2	Eye size		-8.15	19.53		0.681		
	Body mass	-0.023	-5.25	8.73	0.76 (2, 19)	0.554	0.482	199.95
6	RIB		4.97	26.99		0.856		
	Body mass	-0.031	-7.58	6.63	0.68 (2, 19)	0.267	0.516	200.1
1	Eye size		-8.13	20.25		0.693		
	Body mass		-5.24	9.31		0.581		
	Eye size x body mass	-0.080	0.07	10.57	0.48 (3, 18)	0.995	0.701	201.95
5	RIB		6.7	31.49		0.834		
	Body mass		-8.32	9.36		0.386		
	RIB x body mass	-0.088	4.41	37.96	0.44 (3, 18)	0.909	0.729	202.09

Table 4F.4. Phylogenetically independent contrasts analyses for the Indonesian dataset. General linear models and regression analyses of eye size or RIB, body mass, and timing of dawn song in order of AIC score (lowest score indicating best model). Asterisks imply degree of significance with a significant result (*** < 0.0001, ** < 0.001, * < 0.05).

Model number	Explanatory variables	Adjusted R-squared	Regression coefficient	Standard Error	F (d.f.)	Within model p-value	Overall p-value	AIC
5	RIB		81.94	18.89		0.0123 *		
	Body mass		10.14	4.71		0.0979		
	RIB x body mass	0.768	35.40	27.62	8.73 (3, 4)	0.2692	0.031 *	59.38
6	RIB		65.86	15.00		0.00708 **		
	Body mass	0.738	10.94	4.96	19.59 (2, 4)	0.07852	0.009 *	59.79
7	RIB	0.570	60.97	19.02	10.27 (1, 6)	0.0185 *	0.019 *	62.54
4	Body mass	-0.059	7.72	9.87	0.61 (1, 6)	0.4636	0.464	68.85
3	Eye size	0.145	10.30	30.97	0.11 (1, 6)	0.7508	0.751	69.40
2	Eye size		-31.10	58.21		0.616		
	Body mass	0.470	16.37	19.29	3.66 (2, 4)	0.435	0.125	70.46
1	Eye size		-57.68	78.48		0.503		
	Body mass		6.78	26.87		0.813		
	Eye size x body mass	-0.392	-46.02	81.82	0.34 (3, 4)	0.604	0.797	71.93

Discussion

The relationship between visual ability and the onset of dawn song

This study is the first to examine the relationship between visual abilities and the onset of dawn song in a comparative approach, across multiple sites around the world. Both the species level and the phylogenetically independent contrast analyses concur that eye size is an important predictor of the timing of the onset of dawn song for bird species around the world, consistently following a negative relationship; birds with bigger eyes sang earlier than those with smaller eyes. Although variation exists between datasets in the best model to explain the time of onset of dawn chorus, eye size repeatedly occurs in the final best models selected by parsimony and information theory approaches.

These results agree with those of Thomas *et al.* (2002) for a small number of European study sites. As the timing of song during dawn twilight appears to be constrained by visual capability, these results also provide overall support for the inefficient foraging hypothesis for the dawn chorus (Kacelnik and Krebs, 1983), which states that singing is favoured at dawn because light levels are not yet high enough to enable birds to forage efficiently. Berg *et al.* (2006) found in a species level analysis, that eye size correlated with the start time of the neotropical dawn chorus; however, this relationship with eye size was only detectable when controlling for body mass, foraging height and taxonomy, and no significant relationship between eye size and start time was found within their phylogenetically independent contrast analyses when considering all species.

The finding that the timing of dawn song is constrained by visual capability raises the question of what costs may mediate this constraint. Singing in the dark may be a maladaptive strategy for diurnal birds because specialised nocturnal predators (with more sensitive vision), for example owls, may be able to locate the singer without being seen themselves. Remaining asleep (or at least, silent) until visual constraints are lifted would therefore allow a diurnal bird to stay hidden until it can avoid predation.

Keeping quiet may also be a strategy to reduce energetic costs. Ward & Slater (2005a) found that birds (willow warblers, *Phylloscopus trochilus*) singing from relatively exposed song posts are likely to incur costs by increasing their metabolic rate by up to 25% more than birds singing at foraging sites. However, when compared to flight, bird song (at least for those species so far examined) seems to incur low energetic costs overall (Ward & Slater, 2005b). Furthermore, while a bird is singing it is unable to participate in any other behaviour such as foraging, and so singing may confer constraints upon energy intake (Thomas et al. 2003; Ward, Lampe & Slater, 2004). While singing may not be as energetically costly as flight, song at dawn or night is costly when compared to a resting state near the BMR, such as seen during sleep (Ward & Slater, 2005b). Thomas (2002) found that in free living nightingales *Luscinia megarhychos* the rate of overnight mass loss increased with nocturnal song rate, and that in European robins *Erithacus rubecula*, less mass was gained during the day when song production was increased (Thomas et al., 2003).

Whilst not as important as eye size in explaining the variation within the datasets, a significant positive relationship exists between the time of onset of dawn

song and body mass (when controlling statistically for variation in eye size); smaller birds sing earlier than larger birds. This relationship has previously been attributed to energetics due to smaller birds having higher metabolic rates and thus needing to rise earlier in order to recoup the higher proportion of fat reserves lost overnight than bigger birds (Thomas *et al.*, 2002; Thomas 2000). The dawn chorus then allows the bird to advertise the fact that it has successfully survived the night to prospective mates and possible territory intruders (see introduction).

As body mass increases, song frequency decreases as a result of syringeal membrane morphology (Seddon, 2005). As a result, song post height also decreases, in order to maintain optimal sound transference properties, meaning that heavier birds are likely to sing at lower perches (cf. Berg *et al.*, 2006). Song produced at low heights should be of low-frequency to reflect the least-attenuated frequency window (Morton's sound window: Marten & Marler, 1977). Whether or not this relationship explains to some extent the fact that heavy birds sing later (i.e. being lower down in the forest would mean that light would not be perceived as early as those higher up) remains to be explored satisfactorily.

There is a strong positive correlation between eye size and body mass both for phylogenetically independent contrasts and at the species level. This relationship is well documented (Brooke *et al.*, 1999; Garamszegi *et al.*, 2002; Thomas *et al.*, 2002; Burton, 2008), and the exponent of the relationship in my dataset was within the range described in Burton (2008). The highly significant relationship between eye size and body mass may be due to scaling with brain size (bigger eyes require more neural processing power; Garamszegi *et al.*, 2002) or perhaps due to eye size being limited by metabolic rate directly or indirectly (i.e.

metabolic rate constrains brain size which then constrains eye size; Brooke *et al.*, 1999). Such collinearity between eye size and body mass, whilst not especially helpful in determining the best models for each site, does not bias the analyses described above, in part due to standard errors being taken into account when using the model derived parameters. Also, while there is some variability in the best models selected, the modelling procedure is able to partition the variance between the two independent variables relatively well.

Variation in the slope of the eye vs. song relationship with distance from the equator and with twilight length

My analyses indicated that there is a negative relationship between the slopes of association of eye size on the time of onset of dawn song, and distance from the equator (species level analyses) and twilight length (both species level and phylogenetically independent contrast analyses). This implies that the further from the equator the bird community is, the more strongly eye size is related to the time of onset of dawn song. While eye size is perhaps the best predictor of the start time of the dawn chorus globally, these results suggest that visual constraints may be less important in determining the timing of dawn song onset towards the tropics or short twilight lengths. One possible explanation for this is that in the species-rich tropics, the timing of dawn song is strongly influenced by acoustic competition between species.

Sites with longer twilights (e.g. Pwllgloyw, UK) and sites with higher species richness (e.g. Wangi Wangi, Indonesia), had a wider range (quantified as a higher standard deviation) of dawn song start times than at sites with short

twilights or low species richness. It is perhaps intuitive that the dawn chorus should be more spread out in longer twilight periods, because there is greater variation in the time at which light levels reach an intensity by which different species can forage efficiently (Kacelnik & Krebs, 1983).

The wider range of dawn song start times for sites of high species diversity can be explained (at least partially) by acoustic competition. At such sites, if all species sang at the same time, overlapping and masking of signals may prevent effective communication. The use of gaps in song production by coexisting species (i.e. partitioning the multidimensional acoustic space) in noisy environments, perhaps to reduce detection and discrimination error, has been shown in these tropical species: plain-winged antshrike, *Thamnophilus schistaceus*, and wing-barred piprites, *Piprites chloris* (Luther & Wiley, 2009). Similar effects have been shown in amphibians (Woodhouse's Toad, *Bufo woodhousei*, Sullivan & Leek, 1986). Some species are able to demonstrate vocal plasticity in that song structure and length can vary geographically within same species (greenish warbler, *Phylloscopus trochiloides* Irwin, 2000; little greenbuls, Slaabekoorn & Smith, 2002). Slaabekoorn and Peet (2003) and various others, found that vocal plasticity also occurs in great tits *Parus major* in artificially noisy habitats, with birds singing at higher minimum frequencies to prevent the masking effects of low frequency noise within an urban environment. Birds singing their dawn choruses in the tropics may also prevent masking by the similar strategy of spreading their dawn song start times over a longer period that would be explained by visual constraints alone.

Tropical bird species are noted for their differences in song behaviour to temperate species. For example, the females often participate in singing either alone or in duets with their mate, which does not occur to the same degree at temperate latitudes (Slater & Mann, 2004). Temperate bird song is often associated with intense territorial and mate defence or mate attraction during the breeding season. However, in the tropics many species maintain pair-bonds year round in a highly stable social environment (Morton, 1996). Therefore, tropical species perhaps do not utilise the dawn chorus in the same way as temperate species do. Another notable difference is that there is considerable variability in the timing of the tropical breeding season, even within the same species at a particular location, when compared to temperate species, perhaps causing song to function more in territory defence rather than for mate attraction.

Habitat type should also be considered. Different habitats can cause light intensity levels to vary considerably e.g. different forest canopies vary in their light attenuation properties, with some allowing very little light to reach the ground (Montgomery 2004) whereas open grassland is far brighter. Berg *et al.*, (2006) in their study on Neotropical birds found that birds that foraged higher in the canopy sang earlier, supporting the role of light intensity in the onset of the dawn song. Comparisons between the start times of activity between the same species in different habitats may yield interesting insights into how a bird perceives and responds to ambient light conditions. For example, birds living in dense forest habitats may not perceive light levels to have reached acceptable levels to begin singing at the same time as individuals of the same species living in more open habitats.

Comparing eye size and maximum retinal image brightness as predictors of the timing of the onset of dawn song

The results in Results section E for European locations (Chew, Gwaelod-y-Garth and Europe overall) suggest that eye size is a better predictor of the time of onset of dawn song, than RIB_{max} . The relationship between eye size and start time is negative, meaning that the earlier times of onset of dawn song are correlated with larger eyes. Conversely the results for Wangi Wangi, Indonesia suggest that RIB is the better predictor of dawn song, and that the relationship is a positive one, with larger RIB values derived for species that begin their song dawn later. The averaged European analyses do not identify any significant terms, presumably because taking mean song times into account also removes the variation that may be present due to latitude or twilight length.

While both eye size and RIB are measures of visual ability, they are different in their assessment of this ability. RIB allows an estimation of an eye's sensitivity, and so species with very sensitive eyes have large RIB estimates (for example nocturnal species, Martin 1990, see chapter 2). Eye size more generally accounts for the investment placed in vision, with larger eyes relative to body size being more costly than smaller eyes (see Chapter 1), and so having larger eyes must confer a visual advantage of some kind. However, a bird with larger eyes does not necessarily have to be active under low light levels (Land and Nilsson, 2002), and may have maximized eye size in order to increase image resolution, for example to detect small or distant prey items.

All three sites investigated for the eye size vs. RIB comparison (Chew, Gwaelod-y-Garth and Wangi Wangi) have species with similar foraging strategies

(insectivorous or frugivorous), and both of these strategies require good vision in order to be successful. Garamszegi *et al.* (2002) found that eye size increased with increasing prey mobility (on a scale of 1 for herbivorous/ granivorous species, 2 for species which glean prey from vegetation and 3 for species which actively hunt prey in air or water). Frugivorous species are reliant on colour vision to distinguish between palatable and unpalatable fruit. This requires that visual resources are employed in order to process colour information neurally.

The difference between European and Indonesian datasets in the best measure of visual ability for predicting dawn song onset, may also be explained by habitat type. The UK sites Chew and Gwaelod-y-Garth included both wooded and open habitats, in contrast to Indonesia, where most of the species for which RIB information is available inhabit forested areas. As many fruits in the tropical forest are within the dim environment of the canopy level, finding them may require relatively sensitive eyes, allowing a better correlation of activity with RIB than to overall eye size.

As discussed above, the timing of the tropical dawn chorus seems to be less reliant upon eye size, and therefore vision as a whole. However, Indonesian birds that have higher RIB estimates began to sing later. While this is non-intuitive in the sense that earlier song is expected if a bird is able to perceive environmental cues earlier (as seen in the European datasets) it may be explained by tropical birds with high RIBs perhaps foraging before they begin their song, rather than singing before foraging as is typical of temperate songbirds (Thomas *et al.* 2002).

In a tropical environment, there is often extremely high species diversity (e.g. up to 400 different avian species within a few km² in the Amazonian

rainforest; Slater & Mann, 2004). These species generally have larger territories than their temperate counterparts (Terborgh *et al.*, 1990), perhaps in order to gain enough nutrients to survive in a competitive environment: Eberhard & Ewald (1994) found that Anna's hummingbird, *Calypte anna*, territory sizes became larger with decreasing food availability (in addition to decreasing pressure from territory intruders). Reid's (1987) study on the savannah sparrow, *Passerculus sandwichensis*, found that song output was limited by food availability, with less song produced when food resources were low. Theoretical studies on the timing of dawn song suggest that when rewards from foraging are low, then song output should also be low, and the time at which foraging commences is earlier (McNamara *et al.*, 1987). As the tropics are highly variable in their food resources (Slater & Mann, 2004; Karr, 1976), birds with better vision may use the early morning to begin their foraging rather than singing, allowing them to forage without high levels of interspecific competition. However, to fully understand the relationship between RIB and the time of onset of dawn song and/ or activity, further RIB measurements of a wider range of species are needed, from a wider variety of locations around the world.

Chapter 5: Effects of artificial lighting on the behaviour of European robins

Abstract

Throughout most urban and some rural areas, artificial lights are prevalent. While beneficial in some respects, enabling humans to be active day or night, the effects of light pollution (or extraneous light) on the behaviour and ecology of wild birds are poorly understood. I compared the timing and organization of singing and foraging behaviour in a diurnal passerine bird, the European robin *Erithacus rubecula*, under natural and artificial lighting conditions. In a field study of free-living robins, I found that robins with territories artificially lit by street lighting had abnormal song routines, beginning to sing at dawn far earlier than robins with unlit territories. The onset of foraging at dawn was much more variable in artificially lit territories than unlit territories; there was no consistent overall shift in the timing of dawn foraging, but some individuals with artificially lit territories were observed foraging in the middle part of the night. Nocturnal foraging reduces the length of the overnight fast, and would therefore reduce the risk of overnight starvation. I found no significant effects of artificial lighting on either singing or foraging at dusk. In unlit territories, robins normally began to forage soon after starting to sing at dawn, after which they interspersed singing with foraging. In contrast, robins with artificially lit territories maintained a prolonged dawn chorus, delaying their onset of foraging relative to their first song at dawn. A parallel study of wild-caught robins held in aviaries under two common types of street-lighting supported the findings of the field study, that light pollution can change behavioural routines,

energy regulation and hence communication strategies. Given the ubiquitous use of artificial lighting in the modern world, it is clearly important to evaluate the consequences of these behavioural changes for the welfare and fitness of wild animals.

Introduction

Most humans now live in artificially bright environments, and light pollution from the widespread use of artificial outdoor lighting constitutes a major environmental change in many ecosystems around the world. For example, light pollution measured at the Mount Wilson Observatory in California has increased approximately 30 fold between 1900 and 2000 (Garstang, 2004). The impacts of various types of pollution on organisms and ecosystems have been the focus of much research (Warren *et al.*, 2006; Zala and Penn, 2004), but although artificial lights and light pollution are increasingly prevalent, the impacts of light pollution on the welfare, behaviour and ecology of wildlife remain poorly understood (Longcore and Rich, 2004).

Artificial lighting

While artificial lighting began with the advent of man-made fire approximately 790,000 years ago (Goren-Inbar *et al.*, 2004), the first record of modern street lighting was in 1417, when the mayor of London, Sir Henry Barton, ordered lanterns to be hung out on winter evenings (Dickens, 1867). Gas lights, invented in the late 18th century were widely used well into the 20th century (with some parts of

the world still using this form of lighting today). However, electric light sources started to replace gas lights after the invention of the arc lamp (where an electric current “jumps” from one electrode to another, via a gas or air filled gap) and incandescent lamp (light generated when a thin filament is heated electrically) in 1858 and 1878, respectively (Rickwood, 2001). It was then realised that the efficiency of these early lamps could be increased by enclosing the electrodes in a chamber and introducing various gases and metallic compounds; a method used in many of the commonly used modern street lights. For example, low-pressure sodium lights (invented in 1932) have an efficiency of up to 180 lumens per watt, compared with incandescent lamp efficiencies of approximately 20 lumens per watt (Thumann and Mehta, 2001). Low-pressure sodium lamps (henceforth “SOX”) are among the most efficient lighting available, and while there are other lamps which offer a broader colour output (SOX are characteristically orange), most modern street lights are of this type (e.g. 54 % of Buckinghamshire County Council’s lighting scheme is low-pressure sodium, 45% high-pressure sodium and 1% other sources, Allen, K. pers, comm.). However, recent trends in public lighting are towards broad spectrum lighting more similar to daylight (Webster, T. pers. comm.), and LEDs (light emitting diodes). LEDs have very low energetic demands and carbon emissions, but as they are also costly to install, they are likely to be cost-prohibitive to many local councils.

Effects of artificial lighting on the timing of avian behaviour

As artificial light is extremely widespread, its impacts may constitute a major conservation issue. Furthermore, understanding the effects of artificial lighting on

wildlife is an important scientific issue as this can reveal the mechanisms underlying natural behavioural routines (Bolhuis, 2005). Domestic birds are known to perform abnormal behaviours under artificial lighting, which impacts upon their health, fitness and welfare (Bolla, 2001; Moinard *et al.*, 2001). In addition, a wide range of bird species show abnormal behaviour under artificial lighting conditions in the wild. These include normally diurnal birds singing, foraging, and even feeding chicks at night (e.g. Martin, 1990). In the presence of artificial lighting, wild birds such as blue tits, great tits and chaffinches begin to sing earlier in the day when compared to those singing in unlit habitats (Bergen and Abs, 1997). Many otherwise diurnal birds are known to be active at night under artificial illumination, including the European robin *Erithacus rubecula* (Hollom, 1965; England, 1977), song thrush *Turdus philomenos*, wren *Troglodytes troglodytes* (pers. obs), European blackbird *Turdus merula* (Mitchell, 1966), and black redstart *Phoenicurus ochruros* (Patterson, 2000). However, the role of these activities on fitness parameters, e.g. regulation of energy reserves, survival and reproductive success, is unknown.

In this study, I investigated the effects of artificial lighting on the timing of singing and foraging in free-living European robins (*Erithacus rubecula*, henceforth “robin”), and on the timing of foraging and body mass regulation in aviary-held robins. The robin is highly territorial and maintains its territory by singing (Cramp, 1988). At dawn, the robin is one of the first European passerine species to commence singing and foraging, owing to its relatively large eyes and an eye design which confers a relatively high retinal image brightness ($RIB_{\max} = 0.531$, see Chapter 2) and hence good visual capabilities under low light levels

(Thomas *et al.*, 2002; 2004). Robins are known to sing and forage at night near to artificial lights under some circumstances (Hollom, 1965; King, 1965; England, 1977; Fuller *et al.*, 2007).

In a detailed field study by Miller (2006), another relatively large-eyed species, the American robin *Turdus migratorius*, was found to commence song far earlier (i.e. during the latter part of the night) in artificially lit areas than in nearby unlit areas. American robins also started to sing earlier when permanent artificial lighting was introduced into the same previously unlit areas. Whereas Miller's (2006) study focused exclusively on nocturnal singing behaviour under different levels of artificial illumination, my study directly compares the dusk, overnight and dawn routines of song and foraging behaviour, between matched artificially lit and unlit territories in the wild, and in a more controlled aviary setting.

The aims of my study were to investigate how artificial lighting affects the dusk-to-dawn organization of singing and foraging behaviour in the European robin. Preliminary observations of nocturnally singing robins had previously revealed that illuminated territory holders commence song as an early extension of normal dawn song (pers. obs.). As with other diurnal birds, robins appear to start their dawn chorus and then commence foraging as soon as visual constraints allow them to do so efficiently (Kacelnik, 1979; Thomas *et al.*, 2002; McNeil *et al.*, 2005). Therefore, it was predicted that the robins with artificially lit territories would sing and forage earlier at dawn and later at dusk than those with unlit territories. My study also investigated how artificial lighting may influence the overall organisation of singing and foraging behaviour. For example, if artificial lighting allows robins to forage effectively at night, a permanently illuminated

territory may be advantageous by allowing birds to minimize their risk of overnight starvation while maximizing their song output.

Methods

A. Study of free-living robins

Study Design, Study Site and Environmental Measurements

I studied 12 matched pairs of artificially lit robin territories ($N=12$ territories) and unlit territories ($N = 12$ territories). Each pair of territories was monitored overnight on one occasion during the study period, which comprised the period from the 16th November 2005 until 7th March 2006. The study area (around Machen, Wales 51° 35' 55"N, 003° 08' 22"W) consisted of a rural river valley with deciduous woodland, open farmland (pasture), hedges, streams and residential areas on both the north and south sides of the valley. All territories were comprised of similar habitat and, because they were near the same 5km length of road, had comparable traffic levels over the course of each day and throughout the observation period. I chose the matched pairs of unlit and artificially lit territories so that the two territories in each pair did not obviously differ in any respect apart from the absence or presence of public street lighting. All of the street lights had been in situ for at least 4 years (Caerphilly County Council, pers. comm.) and were of high pressure sodium (SON) or low pressure sodium (SOX) type.

I mapped focal robin territories by observing interactions and identifying song posts during the dawn and dusk chorus, for at least two weeks prior to, and

throughout the study period. Some of the robins were colour ringed prior to the study period, to facilitate territory mapping and individual identification. Paired birds were individually identifiable when attending remote weighing stations (see below), by their colour rings and/or by clear differences in their body masses. Only one robin was observed singing in each territory at the time of study; the lone territory holder before pairing and only the male after pairing (Cramp 1988).

Artificially lit territories were illuminated by either SON (7 territories) or SOX (6 territories) street lights, with one type of lamp being situated within or adjacent to each territory. Throughout the study, some of the street lamps were controlled by top mounted phototransistors, which automatically turned on the lights when ambient light intensity fell below approximately 70 lux, and off when it rose above 70 lux. The other street lights were controlled by time switches, and were turned on and off at equivalent times to the phototransistor controlled lights. Both of these devices were under the control of Caerphilly County Borough Council. Unlit territories did not receive any direct artificial light, although indirect sky glow caused by artificial light being scattered and reflected by aerosols and water droplets in the atmosphere inevitably provided some illumination above natural background levels.

I measured light intensity (illuminance, in lux) within each territory, using a 4-in-1 Environment Meter DT-8820 (CEM, China) and a Light Meter N76CC (Precision Gold). Light intensity was measured as illuminance of the ground surface, by holding the light sensor horizontally at a height of 1m, facing the ground surface which consisted of a mix of leaf litter, soil and vegetation. Measures of illuminance quantify the amount of light falling upon an area, i.e.

lumens per m² (lux), where a lumen is defined as all the radiated power emitted by a light source, and which is evaluated with the spectral sensitivity of the human eye and the photometric radiation equivalent k_m (Martin 1990, OSRAM 2005). The spectral sensitivity of birds is different to that of humans (Honkavaara *et al.*, 2002), but measurements in lux allow quantification of the timing and magnitude of the large scale light intensity differences across the day-night cycle and between artificially lit and unlit robin territories.

I measured light intensity within 1m of the feeding station in each territory (see below), at hourly intervals throughout the night. I also measured light intensity at 10 randomly located positions within each territory during true night (between the end and onset of astronomical twilight), during a single night. As the behaviour of robins was monitored in matched pairs of territories on each night, each pair of territories received similar natural ambient light levels (i.e. light other than from artificial sources of illumination) during their observation period.

To check that traffic noise was not a confounding factor in my study (cf. Fuller *et al.*, 2007), the sound pressure levels within each territory were measured at midnight and at sunrise (+/- 40 minutes) using a AZ 8928 sound meter (A-weighted, slow response setting).

Measuring the Effects of Artificial Lighting on Song

To investigate the effects of artificial lighting on song timings and rate, each robin was observed throughout a single night, from approximately 1h before sunset until 1h after sunrise. Matched pairs of robin territories, consisting of one artificially lit territory and one unlit territory, were monitored together on the same night. A

maximum of four individuals (i.e. two matched pairs) were observed per night, though the median number of individuals monitored each night was two birds (1 matched pair).

Every hour, each individual was observed for five minutes and its song rate was measured using a stopwatch. My preliminary observations indicated that when robins were active and singing, their song rates were generally high (see Results), so that 5-minute sampling periods were sufficient to obtain accurate estimates of overall song output. As paired lit and unlit territories were each visited for 5 minutes in every hour, it is unlikely that the first song heard at dawn or the last song heard at dusk in each territory was actually the first or last song to be sung by the territory holder. I therefore categorized the time of song by the 1-hour period relative to the time of sunrise, at which the first or last song was heard.

Measuring the Effects of Artificial Lighting on Foraging Behaviour

I set up remote-weighing feeding stations (cf. Thomas and Cuthill, 2002) in each of the artificially lit and unlit territories. These feeding stations had three main functions: (i) to measure the effects of lighting on foraging behaviour, (ii) to assess differences in body size between individuals and (iii) to eliminate any differences in food availability between territories. To do this, I provided an unlimited supply of mealworms in each robin's territory, in a dish positioned on top of an electronic balance. Robins could be weighed to an accuracy of 0.1g as they collected mealworms from the dish. During monitoring periods, each feeding station was filmed using Sony Handycam® series video cameras. These cameras have an infra-

red NightShot facility, enabling me to monitor the foraging behaviour (and body mass when stable weighings were possible) of each robin throughout the night, from before dusk to after dawn.

Each individual was allowed 24 hour access to the *ad libitum* supply of mealworms at its weighing station for at least two weeks prior to observation. This was long enough to train the robins to forage consistently from the feeders (cf. Thomas, 2000). Each robin therefore had access to an unlimited high quality food supply, which, due to reducing the time needed to search for food, is known to increase song output (Thomas, 1999a; b; and references therein). As all robins regardless of lighting regime had access to this unlimited food supply, this effectively removes any differences in food availability and hence foraging success between territories, allowing me to compare directly the effect of lighting regime on behaviour.

B: Study of aviary-held birds

Ten European robins were captured from the wild, and housed under Countryside Council for Wales licence no. OTH:SB:05:2006. The robins were captured from woodland around Cardiff, using mist-nets and tilting cage traps. Once caught, each individual was immediately brought into the Home Office approved aviaries at Cardiff University Botanical Gardens, Cardiff, Wales, UK. Each robin was kept in an aviary measuring approximately 1.8 m x 1.8 m x 1.8 m. Enrichment of the aviary environment was provided in the form of small trees, shrubs, and branches, with a soil and woodchip floor. A small roost box was also provided in each aviary.

Food (a combination of mealworms dusted in Vitacel vitamin powder, berry suet, insect suet, oats and Haith's softbill mix containing insects, honey and seeds) was provided *ad libitum*, with water for drinking and bathing, and which was renewed on a daily basis. Each robin's feeding and water dishes were regularly cleaned using bird safe Arklens disinfectant to minimise infection risk.

Each robin's aviary was covered in 3-pass blackout fabric to block out any external ambient light, and to prevent the robins from seeing each other (though they could still hear each other). This blackout material was adhered to the aviary walls and ceiling by ties and black gaffer tape, to eliminate any chance of the robins getting between the fabric and the aviary walls.

Each aviary was illuminated by a Philips ® MASTER TL-D 90 De Luxe 58W/965 1SL fluorescent tube light, with a colour temperature of approximately 6500K (cool white light, similar to that of daylight), and a colour rendering index (CRI) of 93, where daylight CRI is 100 (Figure 5.1). The flicker rate of these fluorescent lights was above the level of detection for other passerine birds (Maddocks, Goldsmith and Cuthill, 2001). The lights were dimmed on and off to mimic light intensity changes at dawn and dusk as closely as possible. However, due to the limitations of the circuitry, there was a minimum light intensity of approximately 1 lux, at which the lights abruptly switched on or off.

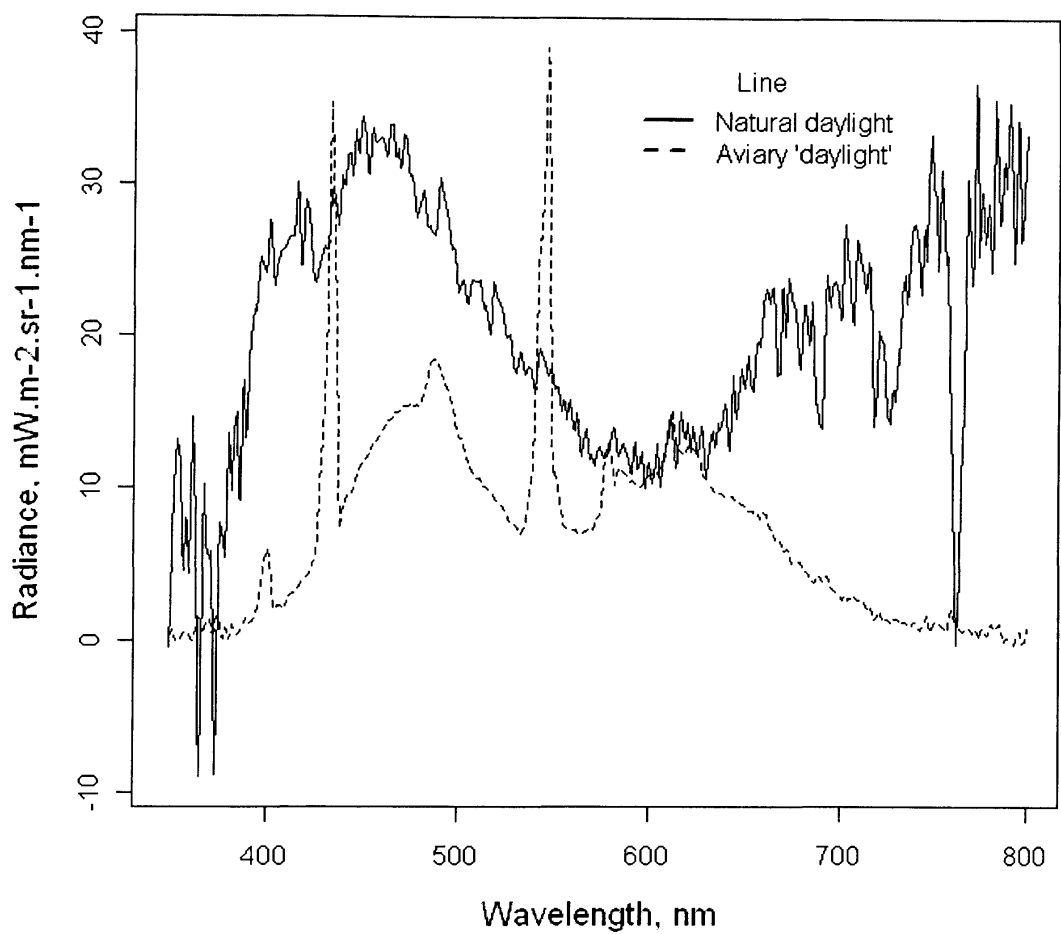


Figure 5.1. The spectral power distribution (in radiance) of winter morning sunlight (solid line), measured on the 15th November 2006, compared with that of aviary fluorescent “day” lighting (Philips ® MASTER TL-D 90 Deluxe Pro 58W/965 1SL, average of 12 readings) (dashed line). The data for the natural light was multiplied by 10 to allow the waveform patterns to be compared.

Each robin was allowed to acclimatise to its new environment for a minimum of one week before any changes to lighting regime or lighting type were made. Subsequently the timing of dawn and dusk was shifted gradually by 12-hours to facilitate the planned experimental work. The robins were then maintained under a 15:9 dark: light regime, mimicking a winter daylight regime, when robins are strongly territorial (BWPI, 2007).

Street lights were obtained from Caerphilly Council (SON and SOX) and DW Windsor Lighting (SON and CDO), and were rewired to allow them to be plugged into a mains source (240V). To assess the differences in the lights used within the aviary, the spectral power distribution of the fluorescent (standard “day” lighting), SON and SOX lamp was determined using a single-beam field spectroradiometer, operating with a 15° field of view, and a spectral range of 350 – 1050 nm (GER-1500, loaned from the NERC Field Spectroscopy Facility). This was fitted with a fibre optic probe with cosine diffuser, mounted upon a tripod, with the sensor facing away from the ground, to obtain spectral information. Data from 800 nm to 1050 nm was discarded due to the high error of measurements within this range (MacLellan, C., NERC Field Spectroscopy Facility, pers. comm.). No measurements were taken from the CDO (MASTER CityWhite CDO-TT 70W) lamp as this lamp arrived after the spectroradiometer loan period had ended. Instead, this information was obtained from the manufacturer’s webpage (Philips, UK: http://www.lighting.philips.com/gb_en).

Each robin was exposed to a series of lighting treatments, in randomised order, and their behaviour under each lighting treatment was recorded (see below). Each robin received each lighting and control treatment to minimise the number of

birds required, and so that each bird acted as its own control. Street lights (SON, SOX and CDO) and the recording equipment were initially introduced to each cage approximately 15 hours before any behavioural recordings were taken, so that the robin could become accustomed to the novel items (i.e. the equipment) in its aviary. Street lights were surrounded by metal mesh to prevent the robins from landing on top of the lamps and burning themselves.

During each experimental regime, a timer switch was used to automatically switch on the street lights at the beginning and end of the robins' "night", simulating the conditions found in artificially lit territories of free-living robins. Each robin was exposed to SOX, SON and CDO lighting treatments, as well as an unlit control (no artificial light during the "night" period). Each individual robin received each treatment twice: once with the behavioural recordings beginning at "dusk" (night-day observations) and once with the recordings beginning at "dawn." (day-night observations). Due to the recording capacity of the video cameras, behavioural recordings were made for approximately 22 hours from the onset of each monitoring period.

Behavioural Observations

Body masses were recorded throughout the course of the experiment using a remote weighing station, comprising of a food dish on top of an electronic balance (MyWeigh iBalance 500) within the aviary. The weighing station was filmed using a Sony Handicam® DCR-SR32 Hard Drive camcorder mounted on a tripod. All equipment was powered by mains electricity to allow recordings to be continuous for 22 hours, and to prevent the risk of battery failure. Each camcorder was

downloaded and reviewed using digital media software (VideoLAN VLC media player and Sony Picture Motion Browser ®). In addition to body mass, any additional behaviour seen on film (e.g. hopping about, flying or foraging on the ground) regarding the robins' activity was also noted, as some of the robins were reluctant to alight on the electronic balance, even after several months of training. Therefore, monitoring of their activity budgets was valuable in assessing if the street lights had any impact on these birds' behaviour.

The start time of the birds' night-time rest period (equivalent to the wild robins fast period) was quantified as the number of minutes relative to daybreak (for night-day observations) and relative to nightfall (for day-night observations), with negative values indicating time before daybreak/nightfall. Daytime body mass gains were calculated as a percentage of each individual's overall body mass, by dividing the total mass gained over the period of activity, by the first recorded morning mass. The rate of mass gain was calculated by dividing the mass gain by the length of the activity period.

Once the study was completed, the robins were gradually re-acclimatised to natural lighting times, and were released at their place of capture. Supplementary food was provided for approximately 2 weeks to allow the robin to become re-habituated to the wild.

Statistical Analyses

Analyses were performed using Minitab Version 14.2 (Minitab Inc.), SPSS Version 12.02 (SPSS Inc.) and R Version 2.8.0 (The R Foundation for Statistical Computing). Data distributions and the diagnostic statistics of each test were

evaluated, with non-parametric tests employed where appropriate. Two-tailed statistical tests were used throughout. Power analyses are presented for non-significant results. Power analyses for non-parametric tests were performed empirically, by randomly resampling the dataset, to determine the sample sizes required to provide a significant result given the observed effect sizes and data distributions.

For practical reasons, it was not possible to obtain complete data for foraging onset/cessation times for the focal robin from all 12 matched pairs of territories in the study of free-living robins. As a result, the sample sizes vary between analyses, depending on the data available. Complete song data was not obtained for all 12 matched pairs because for some territories no song was recorded during any of the hourly 5-minute monitoring periods spanning the first or second half of the night. Specifically, on one territory no song was recorded from the focal bird during the midnight - to end of dawn period, and on four territories no song was recorded from the focal birds during the start of dusk - to midnight period. Where this occurred, the time of first and last song could not be ascertained and so the data for the matched-pair of territories was excluded from the analysis. This resulted in the sample sizes of 11 matched pairs of song data for dawn and 8 matched pairs for dusk.

Similarly, foraging data were not available for both dawn and dusk for all territories used in the study of free-living robins. For some territories, no foraging at the balance was recorded during the dusk –to midnight or midnight – to dawn periods, so the exact time of last or first foraging was unknown. These birds were, however, observed to be active in their territories during these periods, and would

almost certainly have been foraging elsewhere (out of view of our cameras). Where this occurred, the time of the first and last visit to the feeder could not be ascertained and so the data for the matched-pair of territories was excluded from the relevant analysis. This results in the sample sizes of 9 matched pairs of foraging data for dawn and 9 matched pairs for dusk.

In the aviary study, data is also incomplete for some variables due to technical difficulties. In particular, two of the robins died whilst in captivity; one apparently due to natural causes before data were collected, and the other after collision with the cage. The latter bird had already completed half of the experimental protocol, and so was included in the analysis. As a result of these and other practical difficulties, sample size varies from analysis to analysis.

Results

A. Study of Free-Living Robins

Comparisons of Environmental Factors Between Artificially Lit Territories and Unlit Territories

As expected, light intensity at the feeding station during true night was significantly higher in the artificially lit territories than in the unlit territories (median \pm interquartile range: artificially lit territories 0.53 ± 0.45 lux, unlit territories 0.03 ± 0.02 lux, Wilcoxon Signed Ranks test: $T = 0$, $N = 12$ pairs of territories, $P = 0.003$).

Among the territories to which we had sufficient access to the whole territory (N= 10 pairs of artificially lit and unlit territories), the light intensity during true night, measured at randomly selected point across the whole territory, was significantly higher in artificially lit territories (Wilcoxon Signed Ranks test comparing median lux levels in matched lit and unlit territories: $T = 0$, $N = 10$ pairs of territories, $P = 0.002$). The light intensities during true night within unlit territories were uniformly low (minimum recorded light intensity in all unlit territories was 0.00 lux and maximum recorded light intensity ranged from 0.00 – 0.10 lux). In contrast, the spacing of the street lights and vegetation resulted in nocturnal light intensity within artificially lit territories being highly variable, with some parts receiving direct illumination from street lights and other parts being shaded (minimum recorded light intensity ranged from 0.00 - 1.20 lux, maximum recorded light intensity ranged from 3.10 – 28.70 lux).

The distance from the centre of each territory to the road was higher in unlit territories (median \pm interquartile range: 43.6 m \pm 42.9) than in artificially lit territories (median \pm interquartile range: 17.14 m \pm 9.74; Wilcoxon Signed Ranks test: $T = 11$, $N = 12$ pairs of territories, $P = 0.031$). Nevertheless, sound levels were low in both lit and unlit territories. Sound pressure levels at dawn were not significantly different between lit and unlit territories, the median value recorded \pm range was 53.8 \pm 21.9 dB in artificially lit territories and 49.5 \pm 18.0 dB in unlit territories; Wilcoxon Signed Ranks test: $T = 28$, $N = 12$ pairs of territories, $P = 0.424$. Power analysis suggests that the non-significant result is not simply due to the small sample; a sample of $N = 71$ pairs of territories would be required to give

a significant result at $P < 0.05$, given the observed effect size and data distributions.

Comparisons of the Organisation of Singing and Foraging Behaviour Between Artificially Lit Territories and Unlit Territories

Comparisons of the timing of dawn song

The time of the first song at dawn or last song at dusk was quantified in hourly categories relative to the hour in which sunrise occurred (see Methods). The robins with artificially lit territories began to sing significantly earlier before dawn than the matched robins with unlit territories (median \pm interquartile range: artificially lit territories category 3.0 ± 1.5 , unlit territories category 1.0 ± 1.0 , Wilcoxon Signed Ranks test: $T = 66$, $N = 11$ pairs of territories, $P = 0.004$, Figures 5.2 and 5.3). Singing did not occur in discrete bouts throughout the night, and as in our earlier preliminary observations, the robins in our study that began to sing during the latter part of the night sang intensively and more or less continuously until dawn (Figure 5.2). In effect, this was an early and prolonged extension to the dawn chorus. We also noted that robins on lit and unlit territories had similar song rates during their first hour of dawn song. However, by the second hour of dawn singing, robins with artificially lit territories maintained high song rates, while robins with unlit territories tended to sing at a lower rate.

Comparisons of the timing of dusk song

In contrast to dawn, the timing of the last song in the evening did not differ significantly between artificially lit and unlit territories (median \pm interquartile range: artificially lit territories category 11.0 ± 1.0 , unlit territories category 11.0 ± 2.5 , Wilcoxon Signed Ranks test: $T = 10.5$, $N = 8$ pairs of territories, $P = >0.999$). Power analysis suggests that the non-significant result is not simply due to the small sample; a sample of $N = 41$ pairs of territories would be required to give a significant result at $P < 0.05$, given the observed effect size and data distributions.

Comparisons of the light intensity at the time of first song at dawn

The light intensities at the time at which robins start and finish their singing and foraging can be viewed as the critical thresholds required for the birds to begin these activities (Kacelnik, 1979). Despite the large differences in the timing of song described above, we found no significant difference between artificially lit and unlit territories in the light intensities at which singing began (median \pm interquartile range: artificially lit territories 0.330 ± 9.90 lux, unlit territories 0.570 ± 0.453 lux, Wilcoxon Signed Ranks test: $T = 28$, $N = 11$ pairs of territories, $P = 0.689$). Power analysis suggests that the non-significant result is not simply due to the small sample; a sample of $N = 166$ pairs of territories would be required to give a significant result at $P < 0.05$, given the observed effect size and data distributions.

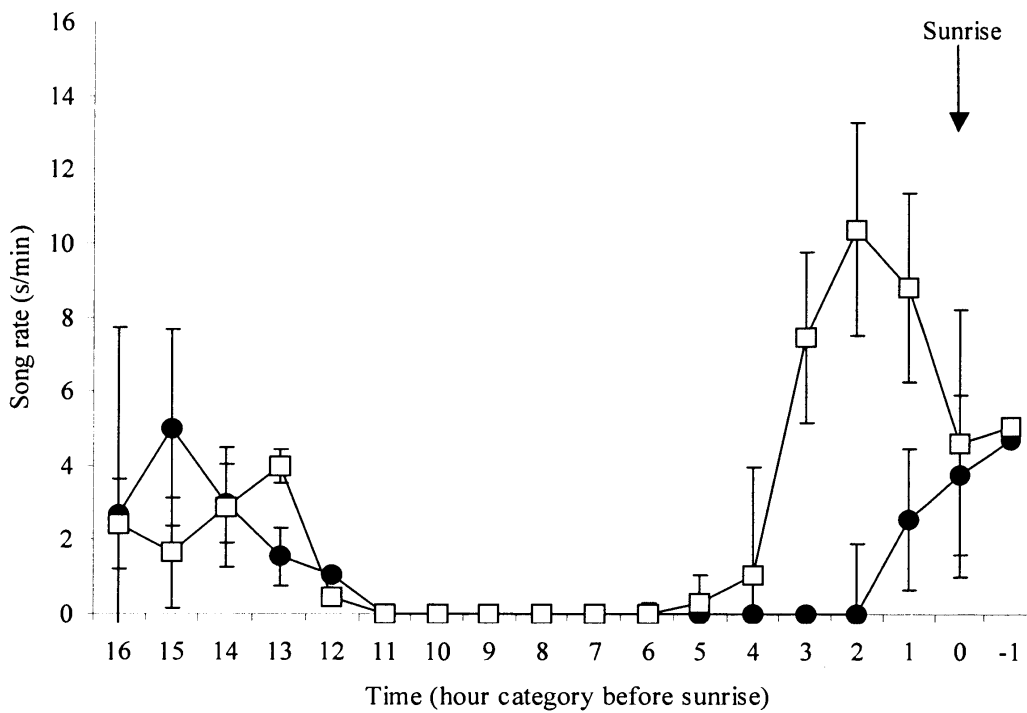


Figure 5.2. Overnight song rates of European robins in artificially lit territories (open squares) and unlit territories (closed circles). N = 12 matched pairs of territories. Error bars represent ± 1 SE. The left hand peak represents the dusk chorus and the right hand peak represents the dawn chorus.

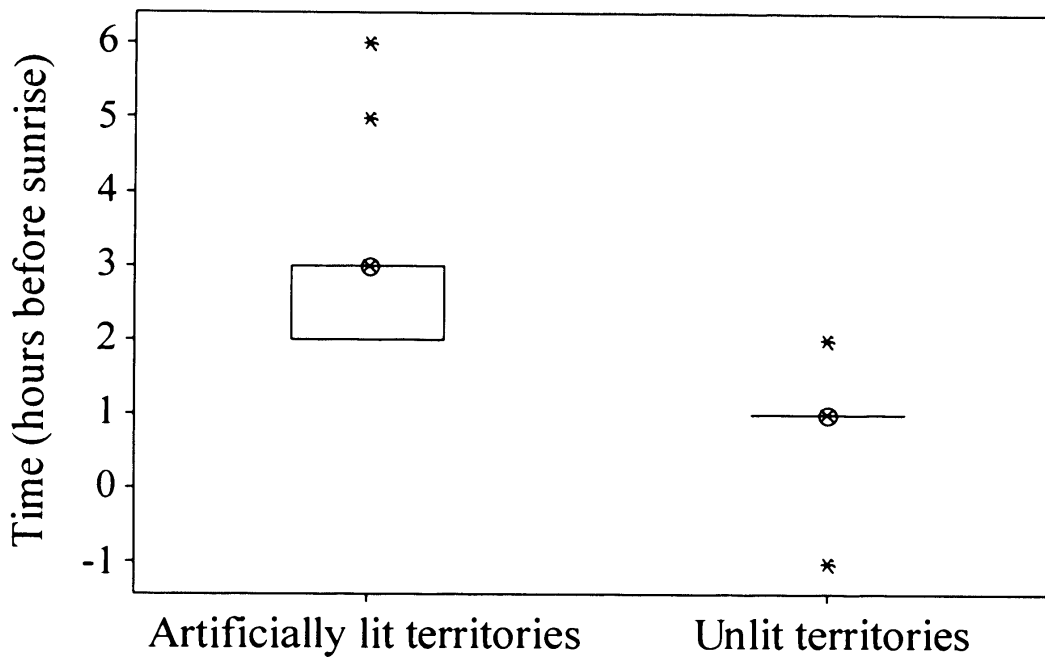


Figure 5.3. Times of first morning song in artificially lit and unlit robin territories. N = 11 matched pairs of territories. The time of song is categorised into hours before sunrise (2nd and 3rd interquartiles in addition to the median and outliers are shown).

Comparisons of the time of first foraging at dawn

There was a marginally non-significant difference in the time of the first visit to the feeder in the morning between robins with unlit territories and those with artificially lit territories (median \pm interquartile range: artificially lit territories 38.0 \pm 136.5 minutes before sunrise, unlit territories 21.0 \pm 30.5 minutes before sunrise, Wilcoxon Signed Ranks test: T = 7, N = 9 pairs of territories, P = 0.074; Figure 5.4). Power analysis suggests that the non-significant result may be due to the small sample of data that could be obtained; a sample of just one extra pair of

territories would be likely to give a significant result at $P < 0.05$, given the observed effect size and data distributions. The inter-quartile range values indicated that the variation between individuals in artificially lit territories was more than four times higher than between individuals with unlit territories.

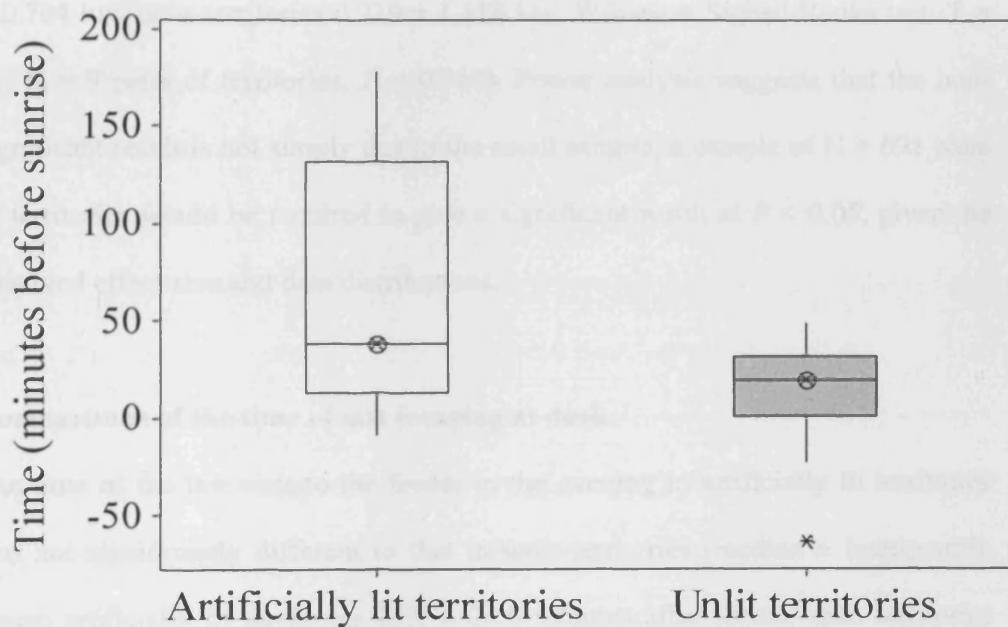


Figure 5.4. Times of first morning visits to ad libitum feeding stations in artificially lit and unlit robin territories. $N = 9$ matched pairs of robin territories (2nd and 3rd interquartiles in addition to the median and outliers are shown).

Comparisons of the light intensity at the time of first foraging at dawn

The light intensity at which foraging commenced was calculated by interpolation from the hourly measurements of light intensity. We found no significant difference between artificially lit and unlit territories in the light intensities at which foraging began (median \pm interquartile range: artificially lit territories 0.475 ± 0.704 lux, unlit territories 0.219 ± 1.118 lux, Wilcoxon Signed Ranks test: $T = 21$, $N = 9$ pairs of territories, $P = 0.910$). Power analysis suggests that the non-significant result is not simply due to the small sample; a sample of $N = 691$ pairs of territories would be required to give a significant result at $P < 0.05$, given the observed effect size and data distributions.

Comparisons of the time of last foraging at dusk

The time of the last visit to the feeder in the evening in artificially lit territories was not significantly different to that in unlit territories (median \pm interquartile range: artificially lit territories 25.0 ± 24.0 minutes after sunset, unlit territories 22.0 ± 15.5 minutes after sunset, Wilcoxon Signed Ranks test: $T = 10$, $N = 9$ pairs of territories, $P = 0.156$). Power analysis suggests that the non-significant result is due to the small sample of data that could be obtained; a sample of just $N = 18$ pairs of territories would give a significant result at $P < 0.05$, given the observed effect size and data distributions.

Instances of nocturnal foraging

Of the 12 matched pairs of territories, for each of which we monitored foraging continuously throughout the dusk-overnight-dawn period, three individuals - all on artificially lit territories - began to forage 2-3 h before sunrise (179, 110 and

143 minutes before the robins on the unlit territories with which they were matched). One of these individuals was also observed to forage at approximately 2 h after sunset (100 minutes later than the robin on the unlit territory on which it was matched) when it made two successive visits to our feeder, with the longest of these visits lasting 5 minutes. Thus, it appears that although nocturnal foraging can be possible under the levels of artificial lighting observed in our study, many of the individuals in our study chose not to do so.

The result of foraging later at dusk during the middle part of the night and/or earlier at dawn (when this occurs) is to reduce the duration of the overnight fast, during which body mass is lost as energy reserves are consumed. We defined the length of the fast as the longest interval between successive visits to our feeding station between sunset and sunrise. The difference in fast length between matched artificially lit and unlit territories was marginally non-significant (median \pm interquartile range: lit territories 747 ± 163 , unlit territories 813 ± 91 , Wilcoxon Signed Ranks test: $T = 7$, $N = 9$ pairs of territories, $P = 0.074$). Power analysis suggests that the non-significant result is due to the small sample of data that could be obtained; a sample of just two extra pairs of territories would give a significant result at $P < 0.05$, given the observed effect size and data distributions.

Comparisons of the timing and light intensities at which singing and foraging began at dawn

We compared the delay between starting to sing in the morning and starting to forage (to the nearest hour before sunrise, with time = 0 at sunrise), between artificially lit and unlit territories. Robins with artificially lit territories commenced foraging significantly later relative to the start of singing than birds

with unlit territories (median \pm interquartile range: artificially lit territory robins 2.0 ± 2.0 hours between starting to sing and starting to forage, unlit territory robins 0.0 ± 1.0 hours between starting to sing and starting to forage, Wilcoxon Signed Ranks test: $T = 0$, $N = 9$ pairs of individuals, $P = 0.009$).

Robins with unlit territories began to forage at dawn at significantly higher light intensities than the light intensities at which they began to sing (median difference in light intensity \pm interquartile range: unlit territories 0.199 ± 1.117 lux, Wilcoxon Signed Ranks test: $T = 33$, $N = 8$ pairs of territories, $P = 0.042$), whereas foraging did not begin at significantly higher light intensities than singing in artificially lit territories (median difference in light intensity \pm interquartile range: artificially lit territories 0.200 ± 0.574 lux, Wilcoxon Signed Ranks test: $T = 14$, $N = 8$ pairs of territories, $P = 0.624$). Power analysis suggests that the non-significant result is not due to the small sample of data that could be obtained; a sample of 112 extra pairs of territories would be needed to give a significant result at $P < 0.05$, given the observed effect size and data distributions.

B. Study of Aviary-Held Robins

Artificial lighting

Figures 5.1, 5.5 and 5.6 show the spectral power distributions of the aviary “daytime” lighting, and the SON and SOX artificial lights (for CDO, please see website above for Philips, UK) used within the aviary study, compared with that of a winter morning (solid line, Figure 5.1). The artificial lights had an overall higher spectral power (radiance) than the natural morning daylight, and the waveform pattern varied considerably between the different types of lamps. The

most marked departure from natural daylight was the low-pressure sodium (SOX) lamp (Figure 5.5) with a single peak at 589 nm (in the yellow region of the light spectrum). The high-pressure sodium (SON) lamp (Figure 5.6) also had a relatively narrow bandwidth, with a main peak from approximately 590 – 620 nm (yellow to orange) and a smaller peak at 498 nm (blue-green), in addition to a very low level output between 400 nm and 800 nm. The metal halide (CDO) lamp also had two peaks at approximately 530 nm (green) and 600 nm (orange), but had a broader and more intense overall coverage of wavelengths from 350 nm to 800 nm than the other street light types. Indeed, the CDO lamp was the artificial light providing the best approximation to true daylight. The radiance of the fluorescent aviary “day” lighting was ten times greater in intensity than the true daylight measured in mid-winter, but was similar in spectral composition (Figure 5.1), in that both natural and fluorescent lights show a peak in the violet and blue ranges (415 nm – 495 nm). However, there were several differences between the natural and fluorescent light spectra. For example, the fluorescent light had two spikes in radiance (one at 430 nm and one at 550 nm), and the red end of the spectra was under represented, when compared to natural light.

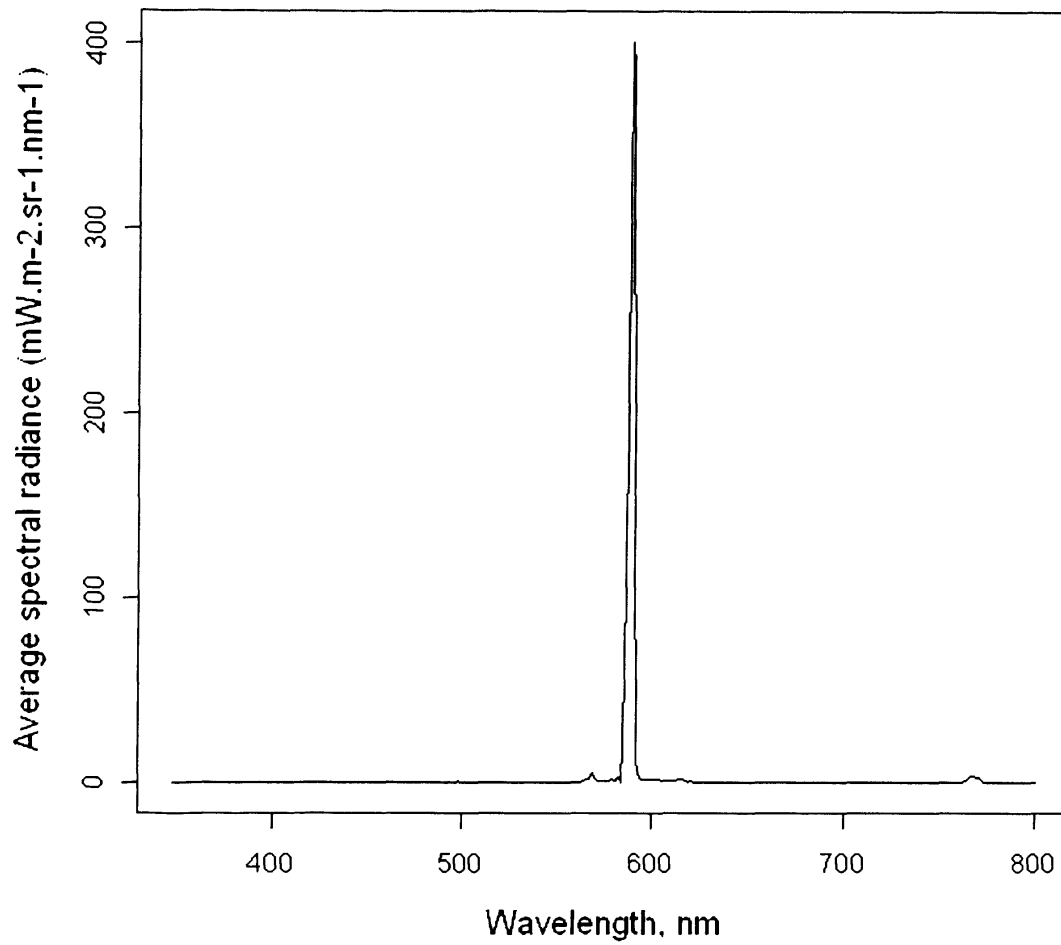


Figure 5.5. The spectral power distribution (radiance) of the low-pressure sodium lamp (manufacturer and model unknown). Spectral power measured as radiance. Average of 25 readings.

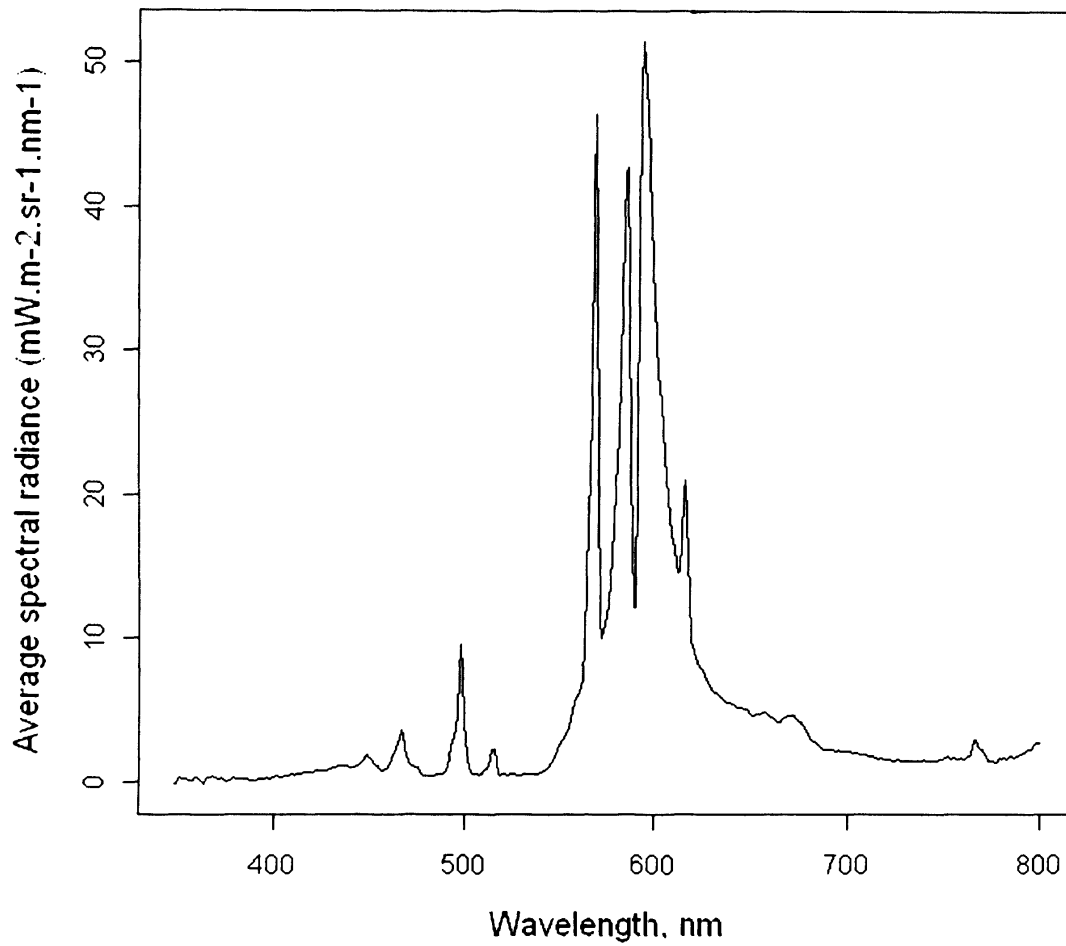


Figure 5.6. The spectral power distribution (radiance) of the high-pressure sodium lamp (Philips ® SON-T 100W). Spectral power measured as radiance. Average of 27 readings.

Analysis of Aviary Behavioural Data

Comparison of the timing of activity between lit and unlit treatments

For the following analyses, robins were classified as active if they were seen on the film footage exhibiting any movement based activity, for example, foraging, bathing, hopping or flying. All birds noted to be active at “night” were seen foraging. There was an overall significant difference in the onset of robin activity relative to “daybreak” in the different experimental conditions (Kruskal-Wallis $\chi^2 = 9.8917$, $df = 3$, $P = 0.020$). Post-hoc Nemenyi-Damico-Wolfe-Dunn tests were used to examine the pairwise differences between experimental conditions (Figure 5.7). There was no significant difference in the onset of activity between the different types of streetlamp (CDO – SON $P > 0.999$, SOX – SON $P > 0.999$, SOX – CDO $P > 0.999$), but the onset of activity was significantly earlier under street-lights than under control (unlit) conditions; except for the SOX – control comparison, for which there was a marginally non-significant difference (SON – control $P = 0.022$, CDO – control $P = 0.027$, SOX – control $P = 0.063$).

Similarly, there was an overall significant difference in the ending of robin activity relative to “nightfall” in the different experimental conditions (Kruskal-Wallis rank test: Kruskal-Wallis $\chi^2 = 19.317$, $df = 3$, $p\text{-value} < 0.001$). Post-hoc Nemenyi-Damico-Wolfe-Dunn tests were used to examine the pairwise differences between experimental conditions. There was no significant difference in the cessation of activity between the different types of streetlamp (CDO – SON $P = 1.000$, SOX – SON $P = 0.725$, SOX – CDO $P = 0.729$) but the cessation of activity was significantly later under street-lights than under control (unlit)

conditions (SON – control P = 0.006, CDO – control P = 0.010, SOX – control P < 0.0001).

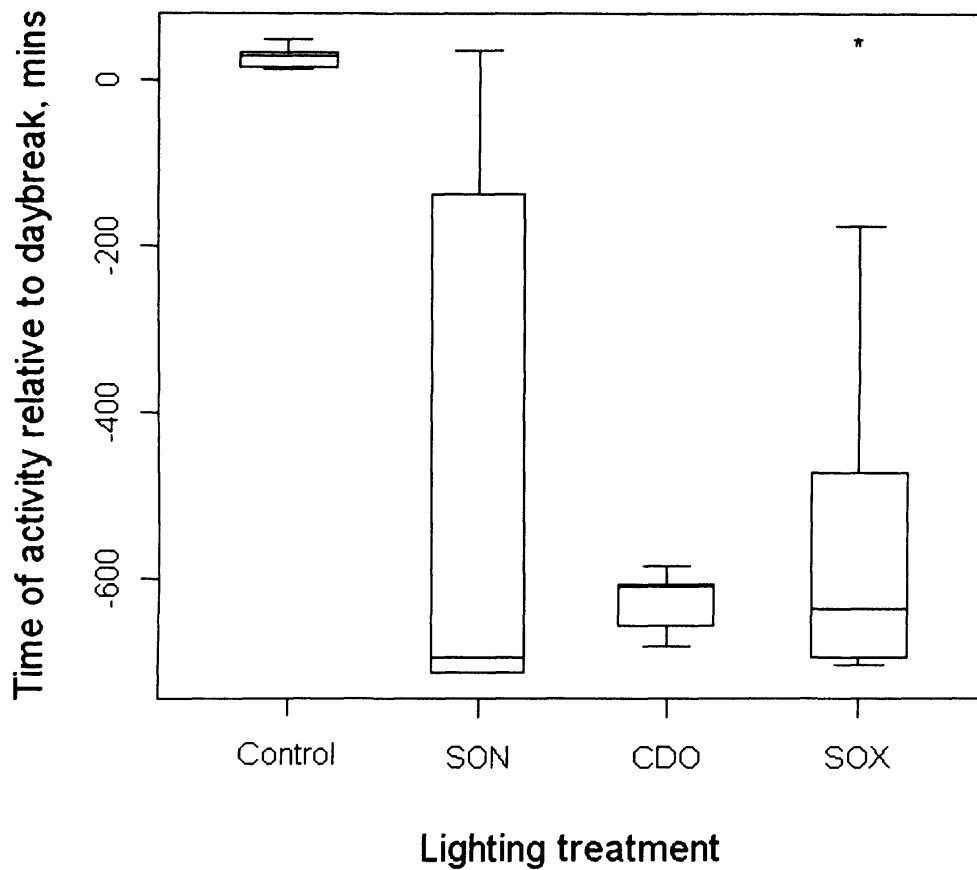


Figure 5.7. Timing of first observed activity of control birds with that of last observed activity before daybreak for birds exposed to artificial lighting treatments. Negative values indicate that the time was before daybreak. Median ± IQR time of activity: Control N = 8: 31.5 ± 22.25 mins, SON N = 5: -695 ± 575 mins, CDO N = 6: -631.5 ± 57.5 mins, SOX N = 8: -639.5 ± 165.25 mins.

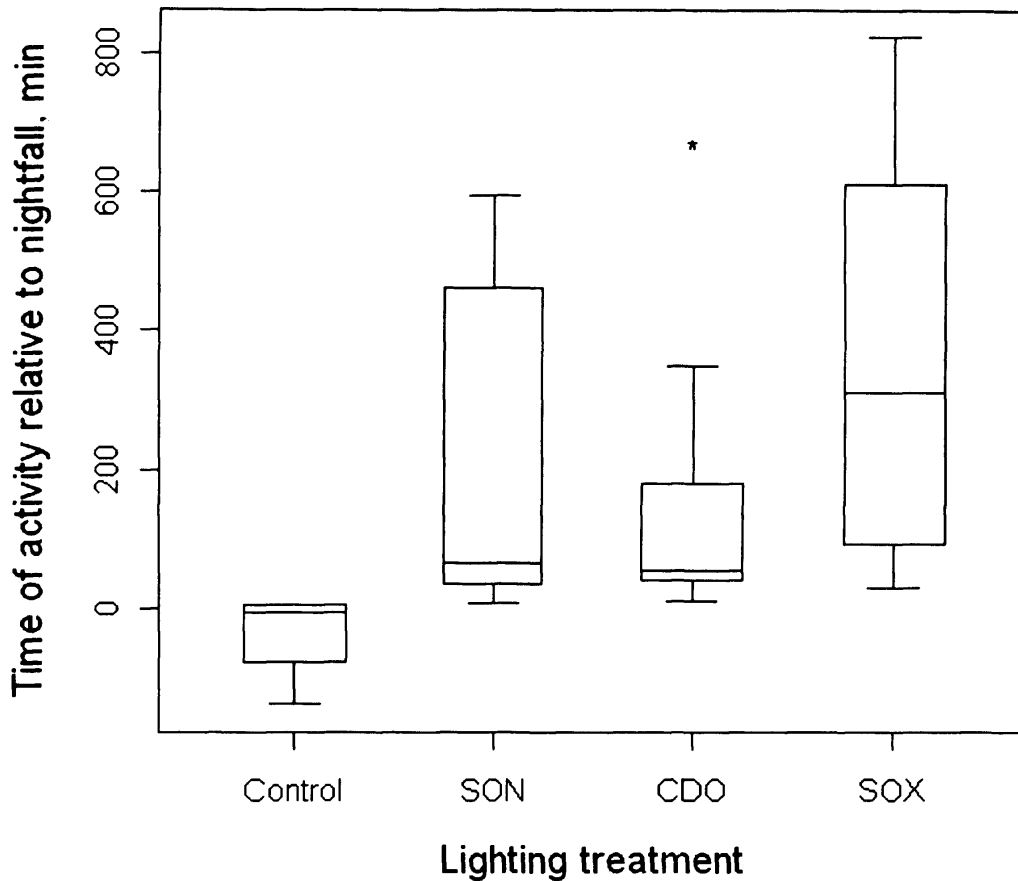


Figure 5.8. Timing of last observed activity of control birds with that of first observed activity after nightfall for birds exposed to artificial lighting treatments. Median \pm IQR time of activity: Control N = 8: -4.5 ± 50.5 mins, SON N = 8: 64.5 ± 389.75 mins, CDO N = 9: 55 ± 140 mins, SOX N = 8: 310 ± 470.75 mins.

Having established these striking effects of artificial lighting on the timing of robin activity, the following analyses of the timing of activity utilised one type of artificial light to allow matched pair analyses which maximise the available sample sizes for each test (SOX only relative to “daybreak” and CDO only relative to “nightfall”). Robins that were observed under artificial light were active

longer relative to “daybreak” than those under control unlit conditions (median \pm IQR_{lit} = 639.5 \pm 165.3 minutes before daybreak, median \pm IQR_{unlit} = 31.5 \pm 22.25 minutes after daybreak, pairwise Wilcoxon test: N = 8 matched pairs, V = 0, P = 0.008). Similarly, birds under artificial lighting treatments (CDO only) were also active longer relative to “nightfall” than were unlit control birds (Figure 5.9, median \pm IQR_{lit} = 163.5 \pm 180.5 minutes after nightfall, median \pm IQR_{unlit} = -4.5 \pm 50.5 minutes after nightfall, pairwise Wilcoxon test: N = 8 matched pairs, V = 0, P = 0.008).

Correspondingly, the length of the night-time rest period of the robins under control conditions was significantly longer than that of the artificially lit robins in both night to day (median \pm IQR_{lit} = 353 \pm 272 minutes, median \pm IQR_{unlit} = 768 \pm 50 minutes, pairwise Wilcoxon test: N = 8 matched pairs, V = 0, P = 0.008) and day to night observation sessions (median \pm IQR_{lit} = 315 \pm 202 minutes, median \pm IQR_{unlit} = 875 \pm 113.3 minutes, pairwise Wilcoxon test: N = 8 matched pairs, V = 36, P = 0.008).

The rate of mass gain over the course of the observed activity period was significantly lower in robins when exposed to artificial lights than under control conditions, for robins observed from night to day (mean rate \pm StDev_{lit} = 0.00120 \pm 8.3E⁻⁴ g min⁻¹, mean rate \pm StDev_{unlit} = 0.00313 \pm 1.26E⁻³ g min⁻¹, paired t-test: t = 3.487, df = 4, P = 0.025). The rate of mass gain in robins observed from day to night were not significantly different between lit and control conditions (mean rate \pm StDev_{lit} = 7.19E⁻⁴ \pm 1.85E⁻³ g min⁻¹, mean rate \pm StDev_{unlit} = 2.74E⁻³ \pm 1.57E⁻³ g min⁻¹, paired t-test: t = 1.611, df = 5, P = 0.168). However a power analysis suggests that this non-significant result is due to the small sample size, as only an additional four extra pairs of territories (i.e. increasing the sample size from N = 6

to N = 10 matched pairs of robins) would be needed to give a significant result at $P < 0.05$, given the observed effect size and data distributions.

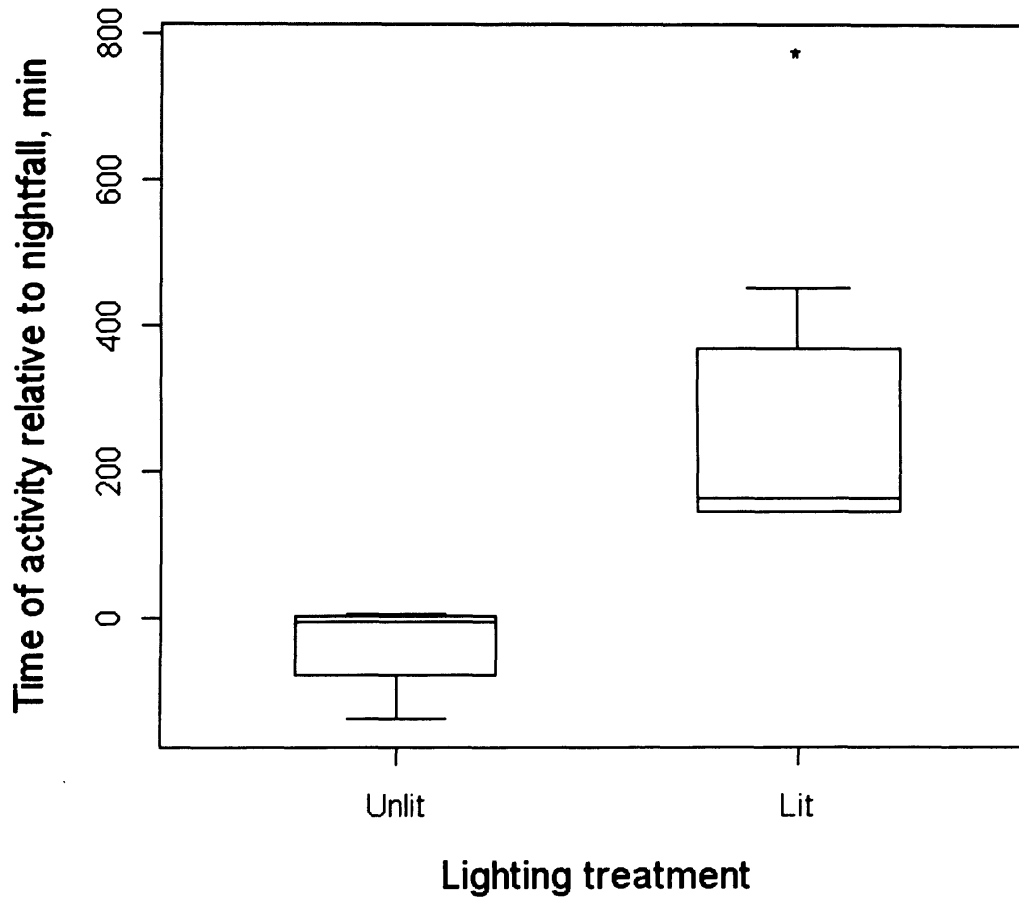


Figure 5.9. The last observed activity of control unlit birds and the time of first activity of artificially lit birds. Artificially lit conditions in this analysis are metal halide (CDO).

Other variables tested (time of start of rest period, rate of mass gain over the course of the daytime period, % mass gained during the daytime period and % mass gained over the activity period) were found to be not significantly different between control unlit conditions or artificially lit conditions (Wilcoxon matched-

pairs comparisons; all $P > 0.05$, see Appendix A 4.1). Power analyses of these non-significant results suggest that the non-significant results are not simply due to small sample sizes.

Discussion

I found that free-living robins with artificially lit territories began singing far earlier at dawn (by approximately 2 hours) than robins with matched unlit territories (Figures 1 & 2), but despite this difference in timing, the ambient light intensity when singing started was similar in the two groups. In addition, although overall the robins with artificially lit territories did not begin to forage significantly earlier than those with unlit territories, several individuals did begin to forage much earlier than the robins on unlit territories with which they were matched (Figure 3), resulting in a shortening of their overnight fast. Overall, the shift in the timing of dawn song due to artificial lighting was much greater than any change in the timing of foraging, leading to a greater lag between the start of singing and the start of foraging on artificially lit territories than on unlit territories. I found no significant differences in the times at which robins on lit and unlit territories ended their singing or foraging at dusk.

Similarly, I found that aviary held robins also modify their activity routines when illuminated by artificial lights: they remained active for much of the “night-time” period, had shorter resting times and lower rates of body mass gain than unlit control birds. However, robins under artificially lit conditions did not gain more mass over the course of the observation period than the control birds. In

addition, I found no significant differences in behaviour of the birds under the different types of street light.

Little is known about the mechanisms underlying the observed changes in behaviour under artificial lights; this study measures the changes but can only provide clues as to the mechanisms. Although there are many non-mutually exclusive hypotheses accounting for the dawn chorus (e.g. Henwood and Fabrick, 1979; Kacelnik and Krebs, 1982; Mace, 1987; Hutchinson *et al.*, 1993; Staicer *et al.*, 1996), my study addresses the role of light in controlling the onset and cessation of daily behaviour. My findings support the hypothesis that light intensity is an important cue for the start of daily activity in diurnally active birds (Kacelnik, 1979; Hutchinson, 2002; Martin, 1990), acting together with the bird's ability to perceive the changes in light intensity (Thomas *et al.*, 2002; McNeil *et al.*, 2005).

These results, showing that artificial lighting appears to trigger an early dawn chorus and sometimes also an earlier start to foraging, raise the question of why light intensity does not appear to influence the timing of song at dusk, and why the robins with artificially lit territories were not always active throughout the night. Rather, they simply initiated their singing activity earlier as an extension to the normal dawn chorus, after a prolonged lull following dusk. All aviary held robins seemed also have a lull in activity after dusk, although the start of this rest period was influenced by artificial lighting. These results suggest that resting for a period after dusk is an optimal strategy.

Song rate at the time of first song was similar across all territories in the study of free-living robins, but I noted that by one hour after the first observed song, the song rate was considerably higher in artificially lit territories than in

unlit territories, showing that the robins with lit territories tend to have a more intense and prolonged dawn chorus than those with unlit territories. This suggests that although the light intensity provided by the street lights was sufficient to initiate singing, it was not usually enough to make foraging profitable, and so these robins may have typically continued to sing intensively without foraging until natural increases in daylight eventually caused light intensities to reach a threshold at which foraging became profitable. In contrast, robins with unlit territories began to forage much sooner after starting to sing at dawn, even though they started to sing later relative to sunrise.

Previous reports of robins singing, foraging and even feeding chicks at night have been largely anecdotal (Hollom, 1965; King, 1965; England, 1977), but a recent study (Fuller *et al.*, 2007) has described an effect of city noise pollution on the tendency of urban robins to sing at night; robins with noisy territories (daytime sound pressure levels of 55-74 dB) were more likely to sing at night than robins with quieter territories, but only if their territories were also brightly lit. My field study was conducted on relatively quiet rural territories, in which sound levels were very similar between artificially lit and unlit territories, and therefore suggests that nocturnal singing can arise even in the absence of the loud noise pollution often associated with artificially lit territories in urban areas. In my aviary study, the robins were held in adjacent aviaries and were exposed to essentially identical levels of background noise. Furthermore, the design of the aviary experiment was such that any differences in background noise levels between days would be balanced across the different treatments. Therefore any differences in robin behaviour between treatments and control conditions cannot

be readily explained by the noise pollution effects suggested by Fuller *et al.* (2007).

It remains unclear whether singing and foraging at night near artificial lights is an adaptive strategy that ultimately leads to increased fitness, or is simply a non-adaptive behaviour triggered by unnaturally high night-time light levels. One might not necessarily expect birds to perform optimal behavioural routines under the changed ecological conditions provided by artificial lights, because widespread use of street-lighting is, in evolutionary terms, a very recent phenomenon, spanning fewer than 100 robin generations. Therefore, the behaviours that I have measured in my field and aviary studies may not be adaptive for two reasons: Firstly, there may be an evolutionary lag between the ecological change and the evolved adaptive response of a population -though other avian behaviours such as migration strategies may evolve rapidly over equivalent time scales (Berthold, 1991). Secondly, not all of the wider robin population is exposed to artificial lighting, so a population-level evolved response may not be adaptive in all circumstances.

The net benefit (or cost) of singing abnormally early and intensively from artificially lit territories is unknown. The primary functions of bird song are mate attraction and territory defence, but it is unclear how effective nocturnal song is for these functions, as many conspecifics are likely to be inactive or asleep. Important costs of singing at night may include increased predation risk and increased metabolic activity. A diurnal bird stores up metabolic reserves during the day in order to survive overnight when it cannot forage effectively (Thomas, 2000), and both wakefulness and singing at night may increase the risk of overnight starvation. The overnight metabolic rate of an awake bird is higher than

that of a sleeping bird. For example, in the pigeon, the metabolic rate decreases by up to 12% during sleep, and 50% of nocturnal energy saving is directly associated with sleep (Phillips and Berger, 1991). Furthermore, there is at least some energetic cost to singing (Chappell *et al.*, 1995; Oberweger and Goller, 2001; Ward *et al.*, 2003), and increased nocturnal song rates are associated with greater overnight mass loss in common nightingales *Luscinia megarhynchos* (Thomas, 2002).

When under artificial lighting conditions in the aviary, robins had a lower rate (approximately three times lower) of body mass gain over their much longer activity period than when under control (unlit) conditions, but with no difference in the total mass gained between the start and end of the activity period or between the times of simulated “dawn” and dusk”. This suggests that while robins are clearly able to forage successfully under artificial lighting, they do not dramatically increase their intake either by night or by day, but consume enough to achieve the daily mass gain needed for maintaining a stable body mass over multiple days. The robins in my aviary study rarely sang, but given that foraging rate and mass gain are traded off against song output in more natural conditions (Thomas *et al.*, 2003), the results of my aviary study imply that street lighting allows more time to be allocated to singing. Therefore, the net result of street lighting on wild robins is likely to be a reduced starvation risk (due to the opportunities for night-time foraging) and a higher song output, both in terms of song rate at any time, and total song output over the extended activity period that becomes possible under street-lighting.

Nocturnal foraging under artificial lighting in the wild may allow robins to reduce their risk of overnight starvation if ambient conditions make this necessary.

A striking result of my study is that while nocturnal foraging under artificial lighting is clearly possible (observed in 3 of the 12 free-living robins with artificially lit territories, and in all aviary-held robins), the majority of free-living robins chose not to forage in the middle part of the night, despite the reliable and unlimited food supply that was available to them. One reason for this might be that sleep is important for survival for all higher animals (e.g. Rechtschaffen *et al.*, 1989; Rattenborg *et al.*, 2004) and so forfeiting sleeping time in order to forage by night may have fitness consequences. Furthermore, the relatively low light intensities and narrow light spectra provided by street lights may make foraging under street-lights at night less efficient than during full daylight, even at familiar *ad libitum* feeders. Furthermore, risk from nocturnal predators may cause more “cautious” and hence less efficient foraging than during daytime.

The free-living robins with artificially lit territories in my field study did not have significantly shorter fast lengths than those with unlit territories. However, the rest length was significantly shorter for aviary held birds under artificially lit conditions than those under control conditions. Therefore, the potential for foraging at night (revealed by the effects of street-lighting in the aviary study and the few free-living individuals on lit territories which foraged in the middle of the night) provides the possibility of reducing overnight fast length if circumstances favour this, such as on very cold and windy nights, when metabolic consumption of energy reserves is likely to be high, or when signing intensively at night. However, the design of my studies did not allow me to test under which circumstances robins may choose to forage at night on artificially lit territories, thereby reducing the length of their overnight fast.

The timing of foraging may also be influenced by the timing of prey activity. Invertebrates normally eaten by robins and found active during the day might not be active under the relatively low light intensities and narrow wavebands provided by street-lights. Some species of invertebrate are attracted to certain wavelengths of light, but are insensitive to others (Ali, 1984; Leverton, 2001). Similar effects may influence the timing of activity under artificial lighting of other invertebrates favoured by the robin.

My field and aviary studies have shown that artificial lighting can have a major impact on the timing of behaviour, but there clearly remain major questions about the underlying mechanisms and fitness consequences of the changes that I have described. The lack of a difference of behaviour under different types of lighting highlights that in addition to understanding these issues, designing efficient lighting schemes to minimise the impacts of light pollution on wildlife is of great importance.

Chapter 6: Conclusions

The aim of my PhD research was to investigate how avian behaviours may be constrained by eye design and visual capabilities. My studies have highlighted that due to the wide variation in avian eye design and ecology, birds are an excellent taxon within which to investigate the links between anatomy, behaviour and ecology. In this chapter I shall give a brief overview of the main findings of each of my studies within the context of my aims, and place these findings in the broader context of behavioural and sensory ecology.

In Chapter 1, I discussed the evolution, anatomy and function of the vertebrate eye, focussing on the anatomical and functional details of the avian eye. This review emphasised the potential for co-evolution of eye design with environmental and ecological conditions. For example, diving birds were presented as a case-study illustrating such adaptation to the visual challenges of vision in both air and water; they have increased lenticular accommodation (Levy and Sivak, 1980), and a flatter, less refracting cornea (Martin, 1998) than terrestrial birds. Additionally, I outlined examples of birds utilising alternative senses, in ecological contexts where visual perception is hindered or non-advantageous. For example, Procellariiforme seabirds are able to use olfaction to find prey in adverse weather conditions in which visual foraging is constrained by the visibility of the prey (Nevitt, 2008). This diversity of eye designs and ecological adaptations allowed me to investigate a series of case-studies of how eye design can constrain, or facilitate, the behaviour of different species, which were described in detail in the subsequent chapters.

To examine and quantify the diversity of avian visual adaptations outlined in Chapter 1, I used a variety of techniques and methods. In Chapter 2, I presented some of the different methods currently available to assess eye design and visual capability in birds, which I used in subsequent chapters to test hypotheses relating to the timing of behaviour in relation to visual constraints and capabilities. These methods included how to measure small-scale variations in eye structure, for example, by examining differences in the thickness of different retinal layers, to larger-scale assessment and measurement of overall eye size and morphology.

To allow future studies to ensure that avian welfare is considered when obtaining information on visual ability, many of the methods that I used and developed were non-invasive, and could be carried out on live birds in the field; for example, measuring pupil aperture, estimating axial and focal lengths, and making estimates of retinal image brightness. Use of non-invasive techniques is valuable to gather information on a wide range of species, where euthanasia or anaesthesia is not an option. I provided a validation and refinement of the existing calculations to estimate retinal image brightness, by examining dead specimens in laboratory-based studies, using MRI as an innovative tool. My refined calculation for retinal image brightness provides a more accurate estimate of visual capability, which in practice would increase the reliability of the measurement, allowing researchers to be confident in using such non-invasive methods. While accurate non-invasive techniques are not only of welfare importance to the bird, they are also more likely to be accessible to a wider researcher audience, and incur less financial costs.

In Chapter 2, I also present results from a case study showing that estimates of maximum retinal image brightness are higher among nocturnally

active than diurnally active species, and that the retinal image brightness estimates for the early bird *Archaeopteryx* fall clearly within the range for diurnal rather than nocturnal activity. By combining knowledge of eye structure obtained from skulls and fossils, with information on eye sensitivities as measured in live birds, such relationships can be revealed. My study raises the possibility that future comparisons involving other fossil birds and more recently extinct birds, for example the moa (family Dinornithidae), could provide an insight into the evolution of avian behaviour, and the light-environments in which early birds were active. Such a study would be valuable as, while some evidence is available on diet (for moa: via gizzard content and coprolite analysis; Wood et al., 2008) very little is known regarding the timing of behaviour of extinct species, with the literature focussing on the extinction model (Holdaway & Jacombe, 2000) or phylogeny (Worthy, 2007).

In Chapter 2 I discovered that the European storm petrel *Hydrobates pelagicus*, a regularly nocturnally active species, had a relatively low retinal image brightness estimate, comparable with that of the European starling *Sturnus vulgaris*; a typical diurnally-active songbird (which exhibits occasional nocturnal activity during migration). This is opposite to my hypothesis that low-light active birds (such as the European storm petrel) will have more sensitive eyes. An explanation of this is that this species is not completely nocturnally active and is active a lot during the day. Therefore the storm petrel may require both nocturnal, and diurnal visual specialisations. This finding is expanded upon in Chapter 3, where I compared additional aspects of the visual ability of the European storm petrel with the diurnal European starling, to investigate how nocturnal activity may be mediated by anatomical and neural adaptation.

Whilst previous studies have examined starling colour vision, visual fields and retinal asymmetry (Martin, 1986a; Hart, Partridge and Cuthill, 1998; 2000), little was known regarding storm petrel vision (Rochon-Duvigneaud, 1943). I compared the retinal structure of the two species, and found that the storm petrel retina to be better adapted to low-light vision than the starling retina, and that an “area of specialisation” may be present in the central storm petrel retina. These findings correspond well with the behaviour of the more nocturnally active storm petrel and the more diurnal starling. However, as starlings are known to migrate at night occasionally, they may utilise alternative navigational cues, for example, olfaction (Wallraff *et al.*, 1995), or magnetoreception (Wiltschko and Wiltschko, 2002), as well as, or even instead of, visual cues. While my results suggest that the storm petrel is otherwise visually well adapted for nocturnal activity, it has a relatively low retinal image brightness. Therefore further study of the storm petrel, perhaps by examination of the visual and olfaction centres of the brain (Martin *et al.*, 2007), may provide further details on the senses by which this species is able to be active nocturnally. It is very important to consider visual ability in birds such as the storm petrel, as they are particularly vulnerable to the effects of light pollution along their long-distance migration, and mitigation measures are required to minimise such impacts (Rodríguez & Rodríguez, 2009). Chapter 3 allowed me to link behaviour with gross anatomy and anatomy at a microscopic level, showing that very small differences (on the scale of μm) in retinal layer thicknesses can represent a useful adaptation to a dramatic difference in ecological conditions, in this case diurnality vs. nocturnality.

In Chapter 4, I used larger scale measurements of overall eye size and estimates of retinal image brightness to examine the timing of singing behaviour,

for species singing in different bird communities around the world. I tested the overall hypothesis that larger-eyed birds would begin their dawn chorus earlier than smaller-eyed birds. I found that birds with better vision at low light intensities began their song earlier at dawn, with eye size being the most important predictor of the time of onset of song, although body mass was also an important independent covariate. The relationship between eye size and time of onset of dawn song was strongest at long twilight durations and high latitudes. This suggests that vision is not the only constraint upon the timing of dawn song, particularly in the tropics, and factors such as acoustic interference (Luther, 2008) may play an important role at locations of high species richness and short twilight duration, as suggested by my analyses. In this chapter, I emphasise that the timing of different species behaviours around the world are likely to be constrained by differing environmental effects. For example, high species abundance and diversity in the tropics increase the levels of acoustic interference, reflecting on the different dawn chorus structure than is observed in temperate regions. Therefore my findings highlight the necessity in undertaking comparative studies to understand behaviour more comprehensively. Single-site studies in the future need to be aware of these latitudinal effects in order for them to address the issues adequately and efficiently.

All of the behavioural differences described above appear to have been due to adaptations to natural conditions. In Chapter 5, I investigated how manipulation of visual constraints affected the timing of behaviour in the European robin *Erithacus rubecula*, which has a relatively large eye with a large retinal image brightness estimate (as found in Chapter 2) and may therefore be expected to be susceptible to the changes in visual constraints imposed by light

pollution. I observed how artificial lighting affects the activity of both free-living and aviary-held robins. I found that the presence of artificial lighting was associated with robins regularly singing, and occasionally foraging, at night in the wild. My aviary study confirmed that robins are able to forage at night under artificial lighting, and that this reduced the duration of the fast period that robins face overnight, with the implication that artificial lighting will tend to reduce overnight starvation risk, and facilitate the optimal regulation of energy reserves. These findings therefore suggest that robins may be able to utilise modified lighting regimes to their advantage in terms of survival and ultimately their fitness, though the postulated fitness benefits of light “pollution” remain to be more fully quantified. Therefore, I could not provide conclusive evidence that artificial lighting or light pollution in general is beneficial or harmful overall. It would therefore be important to assess if birds’ survival, reproductive success and lifetime fitness are affected by artificial lighting. Furthermore, knowledge of the underlying physiology (for example the hormonal basis) of how the effects of artificial lights are mediated may also provide more conclusive evidence of whether lighting is advantageous or disadvantageous to individuals and populations of wild birds. Such information would help to inform the efficient and least damaging placement of artificial lights in the urban and rural environment, not only for the benefit of wildlife, but also enabling the economic costs associated with their provision to be refined.

My studies together comprise a convincing set of evidence for the role of vision in limiting the timing of behaviour under low light intensities, and for the adaptation of eye design to the differing visual tasks that bird species face. However, there is scope for future studies to provide further details. In particular,

investigation into alternative non-visual factors (for example, noise pollution and energetic constraints) that may be important in the timing of behaviour under low-light levels would provide a more holistic view. Similarly, explanation of the asymmetries in the timing of different behaviours at dawn and dusk would shed further light on the mechanisms underlying the organisation of daily behavioural routines, and the role of visual constraints in the timing of different behaviours. Further studies into the structure of the tropical dawn chorus may also yield clarification of the reasons why visual constraints appear to be relatively unimportant in the timing of onset of dawn song in tropical bird communities. Nevertheless, despite the scope for future research into questions raised by the research reported in this thesis, my PhD studies have highlighted the great diversity of avian visual adaptations, and emphasised that understanding the differences between them is intrinsic to appreciating the way in which behaviour is mediated or constrained by visual capabilities.

References

The Wildlife and Countryside Act. 1981. UK: HMSO.

ABOUHEIF, E. 1999. A method for testing the assumption of phylogenetic independence in comparative data. *Evolutionary Ecology Research*, 1, 895-909.

ABRAMOFF, M., MAGALHÃES, P. & RAM, S. 2004. Image Processing with imagej. *Biophotonics International*, 11, 36-42.

ALERSTAM, T., GUDMUNDSSON, G. A., GREEN, M. & HEDENSTROM, A. 2001. Migration along orthodromic sun compass routes by arctic birds. *Science*, 291, 300-303.

ALLEN, F. H., 1913. More notes on the morning awakening. *Auk* 30: 229-235.

ALI, M. A. & KLYNE, M. A. 1985. *Vision in vertebrates*. Plenum Press, New York.

ALI, M.A. 1984. Epilogue. In: Ali MA, editor. *Photoreception and vision in invertebrates*, Proceedings of the NATO Advanced Study Institute on photoreceptors and vision in invertebrates. Plenum Press, New York: 773-788.

ALONSO, P. D., MILNER, A. C., KETCHAM, R. A., COOKSON, M. J. & ROWE, T. B. 2004. The avian nature of the brain and inner ear of Archaeopteryx. *Nature*, 430, 666-669.

ALSTROM, P., OLSSON, U., LEI, F., WANG, H. T., GAO, W. & SUNDBERG, P. 2008. Phylogeny and classification of the Old World Emberizini (Aves, Passeriformes). *Molecular Phylogenetics and Evolution*, 47, 960-973.

AMO, L., GALVAN, I., TOMAS, G. & SANZ, J. J. 2008. Predator odour recognition and avoidance in a songbird. *Functional Ecology*, 22, 289-293.

AMRHEIN, V., KORNER, P. & NAGUIB, M. 2002. Nocturnal and diurnal singing activity in the nightingale: correlations with mating status and breeding cycle. *Animal Behaviour*, 64, 939-944.

ARENDR, D. 2003. Evolution of eyes and photoreceptor cell types. *International Journal of Developmental Biology*, 47, 563-571.

ARENDR, D., TESSMAR-RAIBLE, K., SNYMAN, H., DORRESTEIJN, A. & WITTBRODT, J. 2004. Ciliary photoreceptors with a vertebrate-type opsin in an invertebrate brain. *Science*, 306, 869-71.

ARMSTRONG, E.A., 1963. A study of bird song. Oxford University Press, Oxford.

ARNAIZ-VILLENA, A., MOSCOSO, J., RUIZ-DEL-VALLE, V., GONZALEZ, J., REGUERA, R., WINK, M. & SERRANO-VELA, J. I. 2007. Bayesian phylogeny of Fringillinae birds: status of the singular African oriole finch *Linurgus olivaceus* and evolution and heterogeneity of the genus *Carpodacus*. *Acta Zoologica Sinica*, 53, 826-834.

ARNHOLT, A.T., 2008. BSDA: Basic Statistics and Data Analysis. R package version 0.1.

ASAB, 2006. Guidelines for the treatment of animals in behavioural research and teaching. *Animal Behaviour*, 71, 245-253.

BAKKEN, L. E. & BAKKEN, G. S. 1977. American redstart feeding by artificial light. *Auk* 94: 373-374.

BALAZS, E. A., TOTH, L. Z. J., JUTHEDEN, G. M. & COLLINS, B.-A. 1965. Cytological and biochemical studies on the developing chicken vitreous. *Exp Eye Res*, 4, 237-248.

- BANDAH, D., SWISSA, T., BEN-SHLOMO, G., BANIN, E., OFRI, R. & SHARON, D. 2007. A complex expression pattern of Pax6 in the pigeon retina. *Investigative Ophthalmology & Visual Science*, 48, 2503-2509.
- BANH, A., BANTSEEV, V., CHOH, V., MORAN, K. & SIVAK, J. 2006. The lens of the eye as a focusing device and its response to stress. *Prog Retin Eye Res*, 25, 189-206.
- BARON, J., PINTO, L., DIAS, M. O., LIMA, B. & NEUENSCHWANDER, S. 2007. Directional responses of visual wulst neurones to grating and plaid patterns in the awake owl. *European Journal of Neuroscience*, 26, 1950-1968.
- BEASON, R. & LOEW, E. 2008. Visual pigment and oil droplet characteristics of the bobolink (*Dolichonyx oryzivorus*), a new world migratory bird. *Vision Res*, 48, 1-8.
- BELLINGHAM, J., CHAURASIA, S. S., MELYAN, Z., LIU, C. M., CAMERON, M. A., TARTTELIN, E. E., IUVONE, P. M., HANKINS, M. W., TOSINI, G. & LUCAS, R. J. 2006. Evolution of melanopsin photoreceptors: Discovery and characterization of a new melanopsin in nonmammalian vertebrates. *Plos Biology*, 4, 1334-1343.
- BENNETT, A. T. D. & THERY, M. 2007. Avian color vision and coloration: Multidisciplinary evolutionary biology. *American Naturalist*, 169, S1-S6.
- BERG, K. S., BRUMFIELD, R. T. & APANIUS, V. 2006. Phylogenetic and ecological determinants of the neotropical dawn chorus. *Proceedings of the Royal Society B-Biological Sciences*, 273, 999-1005.
- BERGEN, F. & ABS, M. 1997. Etho-ecological study of the singing activity of the Blue Tit (*Parus caeruleus*), Great Tit (*Parus major*) and Chaffinch (*Fringilla coelebs*). *Journal Fur Ornithologie*, 138, 451-467.

BERTHOLD P. 1991. Genetic-control of migratory behavior in birds. *TREE*. 6 (8): 254-257.

BINGGELI, R. & PAULE, W. 1969. The pigeon retina: quantitative aspects of the optic nerve and ganglion cell layer. *J Comp Neurol*, 137, 1-18.

BINGMAN, V. P. & BENVENUTI, S. 1996. Olfaction and the homing ability of pigeons in the southeastern United States. *Journal of Experimental Zoology*, 276, 186-192.

BIRDLIFE INTERNATIONAL, 2009. Species factsheet: *Strigops habroptila*. Downloaded from <http://www.birdlife.org> on 29/9/2009

BIRDLIFE INTERNATIONAL, 2009. Species factsheet: *Hydrobates pelagicus*. Downloaded from <http://www.birdlife.org> on 29/9/2009

BIRDLIFE INTERNATIONAL, 2009. Species factsheet: *Sturnus vulgaris*. Downloaded from <http://www.birdlife.org> on 29/9/2009

BIRO, D., FREEMAN, R., MEADE, J., ROBERTS, S. & GUILFORD, T. 2007. Pigeons combine compass and landmark guidance in familiar route navigation. *Proceedings of the National Academy of Sciences of the United States of America*, 104, 7471-7476.

BITO, L. Z. & SALVADOR, E. V. 1970. Intraocular fluid dynamics. 2. Postmortem changes in solute concentrations. *Experimental Eye Research*, 10, 273-287.

BITO, L. Z., DIBENEDETTO, F. E. & STETZ, D. 1982. Homeostasis of the retinal micro-environment .I. Magnesium, potassium and calcium distributions in the avian eye. *Experimental Eye Research*, 34, 229-237.

BLACKETT, A., 1970. Blue tits and gulls feeding by artificial light. *Br. Birds* 63: 136.

BLIX, A. S. 2005. Arctic animals: and their adaptations to life on the edge, Norway, Tapir Forlag.

BLOMBERG, S. P., GARLAND, T. & IVES, A. R. 2003. Testing for phylogenetic signal in comparative data: Behavioral traits are more labile. *Evolution*, 57, 717-745.

BOIRE, D., DUFOUR, J. S., THEORET, H. & PTITO, M. 2001. Quantitative analysis of the retinal ganglion cell layer in the ostrich, *Struthio camelus*. *Brain Behavior and Evolution*, 58, 343-355.

BOLHUIS J. J. 2005. Function and mechanism in neuroecology: looking for clues. *Anim. Biol.* 55 (4): 457-490.

BOLLA, G. 2001. Lighting of poultry. 3rd ed. Orange: New South Wales Department of Primary Industries. Agfact A5.1.2

BONADONNA, F. 2009. Olfaction in petrels: from homing to self-odor avoidance. *Ann N Y Acad Sci*, 1170, 428-33.

BONADONNA, F., CARO, S. P., JOUVENTIN, P. & NEVITT, G. A. 2006. Evidence that blue petrel, *Halobaena caerulea*, fledglings can detect and orient to dimethyl sulfide. *Journal of Experimental Biology*, 209, 2165-2169.

BONADONNA, F., HESTERS, F. & JOUVENTIN, P. 2003. Scent of a nest: discrimination of own-nest odours in Antarctic prions, *Pachyptila desolata*. *Behavioral Ecology and Sociobiology*, 54, 174-178.

BOOTE, C., HAYES, S., JONES, S., QUANTOCK, A. J., HOCKING, P. M., INGLEHEARN, C. F., ALI, M. & MEEK, K. M. 2008. Collagen organization in the chicken cornea and structural alterations in the retinopathy, globe enlarged (rge) phenotype - An X-ray diffraction study. *Journal of Structural Biology*, 161, 1-8.

BORES, L. D. 2001. Refractive eye surgery. Blackwell, Oxford.

BORGDORFF, P. 1975. Respiratory fluctuations in pupil size. *American Journal of Physiology*, 228, 1094-1102.

BOUMANS, T., THEUNISSEN, F. E., POIRIER, C. & VAN DER LINDEN, A. 2007. Neural representation of spectral and temporal features of song in the auditory forebrain of zebra finches as revealed by functional MRI. *European Journal of Neuroscience*, 26, 2613-2626.

BOUT, R. G. & ZWEERS, G. A. 2001. The role of cranial kinesis in birds. *Comparative Biochemistry and Physiology a-Molecular and Integrative Physiology*, 131, 197-205.

BOWMAKER, J. K. & MARTIN, G. R. 1978. Visual pigments and color-vision in a nocturnal bird, *Strix aluco* (tawny owl). *Vision Research*, 18, 1125-1130.

BOWMAKER, J. K. & MARTIN, G. R. 1985. Visual pigments and oil droplets in the penguin, *Spheniscus humboldti*. *Journal of Comparative Physiology a-Sensory Neural and Behavioral Physiology*, 156, 71-77.

BOWMAKER, J. K., HEATH, L. A., WILKIE, S. E. & HUNT, D. M. 1997. Visual pigments and oil droplets from six classes of photoreceptor in the retinas of birds. *Vision Research*, 37, 2183-2194.

BOWMAKER, J. K., KOVACH, J. K., WHITMORE, A. V. & LOEW, E. R. 1993. Visual pigments and oil droplets in genetically manipulated and carotenoid deprived quail - a microspectrophotometric study. *Vision Research*, 33, 571-578.

BRACH, V. 1977. Functional significance of avian pecten - REVIEW. *Condor*, 79, 321-327.

BRAEKEVELT, C. R. & RICHARDSON, K. C. 1996. Fine structure of the pecten oculi in the Australian galah (*Eolophus roseicapillus*) (Aves). *Histology and Histopathology*, 11, 565-571.

BRAEKEVELT, C. R. 1993. Fine-structure of the pecten oculi in the great horned owl (*Bubo virginianus*). *Histology and Histopathology*, 8, 9-15.

BRAEKEVELT, C. R. 1994. Fine-structure of the pecten oculi in the american crow (*Corvus brachyrhynchos*). *Anatomia Histologia Embryologia-Journal of Veterinary Medicine Series C-Zentralblatt Fur Veterinarmedizin Reihe C*, 23, 357-366.

BRAEKEVELT, C. R. 1998. Fine structure of the pecten oculi of the emu (*Dromaius novaehollandiae*). *Tissue & Cell*, 30, 157-165.

BRAVO, H. & PETTIGREW, J. D. 1981. The distribution of neurons projecting from the retina and visual-cortex to the thalamus and tectum opticum of the barn owl, *Tyto alba*, and the burrowing owl, *Speotyto cunicularia*. *Journal of Comparative Neurology*, 199, 419-441.

BROOKE, M. D. & COX, J. 2004. Albatrosses and petrels across the world. Oxford University Press, Oxford.

BROOKE, M. D., HANLEY, S. & LAUGHLIN, S. B. 1999. The scaling of eye size with body mass in birds. *Proceedings of the Royal Society of London Series B-Biological Sciences*, 266, 405-412.

BROOKS, D. E., KOMAROMY, A. M. & KALLBERG, M. E. 1999. Comparative retinal ganglion cell and optic nerve morphology. *Veterinary Ophthalmology*, 2, 3-11.

BRUNS, R. R., PRESS, W. & GROSS, J. 1987. A large-scale, orthogonal network of microfibril bundles in the corneal stroma. *Investigative Ophthalmology & Visual Science*, 28, 1939-1946.

BRYANT PA, TRINDER J, CURTIS N. 2004. Sick and tired: Does sleep have a vital role in the immune system? *Nature Rev. Immunology* 4 (6): 457-467.

BUDNIK, V., MPODOZIS, J., VARELA, F. & MATURANA, H. 1984. Regional specialization of the quail retina - ganglion-cell density and oil droplet distribution. *NEUROSCIENCE LETTERS*, 51, 145-150.

BULGARINI F, VISENTIN M. 1997. Nocturnal feeding by barn swallows and house martins. *Br. Birds* 90: 363.

BURNHAM, D. A. 2007. Archaeopteryx - a re-evaluation suggesting an arboreal habitat and an intermediate stage in trees down origin of flight. *Neues Jahrbuch Fur Geologie Und Palaontologie-Abhandlungen*, 245, 33-44.

BURTON, R. F. 2008. The scaling of eye size in adult birds: Relationship to brain, head and body sizes. *Vision Research*, 48, 2345-2351.

CABANAC, A. J. & GUILLEMETTE, M. 2001. Temperature and heart rate as stress indicators of handled common eider. *Physiology & Behavior*, 74, 475-479.

CALCAGNINI, G., CENSI, F., LINO, S. & CERUTTI, S. 2000. Spontaneous fluctuations of human pupil reflect central autonomic rhythms. *Methods of Information in Medicine*, 39, 142-145.

CASINI, G., PORCIATTI, V., FONTANESI, G. & BAGNOLI, P. 1992. Wulst efferents in the little owl *Athene noctua* - an investigation of projections to the optic tectum. *Brain Behavior and Evolution*, 39, 101-115.

CASSIN, B. & SOLOMON, S. 1984. *Dictionary of eye terminology*. Triad, Gainesville, Fla.

CATCHPOLE, C. K. & SLATER, P. J. B. 1995. Bird song: Biological themes and variations, Cambridge University Press; Cambridge.

CHAPPELL MA, ZUK M, KWAN TH, JOHNSEN TS. 1995. Energy-cost of an avian vocal display - crowing in red junglefowl. *Anim. Behav.* 49 (1): 255-257.

CHERNETSOV, N., KISHKINEV, D. & MOURITSEN, H. 2008. A long-distance avian migrant compensates for longitudinal displacement during spring migration. *Current Biology*, 18, 188-190.

CHESSER, R. T. 2004. Molecular systematics of New World suboscine birds. *Molecular Phylogenetics and Evolution*, 32, 11-24.

CHRISTIDIS, L. 1987. Phylogeny and systematics of estrildine finches and their relationships to other seed-eating passerines. *Emu*, 87, 119-123.

CICERO, C. & JOHNSON, N. K. 2002. Phylogeny and character evolution in the Empidonax group of tyrant flycatchers (Aves : Tyrannidae): A test of W. E. Lanyon's hypothesis using mtDNA sequences. *Molecular Phylogenetics and Evolution*, 22, 289-302.

CLARK, J. I. 2004. Order and disorder in the transparent media of the eye. *Experimental Eye Research*, 78, 427-432.

CLAYTON, D. H. & JOHNSON, K. P. 2003. Linking coevolutionary history to ecological process: Doves and lice. *Evolution*, 57, 2335-2341.

CODY, M.L. & BROWN, J.H., 1969. Song asynchrony in neighbouring bird species. *Nature* 222: 778.

COHEN-CORY, S. & LOM, B. 2004. Neurotrophic regulation of retinal ganglion cell synaptic connectivity: from axons and dendrites to synapses. *International Journal of Developmental Biology*, 48, 947-956.

COIMBRA, J. P., MARCELIANO, M. L. V., ANDRADE-DA-COSTA, B. L. D. & YAMADA, E. S. 2006. The retina of tyrant flycatchers: Topographic organization of neuronal density and size in the ganglion cell layer of the great kiskadee *Pitangus sulphuratus* and the rusty margined flycatcher *Myiozetetes cayanensis* (Aves : Tyrannidae). *Brain Behavior and Evolution*, 68, 15-25.

COIMBRA, J. P., TREVIA, N., MARCELIANO, M. L. V., ANDRADE-DA-COSTA, B. L. D., PICANCO-DINIZ, C. W. & YAMADA, E. S. 2009. Number and Distribution of Neurons in the Retinal Ganglion Cell Layer in Relation to Foraging Behaviors of Tyrant Flycatchers. *Journal of Comparative Neurology*, 514, 66-73.

COLVILLE, T. P. & BASSERT, J. M. 2001. *Clinical anatomy & physiology for veterinary technicians*, St. Louis, Mo. ; London, Mosby.

CONNON, C. J., MEEK, K. M., KINOSHITA, S. & QUANTOCK, A. J. 2004. Spatial and temporal alterations in the collagen fibrillar array during the onset of transparency in the avian cornea. *Experimental Eye Research*, 78, 909-915.

COOK, J. E. & PODUGOLNIKOVA, T. A. 2001. Evidence for spatial regularity among retinal ganglion cells that project to the accessory optic system in a frog, a reptile, a bird, and a mammal. *Visual Neuroscience*, 18, 289-297.

COPPACK, T., BECKER, S. F. & BECKER, P. J. J. 2008. Circadian flight schedules in night-migrating birds caught on migration. *Biology Letters*, 4, 619-622.

CORDIER, A. 1927. Some observations on the water ouzel. *The Auk*, 44, 169-178.

COTTRIAL, C. L. & MCBRIEN, N. A. 1996. The M(1) muscarinic antagonist pirenzepine reduces myopia and eye enlargement in the tree shrew. *Investigative Ophthalmology & Visual Science*, 37, 1368-1379.

COX, J. L., FARRELL, R. A., HART, R. W. & LANGHAM, M. E. 1970. Transparency of mammalian cornea. *Journal of Physiology-London*, 210, 601-&.

CRAMP, S. 1977. *Handbook of the birds of Europe the Middle East and North Africa : the birds of the Western Palearctic*, Oxford, Oxford University Press.

CRAMP, S. 1988. *Handbook of the birds of Europe, the Middle East and North Africa: the birds of the Western Palearctic*. Oxford: Oxford University Press.

CRAMP, S., SIMMONS, K. E. L. & PERRINS, C. M., 2004. *The birds of the Western Palearctic interactive*. Sheffield: birdguides Ltd.

CRAMP, S., BROOKS, D. J. & DUNN, E. 1994. *Handbook of the birds of Europe, the Middle East and North Africa : the birds of the western Palearctic*, Oxford, Oxford University Press.

CROWE, T. M., BOWIE, R. C. K., BLOOMER, P., MANDIWANA, T. G., HEDDERSON, T. A. J., RANDI, E., PEREIRA, S. L. & WAKELING, J. 2006. Phylogenetics, biogeography and classification of, and character evolution in. gamebirds (Aves : Galliformes): effects of character exclusion, data partitioning and missing data. *Cladistics*, 22, 495-532.

CURIO, E. 2001. On how birds protect their eyes: division of labour between the upper lid, lower lid and the nictitating membrane. *Journal Fur Ornithologie*, 142, 257-272.

CURTIS, E. & MILLER, R. 1938. The Sclerotic Ring in North American Birds. *The Auk*, 55, 225-243.

DALZIELL, A. H. & COCKBURN, A. 2008. Dawn song in superb fairy-wrens: a bird that seeks extrapair copulations during the dawn chorus. *Animal Behaviour*, 75, 489-500.

DANIELS, R. J. R., JOSHI, N. V. & GADGIL, M. 1992. On the relationship between bird and woody plant-species diversity in the utara kannada district of south-india. *Proceedings of the National Academy of Sciences of the United States of America*, 89, 5311-5315.

DAS, D., WILKIE, S., HUNT, D. & BOWMAKER, J. 1999. Visual pigments and oil droplets in the retina of a passerine bird, the canary *Serinus canaria*: microspectrophotometry and opsin sequences. *Vision Res*, 39, 2801-15.

DE LEON, A., MINGUEZ, E., HARVEY, P., MEEK, E., CRANE, J. E. & FURNESS, R. W. 2006. Factors affecting breeding distribution of Storm-petrels *Hydrobates pelagicus* in Orkney and Shetland. *Bird Study*, 53, 64-72.

D'ELBEE, J. & HEMERY, G. 1998. Diet and foraging behaviour of the British Storm Petrel *Hydrobates pelagicus* in the Bay of Biscay during summer. *Ardea*, 86, 1-10.

DENG, C. & WANG, B. 1993. Convergence of somatic and visual afferent impulses in the wulst of pigeon. *Experimental Brain Research*, 96, 287-290.

DESTEFANO, M. E. & MUGNAINI, E. 1997. Fine structure of the choroidal coat of the avian eye - Lymphatic vessels. *Investigative Ophthalmology & Visual Science*, 38, 1241-1260.

DICKENS, C. 1867. *The first use of gas in London. All the year round.* Chapman and Hall, London.

DONALDSON, D. D. 1971. *Atlas of external diseases of the eye.* Mosby, St Louis.

- DOUGLAS, R. H., WILLIAMSON, R. & WAGNER, H. J. 2005. The pupillary response of cephalopods. *Journal of Experimental Biology*, 208, 261-265.
- DRISKELL, A. C. & CHRISTIDIS, L. 2004. Phylogeny and evolution of the Australo-Papuan honeyeaters (Passeriformes, Meliphagidae). *Molecular Phylogenetics and Evolution*, 31, 943-960.
- DUFFY, J. F. & WRIGHT JR, K. P. 2005. Entrainment of the human circadian system by light. *J Biol. Rhythms* 20 (4): 326- 338.
- DUNNING, J. B. 2008. CRC handbook of avian body masses. CRC, London.
- DURIEZ, O., PASTOUT-LUCCHINI, L., BOOS, M., CHASTEL, O., FRITZ, H., FERRAND, Y. & CLOBERT, J. 2004. Low levels of energy expenditure in a nocturnal, forest-dwelling wader, the Eurasian Woodcock *Scolopax rusticola*. *Ardea* 92 (1): 31-42.
- DVORAK, C. A. & GRANDA, A. M. 1990. Wavelength-dependent temporal properties of retinal horizontal cells in turtles. *Visual Neuroscience*, 4, 427-435.
- EBERHARD, J. R. & EWALD, P. W. 1994. Food availability, intrusion pressure and territory size - an experimental-study of annas hummingbirds (*Calypte anna*). *Behavioral Ecology and Sociobiology*, 34, 11-18.
- EEVA, T., RYÖMÄ, M. & RIIHIMÄKI, J., 2005. Pollution related changes in diets of two insectivorous passerines. *Oecologia* 145: 629-639.
- EMLEN, S. T. 1967. Migratory orientation in indigo bunting *Passerina cyanea* .2. Mechanism of celestial orientation. *Auk*, 84, 463-&.

- EMOND, M. P., MCNEIL, R., CABANA, T., GUERRA, C. G. & LACHAPELLE, P. 2006. Comparing the retinal structures and functions in two species of gulls (*Larus delawarensis* and *Larus modestus*) with significant nocturnal behaviours. *Vision Research*, 46, 2914-2925.
- ENGLAND MD. 1977. Robins foraging at night. *Br. Birds* 71: 88.
- ERICSON, P. G. P. & JOHANSSON, U. S. 2003. Phylogeny of Passerida (Aves : Passeriformes) based on nuclear and mitochondrial sequence data. *Molecular Phylogenetics and Evolution*, 29, 126-138.
- FEDUCCIA, A. & TORDOFF, H. B. 1979. Feathers of Archaeopteryx - asymmetric vanes indicate aerodynamic function. *Science*, 203, 1021-1022.
- FERNALD, R. D. 2004. Evolving eyes. *International Journal of Developmental Biology*, 48, 701-705.
- FERNALD, R. D. 2006. Casting a genetic light on the evolution of eyes. *Science*, 313, 1914-1918.
- FERNANDEZ-JURICIC, E., ERICHSEN, J. T. & KACELNIK, A. 2004. Visual perception and social foraging in birds. *Trends in Ecology & Evolution*, 19, 25-31.
- FIELD, G. D. & CHICHILNISKY, E. J. 2007. Information processing in the primate retina: Circuitry and coding. *Annual Review of Neuroscience*, 30, 1-30.
- FISCHER, A. J. 2005. Neural regeneration in the chick retina. *Progress in Retinal and Eye Research*, 24, 161-182.
- FISLER, G. F. 1962. Variation in the morning awakening time of some birds in south-central Michigan. *Condor*, 64, 184-198.

FLEMING, G. J., LESTER, N. V., STEVENSON, R. & SILVER, X. S. 2003. High field strength (4.7T) magnetic resonance imaging of hydrocephalus in an African Grey parrot (*Psittacus erithacus*). *Veterinary Radiology & Ultrasound*, 44, 542-545.

FOWLER, J. 2002. European Storm-petrel *Hydrobates pelagicus*. In: WERNHAM, C., TOMS, M., MARCHANT, J., CLARK, J., SIRIWARDENA, G. & BAILLIE, S. (eds.) *The migration atlas: movements of the birds of Britain and Ireland*. T. & A.D. Poyser, London.

FOX, J., 2002. *An R and S-PLUS Companion to Applied Regression*, Sage.

FOX, R., LEHMKUHLE, S. W. & WESTENDORF, D. H. 1976. Falcon visual acuity. *Science*, 192, 263-265.

FREEMAN, S. N., ROBINSON, R. A., CLARK, J. A., GRIFFIN, B. M. & ADAMS, S. Y. 2007. Changing demography and population decline in the Common Starling *Sturnus vulgaris*: a multisite approach to Integrated Population Monitoring. *Ibis*, 149, 587-596.

FUCHS, T., MAURY, D., MOORE, F. R. & BINGMAN, V. P. 2009. Daytime micro-naps in a nocturnal migrant: an EEG analysis. *Biology Letters*, 5, 77-80.

FULLER, R. A., WARREN, P. H. & GASTON, K. J., (2007). Daytime noise predicts nocturnal singing in urban robins. *Biol. Lett.* Doi:10.1098/rsbl.2007.0134.

GALLIFRET, Y. 1968. Les divers aires fonctionnelles de la retine du pigeon. *Z. Zellforsch mikrosk. Anat*, 86, 535-545.

GARAMSZEGI, L. Z., MOLLER, A. P. & ERRITZOE, J. 2002. Coevolving avian eye size and brain size in relation to prey capture and nocturnality. *Proceedings of the Royal Society of London Series B-Biological Sciences*, 269, 961-967.

- GARSTANG, R. H. 2004. Mount Wilson Observatory: The sad story of light pollution. *Observatory* 124 (1178): 14-21.
- GARTHE, S. & HUPPOP, O. 1996. Nocturnal scavenging by gulls in the southern North Sea. *Colonial Waterbirds*, 19, 232-241.
- GEHLBACH, F. R. 1995. Eastern screech-owl. *Birds of North America*, 1-24.
- GEISER, M. H., BONVIN, M., QUIBEL, O. & BALUNGA, W. 2003. Corneal and retinal temperatures under various ambient conditions: a model and experimental approach. ARVO Annual Meeting Abstract Search and Program Planner, 2003, Abstract No. 2446.
- GILL, S. A., VONHOF, M. J., STUTCHBURY, B. J. M., MORTON, E. S. & QUINN, J. S. 2005. No evidence for acoustic mate-guarding in duetting buff-breasted wrens (*Thryothorus leucotis*). *Behavioral Ecology and Sociobiology*, 57, 557-565.
- GILLE, U., ZACHEN, F. & SALOMON, F. V. 2000. Brain, eye, and skull growth in embryonic geese. *Condor*, 102, 676-679.
- GLASSER, A. & HOWLAND, H. C. 1996. A history of studies of visual accommodation in birds. *Quarterly Review of Biology*, 71, 475-509.
- GLASSER, A., TROILO, D. & HOWLAND, H. C. 1994. The mechanism of corneal accommodation in chicks. *Vision Research*, 34, 1549-1566.
- GLEN, C. L. & BENNETT, M. B. 2007. Foraging modes of Mesozoic birds and non-avian theropods. *Current Biology*, 17, R911-R912.
- GOLDSMITH, T. H., COLLINS, J. S. & LICHT, S. 1984. The cone oil droplets of avian retinas. *Vision Research*, 24, 1661-1671.

GONDO, M. & ANDO, H. 1995. Comparative histophysiological study of oil droplets in the avian retina. *Japanese Journal of Ornithology*, 44, 81-91.

GOODGE, W. R. 1960. Adaptations for amphibious vision in the dipper (*Cinclus mexicanus*). *Jour Morphol*, 107, 79-91.

GOREN-INBAR, N., ALPERSON, N., KISLEV, M. E., SIMCHONI, O., MELAMED, Y., BEN-NUN, A. & WERKER, E. 2004. Evidence of hominin control of fire at Gesher Benot Ya'aqov, Israel. *Science*, 304, 725-727.

GORISSEN, L. & EENS, M. 2004. Interactive communication between male and female Great Tits (*Parus major*) during the dawn chorus. *Auk*, 121, 184-191.

GORSKA, E., 1991. Roczny cykl rozpoczynania i konczenia aktywnosci dziennej miejskich populacji sierpowki (*Streptopelia decaocto*), wrobla (*Passer domesticus*), kosa (*Turdus merula*), szpaka (*Sturnus vulgaris*) i kawki (*Corvus monedula*) w Slupsku. *Notatki Ornitologiczne* 32, 37-54.

GREENWOOD, V. J., SMITH, E. L., CHURCH, S. C. & PARTRIDGE, J. C. 2003. Behavioural investigation of polarisation sensitivity in the Japanese quail (*Coturnix coturnix japonica*) and the European starling (*Sturnus vulgaris*). *Journal of Experimental Biology*, 206, 3201-3210

GREMILLET, D., KUNTZ, G., GILBERT, C., WOAKES, A. J., BUTLER, P. J. & LE MAHO, Y. 2005. Cormorants dive through the Polar night. *Biology Letters*, 1, 469-471.

GROTH, J. G. 1998. Molecular phylogenetics of finches and sparrows: Consequences of character state removal in cytochrome b sequences. *Molecular Phylogenetics and Evolution*, 10, 377-390.

GUILLEMAIN, M., MARTIN, G. R. & FRITZ, H. 2002. Feeding methods, visual fields and vigilance in dabbling ducks (Anatidae). *Functional Ecology*, 16, 522-529.

GUMPENBERGER, M. & KOLM, G. 2006. Ultrasonographic and computed tomographic examinations of the avian eye: Physiologic appearance, pathologic findings, and comparative biometric measurement. *Veterinary Radiology & Ultrasound*, 47, 492-502.

GUNTURKUN, O. 2000. Sensory Physiology: Vision. In: WHITTOW, G. C. (ed.) *Sturkie's avian physiology*. 5th ed. Academic, San Diego.

GWINNER, E., SCHWABL BENZINGER, I., SCHWABL, H. & DITTAMI, J., 1993. 24-hour melatonin profiles in a nocturnally migrating bird during and between migratory seasons. *Gen. Comp. Endocrin.* 90 (1): 119-124.

GWINNER, E. 1975. Circadian and circannual rhythms in birds. In: Farner, Donald S. and James R. King (Ed.). *Avian Biology*, Vol. 5. Academic Press: New York.

HACKETT, S. J., KIMBALL, R. T., REDDY, S., BOWIE, R. C. K., BRAUN, E. L., BRAUN, M. J., CHOJNOWSKI, J. L., COX, W. A., HAN, K. L., HARSHMAN, J., HUDDLESTON, C. J., MARKS, B. D., MIGLIA, K. J., MOORE, W. S., SHELDON, F. H., STEADMAN, D. W., WITT, C. C. & YURI, T. 2008. A phylogenomic study of birds reveals their evolutionary history. *Science*, 320, 1763-1768.

HAFTORN, S., MEHLUM, F. & BECH, C. 1988. Navigation to nest site in the snow petrel (*Pagodroma nivea*). *Condor*, 90, 484-486.

HAGELIN, J. C. & JONES, I. L. 2007. Bird odors and other chemical substances: A defense mechanism or overlooked mode of intraspecific communication? *Auk*, 124, 741-761.

HALL, M. I. & ROSS, C. F. 2007. Eye shape and activity pattern in birds. *Journal of Zoology*, 271, 437-444.

HALL, M. I. 2008. The anatomical relationships between the avian eye, orbit and sclerotic ring: implications for inferring activity patterns in extinct birds. *Journal of Anatomy*, 212, 781-794.

HALL, M. I. 2009. The relationship between the lizard eye and associated bony features: A cautionary note for interpreting fossil activity patterns. *Anatomical Record -Advances in Integrative Anatomy and Evolutionary Biology*, 292, 798-812.

HARING, E., KVALOY, K., GJERSHAUG, J. O., ROV, N. & GAMAUF, A. 2007. Convergent evolution and paraphyly of the hawk-eagles of the genus *Spizaetus* (Aves, Accipitridae) - phylogenetic analyses based on mitochondrial markers. *Journal of Zoological Systematics and Evolutionary Research*, 45, 353-365.

HARMENING, W. M., VOBIG, M. A., WALTER, P. & WAGNER, H. 2007. Ocular aberrations in barn owl eyes. *Vision Research*, 47, 2934-2942.

HARPER, D. G. C. 1994. Some comments on the repeatability of measurements. *Ring and Migration*, 15, 84-90.

HART, N. S. 2001. The visual ecology of avian photoreceptors. *Progress in Retinal and Eye Research*, 20, 675-703.

HART, N. S. 2004. Microspectrophotometry of visual pigments and oil droplets in a marine bird, the wedge-tailed shearwater *Puffinus pacificus*: topographic variations in photoreceptor spectral characteristics. *Journal of Experimental Biology*, 207, 1229-1240.

HART, N. S. & HUNT, D. M. 2003. Avian visual pigments: Characteristics, spectral tuning, and evolution. In: 2nd European Conference on Avian Colour Vision and Coloration. Univ Chicago Press, Paris. S7-S26.

HART, N. S., PARTRIDGE, J. C. & CUTHILL, I. C. 1998. Visual pigments, oil droplets and cone photoreceptor distribution in the European starling (*Sturnus vulgaris*). *Journal of Experimental Biology*, 201, 1433-1446.

HART, N. S., PARTRIDGE, J. C. & CUTHILL, I. C. 2000. Retinal asymmetry in birds. *Current Biology*, 10, 115-117.

HART, N. S., PARTRIDGE, J. C., BENNETT, A. T. D. & CUTHILL, I. C. 2000. Visual pigments, cone oil droplets and ocular media in four species of estrildid finch. *Journal of Comparative Physiology a-Sensory Neural and Behavioral Physiology*, 186, 681-694.

HART, N. S., PARTRIDGE, J. C., CUTHILL, I. C. & BENNETT, A. T. D. 2000. Visual pigments, oil droplets, ocular media and cone photoreceptor distribution in two species of passerine bird: the blue tit (*Parus caeruleus* L.) and the blackbird (*Turdus merula* L.). *Journal of Comparative Physiology A-Sensory Neural and Behavioral Physiology*, 186, 375-387.

HARVEY, P. H. & PAGEL, M. D. 1991. *Oxford series in ecology and evolution 1. The comparative method in evolutionary biology*. Oxford University Press, Oxford.

HARVEY, P. H. & PURVIS, A. 1991. Comparative methods for explaining adaptations. *Nature*, 351, 619-624.

HAWKINS, B. A., PORTER, E. E. & DINIZ, J. A. F. 2003. Productivity and history as predictors of the latitudinal diversity gradient of terrestrial birds. *Ecology*, 84, 1608-1623.

HAYES, B., MARTIN, G. R. & BROOKE, M. D. 1991. Novel area serving binocular vision in the retinae of procellariiform seabirds. *Brain Behavior and Evolution*, 37, 79-84.

HEALY, S. & GUILFORD, T. 1990. OLFATORY-bulb size and nocturnality in birds. *Evolution*, 44, 339-346.

HEESY, C. P. 2004. On the relationship between orbit orientation and binocular visual field overlap in mammals. *Anatomical Record Part A-Discoveries in Molecular Cellular and Evolutionary Biology*, 281A, 1104-1110.

HELBIG, A. J. & SEIBOLD, I. 1999. Molecular phylogeny of Palearctic-African *Acrocephalus* and *Hippolais* warblers (Aves : Sylviidae). *Molecular Phylogenetics and Evolution*, 11, 246-260.

HEMMINGS, E.A. & DOUGLAS, E. L. 1970. Ultraviolet radiation thresholds for corneal injury in antarctic and temperate-zone animals. *Comparative Biochemistry and Physiology*, 32, 593-&.

HENDERSON, D. M. 2003. The eyes have it: The sizes, shapes, and orientations of theropod orbits as indicators of skull strength and bite force. *Journal of Vertebrate Paleontology*, 22, 766-778.

HENWOOD K, FABRICK A. 1979. A quantitative analysis of the dawn chorus: temporal selection for communicatory optimisation. *Amer. Natur.* 144: 260-274.

HERRERA, G., ZAGAL, J. C., DIAZ, M., FERNANDEZ, M. J., VIELMA, A., CURE, M., MARTINEZ, J., BOZINOVIC, F. & PALACIOS, A. G. 2008. Spectral sensitivities of photoreceptors and their role in colour discrimination in the green-backed firecrown hummingbird (*Sephanoides sephaniodes*). *Journal of Comparative Physiology A-Neuroethology Sensory Neural and Behavioral Physiology*, 194, 785-794.

HEYERS, D., MANNS, M., LUKSCH, H., GUNTURKUN, O. & MOURITSEN, H. 2007. A visual pathway links brain structures active during magnetic compass orientation in migratory birds. *PLOSOne*, 2, e937.

HOLDAWAY, R. N. & JACOMBE, C. 2000. Rapid extinction of the moas (Aves: Dinornithiformes): Model, test, and implications. *Science*, 287 (5461), 2250-2254.

HOLLANDER, M. & WOLFE, D. A. 1999. Nonparametric statistical methods. John Wiley & Sons, Chichester.

HOLLON, P. A. D., 1965. Robins nocturnally singing and feeding. *British Birds*. 59: 501-502.

HONKAVAARA, J., KOIVULA, M., KORPIMÄKI, E., SIITARI, H. & VIITALA, J. 2002. Ultraviolet vision and foraging in terrestrial vertebrates. *Oikos* 98: 505-511.

HOTHORN, T., HORNIK, K., VAN DE WIEL, M. A., & ZEILEIS, A., 2006. A Lego System for Conditional Inference. *The American Statistician* 60(3), 257-263.

HOTHORN, T., BRETZ, F. & WESTFALL, P., 2008. Simultaneous Inference in General Parametric Models. *Biometrical Journal* 50(3), 346-363.

HOUCK, M., GAUTHIER, J. & STRAUSS, R. 1990. Allometric scaling in the earliest fossil bird, *Archaeopteryx lithographica*. *Science*, 247. 195-198.

HOWLAND, H. C. & SIVAK, J. G. 1984. Penguin vision in air and water. *Vision Research*, 24, 1905-1909.

HOWLAND, H. C., MEROLA, S. & BASARAB, J. R. 2004. The allometry and scaling of the size of vertebrate eyes. *Vision Research*, 44, 2043-2065.

HOYO, J. D., ELLIOTT, A., SARGATAL, J. & CABOT, J. Handbook of the birds of the world, Barcelona : Lynx Edicions, c1992-.

HUGHES, J. M. 1996. Phylogenetic analysis of the cuculidae (Aves, Cuculiformes) using behavioral and ecological characters. *Auk*, 113, 10-22.

HUI, C. A. 2002. Concentrations of chromium, manganese, and lead in air and in avian eggs. *Env. Pollution* 120 (2): 201-206.

HUTCHINSON, J. M. C., MCNAMARA, J. M. & CUTHILL, I. C. 1993. Song, sexual selection, starvation and strategic handicaps. *Anim. Behav.* 45: 1153-1177.

HUTCHINSON, J. M. C. 2002. Two explanations of the dawn chorus compared: how monotonically changing light levels favour a short break from singing. *Anim. Behav.* 64 (4): 527-539.

HUTCHISON, L. V. & WENZEL, B. M. 1980. Olfactory guidance in foraging by procellariiforms. *Condor*, 82, 314-319.

IBANEZ, C., JUSTE, J., GARCIA-MUDARRA, J. L. & AGIRRE-MENDI, P. T. 2001. Bat predation on nocturnally migrating birds. *Proceedings of the National Academy of Sciences of the United States of America*, 98, 9700-9702.

IHANAMAKI, T., PELLINIEMI, L. J. & VUORIO, E. 2004. Collagens and collagen-related matrix components in the human and mouse eye. *Progress in Retinal and Eye Research*, 23, 403-434.

INZUNZA, O., BRAVO, H., SMITH, R. L. & ANGEL, M. 1991. Topography and morphology of retinal ganglion-cells in falconiforms - a study on predatory and carrion-eating birds. *Anatomical Record*, 229, 271-277.

IOALE, P. & PAPI, F. 1989. Olfactory-bulb size, odor discrimination and magnetic insensitivity in hummingbirds. *Physiology & Behavior*, 45, 995-999.

IRESTEDT, M., FJELDSA, J., NYLANDER, J. A. A. & ERICSON, P. G. P. 2004. Phylogenetic relationships of typical antbirds (Thamnophilidae) and test of incongruence based on Bayes factors. *BMC Evolutionary Biology*, 4.

IRWIN, D. E. 2000. Song variation in an avian ring species. *Evolution*, 54, 998-1010.

ISLER, K. & VAN SCHAIK, C. P. 2006. Metabolic costs of brain size evolution. *Biology Letters*, 2, 557-560.

IWANIUK, A. N. & WYLIE, D. R. W. 2006. The evolution of stereopsis and the Wulst in caprimulgidiform birds: a comparative analysis. *Journal of Comparative Physiology a-Neuroethology Sensory Neural and Behavioral Physiology*, 192, 1313-1326.

IWANIUK, A. N., CLAYTON, D. H. & WYLIE, D. R. W. 2006. Echolocation, vocal learning, auditory localization and the relative size of the avian auditory midbrain nucleus (MLD). *Behavioural Brain Research*, 167, 305-317.

IWANIUK, A. N., HEESY, C. P., HALL, M. I. & WYLIE, D. R. W. 2008. Relative Wulst volume is correlated with orbit orientation and binocular visual field in birds. *Journal of Comparative Physiology A-Neuroethology Sensory Neural and Behavioral Physiology*, 194, 267-282.

JANE, S. D. & BOWMAKER, J. K. 1988. Tetrachromatic color-vision in the duck (*Anas platyrhynchos* L) - microspectrophotometry of visual pigments and oil droplets. *Journal of Comparative Physiology A-Sensory Neural and Behavioral Physiology*, 162, 225-235.

JEFFERY, G. 2001. Architecture of the optic chiasm and the mechanisms that sculpt its development. *Physiological Reviews*, 81, 1393-1414.

JEZZARD, P. & CLARE, S. 2001. Principles of Nuclear Magnetic Resonance and MRI. In: JEZZARD, MATTHEWS & SMITH (eds.) 'Functional Magnetic Resonance Imaging: An Introduction to Methods. Oxford: Oxford University Press.

JOHANSSON, U. S., IRESTEDT, M., PARSONS, T. J. & ERICSON, P. G. P. 2002. Basal phylogeny of the tyrannoidea based on comparisons of cytochrome b and exons of nuclear c-myc and RAG-1 genes. *Auk*, 119, 984-995.

JOHNSON, K. P., DE KORT, S., DINWOODEY, K., MATEMAN, A. C., TEN CATE, C., LESSELLS, C. M. & CLAYTON, D. H. 2001. A molecular phylogeny of the dove genera *Streptopelia* and *Columba*. *Auk*, 118, 874-887.

JOHNSON, K. P., WILLIAMS, B. L., DROWN, D. M., ADAMS, R. J. & CLAYTON, D. H. 2002. The population genetics of host specificity: genetic differentiation in dove lice (Insecta : Phthiraptera). *Molecular Ecology*, 11, 25-38.

JONES, C. D. & OSORIO, D. 2004. Discrimination of oriented visual textures by poultry chicks. *Vision Research*, 44, 83-89.

JONSSON, K. A. & FJELDSA, J. 2006. A phylogenetic supertree of oscine passerine birds (Aves: Passeri). *Zoologica Scripta*, 35, 149-186.

JOUVENTIN, P., MOURET, V. & BONADONNA, F. 2007. Wilson's storm petrels *Oceanites oceanicus* recognise the olfactory signature of their mate. *Ethology*, 113, 1228-1232.

KACELNIK, A. 1979. Foraging efficiency of great tits (*Parus major* L) in relation to light-intensity. *Animal Behaviour*, 27, 237-241.

KACELNIK, A. & KREBS, J. R. 1983. The dawn chorus in the great tit (*Parus major*) - proximate and ultimate causes. *Behaviour*, 83, 287-309.

KARR, J. R. 1976. Seasonality, resource availability, and community diversity in tropical bird communities. *American Naturalist*, 110, 973-994.

KATZIR, G. & HOWLAND, H. C. 2003. Corneal power and underwater accommodation in great cormorants (*Phalacrocorax carbo sinensis*). *Journal of Experimental Biology*, 206, 833-841.

KAUFMAN, H. E. 1988. *The cornea*. Churchill Livingstone, New York.

KEAST, A. 1994. Temporal vocalization patterns in members of a eucalypt forest bird community - the effects of weather on song production. *Emu*, 94, 172-180.

KERLINGER, P. & MOORE, F. R. 1989. Atmospheric structure and avian migration. *Current Ornithology*, 109-142.

KIAMA, S. G., BHATTACHARJEE, J., MAINA, J. N. & WEYRAUCH, K. D. 1994. A scanning electron-microscope study of the pecten oculi of the black kite (*Milvus migrans*) - possible involvement of melanosomes in protecting the pecten against damage by ultraviolet-light. *Journal of Anatomy*, 185, 637-642.

KIAMA, S. G., MAINA, J. N., BHATTACHARJEE, J. & WEYRAUCH, K. D. 2001. Functional morphology of the pecten oculi in the nocturnal spotted eagle owl (*Bubo bubo africanus*), and the diurnal black kite (*Milvus migrans*) and domestic fowl (*Gallus gallus* var. Domesticus): a comparative study. *Journal of Zoology*, 254, 521-528.

KIAMA, S. G., MAINA, J. N., BHATTACHARJEE, J., MWANGI, D. K., MACHARIA, R. G. & WEYRAUCH, K. D. 2006. The morphology of the pecten oculi of the ostrich, *Struthio camelus*. *Annals of Anatomy-Anatomischer Anzeiger*, 188, 519-528.

KILTIE, R. A. 2000. Scaling of visual acuity with body size in mammals and birds. *Functional Ecology*, 14, 226-234.

KIMBLE, T. D. H., FITZGERALD, M. E. C. & REINER, A. 2006. Sustained upregulation of glial fibrillary acidic protein in Muller cells in pigeon retina following disruption of the parasympathetic control of choroidal blood flow. *Experimental Eye Research*, 83, 1017-1030.

KINNEAR, A. & LAUBER, J. K. 1978. Biochemical studies of chicken vitreous in light-induced avian glaucoma. *Comparative Biochemistry and Physiology B-Biochemistry & Molecular Biology*, 61, 107-110.

KLICKA, J., BURNS, K. & SPELLMAN, G. M. 2007. Defining a monophyletic cardinalini: A molecular perspective. *Molecular Phylogenetics and Evolution*, 45, 1014-1032.

KLICKA, J., VOELKER, G. & SPELLMAN, G. M. 2005. A molecular phylogenetic analysis of the "true thrushes" (Aves : Turdinae). *Molecular Phylogenetics and Evolution*, 34, 486-500.

KING, B. 1965. Robins nocturnally singing and feeding. *Br. Birds* 59: 501.

KNUDSEN, E. I. 1981. The hearing of the barn owl. *Scientific American*, 245, 82-91.

KOHEN, E., SANTUS, R. & HIRSCHBERG, J. G. 1995. *Photobiology*. Academic Press, San Diego

KOLB, H., NELSON, R., AHNELT, P. & CUENCA, N. 2001. Cellular organization of the vertebrate retina. In: DOWLING, J. E., KOLB, H., RIPPS, H. & WU, S. M.-S. (eds.) *Concepts and challenges in retinal biology : a tribute to John E. Dowling*. Elsevier, Amsterdam.

KONISHI, M. & KNUDSEN, E. I. 1979. Oilbird - hearing and echolocation. *Science*, 204, 425-427.

LAMB, T. D., COLLIN, S. P. & PUGH, E. N. 2007. Evolution of the vertebrate eye: opsins, photoreceptors, retina and eye cup. *Nature Reviews Neuroscience*, 8, 960-975.

LAND, M. F. 1999. The roles of head movements in the search and capture strategy of a tern (Aves, Laridae). *Journal of Comparative Physiology a-Neuroethology Sensory Neural and Behavioral Physiology*, 184, 265-272.

LAND, M. F. 2005. The optical structures of animal eyes. *Current Biology*, 15, R319-R323.

LAND, M. F. & FERNALD, R. D. 1992. The evolution of eyes. *Annual Review of Neuroscience*, 15, 1-29.

LAND, M. F. & NILSSON, D.-E. 2002. Oxford Animal Biology Series. Animal eyes. Oxford Animal Biology Series.

LATENDRESSE, J. R., WARBRITTON, A. R., JONASSEN, H. & CREASY, D. M. 2002. Fixation of testes and eyes using a modified Davidson's fluid: Comparison with Bouin's fluid and conventional Davidson's fluid. *Toxicologic Pathology*, 30, 524-533.

LEGER, J. & LAROCHELLE, J. 2006. On the importance of radiative heat exchange during nocturnal flight in birds. *Journal of Experimental Biology*, 209, 103-114.

LEI, F.-M., ZHANG, Y.-H. & YIN, Z.-H. 1999. Comparative studies on morphology of optic organs in *Bubo bubo*, *Athene noctua* and *Falco tinnunculus*. *Acta Zoologica Sinica*, 45, 371-377.

LERNER, H. R. L. & MINDELL, D. P. 2005. Phylogeny of eagles, Old World vultures, and other Accipitridae based on nuclear and mitochondrial DNA. *Molecular Phylogenetics and Evolution*, 37, 327-346.

LETTVIN, J., MATURANA, H., MCCULLOCH, W. & PITTS, W. 1968. What the frog's eye tells the frog's brain. In: CORNING, W. C. E. & BALABAN, M. E. (eds.). The mind: biological approaches to its functions. Interscience, New York.

LEVERTON, R. 2001. Enjoying moths. T & A D Poyser Natural History, London.

LEVIN, R. N. 1996. Song behaviour and reproductive strategies in a duetting wren, *Thryothorus nigricapillus*. 2. Playback experiments. *Animal Behaviour*, 52, 1107-1117.

LEVY, B. & SIVAK, J. G. 1980. Mechanisms of accommodation in the bird eye. *Journal of Comparative Physiology*, 137, 267-272.

LI, N., GONG, Z., SAUCIER, D., KENDALL, E. J. & SARTY, G. E. 2003. Water self-diffusion tensor changes in an avian genetic developmental model of epilepsy. *Magnetic Resonance Materials in Physics Biology and Medicine*, 16, 121-128.

LIMA, S. L., RATTENBORG NC, LESKU, JA, AMLANER CJ. 2005. Sleeping under the risk of predation. *Anim. Behav.* 70: 723-736.

LIMAN, E. R. 2006. Use it or lose it: molecular evolution of sensory signaling in primates. *Pflugers Archiv-European Journal of Physiology*, 453, 125-131.

LIND, O. E., KELBER, A. & KROGER, R. H. H. 2008. Multifocal optical systems and pupil dynamics in birds. *Journal of Experimental Biology*, 211, 2752-2758.

LINDSTROM, S., NACSA, N., BLANKENSHIP, T., FITZGERALD, P., WELLER, C., VANEY, D. & WILSON, M. 2009. Distribution and structure of efferent synapses in the chicken retina. *Visual Neuroscience*, 26, 215-226.

LISENMAYER, T. F., FITCH, J. M., GORDON, M. K., CAI, C. X., IGOE, F., MARCHANT, J. K. & BIRK, D. E. 1998. Development and roles of collagenous matrices in the embryonic avian cornea. *Progress in Retinal and Eye Research*, 17, 231-265.

LISENMAYER, T. F., GIBNEY, E. & FITCH, J. M. 1986. Embryonic avian cornea contains layers of collagen with greater than average stability. *Journal of Cell Biology*, 103, 1587-1594.

LO, W. K. & REESE, T. S. 1993b. Multiple structural types of gap-junctions in mouse lens. *Journal of Cell Science*, 106, 227-235.

LOWDEN, A., AKERSLEDT, T. & WIBOM, R. 2004. Suppression of sleepiness and melatonin by bright light exposure during breaks in night work. *J Sleep Res.* 13: 37-43.

LUKSCH, H., KHANBABAIE, R. & WESSEL, R. 2004. Synaptic dynamics mediate sensitivity to motion independent of stimulus details. *Nature Neuroscience*, 7, 380-388.

LUTHER, D. A. 2008. Signaller: receiver coordination and the timing of communication in Amazonian birds. *Biology Letters*, 4, 651-654.

LUTHER, D. A. & WILEY, R. H. 2009. Production and perception of communicatory signals in a noisy environment. *Biology Letters*, 5, 183-187.

LYNN, S. E. & PORTER, A. J. 2008. Trapping initiates stress response in breeding and non-breeding house sparrows *Passer domesticus*: implications for using unmonitored traps in field studies. *Journal of Avian Biology*, 39, 87-94.

LYTHGOE, J. N. 1984. Visual pigments and environmental light. *Vision Research*, 24, 1539-1550.

MACE, R. H. 1987. Why do birds sing at dawn? *Ardea* 75: 123-132.

MADDOCKS, S. A., GOLDSMITH, A. R. & CUTHILL, I. C. 2001. The influence of flicker rate on plasma corticosterone levels of European starlings, *Sturnus vulgaris*. *General and Comparative Endocrinology*, 124, 315-320.

MAIER, E. J. & BOWMAKER, J. K. 1993. Color-vision in the passeriform bird, *Leiothrix lutea* - correlation of visual pigment absorbency and oil droplet transmission with spectral sensitivity. *Journal of Comparative Physiology a-Sensory Neural and Behavioral Physiology*, 172, 295-301.

MALMSTROM, T. & KROGER, R. H. H. 2006. Pupil shapes and lens optics in the eyes of terrestrial vertebrates. *Journal of Experimental Biology*, 209, 18-25.

MARCOS, S., BURNS, S., MORENO-BARRIUSOP, E. & NAVARRO, R. 1999. A new approach to the study of ocular chromatic aberrations. *Vision Research*, 39, 4309-4323.

MARGARITIS, L. H., POLITOF, T. K. & KOLIOPOULOS, J. X. 1976. Quantitative and comparative ultrastructure of vertebrate cornea .1. *Urodele amphibia*. *Tissue & Cell*, 8, 591-602.

MARIANO-JELICICH, R., FAVERO, M. & SILVA, M. P. 2003. Fish prey of the Black Skimmer *Rynchops niger* at Mar Chiquita, Buenos Aires Province, Argentina. *Marine Ornithology*, 31, 199-202.

MARKMAN, S., LEITNER, S., CATCHPOLE, C., BARNSLEY, S., MUELLER, C. T., PASCOE, D. & BUCHANAN, K. L. 2008. Pollutants increase song complexity and the volume of the brain area HVC in a songbird. *Plos ONE*, 3, e1674, 1-6.

MARPLES, G., 1939. Some notes on the diurnal song of birds. *British Birds* 33: 4-11.

MARSHALL, J., MELLERIO, J. & PALMER, D. A. 1973. Schematic eye for pigeon. *Vision Research*, 13, 2449-2453

- MARTEN, K. & MARLER, P. 1977. Sound-transmission and its significance for animal vocalization .I. Temperate habitats. *Behavioral Ecology and Sociobiology*, 2, 271-290.
- MARTIN, G. R. 1986a. The eye of a passeriform bird, the european starling (*Sturnus vulgaris*) - eye-movement amplitude, visual-fields and schematic optics. *Journal of Comparative Physiology a-Sensory Neural and Behavioral Physiology*, 159, 545-557.
- MARTIN, G. R. 1986b. Vision - shortcomings of an eagles eye. *Nature*, 319, 357-357.
- MARTIN, G. R. 1990. *Birds by night*. T & A D Poyser Ltd, London.
- MARTIN, G. R. 1993. *Producing the image. Vision, Brain and Behaviour in Birds*. MIT Press Cambridge.
- MARTIN, G. R. 1998. Eye structure and amphibious foraging in albatrosses. *Proceedings of the Royal Society of London Series B-Biological Sciences*, 265, 665-671.
- MARTIN, G. R. 1999. Eye structure and foraging in King Penguins *Aptenodytes patagonicus*. *Ibis*, 141, 444-450.
- MARTIN, G. R. & BROOKE, M. D. 1991. The eye of a procellariiform seabird, the Manx shearwater, *Puffinus puffinus* - visual-fields and optical structure. *Brain Behavior and Evolution*, 37, 65-78.
- MARTIN, G. R. & COETZEE, H. C. 2004. Visual fields in hornbills: precision-grasping and sunshades. *Ibis*, 146, 18-26.
- MARTIN, G. R. & GORDON, I. E. 1974. Visual-acuity in tawny owl (*Strix aluco*). *Vision Research*, 14, 1393-1397.

MARTIN, G. R. & KATZIR, G. 1994. Visual-fields and eye-movements in herons (Ardeidae). *Brain Behavior and Evolution*, 44, 74-85.

MARTIN, G. R. & KATZIR, G. 1999. Visual fields in short-toed eagles, *Circaetus gallicus* (Accipitridae), and the function of binocularity in birds. *Brain Behavior and Evolution*, 53, 55-66.

MARTIN, G. R. & MUNTZ, W. R. A. 1978. Spectral sensitivity of red and yellow oil droplet fields of pigeon (*Columba livia*). *Nature*, 274, 620-621.

MARTIN, G. R. & PRINCE, P. A. 2001. Visual fields and foraging in procellariiform seabirds: Sensory aspects of dietary segregation. *Brain Behavior and Evolution*, 57, 33-38.

MARTIN, G. R. & YOUNG, S. R. 1984. The eye of the humboldt penguin, *Spheniscus-humboldti* - visual-fields and schematic optics. *Proceedings of the Royal Society of London Series B-Biological Sciences*, 223, 197-222.

MARTIN, G. R., JARRETT, N. & WILLIAMS, M. 2007a. Visual fields in Blue Ducks *Hymenolaimus malacorhynchos* and Pink-eared Ducks *Malacorhynchus membranaceus*: visual and tactile foraging. *IBIS*, 149, 112-120.

MARTIN, G. R., MCNEIL, R. & ROJAS, L. M. 2007. Vision and the foraging technique of skimmers (Rynchopidae). *Ibis*, 149, 750-757.

MARTIN, G. R., ROJAS, L. M., RAMIREZ, Y. & MCNEIL, R. 2004. The eyes of oilbirds (*Steatornis caripensis*): pushing at the limits of sensitivity. *Naturwissenschaften*, 91, 26-29.

MARTIN, G. R., WILSON, K.-J., MARTIN WILD, J., PARSONS, S., FABIANA KUBKE, M. & CORFIELD, J. 2007. Kiwi forego vision in the guidance of their nocturnal activities. *PLOSOne*, 2, e198.

MAYR, G., POHL, B., HARTMAN, S. & PETERS, D. S. 2007. The tenth skeletal specimen of *Archaeopteryx*. *Zoological Journal of the Linnean Society*, 149, 97-116.

MCFADDEN, S. A. & WILD, J. M. 1986. Binocular depth-perception in the pigeon. *Journal of the Experimental Analysis of Behavior*, 45, 149-160.

MCNAMARA, J. M., BARTA, Z., WIKELSKI, M. & HOUSTON, A. I. 2008. A theoretical investigation of the effect of latitude on avian life histories. *American Naturalist*, 172, 331-345.

MCNAMARA, J. M., MACE, R. H. & HOUSTON, A. I. 1987. Optimal daily routines of singing and foraging in a bird singing to attract a mate. *Behavioral Ecology and Sociobiology*, 20, 399-405.

MCNEIL, R., MCSWEEN, A. & LACHAPELLE, P. 2005. Comparison of the retinal structure and function in four bird species as a function of the time they start singing in the morning. *Brain Behavior and Evolution*, 65, 202-214.

MICELI, D., REPERANT, J., MEDINA, M., VOLLE, M. & RIO, J. P. 2006. Distribution of ganglion cells in the pigeon retina labeled via retrograde transneuronal transport of the fluorescent dye rhodamine beta-isothiocyanate from the telencephalic visual Wulst. *Brain Research*, 1098, 94-105.

MILLAR, W. 1995. Basic principles. In: DE POTTER, P., SHIELDS, J. A. & SHIELDS, C. L. (eds.) *MRI of the eye and orbit*. Lippincott, Philadelphia.

MILLER, M. W. 2006. Apparent effects of light pollution on singing behaviour of American robins. *Condor* 108: 130-139.

MINGUEZ, E. 1997. Olfactory nest recognition by British storm-petrel chicks. *Animal Behaviour*, 53, 701-707.

MITCHELL, K. D. G. 1966. Nocturnal singing blackbird. *Br. Birds* 60: 373-374.

MOINARD, C., LEWIS, P. D., PERRY, G. C. & SHERWIN, C. M. 2001. The effects of light intensity and light source on injuries due to pecking of male domestic turkeys (*Meleagris gallopavo*). *Animal Welfare* 10: 131-139.

MONTGOMERY, R. A. 2004. Effects of understory foliage on patterns of light attenuation near the forest floor. *Biotropica*, 36, 33-39.

MORGAN, I. G. & BOELEN, M. K. 1996. A retinal dark-light switch: A review of the evidence. *Visual Neuroscience*, 13, 399-409.

MORONEY, M. K. & PETTIGREW, J. D. 1987. Some observations on the visual optics of kingfishers (aves, coraciformes, alcedinidae). *Journal of Comparative Physiology a-Sensory Neural and Behavioral Physiology*, 160, 137-149.

MORRIS, V. B. & SHOREY, C. D. 1967. An electron microscope study of types of receptor in chick retina. *Journal of Comparative Neurology*, 129, 313-340.

MORTON, E. S. 1996. A comparison of vocal behavior among tropical and temperate passerine birds. *Ecology and evolution of acoustic communication in birds*, 258-268.

MOUGEOT, F., GENEVOIS, F. & BRETAGNOLLE, V. 1998. Predation on burrowing petrels by the brown skua (*Catharacta skua lonnbergi*) at Mayes Island, Kerguelen. *Journal of Zoology*, 244, 429-438.

MOURITSEN, H. & RITZ, T. 2005. Magnetoreception and its use in bird navigation. *Current Opinion in Neurobiology*, 15, 406-414.

MOURITSEN, H., FEENDERS, G., LIEDVOGEL, M., WADA, K. & JARVIS, E. D. 2005. Night-vision brain area in migratory songbirds. *Proceedings of the National Academy of Sciences of the United States of America*, 102, 8339-8344.

MOYLE, R. G. & MARKS, B. D. 2006. Phylogenetic relationships of the bulbuls (Aves: Pycnonotidae) based on mitochondrial and nuclear DNA sequence data. *Molecular Phylogenetics and Evolution*, 40, 687-695.

MUKHIN, A., GRINKEVICH, V. & HELM, B. 2009. Under Cover of Darkness: Nocturnal Life of Diurnal Birds. *Journal of Biological Rhythms*, 24, 225-231.

MUNIZ, A., BETTS, B. S., TREVINO, A. R., BUDDAVARAPU, K., ROMAN, R., MA, J. X. & TSIN, A. T. C. 2009. Evidence for Two Retinoid Cycles in the Cone-Dominated Chicken Eye. *Biochemistry*, 48, 6854-6863.

MURPHY, C. J. & HOWLAND, H. C. 1983. Owl eyes - accommodation, corneal curvature and refractive state. *Journal of Comparative Physiology*, 151, 277-284.

MURPHY, C. J. & HOWLAND, H. C. 1987. The optics of comparative ophthalmoscopy. *Vision Research*, 27, 599-607.

MYERS, N., MITTERMEIER, R. A., MITTERMEIER, C. G., DA FONSECA, G. A. B. & KENT, J. 2000. Biodiversity hotspots for conservation priorities. *Nature*, 403, 853-858.

NAITO, J. & CHEN, Y. X. 2004. Morphologic analysis and classification of ganglion cells of the chick retina by intracellular injection of lucifer yellow and retrograde labeling with dii. *Journal of Comparative Neurology*, 469, 360-376.

NAKABAYASHI, M. 1999. Anatomical and physiological studies on the aqueous sinus artery of the pigeon eye. *Japanese Journal of Ophthalmology*, 43, 262-271.

NAKAZAKI, S., NAO-I, N. & SAWADA, A. 1998. Effects of hypoxia and post-hypoxic recovery on chick retinal pigment epithelium potentials and light-evoked responses in vitro. *Current Eye Research*, 17, 384-391.

NEVITT, G. A. 2008. Sensory ecology on the high seas: the odor world of the procellariiform seabirds. *Journal of Experimental Biology*, 211, 1706-1713.

NEVITT, G. A. & BONADONNA, F. 2005a. Seeing the world through the nose of a bird: new developments in the sensory ecology of procellariiform seabirds. *Marine Ecology-Progress Series*, 287, 292-295.

NEVITT, G. A. & BONADONNA, F. 2005b. Sensitivity to dimethyl sulphide suggests a mechanism for olfactory navigation by seabirds. *Biology Letters*, 1, 303-305.

NEVITT, G. A., LOSEKOOT, M. & WEIMERSKIRCH, H. 2008. Evidence for olfactory search in wandering albatross, *Diomedea exulans*. *Proceedings of the National Academy of Sciences of the United States of America*, 105, 4576-4581.

NEVITT, G. A., REID, K. & TRATHAN, P. 2004. Testing olfactory foraging strategies in an Antarctic seabird assemblage. *Journal of Experimental Biology*, 207, 3537-3544.

NEWSOME, D. A., LINSENMYER, T. F. & TRELSTAD, R. L. 1976. Vitreous body collagen - evidence for a dual origin from neural retina and hyalocytes. *Journal of Cell Biology*, 71, 59-67.

NGUEMBOCK, B., FJELDSA, J., TILLIER, A. & PASQUET, E. 2007. A phylogeny for the Cisticolidae (Aves : Passeriformes) based on nuclear and mitochondrial DNA sequence data, and a re-interpretation of an unique nest-building specialization. *Molecular Phylogenetics and Evolution*, 42, 272-286.

NICOL, J. A. C. & ARNOTT, H. J. 1974. Tapeta lucida in eyes of goatsuckers (Caprimulgidae). *Proceedings of the Royal Society of London Series B-Biological Sciences*, 187, 349-352.

NILSSON, D. E. & PELGER, S. 1994. A pessimistic estimate of the time required for an eye to evolve. *Proceedings of the Royal Society of London Series B-Biological Sciences*, 256, 53-58.

NILSSON, D. E. 2005. Photoreceptor evolution: Ancient siblings serve different tasks. *Current Biology*, 15, R94-R96.

NISHIDA, T. 2005. Neutrotrophic mediators and corneal wound healing. *Ocular Surface*, 3, 194-202.

NORBERG, U. M. 1985. Evolution of vertebrate flight - an aerodynamic model for the transition from gliding to active flight. *American Naturalist*, 126, 303-327.

OBERWEGER, K. & GOLLER, F. 2001. The metabolic cost of birdsong production. *J Exp. Biol.* 204 (19): 3379-3388.

ODEEN, A. & HASTAD, O. 2003. Complex distribution of avian color vision systems revealed by sequencing the SWS1 opsin from total DNA. *Molecular Biology and Evolution*, 20, 855-861.

OHNO, H., YONEZAWA, S., ARIMURA, F. & UCHIYAMA, H. 2004. The avian centrifugal visual system and its possible contribution to focal attention. *Brain-Inspired It I*, 1269, 61-64.

OLIPHANT, L. W., JOHNSON, M. R., MURPHY, C. & HOWLAND, H. 1983. The musculature and pupillary response of the great horned owl iris. *Experimental Eye Research*, 37, 583-595.

OLIVIER, F. & WOTHERSPOON, S. J. 2005. GIS-based application of resource selection functions to the prediction of snow petrel distribution and abundance in East Antarctica: Comparing models at multiple scales. *Ecological Modelling*, 189, 105-129.

OLLIVIER, F. J., SAMUELSON, D. A., BROOKS, D. E., LEWIS, P. A., KALLBERG, M. E. & KOMAROMY, A. M. 2004. Comparative morphology of the tapetum lucidum (among selected species). *Veterinary Ophthalmology*, 7, 11-22.

ORO, D., DE LEON, A., MINGUEZ, E. & FURNESS, R. W. 2005. Estimating predation on breeding European storm-petrels (*Hydrobates pelagicus*) by yellow-legged gulls (*Larus Michahellis*). *Journal of Zoology*, 265, 421-429.

OSRAM. 2005. Catalogue of indoor and outdoor lighting 2005/2006: General lighting, electronic control gear. Munchen: OSRAM gmbh.

OWEN, J. C. & MOORE, F. R. 2008. Swainson's thrushes in migratory disposition exhibit reduced immune function. *Journal of Ethology*, 26, 383-388.

PAINÉ, R. T., WOOTTON, J. T. & BOERSMA, P. D. 1990. Direct and indirect effects of peregrine falcon predation on seabird abundance. *Auk*, 107, 1-9.

PARDUE, M. T. & SIVAK, J. G. 1997. The functional anatomy of the ciliary muscle in four avian species. *Brain Behavior and Evolution*, 49, 295-311.

PARKER, A. 2003. *In the blink of an eye*. Free Press, London.

PARTRIDGE, J. C. 1989. The visual ecology of avian cone oil droplets. *Journal of Comparative Physiology a-Sensory Neural and Behavioral Physiology*, 165, 415-426.

PAUL, G. S. 2001. *Dinosaurs of the air: the evolution and loss of flight in dinosaurs and birds*. Johns Hopkins University Press, Baltimore, MD;

PETTIGREW, J. D. & KONISHI, M. 1976. Neurons selective for orientation and binocular disparity in visual wulst of barn owl (*Tyto alba*). *Science*, 193, 675-678.

PETTIGREW, J. D., WALLMAN, J. & WILDSOET, C. F. 1990. Saccadic oscillations facilitate ocular perfusion from the avian pecten. *Nature*, 343, 362-363.

PHILLIPS NH, BERGER RJ. 1991. Regulation of body temperature, metabolic rate and sleep in fasting pigeons diurnally infused with glucose or saline. *J Comp. Physiol. B* 161 (3): 311-318.

POPP, J.W., FICKEN, R.W. & REINARTZ, J.A.,1985. Short-term temporal avoidance of interspecific acoustic interference among forest birds. *Auk* 102: 744-748.

POSADA, D. & BUCKLEY, T. R. 2004. Model selection and model averaging in phylogenetics: Advantages of akaike information criterion and Bayesian approaches over likelihood ratio tests. *Systematic Biology*, 53, 793-808.

PRASAD, B. K. 2003. Post-mortem ocular changes: a study on autopsy cases in Bharatpur Hospital. *Kathmandu Univ Medical Journal*, 1, 276-7.

PRICE, J. J., JOHNSON, K. P. & CLAYTON, D. H. 2004. The evolution of echolocation in swiftlets. *Journal of Avian Biology*, 35, 135-143.

- PRICE, J. J., JOHNSON, K. P., BUSH, S. E. & CLAYTON, D. H. 2005. Phylogenetic relationships of the Papuan Swiftlet *Aerodramus papuensis* and implications for the evolution of avian echolocation. *Ibis*, 147, 790-796.
- QIAN, H., BADGLEY, C. & FOX, D. L. 2009. The latitudinal gradient of beta diversity in relation to climate and topography for mammals in North America. *Global Ecology and Biogeography*, 18, 111-122.
- QUESADA, A., GARCIALOMAS, V. & GENISGALVEZ, J.M. 1986. The midget bipolar cells in the chick retina. *Current Eye Research*, 5, 85-92.
- RABOSKY, D. L. & LOVETTE, I. J. 2008. Density-dependent diversification in North American wood warblers. *Proceedings of the Royal Society B-Biological Sciences*, 275, 2363-2371.
- RAHMAN, M. L., AOYAMA, M. & SUGITA, S. 2007a. Number and density of retinal photoreceptor cells with emphasis on oil droplet distribution in the Mallard Duck (*Anas platyrhynchos* var. Domesticus). *Animal Science Journal*, 78, 639-649.
- RAHMAN, M. L., AOYAMA, M. & SUGITA, S. 2007b. Topography of retinal photoreceptor cells in the Jungle Crow (*Corvus macrorhynchos*) with emphasis on the distribution of oil droplets. *Ornithological Science*, 6, 29-38.
- RAHMAN, M. L., AOYAMA, M. & SUGITA, S. 2008. Ganglion cell density and oil droplet distribution in the retina of brown-eared bulbul (*Hypsipetes amaurotis*). *Anatomical Science International*, 83, 239-246.
- RAMON Y CAJAL, S. 1889. Sur la morphologie et les connexions des elements de la retine des oiseaux. *Anatomischer Anzeiger*, 4, 111-121.

RAO, S. C., SRINIVAS, V. & BALASUBRAMANIAN, D. 1994. Conformational studies on delta-crystallin, the core protein of the bird eye lens. Proceedings of the Indian Academy of Sciences-Chemical Sciences, 106, 1399-1414.

RATTENBORG, N. C., LIMA, S. L. & AMLANER, C. J. 1999. Facultative control of avian unihemispheric sleep under the risk of predation. Behav. Brain Res. 105: 163-172.

RATTENBORG, N. C., MANDT BH, OBERMEYER WH, WINSAUER PJ, HUBER R, WIKELSKI M, BENCA RM. 2004. Migratory sleeplessness in the white-crowned sparrow (*Zonotrichia leucophrys gambelii*). PLOS Biol. 2 (7): 924-936.

RATTENBORG, N. C., OBERMEYER WH, VACHA E, BENCA RM. 2005. Acute effects of light and darkness on sleep in the pigeon (*Columba livia*). Physiol. Behav. 84: 635-640.

RAYER, B., NAYNERT, M. & STIEVE. H. 1990. Phototransduction - different mechanisms in vertebrates and invertebrates. Journal of Photochemistry and Photobiology B-Biology, 7, 107-148.

RECHTSCHAFFEN, A., BERGMANN, B. M., EVERSON, C. A., KUSHIDA, C. A. & GILLILAND, M. A. 1989. Sleep deprivation in the rat: X, integration and discussion of the findings. Sleep 12 (1): 68-87.

REDFERN, C. & CLARK, J. 2001. Ringers' Manual. British Trust for Ornithology, Thetford.

REEVE, J. & ABOUHEIF, E., 2003. Phylogenetic independence. Department of Biology, McGill University.

REID, M. L. 1987. Costliness and reliability in the singing vigor of ipswich sparrows. Animal Behaviour, 35, 1735-1743.

REINER, A., BRECHA, N. & KARTEN, H. J. 1979. Specific projection of retinal displaced ganglion-cells to the nucleus of the basal optic root in the chicken. *Neuroscience*, 4, 1679-1688.

REISS, G. R., WERNESS, P. G., ZOLLMAN, P. E. & BRUBAKER, R. F. 1986. Ascorbic-acid levels in the aqueous-humor of nocturnal and diurnal mammals. *Archives of Ophthalmology*, 104, 753-755.

REPERANT, J., MEDINA, M., WARD, R., MICELI, D., KENIGFEST, N. B., RIO, J. P. & VESSELKIN, N. P. 2007. The evolution of the centrifugal visual system of vertebrates. A cladistic analysis and new hypotheses. *Brain Research Reviews*, 53, 161-197.

REPERANT, J., WARD, R., MICELI, D., RIO, J. P., MEDINA, M., KENIGFEST, N. B. & VESSELKIN, N. P. 2006. The centrifugal visual system of vertebrates: A comparative analysis of its functional anatomical organization. *Brain Research Reviews*, 52, 1-57.

REYMOND, L. 1985. Spatial visual-acuity of the eagle *Aquila-audax* - a behavioral, optical and anatomical investigation. *Vision Research*. 25, 1477-1491.

RICH, C. & LONGCORE, T. 2006. Ecological consequences of artificial night lighting, Island, Washington, D.C.

RICKWOOD, K. 2001. Lighting up Colchester. Lessenden, Colchester.

RINGVOLD, A., ANDERSSEN, E. & KJONNIKSEN, I. 2000. UV absorption by uric acid in diurnal bird aqueous humor. *Investigative Ophthalmology & Visual Science*, 41, 2067-2069.

RINGVOLD, A., ANDERSSEN, E., JELLUM, E., BJERKAS, E., SONERUD, G. A., HAALAND, P. J., DEVOR, T. P. & KJONNIKSEN, I. 2003. UV-absorbing compounds in the aqueous humor from aquatic mammals and various non-mammalian vertebrates. *Ophthalmic Research*, 35, 208-216.

ROCHON-DUVIGNEAUD, A. 1943. Les yeux et la vision des vertebres, Paris, Masson.

RODGERS, C. T. & HORE, P. J. 2009. Chemical magnetoreception in birds: The radical pair mechanism. *Proceedings of the National Academy of Sciences of the United States of America*, 106, 353-360.

RODRIGUEZ, A. & RODRIGUEZ, B. 2009. Attraction of petrels to artificial lights in the Canary Islands: effects of the moon phase and age class. *Ibis*, 151, 299-310.

ROGERS, L. 1996. Behavioral, structural and neurochemical asymmetries in the avian brain: A model system for studying visual development and processing. *Neuroscience and Biobehavioral Reviews*, 20, 487-503.

ROLLIN, 1953. Dataset, In: ARMSTRONG E. A. A study of bird song, 1963.. Oxford University Press, Oxford.

ROJAS, L. M., MCNEIL, R., CABANA, T. & LACHAPELLE, P. 1999. Behavioral, morphological and physiological correlates of diurnal and nocturnal vision in selected wading bird species. *Brain Behavior and Evolution*, 53, 227-242.

ROMAGNANO, A., SHIROMA, J. T., HEARD, D. J., JOHNSON, R. D., SCHIERING, M. R. & MLADINICH, C. R. J. 1996. Magnetic resonance imaging of the brain and coelomic cavity of the domestic pigeon (*Columba livia domestica*). *Veterinary Radiology & Ultrasound*, 37, 431-440.

ROTH, L. S. V., LUNDSTROM, L., KELBER, A., KROGER, R. H. H. & UNSBO, P. 2009. The pupils and optical systems of gecko eyes. *Journal of Vision*, 9 (3), 27.1-11.

ROTH, T. C., COX, J. G. & LIMA, S. L. 2008. Can foraging birds assess predation risk by scent? *Animal Behaviour*, 76, 2021-2027.

ROTH, T. C., LESKU, J. A., AMLANER, C. J. & LIMA, S. L. 2006. A phylogenetic analysis of the correlates of sleep in birds. *J. Sleep Res.* 15: 395-402

ROTH, T. C., SPRAU, P., SCHMIDT, R., NAGUIB, M. & AMRHEIN, V. 2009. Sex-specific timing of mate searching and territory prospecting in the nightingale: nocturnal life of females. *Proceedings of the Royal Society B-Biological Sciences*, 276, 2045-2050.

RUCKER, F. J. & WALLMAN, J. 2008. Cone signals for spectacle-lens compensation: Differential responses to short and long wavelengths. *Vision Research*, 48, 1980-1991.

SAMPALEANU, L. M., DAVIDSON, A. R., GRAHAM, C., WISTOW, G. J. & HOWELL, P. L. 1999. Domain exchange experiments in duck delta-crystallins: Functional and evolutionary implications. *Protein Science*, 8, 529-537.

SARKAR, D., 2008. *Lattice: Multivariate Data Visualization with R*. Springer

SATO, A., TICHY, H., O'HUIGIN, C., GRANT, P. R., GRANT, B. R. & KLEIN, J. 2001. On the origin of Darwin's finches. *Molecular Biology and Evolution*, 18, 299-311.

SCHAEFER, H. M., MCGRAW, K. & CATONI, C. 2008. Birds use fruit colour as honest signal of dietary antioxidant rewards. *Functional Ecology*, 22, 303-310.

SCHEER, 1950 Dataset, In: ARMSTRONG E. A. *A study of bird song, 1963*.. Oxford University Press, Oxford.

SCHMALJOHANN, H., BRUDERER, B. & LIECHTI, F. 2008. Sustained bird flights occur at temperatures far beyond expected limits. *Animal Behaviour*, 76, 1133-1138.

SCHMALJOHANN, H., LIECHTI, F. & BRUDERER, B. 2007. Songbird migration across the Sahara: the non-stop hypothesis rejected! *Proceedings of the Royal Society B-Biological Sciences*, 274, 735-739.

SCHMID, V. 2006. Imaging of the eye and orbit. In: MANNION, P. (ed.) *Diagnostic ultrasound in small animal practice*. 2 ed. Blackwell, Oxford.

SCHMIDT, A. & BISCHOF, H. J. 2001. Integration of information from both eyes by single neurons of nucleus rotundus, ectostriatum and lateral neostriatum in the zebra finch (*Taeniopygia guttata castanotis* Gould). *Brain Research*, 923, 20-31.

SCHMIDT-NIELSEN, K. 1984. *Scaling: Why is animal size so important?* Cambridge University Press, Cambridge.

SCHMITZ, L. & MOTANI, R. 2007. Diel activity pattern of *Archaeopteryx*. *Journal of Vertebrate Paleontology*, 27, 142A-142A.

SCHRAERMEYER, U. & HEIMANN, K. 1999. Current understanding on the role of retinal pigment epithelium and its pigmentation. *Pigment Cell Research*, 12, 219-236.

SCHROEDL, F., DE STEFANO, M. E., REESE, S., BREHMER, A. & NEUHUBER, W. L. 2004. Comparative anatomy of nitrenergic intrinsic choroidal neurons (ICN) in various avian species. *Experimental Eye Research*, 78, 187-196.

SEAMAN, A. R. & STORM, H. K. 1965. Electron microscope observations on hyalocytes of vitreous body in domestic fowl (*Gallus domesticus*). *Experimental Eye Research*, 4, 13-17.

SEDDON, N. 2005. Ecological adaptation and species recognition drives vocal evolution in neotropical suboscine birds. *Evolution*, 59, 200-215.

SILLMAN, A. 1969. The visual pigments of several species of birds. *Vision Res*, 9, 1063-77.

SIMONS, T. R. 1985. Biology and behavior of the endangered Hawaiian dark-rumped petrel. *Condor*, 87, 229-245.

SIVAK, J. 2004. Through the lens clearly: phylogeny and development: the Proctor lecture. *Invest Ophthalmol Vis Sci*, 45, 740-7; 739.

SIVAK, J. G. & MANDELMAN, T. 1982. Chromatic dispersion of the ocular media. *Vision Research*, 22, 997-1003.

SIVAK, J. G. & MILLODOT, M. 1977. Optical performance of penguin eye in air and water. *Journal of Comparative Physiology*, 119, 241-247.

SIVAK, J. G., BOBIER, W. R. & LEVY, B. 1978. Refractive significance of nictitating-membrane of bird eye. *Journal of Comparative Physiology*, 125, 335-339.

SIVAK, J. G., HILDEBRAND, T. & LEBERT, C. 1985. Magnitude and rate of accommodation in diving and nondiving birds. *Vision Research*, 25, 925-933.

SIVAK, J. G., HOWLAND, H. C. & MCGILLHARELSTAD, P. 1987. Vision of the Humboldt penguin (*Spheniscus humboldti*) in air and water. *Proceedings of the Royal Society of London Series B-Biological Sciences*, 229, 467-472.

SLABBEKOORN, H. & PEET, M. 2003. Ecology: Birds sing at a higher pitch in urban noise - Great tits hit the high notes to ensure that their mating calls are heard above the city's din. *Nature*, 424, 267-267.

SLABBEKOORN, H. & SMITH, T. B. 2002. Habitat-dependent song divergence in the little greenbul: An analysis of environmental selection pressures on acoustic signals. *Evolution*, 56, 1849-1858.

SLATER, P. J. B. & MANN, N. I. 2004. Why do the females of many bird species sing in the tropics? *Journal of Avian Biology*, 35, 289-294.

SLONAKER, J. R. 1918. A physiological study of the anatomy of the eye and its accessory parts of the English sparrow (*Passer domesticus*). *Journal of Morphology*, 31, 351-459.

SMITH, K. A., SCHOEN, M. W. & CZEISLER, C. A. 2004. Adaptation of human pineal melatonin suppression by recent photic history. *J Clin. Endocrin. Metab.* 89 (7): 3610-3614.

SMITH, B. J., SMITH, S. A. & BRAEKEVELT, C. R. 1996. Fine structure of the pecten oculi of the barred owl (*Strix varia*). *Histology and Histopathology*, 11, 89-96.

SÖDERSTRÖM, B. 1999. Artificial nest predation rates in tropical and temperate forests: a review of the effects of edge and nest site. *Ecography*, 22 (4), 455-463.

SOLOV'YOV, I. A. & GREINER, W. 2009. Iron-mineral-based magnetoreceptor in birds: polarity or inclination compass? *European Physical Journal D*, 51, 161-172.

STAFFORD, M. 2001. Histology and biology of the lens. *Optometry Today*.

STAIKER, C. A., SPECTOR, D. A., HORN, A. G. 1996. The dawn chorus and other diel patterns in acoustic signalling. In: Kroodsma DE, Miller EH, editors. *Ecology and evolution of acoustic communication in birds*. Cornell University Press, Ithaca, 426-453

STAPPUT, K., THALAU, P., WILTSCHKO, R. & WILTSCHKO, W. 2008. Orientation of birds in total darkness. *Current Biology*, 18, 602-606.

STARK, L., CAMPBELL, F. W. & ATWOOD, J. 1958. Pupil unrest - example of noise in a biological servomechanism. *Nature*, 182, 857-858.

STAUBER, E., HOLMES, S., DEGNETTO, D. L. & FINCH, N. 2007. Magnetic resonance imaging is superior to radiography in evaluating spinal cord trauma in three bald eagles (*Haliaeetus leucocephalus*). *Journal of Avian Medicine and Surgery*, 21, 196-200.

STEIGER, S. S., FIDLER, A. E., VALCU, M. & KEMPENAERS, B. 2008. Avian olfactory receptor gene repertoires: evidence for a well-developed sense of smell in birds? *Proceedings of the Royal Society B-Biological Sciences*, 275, 2309-2317.

STONE, J. 1981. *The whole mount handbook: a guide to the preparation and analysis of retinal whole mounts*. Maitland Publications, Sydney.

STRAZNICKY, C. & CHEHADE, M. 1987. The formation of the area centralis of the retinal ganglion-cell layer in the chick. *Development*, 100, 411-420.

STURMBAUER, C., BERGER, B., DALLINGER, R. & FOGER, M. 1998. Mitochondrial phylogeny of the genus *Regulus* and implications on the evolution of breeding behavior in Sylvioid songbirds. *Molecular Phylogenetics and Evolution*, 10, 144-149.

SUBURO, A. M. & SCOLARO, J. A. 1990. The eye of the magellanic penguin (*Spheniscus magellanicus*) - structure of the anterior segment. *American Journal of Anatomy*, 189, 245-252.

SUBURO, A. M., HERRERO, M. V. & SCOLARO, J. A. 1991. Regionalization of the ganglion-cell layer in the retina of the magellanic penguin (*Spheniscus magellanicus*). *Colonial Waterbirds*, 14, 17-24.

SULLIVAN, B. K. & LEEK, M. R. 1986. Acoustic communication in woodhouses toad (*Bufo woodhousei*) .1. Response of calling males to variation in spectral and temporal components of advertisement calls. *Behaviour*, 98, 305-319.

- SUTHERS, R. A. & WALLIS, N. E. 1970. Optics of eyes of echolocating bats. *Vision Research*, 10, 1165-1173.
- TANSLEY, K. & ERICHSEN, J. T. 1985. Vision. In: CAMPBELL, B. & LACK, E. (eds.) *A Dictionary of Birds*. Poyser, Berkamsted.
- TARRES, M. A. G., BARON, M. & GALLEGO, A. 1986. The horizontal cells in the retina of the owl, *Tyto alba*, and owllet, *Carinae noctua*. *Experimental Eye Research*, 42, 315-321.
- TEMPLETON, J. J. & CHRISTENSEN-DYKEMA, J. M. 2008. A behavioral analysis of prey detection lateralization and unilateral transfer in European starlings (*Sturnus vulgaris*). *Behavioural Processes*, 79, 125-131.
- TEMPLETON, J. J. & GONZALEZ, D. P. 2004. Reverse lateralization of visual discriminative abilities in the European starling. *Animal Behaviour*, 67, 783-788.
- TERBORGH, J., ROBINSON, S. K., PARKER, T. A., MUNN, C. A. & PIERPONT, N. 1990. Structure and organization of an amazonian forest bird community. *Ecological Monographs*, 60, 213-238.
- TESSMAR-RAIBLE, K., JEKELY, G., GUY, K., RAIBLE, F., WITTBRODT, J. & ARENDT, D. 2005. Ancestry of photic and mechanic sensation? Response. *Science*, 308, 1114-1114.
- THOMAS, C. I. 1955. *The Cornea*, C C Thomas.
- THOMAS, R. J., 1997. Functions of daily signing routines in birds. Unpublished D.Phil. thesis, University of Sussex.
- THOMAS, R. J. 1999a. Two tests of a stochastic dynamic programming model of daily singing routines in birds. *Anim. Behav.* 57: 277-284.

THOMAS, R. J. 1999b. The effect of variability in the food supply on the daily singing routines of European robins: a test of a stochastic dynamic programming model. *Animal Behaviour*, 57, 365-369.

THOMAS, R. J. 2000. Strategic diel regulation of body mass in European robins. *Animal Behaviour*, 59, 787-791.

THOMAS, R. J. 2002. The costs of singing in nightingales. *Animal Behaviour*, 63, 959-966.

THOMAS, R. J. & CUTHILL, I. C. 2002. Body mass regulation and the daily singing routines of European robins. *Animal Behaviour*, 63, 285-292.

THOMAS, R. J., CUTHILL, I. C., GOLDSMITH, A. R., COSGROVE, D. F., LIDGATE, H. C. & PROCTOR, S. L. B. 2003. The trade-off between singing and mass gain in a daytime-singing bird, the European robin. *Behaviour*, 140, 387-404.

THOMAS, R. J., KELLY, D. J. & GOODSHIP, N. M. 2004. Eye design in birds and visual constraints on behavior. *Ornitologia Neotropical*, 15, 243-250.

THOMAS, R. J., MEDEIROS, R. & POLLARD, A. 2006. Evidence for intertidal foraging by European Storm Petrels *Hydrobates pelagicus* during migration. *Atlantic Seabirds*, 8, 87-94.

THOMAS, R. J., SZEKELY, T., CUTHILL, I. C., HARPER, D. G. C., NEWSON, S. E., FRAYLING, T. D. & WALLIS, P. D. 2002. Eye size in birds and the timing of song at dawn. *Proceedings of the Royal Society of London Series B-Biological Sciences*, 269, 831-837.

THOMAS, R. J., SZEKELY, T., POWELL, R. F. & CUTHILL, I. C. 2006b. Eye size, foraging methods and the timing of foraging in shorebirds. *Functional Ecology*, 20, 157-165.

THOMASSEN, H. A., GEA, S., MAAS, S., BOUT, R. G., DIRCKX, J. J. J., DECRAEMER, W. F. & POVEL, G. D. E. 2007. Do Swiftlets have an ear for echolocation? The functional morphology of Swiftlets' middle ears. *Hearing Research*, 225, 25-37.

THUMANN, A. & MEHTA, D. P. 2001. *Handbook of energy engineering*. Fairmont Press, Prentice-Hall, London.

TIELEMAN, B. I., DIJKSTRA, T. H., LASKY, J. R., MAUCK, R. A., VISSER, G. H. & WILLIAMS JB. 2006. Physiological and behavioural correlates of life-history variation: a comparison between tropical and temperate zone house wrens. *Func. Ecol.* 20 (3): 491-499.

TINBERGEN, J. M. 1981. Foraging decisions in starlings (*Sturnus-vulgaris*). *Ardea*, 69, 1-67.

TOMBS, S. & SILVERMAN, I. 2004. Pupillometry - A sexual selection approach. *Evolution and Human Behavior*, 25, 221-228.

TRELSTAD, R. L. & KANG, A. H. 1974. Collagen heterogeneity in avian eye - lens, vitreous body, cornea and sclera. *Experimental Eye Research*, 18, 395-406.

UCHIYAMA, H. & STELL, W. K. 2005. Association amacrine cells of Ramon y Cajal: Rediscovery and reinterpretation. *Visual Neuroscience*, 22, 881-891.

VAN MEIR, V., PAVLOVA, D., VERHOYE, M., PINXTEN, R., BALTHAZART, J., EENS, M. & VAN DER LINDEN, A. 2006. In vivo MR imaging of the seasonal volumetric and functional plasticity of song control nuclei in relation to song output in a female songbird. *Neuroimage*, 31, 981-992.

VARELA, F., PALACIOS, A. & GOLDSMITH, T. 1993. Color vision of Birds. In: BISCHOFF, H. (ed.) *Bird Vision and Cognition*. MIT Press, Cambridge.

VENABLES, W. N. & RIPLEY, B. D., 2002. Modern Applied Statistics with S. Fourth Edition. Springer, New York.

VERKMAN, A. S. 2003. Role of aquaporin water channels in eye function. *Experimental Eye Research*, 76, 137-143.

VOELKER, G. & SPELLMAN, G. M. 2004. Nuclear and mitochondrial DNA evidence of polyphyly in the avian superfamily Muscicapidae. *Molecular Phylogenetics and Evolution*, 30, 386-394.

VOELKER, G., ROHWER, S., BOWIE, R. C. K. & OUTLAW, D. C. 2007. Molecular systematics of a speciose, cosmopolitan songbird genus: Defining the limits of, and relationships among, the *Turdus* thrushes. *Molecular Phylogenetics and Evolution*, 42, 422-434.

VOSS, J. & BISCHOF, H. J. 2003. Regulation of ipsilateral visual information within the tectofugal visual system in zebra finches. *Journal of Comparative Physiology a-Neuroethology Sensory Neural and Behavioral Physiology*, 189, 545-553.

VOTIER, S. C., CRANE, J. E., BEARHOP, S., DE LEON, A., MCSORLEY, C. A., MINGUEZ, E., MITCHELL, I. P., PARSONS, M., PHILLIPS, R. A. & FURNESS, R. W. 2006. Nocturnal foraging by great skuas *Stercorarius skua*: implications for conservation of storm-petrel populations. *Journal of Ornithology*, 147, 405-413.

WALLMAN, J., WILDSOET, C., XU, A. M., GOTTLIEB, M. D., NICKLA, D. L., MARRAN, L., KREBS, W. & CHRISTENSEN, A. M. 1995. Moving the retina - choroidal modulation of refractive state. *Vision Research*, 35, 37-50.

WALLRAFF, H. G. 2004. Avian olfactory navigation: its empirical foundation and conceptual state. *Animal Behaviour*, 67, 189-204.

WALLRAFF, H. G., KIEPENHEUER, J., NEUMANN, M. F. & STRENG, A. 1995. Homing experiments with starlings deprived of the sense of smell. *Condor*, 97, 20-26.

WALLS, G. 1967. The vertebrate eye and its adaptive radiation. Hafner, New York.

WANLESS, S., FINNEY, S. K., HARRIS, M. P. & MCCAFFERTY, D. J. 1999. Effect of the diel light cycle on the diving behaviour of two bottom feeding marine birds: the blue-eyed shag *Phalacrocorax atriceps* and the European shag *P. aristotelis*. *Marine Ecology-Progress Series*, 188, 219-224.

WARD, S. & SLATER, P. J. B. 2005a. Heat transfer and the energetic cost of singing by canaries *Serinus canaria*. *Journal of Comparative Physiology A-Neuroethology Sensory Neural and Behavioral Physiology*, 191, 953-964.

WARD, S. & SLATER, P. J. B. 2005b. Raised thermoregulatory costs at exposed song posts increase the energetic cost of singing for willow warblers *Phylloscopus trochilus*. *Journal of Avian Biology*, 36, 280-286.

WARD, S., SPEAKMAN, J. R. & SLATER, P. J. B. 2003. The energy cost of song in the canary, *Serinus canaria*. *Anim. Behav.* 66 (5): 893-902.

WARD, S., LAMPE, H. M. & SLATER, P. J. B. 2004. Singing is not energetically demanding for pied flycatchers, *Ficedula hypoleuca*. *Behavioral Ecology*, 15, 477-484.

WARNES G. R., BOLKER, B & LUMLEY, T., 2009. gplots: Various R programming tools for plotting data includes R source code and/or documentation. R package version 2.6.0.

WARRANT, E. J. & NILSSON, D. E. 1998. Absorption of white light in photoreceptors. *Vision Research*, 38, 195-207.

WARREN, P. S., KATTI, M., ERMANN, M. & BRAZEL, A. 2006. Urban bioacoustics: it's not just noise. *Anim. Behav.* 71 (3): 491-502.

WATANUKI, Y. 1986. Moonlight avoidance-behavior in leach storm-petrels as a defense against slaty-backed gulls. *Auk*, 103, 14-22.

WEIDNER, C., REPERANT, J., MICELI, D., HABY, M. & RIO, J. P. 1985. An anatomical study of ipsilateral retinal projections in the quail using autoradiographic, horseradish-peroxidase, fluorescence and degeneration techniques. *Brain Research*, 340, 99-108.

WILKIE, S. E., VISSERS, P., DAS, D., DEGRIP, W. J., BOWMAKER, J. K. & HUNT, D. M. 1998. The molecular basis for UV vision in birds: spectral characteristics, cdna sequence and retinal localization of the UV-sensitive visual pigment of the budgerigar (*Melopsittacus undulatus*). *Biochemical Journal*, 330, 541-547.

WILLEKENS, B. & VRENSEN, G. 1985. Lens fiber organization in 4 avian species - a scanning electron-microscopic study. *Tissue & Cell*, 17, 359-377.

WILTSCHKO, W. & WILTSCHKO, R. 2002. Magnetic compass orientation in birds and its physiological basis. *Naturwissenschaften*, 89, 445-452.

WIRTSCHAFTER, J., BERMAN, E. & MCDONALD, C. 1992. *Magnetic Resonance Imaging and Computed Tomography*, San Francisco, American Academy of Ophthalmology.

WISTOW, G. J. & PIATIGORSKY, J. 1988. Lens crystallins - the evolution and expression of proteins for a highly specialized tissue. *Annual Review of Biochemistry*, 57, 479-504.

WITMER, L. M., CHATTERJEE, S., FRANZOSA, J. & ROWE, T. 2003. Neuroanatomy of flying reptiles and implications for flight, posture and behaviour. *Nature*, 425, 950-953.

WOOD, J. R., RAWLENCE, N. J., ROGERS, G. M., AUSTIN, J. J., WORTHY, T. H. & COOPER, A. 2008. Coprolite deposits reveal the diet and ecology of the extinct New Zealand megaherbivore moa (Aves, Dinornithiformes). *Quaternary Science Reviews*, 27 (27-28), 2593-2602,

WOOD, S.N., 2003. Thin-plate regression splines. *Journal of the Royal Statistical Society (B)* 65 (1): 95-114.

WOOD, S.N., 2006. *Generalized Additive Models: An Introduction with R*. Chapman and Hall/CRC Press, UK.

WOODS, C. Year. Corneal ulceration. In: Conference on Veterinary Ophthalmology, Nov 29-30 2003 Dublin, IRELAND. *Veterinary Ireland*, 285-289.

WORTHY, T. H. 2007. Moas and phylogenomics: How nomenclatural errors do a disservice to the understanding of moa taxonomy. *Auk*, 124 (4), 1447-1449.

WRIGHT, H. W., 1912. Morning awakening and even-song. *Auk* 29: 150-160.

WRIGHT, H. W., 1913. Morning awakening and even-song. *Auk* 30: 512-537.

WRIGHT, M. W. & BOWMAKER, J. K. 2001. Retinal photoreceptors of paleognathous birds: the ostrich (*Struthio camelus*) and rhea (*Rhea americana*). *Vision Research*, 41, 1-12.

WYLIE, D. R. & FROST, B. J. 1990. Binocular neurons in the nucleus of the basal optic root (nbor) of the pigeon are selective for either translational or rotational visual flow. *Visual Neuroscience*, 5, 489-495.

WYLIE, D. R. & FROST, B. J. 1999. Responses of neurons in the nucleus of the basal optic root to translational and rotational flowfields. *Journal of Neurophysiology*, 81, 267-276.

YAU, K. W. 1994. Phototransduction mechanism in retinal rods and cones - the Friedenwald lecture. *Investigative Ophthalmology & Visual Science*, 35, 9-32.

YU, C. Q., SCHWAB, I. R. & DUBIELZIG, R. R. 2009. Feeding the vertebrate retina from the Cambrian to the Tertiary. *Journal of Zoology*, 278, 259-269.

ZALA, S. M. & PENN, D. J. 2004. Abnormal behaviours induced by chemical pollution: a review of the evidence and new challenges. *Animal Behaviour*, 68, 649-664.

ZAMMUTO, R. M. & JAMES, D. 1982. Relationships of environmental factors to onset of autumn morning vocalizations in an Ozark community USA. *Wilson Bulletin*, 94, 74-79.

ZEISS, C. J. & DUBIELZIG, R. R. 2006. Lentoid bodies in the avian retina. *Journal of Comparative Pathology*, 135, 243-248.

ZUSI, R. L. & BRIDGE, D. 1981. On the slit pupil of the black skimmer (*Rynchops niger*). *Journal of Field Ornithology*, 52, 338-340.

Appendices

Appendix A 1.1. Estimates of retinal image brightness (RIB) from the non-invasive photographic method. N = number of individuals per species.

Common name	Latin name	Focal length, mm	Pupil diameter, mm	RIB estimate	N
Oriental great reed warbler	<i>Acrocephalus arundinaceus</i>	4.712	2.545	0.292	1
Sedge warbler	<i>Acrocephalus schoenobaenus</i>	3.352	2.107	0.396	2
Reed warbler	<i>Acrocephalus scirpaceus</i>	3.641	2.137	0.349	3
Common sandpiper	<i>Actitis hypoleucos</i>	4.860	3.808	0.614	1
Kingfisher	<i>Alcedo atthis</i>	5.162	3.308	0.411	1
Nicobar pigeon	<i>Caloenas nicobarica</i>	7.859	6.086	0.606	3
Red necked nightjar	<i>Caprimulgus ruficollis</i>	10.601	9.325	0.772	2

Goldfinch	<i>Carduelis carduelis</i>	3.584	1.888	0.278	1
Greenfinch	<i>Carduelis chloris</i>	4.845	2.497	0.266	1
Short toed treecreeper	<i>Certhia brachydactyla</i>	2.956	1.956	0.438	1
Cettis warbler	<i>Cettia cetti</i>	3.655	2.493	0.465	2
Pigeon	<i>Columba livia</i>	7.371	4.701	0.420	17
Mauritius pink pigeon	<i>Columba mayeri</i>	6.728	4.641	0.476	1
Raven	<i>Corvus corax</i>	15.312	5.828	0.145	1
Jackdaw	<i>Corvus monedula</i>	8.475	4.594	0.294	1
Barefaced curassow	<i>Crax fasciolata</i>	11.790	9.111	0.597	1
Azure winged magpie	<i>Cyanopica cyana</i>	6.889	3.597	0.273	1
Lesser spotted woodpecker	<i>Dendrocopos minor</i>	4.703	2.384	0.257	1
Graysided flowerpecker	<i>Dicaeum celebicum</i>	3.284	2.932	0.797	1
Pied imperial	<i>Ducula bicolor</i>	7.909	4.942	0.399	2

Reed Bunting	<i>Emberiza schoeniclus</i>	3.981	2.214	0.310	2
European robin	<i>Erithacus rubecula</i>	4.577	3.105	0.463	3
Common waxbill	<i>Estrilda astrild</i>	3.071	1.553	0.256	1
GreatEared Nightjar	<i>Eurostopodus macrotis</i>	10.877	11.390	1.097	1
Pied Flycatcher	<i>Ficedula hypoleuca</i>	4.527	2.927	0.418	3
Chaffinch	<i>Fringella coelebs</i>	4.465	2.153	0.232	1
Blackthroated laughing thrush	<i>Garrulax chinensis</i>	7.008	4.692	0.450	2
Victoria Crown Pigeon	<i>Goura victoria</i>	11.422	9.197	0.648	1
Barn swallow	<i>Hirundo rustica</i>	5.483	3.147	0.330	1
European storm petrel	<i>Hydrobates pelagicus</i>	5.495	2.787	0.257	2
Little Bittern	<i>Ixobrychus minutus</i>	5.391	4.604	0.729	1
Herring gull	<i>Larus argentatus</i>	11.515	5.217	0.205	1
Grasshopper warbler	<i>Locustella naevia</i>	3.377	2.306	0.468	2

Nightingale	<i>Luscinia megarhynchos</i>	4.483	2.997	0.454	2
Red Breasted Merganser	<i>Mergus serrator</i>	8.410	4.219	0.252	1
Red kite	<i>Milvus milvus</i>	12.433	6.536	0.276	1
Blue-crowned motmot	<i>Momotus momota</i>	7.861	5.832	0.550	1
Island monarch	<i>Monarcha cinerascens</i>	5.258	2.888	0.302	1
Olive-backed sunbird	<i>Nectarina jugularis</i>	3.394	2.216	0.432	3
Black-naped oriole	<i>Oriolus chinensis</i>	73.360	41.067	0.318	2
Coal tit	<i>Parus ater</i>	3.383	2.292	0.459	1
Blue tit	<i>Parus caeruleus</i>	3.579	2.298	0.412	4
Great tit	<i>Parus major</i>	4.378	2.609	0.356	3
Marsh tit	<i>Parus palustris</i>	3.865	2.168	0.315	1
House Sparrow	<i>Passer domesticus</i>	4.399	2.457	0.312	2
Cormorant	<i>Phalacrocorax carbo</i>	10.087	4.758	0.225	4
Redstart	<i>Phoenicurus phoenicurus</i>	4.348	2.816	0.420	1

Chiffchaff	<i>Phylloscopus collybita</i>	3.136	2.003	0.408	2
Magpie	<i>Pica pica</i>	8.951	4.414	0.251	2
Palawan peacock-pheasant	<i>Polyplectron emphanum</i>	8.194	5.342	0.427	2
Black-naped fruit dove	<i>Ptilinopus melanospila</i>	59.067	36.829	0.389	1
Manx shearwater	<i>Puffinus puffinus</i>	8.571	4.309	0.256	9
Rouloul	<i>Rollulus rouloul</i>	6.378	5.491	0.746	2
Pied chat	<i>Saxicola caprata</i>	4.631	2.909	0.395	1
Serin	<i>Serinus serinus</i>	3.156	1.638	0.269	1
Nuthatch	<i>Sitta europaea</i>	4.459	2.804	0.395	1
Collared dove	<i>Streptopelia decaocto</i>	6.404	4.433	0.479	1
Jerdon's starling	<i>Sturnus burmannicus</i>	5.822	3.787	0.423	1
Blackcollared starling	<i>Sturnus nigricollis</i>	6.938	4.109	0.352	3
Blackcap	<i>Sylvia atricapilla</i>	4.293	3.130	0.531	2
Sardinian warbler	<i>Sylvia melanocephala</i>	3.944	2.511	0.408	2

Zebra finch	<i>Taeniopygia guttata</i>	3.363	2.001	0.355	2
Collared kingfisher	<i>Todirhamphus chloris</i>	7.022	4.456	0.403	1
Wren	<i>Troglodytes troglodytes</i>	3.387	2.249	0.446	3
Blackbird	<i>Turdus merula</i>	6.802	5.200	0.584	1
Hoopoe	<i>Upupa epops</i>	6.477	3.175	0.241	2
Lemon bellied white eye	<i>Zosterops chloris</i>	3.468	1.927	0.316	3
Wangi wangi white eye	<i>Zosterops sp</i>	3.948	2.301	0.340	1

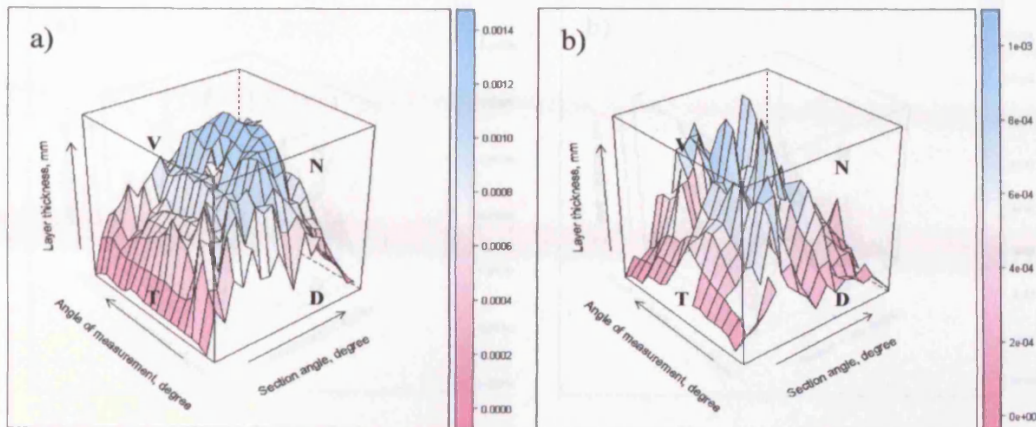
Appendix A 1.2 The angles of convergences used in refining the calculation for RJB estimates. Angles of convergence were averaged for both eyes where available. The angle of convergence was obtained from either skull or MRI datasets. Continued overleaf.

Common name	Latin name	Body mass, g	Angle of convergence, degree	From MRI or skull?	Septum, mm
Sedge warbler	<i>Acrocephalus schoenobaenus</i>	13.5	72.11	MRI	1.381
Reed warbler	<i>Acrocephalus scirpaceus</i>	11.3	61.26	Skull	*
Common sandpiper	<i>Actitis hypoleucos</i>	48.0	65.98	Skull	*
Kingfisher	<i>Alcedo atthis</i>	33.0	77.95	Skull	*
Goldfinch	<i>Carduelis carduelis</i>	13.3	62.38	Skull	*
Greenfinch	<i>Carduelis chloris</i>	24.2	68.08	Skull	*
Siskin	<i>Carduelis spinus</i>	15.0	57.14	MRI	1.283
Cetti's warbler	<i>Cettia cetti</i>	11.8	62.92	Skull	*
Blue tit	<i>Cyanistes caeruleus</i>	10.7	55.27	Skull	*

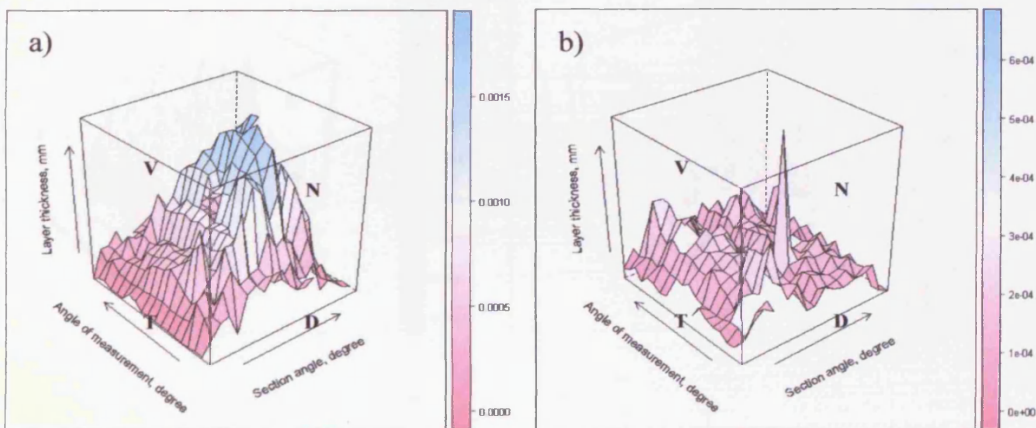
Azure-winged magpie	<i>Cyanopica cyana</i>	61.0	59.78	Skull	*
House martin	<i>Delichon urbica</i>	14.5	67.40	MRI	0.877
Reed bunting	<i>Emberiza schoeniclus</i>	19.8	62.55	Skull	*
European robin	<i>Erithacus rubecula</i>	19.5	68.33	MRI	0.904
Common waxbill	<i>Estrilda astrild</i>	8.7	61.92	Skull	*
Pied flycatcher	<i>Ficedula hypoleuca</i>	13.1	66.44	Skull	*
Chaffinch	<i>Fringilla coelebs</i>	17.5	69.77	MRI	2.000
Snipe	<i>Gallinago gallinago</i>	105.0	83.30	MRI	2.876
Barn swallow	<i>Hirundo rustica</i>	18.3	65.83	MRI	2.048
European storm petrel	<i>Hydrobates pelagicus</i>	25.2	72.23	MRI	4.800
Little bittern	<i>Ixobrychus minutus</i>	148.0	82.69	Skull	*
Grasshopper warbler	<i>Locustella naevia</i>	13.9	67.49	MRI	1.370
Nightingale	<i>Luscinia megarhynchos</i>	20.6	63.17	Skull	*
Red breasted merganser	<i>Mergus serrator</i>	1100.0	53.51	Skull	*

Leach's storm petrel	<i>Oceanodroma leucorhoa</i>	41.4	*	MRI	5.603
Great tit	<i>Parus major</i>	18.5	64.72	Skull *	
Marsh tit	<i>Parus palustris</i>	10.6	57.06	Skull *	
House sparrow	<i>Passer domesticus</i>	28.2	65.85	Skull *	
Common redstart	<i>Phoenicurus phoenicurus</i>	14.7	67.58	Skull *	
Chiffchaff	<i>Phylloscopus collybita</i>	7.1	58.72	Skull *	
Willow warbler	<i>Phylloscopus trochilus</i>	8.5	66.65	MRI	0.759
Manx shearwater	<i>Puffinus puffinus</i>	450.0	79.03	MRI	4.265
Kittiwake	<i>Rissa tridactyla</i>	410.0	69.47	MRI	4.844
Serim	<i>Serinus serinus</i>	11.2	67.55	Skull *	
Starling	<i>Sturnus vulgaris</i>	80.0	67.52	MRI	3.513
Blackcap	<i>Sylvia atricapilla</i>	17.5	71.56	MRI	1.724
Whitethroat	<i>Sylvia communis</i>	14.6	65.21	MRI	1.241
Sardinian warbler	<i>Sylvia melanocephala</i>	11.2	61.16	Skull *	

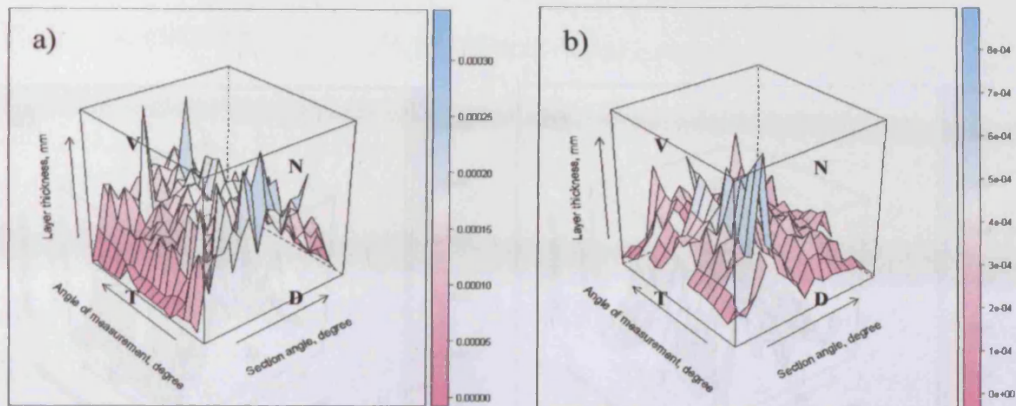
Winter wren	<i>Troglodytes troglodytes</i>	10.1	61.80	Skull	*
Redwing	<i>Turdus iliacus</i>	61.2	75.28	MRJ	1.633
Blackbird	<i>Turdus merula</i>	92.2	74.17	MRJ	3.027
Song thrush	<i>Turdus philomelos</i>	76.5	72.93	MRJ	2.143
Hoopoe	<i>Upupa epops</i>	63.8	76.84	Skull	*



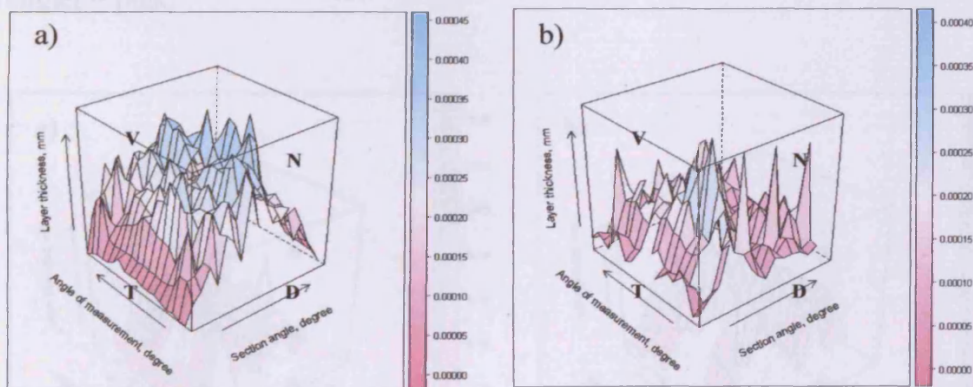
Appendix A 2.1. Inner plexiform layer topographies for a) starling and b) storm petrel. N = nasal, V = ventral, D = dorsal, T = temporal. The centre of the x axis and y axis corresponds to 90°. Colour scale (mm) runs from thicker = blue to thinner = pink.



Appendix A 2.2 Inner nuclear layer topographies for a) starling and b) storm petrel. N = nasal, V = ventral, D = dorsal, T = temporal. The centre of the x axis and y axis corresponds to 90°. Colour scale (mm) runs from thicker = blue to thinner = pink.

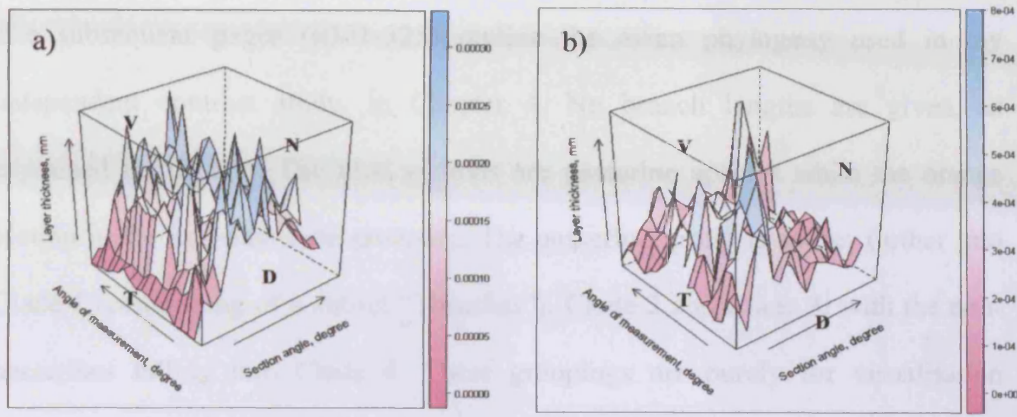


Appendix A 2.3 Outer plexiform layer topographies for a) starling and b) storm petrel. N = nasal, V = ventral, D = dorsal, T = temporal. The centre of the x axis and y axis corresponds to 90° . Colour scale (mm) runs from thicker = blue to thinner = pink.

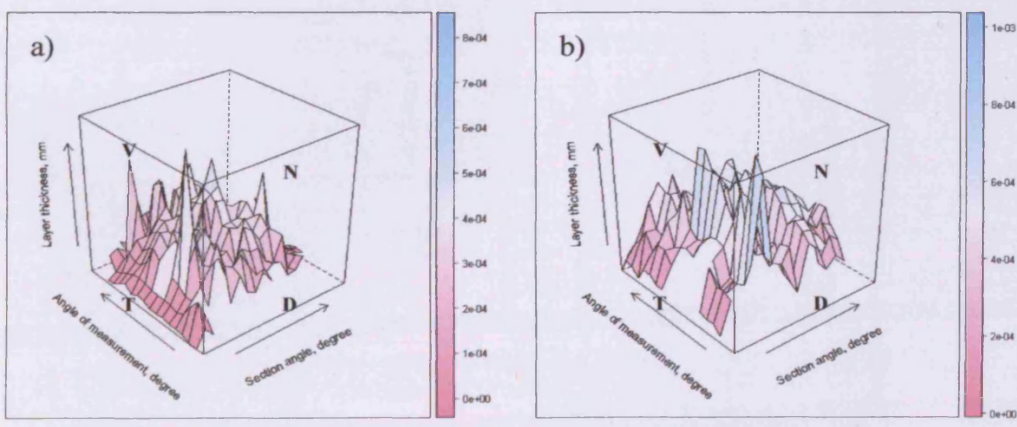


Appendix A 2.4 Outer nuclear layer topographies for a) starling and b) storm petrel. N = nasal, V = ventral, D = dorsal, T = temporal. The centre of the x axis and y axis corresponds to 90° . Colour scale (mm) runs from thicker = blue to thinner = pink.

Appendix A.3.1



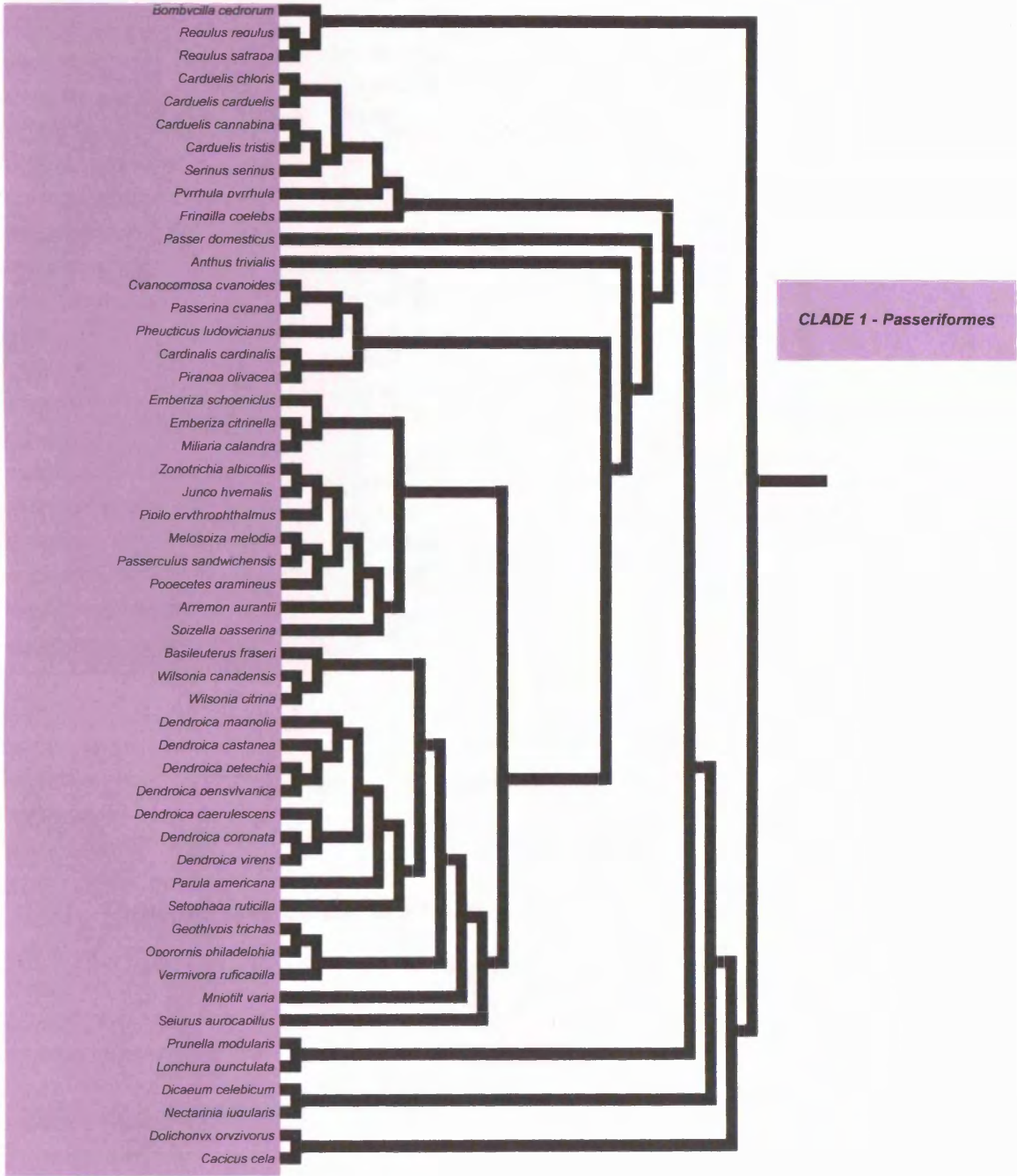
Appendix A 2.5 Photoreceptor inner segment topographies for a) starling and b) storm petrel. N = nasal, V = ventral, D = dorsal, T = temporal. The centre of the x axis and y axis corresponds to 90°. Colour scale (mm) runs from thicker = blue to thinner = pink.



Appendix A 2.6 Photoreceptor outer segment topographies for a) starling and b) storm petrel. N = nasal, V = ventral, D = dorsal, T = temporal. The centre of the x axis and y axis corresponds to 90°. Colour scale (mm) runs from thicker = blue to thinner = pink.

Appendix A.3.1.

The subsequent pages (p321-325) outline the avian phylogeny used in my independent contrast study, in Chapter 4. No branch lengths are given, as explained in the text. The lilac sections are passerine species while the orange section is the non-passerine grouping. The passerine group is subset further into Clade 1 (comprising of a subset “Thrushes”), Clade 2 and Clade 3, with the non-passerines falling into Clade 4. These groupings are purely for visualisation purposes. Please see Chapter 4 for details on how this phylogeny was constructed.

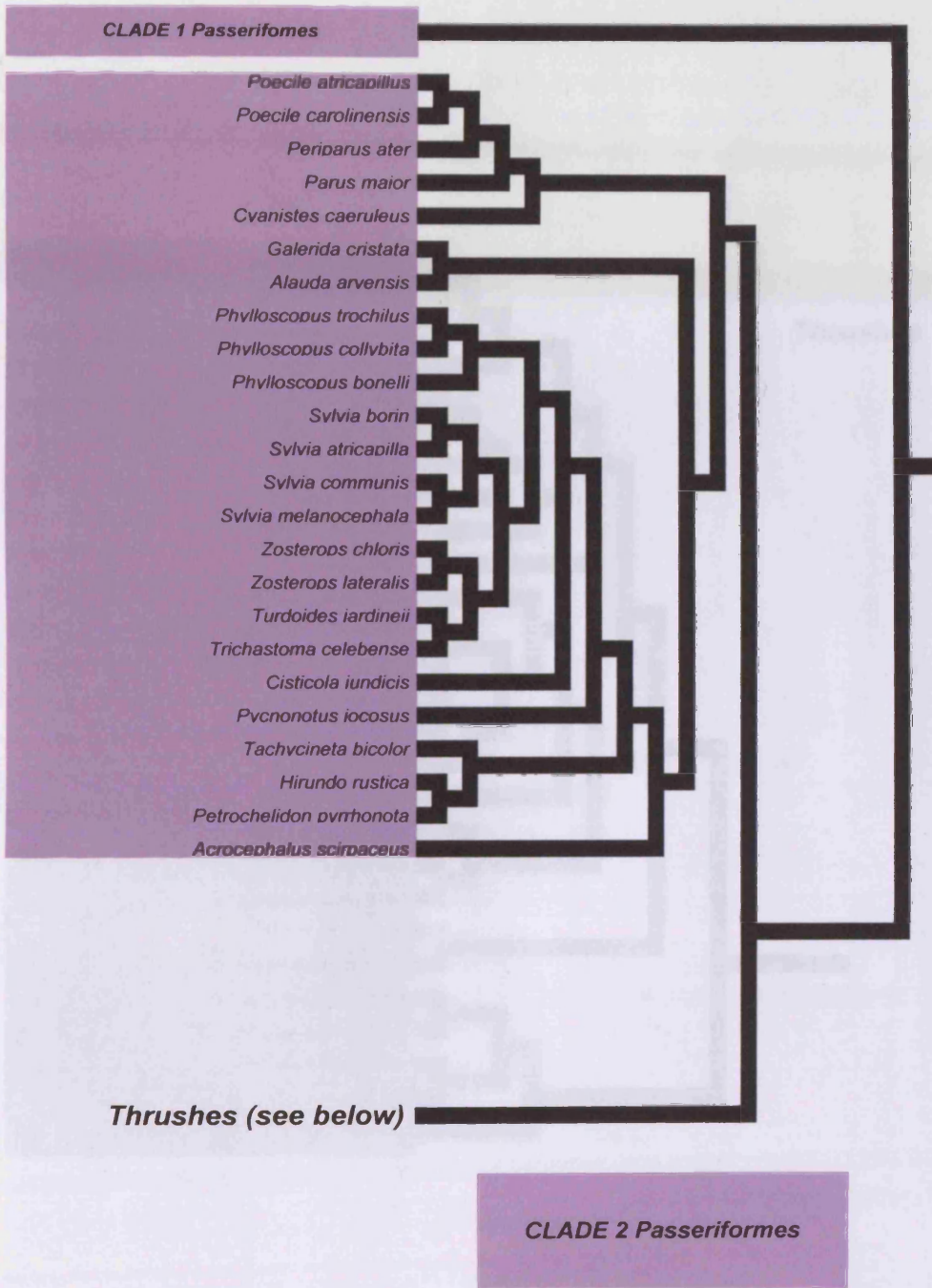


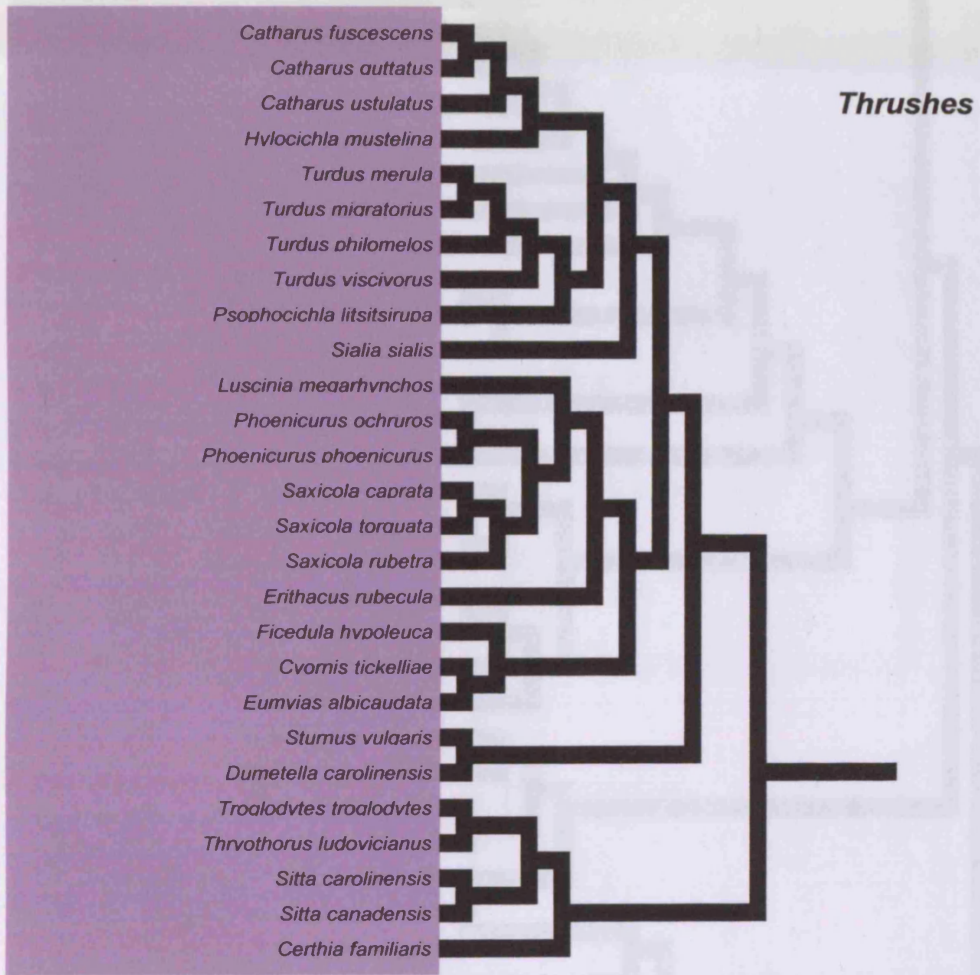
CLADE 1 Passeriformes

Poecile atricapillus
Poecile carolinensis
Periparus ater
Parus major
Cyanistes caeruleus
Galerida cristata
Alauda arvensis
Phylloscopus trochilus
Phylloscopus collybita
Phylloscopus bonelli
Sylvia borin
Sylvia atricapilla
Sylvia communis
Sylvia melanocephala
Zosterops chloris
Zosterops lateralis
Turdoides jardineii
Trichastoma celebense
Cisticola iundicis
Pycnonotus iocosus
Tachycineta bicolor
Hirundo rustica
Petrochelidon pyrrhonota
Acrocephalus scirpaceus

Thrushes (see below)

CLADE 2 Passeriformes

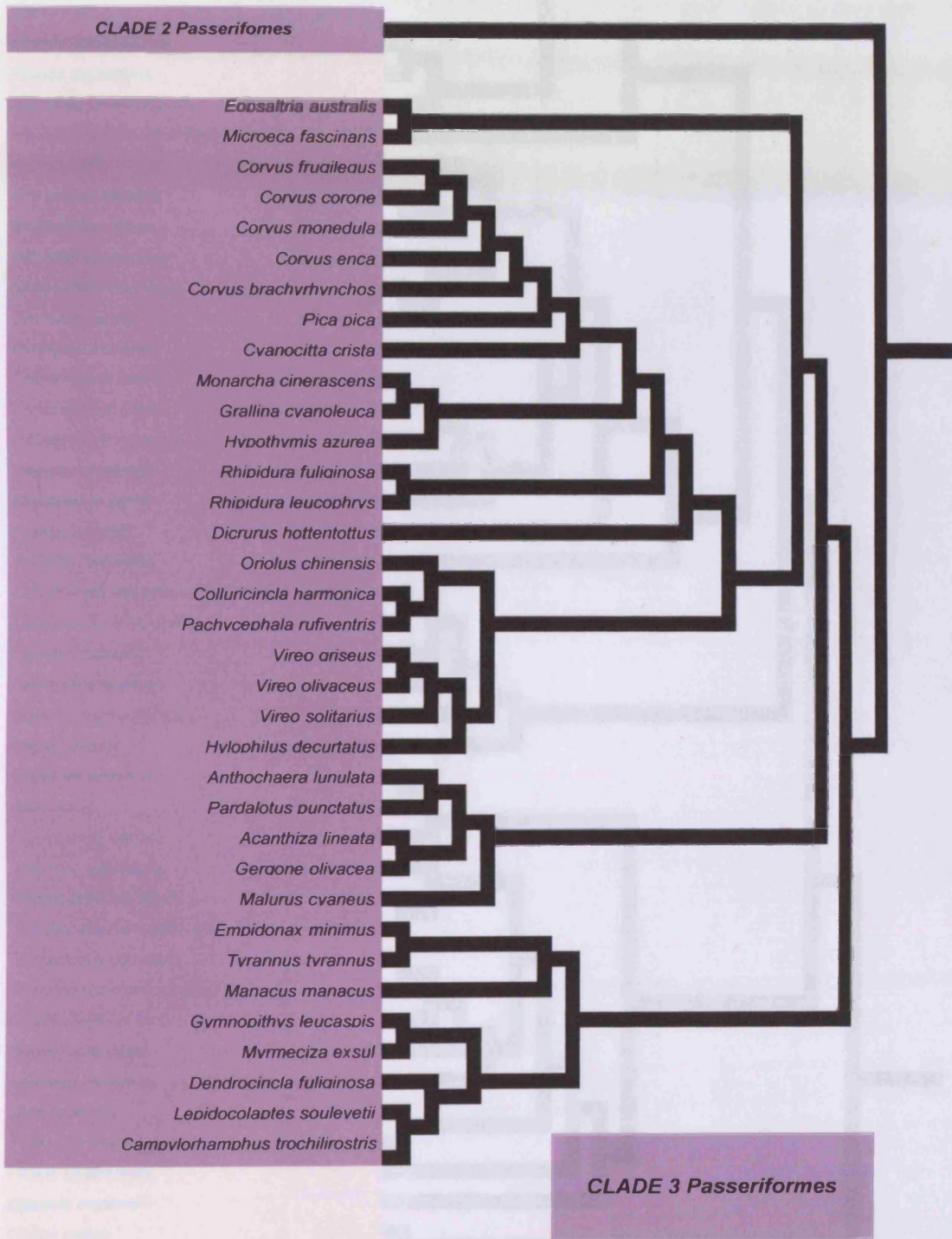




CLADE 2 Passeriformes

Eopsaltria australis
Microeca fascinans
Corvus fruileaus
Corvus corone
Corvus monedula
Corvus enca
Corvus brachyrhynchos
Pica pica
Cyanocitta cristata
Monarcha cinerascens
Grallina cyanoleuca
Hypothymis azurea
Rhipidura fuliginosa
Rhipidura leucophrys
Dicurus hottentottus
Oriolus chinensis
Colluricincla harmonica
Pachycephala rufiventris
Vireo ariseus
Vireo olivaceus
Vireo solitarius
Hylophilus decurtatus
Anthochaera lunulata
Pardalotus punctatus
Acanthiza lineata
Geræone olivacea
Malurus cyaneus
Empidonax minimus
Tyrannus tyrannus
Manacus manacus
Gymnophis leucaspis
Mymeciza exsul
Dendrocincla fuliginosa
Lepidocolaptes souleyetii
Campylorhamphus trochilirostris

CLADE 3 Passeriformes



CLADE 3 Passeriformes

Pionus chalcopterus
Pionus menstruus
Aratinga erythrogastra
Herpetotheres cachinnans
Picus viridis
Dryocopus pileatus
Mulleripicus fulvus
Picoides pubescens
Melanerpes carolinus
Sphyrapicus varius
Momotus momota
Todiramphus sancta
Todiramphus chloris
Dacelo novaeguineae
Halcyon chelicuti
Microceryle alcyon
Aceros cassidix
Accipiter trinotatus
Cacomantis merulinus
Cacomantis sepulcralis
Cuculus canorus
Surmiculus luabris
Coccyzus americanus
Piaya cayana
Chaetura pelagica
Apus apus
Phaethornis baroni
Columba palumbus
Streptopelia chinensis
Streptopelia senegalensis
Streptopelia decaocto
Streptopelia semitorquata
Streptopelia capicola
Streptopelia turtur
Leptotila verreauxi
Ducula aenea
Ptilinopus melanospilus
Phaps chalcoptera
Claravis pretiosa
Gallus gallus
Phasianus colchicus

CLADE 4 Non-passeriformes

Appendix A3.2. Results of General Linear Model analyses of the model: Contrasts of the time of onset of dawn song ~ contrasts of body mass + 0, for each site, for combined regional areas and overall. Cells are hatched where no data is available due to averaging across sites or study took place over several months, cells are hatched. Significance scoring: * $P < 0.05$, ** $P < 0.01$, n = not significant.

Site	Latitude	Twilight length (minutes)	Slope of association of mass upon start time of dawn song	Mass significant?	SE	T value	P value	AIC
Coonor, India	11.35	22:56	16.450	n	23.950	0.687	0.530	48.34
Darwendale, Zimbabwe	-17.70	21:59	-19.030	n	14.380	-1.324	0.256	46.90
Wangi Wangi, Indonesia	-5.31	20:51	4.563	n	5.182	0.881	0.388	222.83
Ebenezer, Australia	-33.52	25:46	0.069	n	2.882	0.024	0.981	119.28
Manabi Province, Ecuador	-0.69	21:27	-5.385	n	4.083	-1.319	0.203	184.62
Cruzinha, Portugal	37.14	25:57	-2.381	n	5.544	-0.430	0.675	116.04

Site	Latitude	Twilight length (minutes)	Slope of association of mass upon start time of dawn song	Mass significant?	SE	T value	P value	AIC
Guarda, Switzerland	46.77	39:06	-10.298	n	7.284	-1.414	0.195	82.24
Darmstadt, Germany	49.87	38:38	-0.493	n	5.930	-0.083	0.936	86.32
Gianton, UK	55.42	39:18	-5.695	n	6.001	-0.949	0.379	71.77
Dublin, Ireland	53.36	39:10	-7.441	*	3.190	-2.333	0.038	110.14
Pwllgloyw, UK	51.99	48:54	-8.742	n	5.805	-1.506	0.163	92.52
Gwaelod-y-Garth, UK	51.54	47:52	-10.378	n	7.247	-1.432	0.171	156.57
Chew, UK	51.35	40:46	-2.997	n	8.610	-0.348	0.731	213.38
Henfield, UK	50.93	38:39	-10.357	n	6.511	-1.591	0.146	85.92
Slupsk, Poland	54.46		-5.833	n	9.222	-0.633	0.572	37.47
South Hampshire, UK	50.91		-9.388	n	5.808	-1.616	0.119	239.07

Site	Latitude	Twilight length (minutes)	Slope of association of mass upon start time of dawn song	Mass significant?	SE	T value	P value	AIC
Average Europe	49.82		-12.463	**	4.166	-2.992	0.004	477.11
Mt Katahdin, USA	45.85	38:19	-1.244	n	6.367	-0.195	0.850	75.06
Jefferson Highlands, USA	44.38	36:44	1.030	n	3.463	0.297	0.767	474.82
East Lansing, USA	42.74		-1.120	n	7.802	-0.144	0.890	70.06
Ozark, USA	35.66		-4.234	n	2.311	-1.833	0.088	118.34
Average USA	42.16		1.313	n	3.114	0.421	0.675	560.23
Average Global			-0.439	n	2.407	-0.183	0.855	1700.20

Appendix A3.3. Sign tests of the slopes of associations of body mass with the onset of dawn song (either the direct association, or body mass controlled statistically for eye size, or body mass controlled statistically for eye size and their interaction), showing that slopes tend to negative when body mass is the only independent variable, but are frequently positive when eye size is controlled for statistically.

Slope from model containing:	Category	N	Proportion	P value
Body mass	<0	18	0.78	0.011
	>0	5	0.22	
Eye size + body mass	<0	8	0.35	0.21
	>0	15	0.65	
Eye size * body mass	<0	9	0.39	0.405
	>0	14	0.61	

Appendix A3.4. Results of General Linear Model analyses of the model: Time of onset of dawn song ~ eye size, for each site, for combined

regional areas and overall. Bold site names are those which are used at a regional or global comparison level. Where no data is available due to

averaging across sites or study took place over several months, cells are hatched. Significance scoring: * $P < 0.05$, ** $P < 0.01$, n = not

significant. Continued overleaf.

Site	Latitude	Twilight length (minutes)	Slope of association of eye upon start time of dawn song	Eye significant?	SE	T value	P value	AIC
Coonor, India	11.35	22:56	38.750	n	62.610	0.619	0.569	56.89
Darwendale, Zimbabwe	-17.7	21:59	-98.920	n	88.160	-1.122	0.325	56.14
Wangi Wangi, Indonesia	-5.31	20:51	14.640	n	13.180	1.111	0.279	224.63
Ebenezer, Australia	-33.52	25:46	-1.597	n	8.523	-0.187	0.854	122.16
Manabi Province, Ecuador	-0.69	21:27	-11.720	n	12.660	-0.925	0.366	189.81
Cruzinha, Portugal	37.14	25:57	-31.260	*	11.390	-2.745	0.017	118.53
Guarda, Switzerland	46.77	39:06	-56.420	*	22.230	-2.538	0.035	87.86
Darmstadt, Germany	49.87	38:38	-17.440	n	22.790	-0.765	0.464	98.59
Glanton, UK	55.42	39:18	-71.590	**	17.690	-4.048	0.007	72.99
Dublin, Ireland	53.36	39:10	-44.640	**	14.280	-3.125	0.009	121.67
Pwllgloyw, UK	51.99	48:54	-61.100	**	19.030	-3.211	0.009	103.17
Gwaelod-y-Garth, UK	51.54	47:52	-68.930	**	21.440	-3.215	0.005	163.48
Chew, UK	51.35	40:46	-57.600	*	24.750	-2.327	0.030	217.93

Site	Latitude	Twilight length (minutes)	Slope of association of eye upon start time of dawn song	Eye significant?	SE	T value	P value	AIC
Henfield, UK	50.93	38:39	-49.620	*	16.390	-3.028	0.014	91.86
Slupsk, Poland	54.46		-29.270	n	27.050	-1.082	0.358	42.74
South Hampshire, UK	50.91		-22.364	*	9.671	-2.312	0.030	236.67
Average EU	49.82		-39.484	***	8.692	-4.542	<0.001	480.46
Mt Katahdin, US	45.85	38:19	-18.600	n	16.180	-1.150	0.288	81.29
Jefferson Highlands, US	44.38	36:44	5.164	n	12.957	0.399	0.692	490.16
East Lansing, US	42.74		-9.995	n	14.264	-0.701	0.510	67.59
Ozark, US	35.66		-5.412	n	9.205	-0.588	0.566	126.04
Average US	42.16		4.833	n	11.028	0.438	0.663	572.79
Overall Global			-10.698	n	5.838	-1.832	0.069	1721.60

Appendix A3.5. Results of General Linear Model analyses of the model: Time of onset of dawn song ~ body mass, for each site, for combined regional areas and overall. Bold site names are those which are used at a regional or global comparison level. Where no data is available due to averaging across sites or study took place over several months, cells are hatched. Significance scoring: * $P < 0.05$, ** $P < 0.01$, n = not significant. Continued overleaf.

Site	Latitude	Twilight length (minutes)	Slope of association of body mass upon start time of dawn song	Body mass significant?	SE	T value	P value	AIC
Coonor, India	11.35	22:56	7.903	n	28.821	0.274	0.797	57.33
Darwendale, Zimbabwe	-17.7	21:59	-23.830	n	12.580	-1.894	0.131	53.94
Wangi Wangi, Indonesia	-5.31	20:51	3.578	n	4.034	0.887	0.385	225.10
Ebenezer, Australia	-33.52	25:46	0.769	n	2.478	0.310	0.761	122.08
Manabi Province, Ecuador	-0.69	21:27	-3.817	n	3.709	-1.029	0.316	189.60
Cruzinha, Portugal	37.14	25:57	-8.109	n	4.384	-1.850	0.087	121.89
Guarda, Switzerland	46.77	39:06	-16.770	n	7.670	-2.186	0.060	89.08
Darmstadt, Germany	49.87	38:38	-0.780	n	8.568	-0.091	0.930	99.27
Glanton, UK	55.42	39:18	-17.251	**	3.862	-4.466	0.004	71.81
Dublin, Ireland	53.36	39:10	-11.033	*	3.669	-3.007	0.011	122.14
Pwllgloyw, UK	51.99	48:54	-15.077	n	6.919	-2.179	0.054	107.01
Gwaelod-y-Garth, UK	51.54	47:52	-12.376	n	8.229	-1.504	0.152	170.07
Chew, UK	51.35	40:46	-5.164	n	8.133	-0.635	0.532	222.77

Site	Latitude	Twilight length (minutes)	Slope of association of body mass upon start time of dawn song	Body mass significant?	SE	T value	P value	AIC
Henfield, UK	50.93	38:39	-14.323	*	5.814	-2.463	0.036	93.92
Slupsk, Poland	54.46		-3.671	n	8.691	-0.422	0.701	44.10
South Hampshire, UK	50.91		-8.090	**	2.798	-2.891	0.008	234.13
Average EU	49.82		-10.798	***	2.672	-4.042	0.000	483.73
Mt Katahdin, US	45.85	38:19	-4.664	n	4.935	-0.945	0.376	81.77
Jefferson Highlands, US	44.38	36:44	3.970	n	3.653	1.087	0.282	489.11
East Lansing, US	42.74		-1.671	n	4.332	-0.386	0.713	68.03
Ozark, US	35.66		-1.788	n	2.510	-0.712	0.488	125.86
Average US	42.16		3.201	n	3.159	1.013	0.315	571.94
Overall Global			-2.073	n	1.760	-1.178	0.241	1723.50

Appendix A3.6. Results of General Linear Model analyses of the model: Time of onset of dawn song ~ eye size + body mass, for each site, for combined regional areas and overall. Bold site names are those which are used at a regional or global comparison level. Where no data is available due to averaging across sites or study took place over several months, cells are hatched. Significance scoring: * $P < 0.05$, ** $P < 0.01$, n = not significant. Continued overleaf. Lat. = Latitude, TL = Twilight length (minutes), SAE = Slope of association of eye size upon start time of dawn song, SAB = Slope of association of body mass upon start time of dawn song, E*?= Eye size significant?, B*?= Body mass significant?.

Site	Lat.	TL	SAE	SAB	E*?	B*?	SE (eye size)	T (eye size)	P (eye size)	SE (mass)	T (mass)	P (mass)	AIC
Coonoor, India	11.35	22:56	41.530	7.903	n	n	71.63 0	0.58 0	0.60 3	84.15 9	0.27 4	0.79 7	57.33
Darwendale, Zimbabwe	-17.7	21:59	-29.910	-20.930	n	n	101.2 60	0.29 5	0.78 7	17.36 0	1.20 6	0.31 4	55.77
Wangi Wangi, Indonesia	-5.31	20:51	25.090	-3.430	n	n	34.86 0	0.72 0	0.48 0	10.56 0	0.32 5	0.74 9	226.5 1
Ebenezer, Australia	-33.52	25:46	-65.838	19.341	*	*	29.67 8	2.21 8	0.04 7	8.649	2.23 6	0.04 5	118.9 3
Manabi Province, Ecuador	-0.69	21:27	4.772	-5.143	n	n	39.21 2	0.12 2	0.90 4	11.54 7	0.44 5	0.66 1	191.5 8
Cruzinha, Portugal	37.14	25:57	-54.551	8.871	n	n	26.71 2	2.04 2	0.06 4	9.197	0.96 5	0.35 4	119.4 1

Site	Lat.	TL	SAE	SAB	E*?	B*?	SE (eye)	T (eye size)	P (eye size)	SE (mass)	T (mass)	P (mass)	AIC
Guarda, Switzerland	46.77	39:06	-68.149	4.043	n	n	70.08 4	0.97 2	0.36 3	22.74 2	0.17 8	0.86 4	89.82
Darmstadt, Germany	49.87	38:38	-94.580	30.740	n	n	51.78 0	1.82 7	0.10 5	18.87 0	1.62 9	0.14 2	97.43
Glanton, UK	55.42	39:18	11.810	-19.980	n	n	94.12 0	0.12 5	0.90 5	22.13 0	0.90 3	0.40 8	73.79
Dublin, Ireland	53.36	39:10	-33.707	-2.884	n	n	51.39 4	0.65 6	0.52 5	12.98 1	0.22 2	0.82 8	123.6 0
Pwllgloyw, UK	51.99	48:54	-175.970	37.150	*	n	57.38 0	3.06 7	0.01 3	17.78 0	2.09 0	0.06 6	100.4 3
Gwaelod-y-Garth, UK	51.54	47:52	-166.050	34.870	***	*	39.60 0	4.19 3	0.00 1	12.66 0	2.75 5	0.01 5	158.1 1
Chew, UK	51.35	40:46	-197.840	46.760	***	**	42.10 0	4.70 0	0.00 0	12.45 0	3.75 5	0.00 1	207.6 6
Henfield, UK	50.93	38:39	-99.170	16.590	n	n	63.62 0	1.55 9	0.15 8	20.55 0	0.80 7	0.44 3	93.00
Slupsk, Poland	54.46		-68.350	12.780	n	n	55.87 0	1.22 3	0.34 6	15.67 0	0.81 5	0.50 1	43.30

Site	Lat.	TL	SAE	SAB	E*?	B*?	SE (eye)	T (eye size)	P (eye size)	SE (mass)	T (mass)	P (mass)	AIC
South Hampshire, UK	50.91		4.657	-9.335	n	n	19.746	0.236	0.816	5.999	1.556	0.133	236.07
Average EU	49.82		-35.020	-1.490	n	n	19.442	1.801	0.078	5.791	0.257	0.798	482.39
Mt Katahdin, US	45.85	38:19	-222.420	60.970	n	n	124.670	1.784	0.125	37.040	1.646	0.151	79.94
Jefferson Highlands, US	44.38	36:44	-61.390	20.290	n	*	35.170	1.746	0.087	10.010	2.027	0.048	487.98
East Lansing, US	42.74		-232.070	66.270	**	**	53.300	4.354	0.007	15.750	4.206	0.008	57.49
Ozark, US	35.66		32.450	-10.550	n	n	53.190	0.610	0.552	14.580	0.723	0.482	127.41
Average US	42.16		-47.207	15.862	n	n	31.515	1.498	0.139	9.155	1.733	0.088	571.62
Overall Global			-28.829	5.897	n	n	15.042	1.917	0.057	4.511	1.307	0.193	1721.80

Appendix A3.7. Results of General Linear Model analyses of the model: Time of onset of dawn song ~ eye size * body mass, for each site, for

combined regional areas and overall. Bold site names are those which are used at a regional or global comparison level. Where no data is

available due to averaging across sites or study took place over several months, cells are hatched. Significance scoring: * $P < 0.05$, ** $P < 0.01$, n

= not significant. Continued overleaf. Lat. = Latitude, TL = Twilight length (minutes), SAE = Slope of association of eye size upon start time of

dawn song, SAB = Slope of association of body mass upon start time of dawn song, SAE*B = Slope of association of eye size*body mass upon

start time of dawn song, E*?= Eye size significant?, B*? = Body mass significant?, E*M*? = Eye size * body mass significant?.

Site	Lat	TL	SAE	SAB	SAE*B	E*?	B*?	E*M*?	SE (eye size)	T (eye size)	P (eye size)
Coonoor, India	11.35	22:56	-872.900	-1214.900	329.900	n	n	n	789.000	-1.106	0.384
Darwendale, Zimbabwe	-17.7	21:59	1242.610	1070.780	-267.330	**	**	**	112.610	11.030	0.008
Wangi Wangi, Indonesia	-5.31	20:51	-18.194	-67.623	13.862	n	n	n	40.973	-0.444	0.662
Ebenezer, Australia	-33.52	25:46	-56.106	31.693	-3.009	n	n	n	39.060	-1.436	0.179
Manabi Province, Ecuador	-0.69	21:27	54.530	33.550	-10.220	n	n	n	62.850	0.868	0.398
Cruzinha, Portugal	37.14	25:57	-63.229	-1.576	2.753	n	n	n	53.658	-1.178	0.264

Site	Lat	TL	SAE	SAB	SAE*B	E*?	B*?	E*M*?	SE (eye size)	T (eye size)	P (eye size)
Guarda, Switzerland	46.77	39:06	-112.040	-68.750	18.050	n	n	n	105.850	-1.058	0.331
Darmstadt, Germany	49.87	38:38	-66.590	91.180	-14.280	n	n	n	85.610	-0.778	0.462
Glanton, UK	55.42	39:18	15.790	41.520	-11.980	n	n	n	99.170	0.159	0.881
Dublin, Ireland	53.36	39:10	-45.191	-38.049	7.926	n	n	n	56.836	-0.795	0.445
Pwllgloyw, UK	51.99	48:54	-142.300	108.930	-16.860	n	n	n	82.560	-1.724	0.123
Gwaelod-y-Garth, UK	51.54	47:52	-164.704	36.543	-0.437	n	n	n	78.021	-2.111	0.053
Chew, UK	51.35	40:46	-241.630	-0.197	12.735	*	n	n	88.651	-2.726	0.013
Henfield, UK	50.93	38:39	-137.860	-55.380	17.290	n	n	n	82.490	-1.671	0.139
Slupsk, Poland	54.46		152.050	250.690	-58.850	n	n	n	261.040	0.582	0.664
South Hampshire, UK	50.91		-3.922	-17.146	1.933	n	n	n	45.845	-0.086	0.933
Average EU	49.82		-54.576	-20.587	4.768	n	n	n	35.530	-1.536	0.131
Mt Katahdin, US	45.85	38:19	-150.550	-85.070	24.120	n	n	n	127.590	-1.180	0.291

Site	Lat	TL	SAE	SAB	SAE*B	E*?	B*?	E*M*?	SE (eye size)	T (eye size)	P (eye size)
Jefferson Highlands, US	44.38	36.44	-94.839	-22.247	10.494	*	n	n	46.532	-2.038	0.047
East Lansing, US	42.74		-228.193	53.302	2.228	*	n	n	61.095	-3.735	0.020
Ozark, US	35.66		-7.022	-69.109	13.406	n	n	n	55.084	-0.127	0.901
Average US	42.16		-95.180	-40.520	13.940	*	n	n	41.030	-2.319	0.024
Overall Global			-46.271	-12.021	4.405	*	n	n	21.908	-2.112	0.036

Appendix A3.7 continued.

Site	SE (body mass)	T (body mass)	P (body mass)	SE (E*M)	T (E*M)	P (E*M)	AIC
Coonor, India	1053.600	-1.153	0.368	283.600	1.163	0.365	57.59
Darwendale, Zimbabwe	95.760	11.180	0.008	23.440	-11.400	0.008	32.63
Wangi Wangi, Indonesia	37.229	-1.816	0.085	7.743	1.790	0.089	224.92
Ebenezer, Australia	31.830	0.996	0.341	7.441	-0.404	0.694	120.71
Manabi Province, Ecuador	39.910	0.841	0.412	10.090	-1.013	0.325	192.35
Cruzinha, Portugal	56.040	-0.028	0.978	14.553	0.189	0.853	121.36
Guarda, Switzerland	128.300	-0.536	0.611	31.260	0.577	0.585	91.28
Darmstadt, Germany	143.670	0.635	0.546	33.630	-0.425	0.684	99.15

Site	SE (body mass)	T (body mass)	P (body mass)	SE (E*M)	T (E*M)	P (E*M)	AIC
Glantou, UK	88.560	0.469	0.664	16.640	-0.720	0.512	74.81
Dublin, Ireland	63.765	-0.597	0.564	14.052	0.564	0.585	125.16
Pwllgloyw, UK	123.220	0.884	0.402	28.620	-0.589	0.572	101.92
Gwaelod-y-Garth, UK	83.252	0.439	0.667	21.512	-0.020	0.984	160.11
Chew, UK	84.187	-0.002	0.998	22.573	0.564	0.579	209.28
Henfield, UK	96.040	-0.577	0.582	22.510	0.768	0.468	94.11
Slupsk, Poland	274.820	0.912	0.529	67.860	-0.867	0.545	42.50
South Hampshire, UK	37.987	-0.451	0.656	9.279	0.208	0.837	238.02
Average EU	29.549	-0.697	0.489	7.232	0.659	0.513	483.92
Mt Katahdin, US	111.800	-0.761	0.481	17.560	1.374	0.228	79.05
Jefferson Highlands, US	40.126	-0.554	0.582	9.586	1.095	0.279	488.70
East Lansing, US	54.362	0.980	0.382	8.846	0.252	0.814	59.37
Ozark, US	37.449	-1.845	0.090	7.982	1.679	0.119	126.03
Average US	36.170	-1.120	0.267	8.660	1.610	0.113	570.32
Overall Global	16.979	-0.708	0.480	4.024	1.095	0.275	1722.60

Appendix A 3.8. Species level analysis for the Indonesian dataset. General linear models and regression analyses of eye size or RIB, body mass, and timing of dawn song in order of AIC score (lowest score indicating best model). Asterisks imply degree of significance with a significant result (**<math>< 0.0001</math>, **<math>< 0.001</math>, *<math>< 0.05</math>).

Model number	Explanatory variables	Adjusted R ²	Regression coefficient	Standard error	F (d.f.)	Within model P-value	Overall P-value	AIC
5	RIB Body mass RIB * Body mass	0.869	177.240 -39.930 -53.340	39.70 16.00 17.03	16.51 (3, 4)	0.011 * 0.067 0.035 *	0.010 *	58.25
6	RIB Body mass	0.639	56.369 9.495	15.48 4.34	7.19 (2, 5)	0.015 * 0.080	0.034 *	66.17
7	RIB	0.411	45.319	18.68	5.89 (1, 6)	0.051	0.051	69.54
4	Body mass	-0.100	4.332	7.16	0.37 (1, 6)	0.567	0.567	74.53
3	Eye size	0.013	6.253	22.62	0.08 (1, 6)	0.791	0.792	74.90
1	Eye size Body mass Eye size * Body mass	-0.110	-137.030 -183.450 46.610	98.82 156.63 36.95	0.77 (3, 4)	0.238 0.307 0.276	0.569	75.37
2	Eye size Body mass	-0.242	-29.970 13.060	53.55 17.35	0.32 (2, 5)	0.600 0.486	0.741	76.04

Appendix A 3.9. Species level analysis for the European dataset. General linear models and regression analyses of eye size or RIB, body mass, and timing of dawn song in order of AIC score (lowest score indicating best model). Asterisks imply degree of significance with a significant result (*** < 0.0001, ** < 0.001, * < 0.05).

Model number	Explanatory variables	Adjusted R ²	Regression coefficient	Standard error	F (d.f.)	Within model P-value	Overall P-value	AIC
1	Eye size		-212.890	78.10		0.014 *		
	Body mass		-138.170	59.41		0.032 *		
	Eye size * Body mass	0.260	38.180	15.93	3.46 (3, 18)	0.028 *	0.038 *	209.11
3	Eye size	0.119	-29.140	14.88	3.83 (1, 20)	0.064	0.064	211.26
6	RIB		-41.649	23.14		0.088		
	Body mass	0.138	-11.414	6.04	2.68 (2, 19)	0.074	0.094	211.65
4	Body mass	0.042	-8.470	6.13	1.91 (1, 20)	0.182	0.182	213.12
2	Eye size		-34.230	26.02		0.204		
	Body mass	0.075	2.480	10.27	1.86 (2, 19)	0.812	0.184	213.20
7	RIB	0.027	-29.790	23.66	1.59 (1, 20)	0.222	0.223	213.44
5	RIB		-59.641	78.11		0.455		
	Body mass		-6.495	21.27		0.764		
	RIB * Body mass	0.093	5.290	21.88	1.72 (3, 18)	0.812	0.199	213.58

Appendix A 3.10. Species level analysis for the Gwaelod-y-Garth dataset. General linear models and regression analyses of eye size or RIB, body mass, and timing of dawn song in order of AIC score (lowest score indicating best model). Asterisks imply degree of significance with a significant result (***) < 0.0001, ** < 0.001, * < 0.05).

Model number	Explanatory variables	Adjusted R ²	Regression coefficient	Standard error	F (d.f.)	Within	
						model P-value	Overall P-value
1	Eye size		-147.360	72.75		0.099	
	Body mass		175.210	101.05		0.144	
	Eye size * Body mass	0.849	-29.710	24.50	15.95 (3, 5)	0.279	0.005 *
3	Eye size		-224.600	36.50		0.001 *	
	Body mass	0.837	53.470	11.95	21.51 (2, 6)	0.004 *	0.002 *
2	Eye size	0.393	-78.680	31.65	6.18 (1, 7)	0.042 *	0.042 *
7	RIB	0.194	-47.380	27.71	2.92 (1, 7)	0.131	0.131
6	RIB		69.410	69.86		0.366	
	Body mass		-481.910	394.01		0.276	87.23
5	RIB * Body mass	0.142	154.060	137.88	1.44 (3, 5)	0.315	0.335
	RIB		-42.908	30.23		0.206	
	Body mass	0.107	-7.340	13.02	1.48 (2, 6)	0.593	0.301
4	Body mass	-0.023	-12.190	13.45	0.82 (1, 7)	0.395	0.395
							87.84

Appendix A 3.11. Species level analysis for the Chew dataset. General linear models and regression analyses of eye size or RIB, body mass, and timing of dawn song in order of AIC score (lowest score indicating best model). Asterisks imply degree of significance with a significant result (***) < 0.0001, ** < 0.001, * < 0.05).

Model number	Explanatory variables	Adjusted R ²	Regression coefficient	Standard error	F (d.f.)	Within model p-value	Overall p-value	AIC
2	Eye size	0.507	-212.710	54.60	7.69 (2, 11)	0.002 *	0.008 *	128.20
1	Body mass		56.440	18.04		0.010 *		
	Eye size		-207.446	114.87		0.101		
	Body mass		62.776	121.14		0.616		
	Eye size * Body mass	0.458	-1.663	31.43	4.66 (3, 10)	0.959	0.028 *	130.20
3	Eye size	0.146	-65.560	36.53	3.22 (1, 12)	0.098	0.098	135.12
7	RIB	0.124	-46.660	27.69	2.84 (1, 12)	0.118	0.118	135.47
6	RIB		-1.940	12.82		0.882		
	Body mass	0.046	-46.200	29.05	1.32 (2, 11)	0.140	0.308	137.45
4	Body mass	-0.075	-4.069	13.54	0.09 (1, 12)	0.769	0.769	138.34
5	RIB		19.960	237.16		0.935		
	Body mass		-14.810	47.68		0.762		
	RIB * Body mass	-0.041	-21.480	76.36	0.83 (3, 10)	0.784	0.507	139.34

Appendix A 4.1. Non significant results of the aviary study; comparisons between birds under artificially lit and control (unlit) “night-time” treatments. Power analyses were completed by calculating the minimum sample size (N_{min}) required for a significant ($P < 0.05$) result given the observed effect sizes and data distributions.

Variable tested	Day-night order	Test statistic V	N	P	Power analysis (N_{min})	Median \pm IQR unlit			Median \pm IQR lit		
							\pm			\pm	
Start time of rest	Day-Night	10	8	0.293	> 31	4.00	\pm	42.00	95.00	\pm	180.25
Daytime rate of mass gain	Day-Night	10	6	1.000	> 148	2.79E-03	\pm	6.26E-04	3.48E-03	\pm	2.32E-03
% Mass gain during day	Day-Night	5	6	0.590	> 48	6.02	\pm	2.20	7.16	\pm	6.36
% Mass gain throughout activity period	Day-Night	5	6	1.000	> 227	6.65	\pm	3.57	2.15	\pm	5.11
Start time of rest	Night-Day	13	8	0.547	> 51	-676.50	\pm	74.75	-625.00	\pm	151.75
Daytime rate of mass gain	Night-Day	6	5	0.813	> 69	2.87E-03	\pm	2.38E-03	2.25E-03	\pm	9.31E-04
% Mass gain during day	Night-Day	6	5	0.813	> 70	7.89	\pm	3.95	5.97	\pm	1.60
% Mass gain throughout activity period	Night-Day	4	5	0.875	> 84	7.89	\pm	3.95	7.14	\pm	2.72

